ROLES OF GLYCOSYLTRANSFERASES IN DROSOPHILA DEVELOPMENT

by

Matthew Jason Moulton

A dissertation submitted to the faculty of
The University of Utah
in partial fulfillment of the requirements for the degree of

Doctor of Philosophy

Department of Human Genetics

The University of Utah

August 2017

The University of Utah Graduate School

STATEMENT OF DISSERTATION APPROVAL

The dissertation of **Matthew Jason Moulton**

has been approved by the following supervisory committee members:

Anthea Letsou	, Chair	**5/31/2017**
		Date Approved
Jan Christian	, Member	**5/31/2017**
		Date Approved
David Grunwald	, Member	**5/31/2017**
		Date Approved
Shigeru Sakonju	, Member	
		Date Approved
Michael Shapiro	, Member	**5/31/2017**
		Date Approved

and by **Lynn Jorde**, Chair/Dean of

the Department/College/School of **Human Genetics**

and by David B. Kieda, Dean of The Graduate School.

ABSTRACT

It is surprising that there are only about 80 described congenital diseases that result from mutations in any of the 1% of genes in the human genome (~200-250 genes) dedicated to protein glycosylation. It is these glycosylation events that provide tremendous protein diversity and contribute to proper protein folding, function, and subcellular localization. Thus, the rarity with which human congenital disorders of glycosylation (CDGs) are observed despite the myriad of genes involved in this process and the apparent critical role for proper protein form and function suggests that glycosylation is critical for proper development. However, the role of glycans in development has been largely understudied and there are only a few genetic models of human CDGs in existence.

Glycosylation occurs by the enzymatic addition of sugar-derived molecules and is estimated to provide 10-10^4 times more diversity than the unmodified proteome alone. Glycans are present on the surface of nearly every cell within multicellular organisms and are capable of facilitating communication with the cell and its environment and with other cells and also have structural roles as critical components of extracellular matrix. However, the complexity of glycan formation makes it difficult to understand the diverse and pleiotropic roles glycans play in cellular biology.

The utility of *Drosophila* to elucidate the role of glycans in development as well as disease has only been appreciated recently. Herein, I further demonstrate the utility of *Drosophila* to understand the roles of both N- and O-glycans in development and cell signaling. Furthermore, I utilize the fly to understand the biology of glycans in a human disorder of congenital disease, Peters' Plus Syndrome.

I demonstrate that the previously reported Dpp signal antagonism achieved by the sugar derivative UDP-*N*-Acetyglucosamine (GlcNAc) is carried out by the synthesis of a chondroitin-sulfate sink produced in the embryonic cardiac mesoderm and by the addition of GlcNAc to the type I receptor Saxophone to limit Dpp signal through Tkv exclusively. Furthermore, loss of the *Drosophila* ortholog of the human *B3GLCT* gene, *sugarcoated*, demonstrates a critical role for O-linked mucins in cell hypertrophic growth during larval development and oogenesis and demonstrates a potential role for human mucins in chondrocyte hypertrophy—an event required for the majority of human bone growth—and a potential mechanistic reason for growth defects observed in Peters' Plus Syndrome patients.

I dedicate this to my tremendously supportive wife who encourages me and sustains me in all aspects of my life. This is also dedicated to my two sons who are never ending sources of happiness and fun as well as to my mother who has always pushed me to learn and discover.

TABLE OF CONTENTS

LIST OF TABLES

Tables

LIST OF FIGURES

Figures

ACKNOWLEDGEMENTS

I am indebted to all those who helped me in my graduate studies and completion of my research and this dissertation. I learned some of my most valued lessons from my fellow graduate students within and outside of the Letsou Lab who are too numerous to name. I extend a special thanks to the current and former members of the Letsou Lab: Greg Humphreys, Shaili Jori, Hannah Gordon, Molly Jud, Suzanne Kimball, Sandy Kazuko, and an undergraduate researcher who has been with me almost the entirety of my graduate studies, Alex Kim. Without the help and guidance from these people, this work would have never have been possible.

I especially thank Anthea for her kind and generous way of mentoring her students. Anthea is a constant source of support through good and bad times and always had my back. I thank her for always making herself available for me to get help from her, even though I know she often had more pressing matters to deal with. I am especially grateful to her for taking up extra commitments at the NSF to keep the lab running and for maintain a constant mentorship of me even while she was away. Thank you, Anthea, for taking a chance on me and always believing I could do it.

I have benefitted greatly from the scientific community at the University and beyond. Thank you to our department chair, Lynn Jorde, the graduate advisor, Carl Thummel, and the organizers of many insightful conferences and retreats. A special thanks also goes out to those who manage the Human Genetics and Bioscience offices who have ensured all the administrative obligations are fulfilled. I also acknowledge the researchers who provided me with reagents to ensure the successful completion of my studies. These include: Kristi Wharton, who provided me with the Sax-Flag transgenic

line, John Hanover, who provided me the *sxc* lines, Tom Kornberg, who provided me with the Tkv-GFP line, and Michael O'Connor who provided numerous reagents and helpful feedback throughout my graduate research.

I am also indebted to numerous mentors I've had the pleasure of learning from throughout my life. Thank you to Michael Whiting, my undergraduate research mentor who taught me how do research and helped me get a first-author publication out while I was an undergraduate. Thank you also to my music teacher and life-long friend Iain McKay who not only taught me to love music but to enjoy life and face its problems head on.

Lastly, I thank my wife, our children, and our families for their constant support and love throughout the years. To my son, Thomas, thank you for being kind and gentle and always being excited to see me when I get home. To my son, Derek, thank you for being a never-ending source of humor and fun and making sure we don't take ourselves too seriously. To my wife, a tremendous thank you for your willingness to spend the majority of our married lives still in school and living in basement apartments. Thank you for being my greatest champion and for your eternal love and support.

CHAPTER 1

INTRODUCTION

Glycosylation in cell signaling, development and disease

Glycan biology

Although the human genome encodes in excess of 20,000 genes, the protein diversity that can be generated from these genes is vastly increased due to alternative splicing and post-translational modification (PTM) (Fig. 1.1). One of the most diverse and abundant PTMs is glycosylation, which occurs by enzymatic addition of sugar-derived molecules. Glycosylation can be a major contributor to protein mass and can alter subcellular localization and function of a protein (Pandey and Mann, 2000; Varki, 2017). The collective group of glycan structures, or the glycome, is estimated to be 10-10^4 times more diverse than the translated proteome, and upwards of 1% or more of the genes in the genome are dedicated to glycosylating proteins (Freeze, 2006; Marquardt and Denecke, 2003). It is, therefore, somewhat surprising that the role of glycosylation in development and disease has only been recently appreciated. This may be due, in part, to the heterogeneous nature of disorders of glycosylation and the relative rarity with which many of these diseases occur in the human population. A critical developmental role for glycosylation has lately become well-established and may provide a reason why glycosylation disorders are rare (Haltiwanger, 2002; Haltiwanger and Lowe, 2004; Moremen et al., 2012). For example, pathogenic mutations of the catalytic subunit of the oligosaccharyltransferase complex, *STT3A*, result in aberrations in the glycosylation pattern of transferrin glycoconjugates (Ghosh et al., 2017). Clinical symptoms manifest

in these patients include intellectual disability, developmental delay, seizures, and absent speech. Additionally, some patients developed episodic hypothermia and altered consciousness. Clinical manifestations like these may not be properly attributed to disorders in glycosylation until after extensive mutation mapping and laboratory verification. Indeed the rarity with which disorders of glycosylation are observed in humans may be due not only to the important developmental roles of glycans, but also our inability to distinguish disorders of glycosylation from the myriad of other disorders with overlapping symptoms.

The glycome encompasses all sugar-modified compounds including glycoproteins, proteoglycans, glycosphingolipids, and glycosylphosphatidylinositol (GPI) anchors, collectively termed glycans. Glycans are categorized by the types of sugars found in them, by the presence or absence of sugar chain branches, and by the substrate on which the sugars are attached (Varki, 2017). Glycoproteins are broadly defined as any protein with a carbohydrate group attached whereas proteoglycans are glycoproteins that are modified by one or more nonbranched glycosaminoglycan chain (i.e., heparin, chondroitin, and dermatan sulfate). Glycosphingolipids are branched or nonbranched sugar chains attached to the cell membrane via a ceramide-derived lipid and can also be attached to the carboxy-terminus of a glycoprotein making up a GPI anchor. Glycans surround the surface of virtually every cell of multicellular organisms capable of differentiation and tissue formation. These glycans are positioned around the cell to facilitate cellular communication with the environment and perform essential cellular functions including the regulation of cell-cell communication (Haltiwanger, 2002; Haltiwanger and Lowe, 2004; Haltiwanger and Stanley, 2002; Shao et al., 2002). Additionally, secreted proteoglycans (like hyaluronan) function to define the structural properties within bone and cartilage and are critical components of extracellular matrix (Bastow et al., 2008; Vincent et al., 2003). Glycans are found in ordered arrays across

diverse tissues throughout developmental time, leading to the hypothesis that they serve a critical role in development. However, the astounding complexity with which glycans alter cellular function makes the understanding of their specific developmental roles difficult to assess with rapidity.

Genetic models of glycosylation disease

Drosophila has proven itself to be an invaluable model in which to elucidate the function of glycans and implies that similar mechanisms may be utilized across diverse evolutionary lineages. Both N- and O-glycans play critical roles in modulation of signaling pathways in the fly (Haltiwanger, 2002; Haltiwanger and Stanley, 2002; Shao et al., 2002). It has been demonstrated that Notch signaling is regulated by both O-glucose and the subsequent elongation by xylose. O-glucose modification of Notch alters the conformation of the Notch extracellular domain and promotes efficient proteolytic processing of Notch (Haltiwanger and Lowe, 2004; Haltiwanger and Stanley, 2002). However, further addition of xylose to O-glucose modifications in one protein domain of Notch leads to inhibition of Notch signaling in some developmental contexts (Lee et al., 2017; Lee et al., 2013; Lee et al., 2010). Lack of O-fucose completely abrogates Notch signaling as nonfucosylated Notch cannot bind to the receptor Delta (Stanley, 2007). For an in-depth review of glycosylation-mediated regulation of Notch signaling, see Haines and Irvine (2003). N-glycosylation plays important modulatory roles in other signaling pathways as well. For example, loss of heparin and chondroitin sulfate, as in a *suppenkasper* (*ska*) mutant, results in *wingless* loss of function phenotypes and demonstrates the essential role for N-linked GAGs in Wingless signaling (Haerry et al., 1997). Heparin sulfated proteoglycans like Syndecan have also been implicated in facilitating Dpp signaling in the wing imaginal disc (Yan and Lin, 2009). These studies demonstrate that the fly has been well-utilized in understanding

the complex roles glycans play in development, especially cell signaling and is poised to aid our understanding of glycans in human developmental disease.

Although there are over 80 described human congenital disorders of glycosylation (NORD website, May 15, 2017), most of these diseases currently lack adequate genetic models in which to understand disease etiology and develop effective therapeutic interventions (see Table 1.1 for list of animal models of CDGs). Human disorders of glycosylation are among the more complicated human congenital diseases to understand and treat owing to the complexity of the metabolic pathways required to carry out glycosylation and the pleiotropic effects that can be caused by mutations in even a single gene (i.e., loss of any sugar/enzyme can affect many downstream pathways). *Drosophila* provides a superb platform in which models of glycosylation defects can be tested and utilized to inform research into disease therapies (Moulton and Letsou, 2016). This is in no small part due to the high degree of conservation of developmental and homeostatic pathways and biological processes between human and fly. Its utility is further bolstered by an immense and ever expanding genetic toolkit to generate mutations with increased ease and specificity and with decreasing cost and time.

Drosophila has recently been used in diverse ways to understand glycosylation and disorders of glycosylation. Analyses of O-mannose modifications on the protein dystroglycan have been instrumental in establishing a *Drosophila* model of muscular dystrophy (Haltiwanger and Lowe, 2004; Nakamura et al., 2010), and elimination of *Gfr* RNA in *Drosophila* mimics Notch loss-of-function mutations and serves as a model for the human disease congenital disorder of glycosylation IIc (Ishikawa et al., 2005). Drosophila geneticists have also successfully developed models of the glycosylation-affected disorders CGD-la (Jumbo-Lucioni et al., 2014; Parkinson et al., 2016) and classic galactosemia (Jumbo-Lucioni et al., 2014). Despite these clear victories in

disease modeling, many glycosylation-related human diseases such as X-linked intellectual disability resulting from mutations in the O-linked GlcNAc transferase (Niranjan et al., 2015), Peters' Plus Syndrome resulting from mutations in *β3GLCT* (Maillette de Buy Wenniger-Prick and Hennekam, 2002), and others, still lack genetic models (Table 1.1). Thus although *Drosophila* has proven fruitful in delineating roles for glycosylation in human disease, there is still more that can be done in *Drosophila* to expand our understanding of glycosylation-related human diseases.

Research summary

Building on work to understand the role of glycans in modulating cell signaling, our lab has identified several unique ways in which glycans are required for proper development, cell signaling, and embryonic patterning using *Drosophila* as a model. Specifically, our lab has discovered a critical role for *N*-acetylglucosamine (GlcNAc) in embryonic development and patterning. Loss of the *mummy* (*mmy*)–encoded *N*-acetylglucasamine pyrophosphorylase, which catalyzes the last step in the synthesis of GlcNAc, results in ectopic Dpp signaling in the embryonic epidermis and hypotrophy of ventral structures, the ventral denticle belts (Humphreys et al., 2013). We and others have identified a group of mutants, namely *raw*, *ribbon* (*rib*), and *puckered* (*puc*), with shared loss-of-function cuticle phenotypes and demonstrated that these mutants also share defects in Dpp signal antagonism. While *raw*, *rib*, and *puc* all mediate their effects on Dpp via regulation of JNK signaling, the signaling pathway that is required for *dpp* production in the epidermis, *mmy's* effects on Dpp are direct. We now seek to understand the role of GlcNAc in direct antagonism of Dpp signaling. To this end, we have discovered two novel mechanisms of GlcNAc-mediated Dpp signal antagonism. The first via O-GlcNAcylation-mediated repression of the Type I receptor Saxophone (Sax), which functions as a nutrient sensitive arm of Dpp signaling (Chapter 2). The

second via the synthesis of a chondroitin-sulfate sink that is generated in the mesoderm underlying the dorsolateral epidermis which functions to sequester Dpp and prevent it from signaling (Chapter 4). Additionally, we have discovered a novel developmental role for mucins containing β1-3 glucose additions to O-Fucose, which are added using the enzyme encoded by the *CG9109* gene, which we have named *sugarcoated* (*sgct*) (Chapter 3).

Specifically, herein I describe our discovery that while Dpp signaling is required in both the embryonic epidermis and the underlying cardiac mesoderm, proper Dpp signal propagation in both of these tissues requires the expression of a chondroitin-modified signaling sink in the mesoderm. Loss of either of two genes required for the formation of chondroitin (*gale* and *wand*) results in expanded Dpp signaling in the epidermis and cardiac mesoderm. These data are the first to demonstrate a role for a signaling sink specifically targeting Dpp for elimination from its signaling capacity.

I also describe a novel role for the O-GlcNAc transferase, Sxc, in Dpp signal antagonism. Loss of Sxc results in ectopic Dpp signaling phenotypes dependent on the Type I BMP receptor Sax, but not the canonical Type I Dpp receptor, Tkv. This demonstrates that Sax is capable of transducing a Dpp signal in the embryonic epidermis, but its ability to do so is limited by Sxc-mediated glycosylation of the Sax receptor. Furthermore, I demonstrate that Dpp signaling is responsive to dietary sugar and hypothesize that Sax represents a nutrient sensitive arm of the Dpp signaling pathway to modulate Dpp signal capacity in response to glucose availability. Activating mutations in the human homolog of Sax, *ALK2/5*, result in a progressive ossification of soft tissue disorder known as Fibrodysplasia Ossificans Progressiva, or FOP (Petrie et al., 2009). The finding that O-GlcNAc can be used to inhibit Sax function may prove useful in developing therapeutics to combat FOP.

Lastly, I describe our discovery of that *sgct* plays an essential role in cell

hypertrophy during oogenesis and larval development. I have demonstrated that loss of *sgct* in vivo results in failure of developing fly larvae to grow in size and progress through their normal stages of development (i.e., failure to molt). Furthermore, specific loss of *sgct* in female ovaries results in infertility and severe growth defects of developing egg chambers. I have discovered that these phenotypes are due to the failure of cells to undergo hypertrophic growth, a process critical for egg chamber and larval growth. Given the predicted function of sgct as a glycosyltransferase required for mucin formation, our data suggest a role for mucins in hypertrophic growth of nonmitotic cells. I hypothesize that growth defects observed in patients with Peters' Plus Syndrome, which is caused by defects in the *B3GLCT* gene, the human homolog of *sgct*, could be explained by a failure in cells to grow by hypertrophy.

The discovery of these novel ways in which glycosylation regulates cell signaling, cell growth, and development have aided us in developing a broad understanding of the critical and diverse role of cellular glycans and allowed us to develop a *Drosophila* models of human disease.

References

Asano, M., Furukawa, K., Kido, M., Matsumoto, S., Umesaki, Y., Kochibe, N., and Iwakura, Y. (1997). Growth retardation and early death of beta-1,4-galactosyltransferase knockout mice with augmented proliferation and abnormal differentiation of epithelial cells. EMBO J *16*, 1850-1857.

Bastow, E.R., Byers, S., Golub, S.B., Clarkin, C.E., Pitsillides, A.A., and Fosang, A.J. (2008). Hyaluronan synthesis and degradation in cartilage and bone. Cell Mol Life Sci *65*, 395-413.

Cantagrel, V., Lefeber, D.J., Ng, B.G., Guan, Z., Silhavy, J.L., Bielas, S.L., Lehle, L., Hombauer, H., Adamowicz, M., Swiezewska, E*., et al.* (2010). SRD5A3 is required for converting polyprenol to dolichol and is mutated in a congenital glycosylation disorder. Cell *142*, 203-217.

Dickinson, M.E., Flenniken, A.M., Ji, X., Teboul, L., Wong, M.D., White, J.K., Meehan, T.F., Weninger, W.J., Westerberg, H., Adissu, H*., et al.* (2016). High-throughput discovery of novel developmental phenotypes. Nature *537*, 508-514.

Evrard, Y.A., Lun, Y., Aulehla, A., Gan, L., and Johnson, R.L. (1998). Lunatic fringe is an essential mediator of somite segmentation and patterning. Nature *394*, 377-381.

Freeze, H.H. (2006). Genetic defects in the human glycome. Nat Rev Genet *7*, 537-551.

Galeano, B., Klootwijk, R., Manoli, I., Sun, M., Ciccone, C., Darvish, D., Starost, M.F., Zerfas, P.M., Hoffmann, V.J., Hoogstraten-Miller, S.*, et al.* (2007). Mutation in the key enzyme of sialic acid biosynthesis causes severe glomerular proteinuria and is rescued by N-acetylmannosamine. J Clin Invest *117*, 1585-1594.

Ghosh, A., Urquhart, J., Daly, S., Ferguson, A., Scotcher, D., Morris, A.A.M., and Clayton-Smith, J. (2017). Phenotypic Heterogeneity in a congenital disorder of glycosylation caused by mutations in STT3A. J Child Neurol *32*, 560-565.

Haerry, T.E., Heslip, T.R., Marsh, J.L., and O'Connor, M.B. (1997). Defects in glucuronate biosynthesis disrupt Wingless signaling in Drosophila. Development *124*, 3055-3064.

Haines, N., and Irvine, K.D. (2003). Glycosylation regulates Notch signalling. Nat Rev Mol Cell Biol *4*, 786-797.

Haltiwanger, R.S. (2002). Regulation of signal transduction pathways in development by glycosylation. Curr Opin Struct Biol *12*, 593-598.

Haltiwanger, R.S., and Lowe, J.B. (2004). Role of glycosylation in development. Annu Rev Biochem *73*, 491-537.

Haltiwanger, R.S., and Stanley, P. (2002). Modulation of receptor signaling by glycosylation: fringe is an O-fucose-beta1,3-N-acetylglucosaminyltransferase. Biochim Biophys Acta *1573*, 328-335.

Hellbusch, C.C., Sperandio, M., Frommhold, D., Yakubenia, S., Wild, M.K., Popovici, D., Vestweber, D., Grone, H.J., von Figura, K., Lubke, T.*, et al.* (2007). Golgi GDP-fucose transporter-deficient mice mimic congenital disorder of glycosylation IIc/leukocyte adhesion deficiency II. J Biol Chem *282*, 10762-10772.

Hiraoka, S., Furuichi, T., Nishimura, G., Shibata, S., Yanagishita, M., Rimoin, D.L., Superti-Furga, A., Nikkels, P.G., Ogawa, M., Katsuyama, K.*, et al.* (2007). Nucleotide-sugar transporter SLC35D1 is critical to chondroitin sulfate synthesis in cartilage and skeletal development in mouse and human. Nat Med *13*, 1363-1367.

Humphreys, G.B., Jud, M.C., Monroe, K.M., Kimball, S.S., Higley, M., Shipley, D., Vrablik, M.C., Bates, K.L., and Letsou, A. (2013). Mummy, A UDP-N-acetylglucosamine pyrophosphorylase, modulates DPP signaling in the embryonic epidermis of Drosophila. Dev Biol *381*, 434-445.

Ishikawa, H.O., Higashi, S., Ayukawa, T., Sasamura, T., Kitagawa, M., Harigaya, K., Aoki, K., Ishida, N., Sanai, Y., and Matsuno, K. (2005). Notch deficiency implicated in the pathogenesis of congenital disorder of glycosylation IIc. Proc Natl Acad Sci U S A *102*, 18532-18537.

Jumbo-Lucioni, P., Parkinson, W., and Broadie, K. (2014). Overelaborated synaptic architecture and reduced synaptomatrix glycosylation in a Drosophila classic galactosemia disease model. Dis Model Mech *7*, 1365-1378.

Keller, P., Tremml, G., Rosti, V., and Bessler, M. (1999). X inactivation and somatic cell selection rescue female mice carrying a Piga-null mutation. Proc Natl Acad Sci U S A *96*, 7479-7483.

Kotani, N., Asano, M., Iwakura, Y., and Takasaki, S. (2001). Knockout of mouse beta 1,4-galactosyltransferase-1 gene results in a dramatic shift of outer chain moieties of N-glycans from type 2 to type 1 chains in hepatic membrane and plasma glycoproteins. Biochem J *357*, 827-834.

Lee, T.V., Pandey, A., and Jafar-Nejad, H. (2017). Xylosylation of the Notch receptor preserves the balance between its activation by trans-Delta and inhibition by cis-ligands in Drosophila. PLoS Genet *13*, e1006723.

Lee, T.V., Sethi, M.K., Leonardi, J., Rana, N.A., Buettner, F.F., Haltiwanger, R.S., Bakker, H., and Jafar-Nejad, H. (2013). Negative regulation of Notch signaling by xylose. PLoS Genet *9*, e1003547.

Lee, T.V., Takeuchi, H., and Jafar-Nejad, H. (2010). Regulation of Notch signaling via O-glucosylation insights from Drosophila studies. Methods Enzymol *480*, 375-398.

Li, M., Cheng, R., Liang, J., Yan, H., Zhang, H., Yang, L., Li, C., Jiao, Q., Lu, Z., He, J.*, et al.* (2013). Mutations in POFUT1, encoding protein O-fucosyltransferase 1, cause generalized Dowling-Degos disease. Am J Hum Genet *92*, 895-903.

Li, Y., Laue, K., Temtamy, S., Aglan, M., Kotan, L.D., Yigit, G., Canan, H., Pawlik, B., Nurnberg, G., Wakeling, E.L.*, et al.* (2010). Temtamy preaxial brachydactyly syndrome is caused by loss-of-function mutations in chondroitin synthase 1, a potential target of BMP signaling. Am J Hum Genet *87*, 757-767.

Lo, N.W., Shaper, J.H., Pevsner, J., and Shaper, N.L. (1998). The expanding beta 4-galactosyltransferase gene family: messages from the databanks. Glycobiology *8*, 517-526.

Maillette de Buy Wenniger-Prick, L.J., and Hennekam, R.C. (2002). The Peters' Plus Syndrome: a review. Ann Genet *45*, 97-103.

Malicdan, M.C., Noguchi, S., Nonaka, I., Hayashi, Y.K., and Nishino, I. (2007). A Gne knockout mouse expressing human GNE D176V mutation develops features similar to distal myopathy with rimmed vacuoles or hereditary inclusion body myopathy. Hum Mol Genet *16*, 2669-2682.

Marek, K.W., Vijay, I.K., and Marth, J.D. (1999). A recessive deletion in the GlcNAc-1-phosphotransferase gene results in peri-implantation embryonic lethality. Glycobiology *9*, 1263-1271.

Marquardt, T., and Denecke, J. (2003). Congenital disorders of glycosylation: review of their molecular bases, clinical presentations and specific therapies. Eur J Pediatr

162, 359-379.

Mizuguchi, S., Uyama, T., Kitagawa, H., Nomura, K.H., Dejima, K., Gengyo-Ando, K., Mitani, S., Sugahara, K., and Nomura, K. (2003). Chondroitin proteoglycans are involved in cell division of Caenorhabditis elegans. Nature *423*, 443-448.

Moremen, K.W., Tiemeyer, M., and Nairn, A.V. (2012). Vertebrate protein glycosylation: diversity, synthesis and function. Nat Rev Mol Cell Biol *13*, 448-462.

Moulton, M.J., and Letsou, A. (2016). Modeling congenital disease and inborn errors of development in Drosophila melanogaster. Dis Model Mech *9*, 253-269.

Nakamura, N., Stalnaker, S.H., Lyalin, D., Lavrova, O., Wells, L., and Panin, V.M. (2010). Drosophila Dystroglycan is a target of O-mannosyltransferase activity of two protein O-mannosyltransferases, Rotated Abdomen and Twisted. Glycobiology *20*, 381-394.

Niranjan, T.S., Skinner, C., May, M., Turner, T., Rose, R., Stevenson, R., Schwartz, C.E., and Wang, T. (2015). Affected kindred analysis of human X chromosome exomes to identify novel X-linked intellectual disability genes. PLoS One *10*, e0116454.

Pandey, A., and Mann, M. (2000). Proteomics to study genes and genomes. Nature *405*, 837-846.

Parkinson, W.M., Dookwah, M., Dear, M.L., Gatto, C.L., Aoki, K., Tiemeyer, M., and Broadie, K. (2016). Synaptic roles for phosphomannomutase type 2 in a new Drosophila congenital disorder of glycosylation disease model. Dis Model Mech *9*, 513-527.

Petrie, K.A., Lee, W.H., Bullock, A.N., Pointon, J.J., Smith, R., Russell, R.G., Brown, M.A., Wordsworth, B.P., and Triffitt, J.T. (2009). Novel mutations in ACVR1 result in atypical features in two fibrodysplasia ossificans progressiva patients. PLoS One 4, e5005.

Sakaidani, Y., Ichiyanagi, N., Saito, C., Nomura, T., Ito, M., Nishio, Y., Nadano, D., Matsuda, T., Furukawa, K., and Okajima, T. (2012). O-linked-N-acetylglucosamine modification of mammalian Notch receptors by an atypical O-GlcNAc transferase Eogt1. Biochem Biophys Res Commun *419*, 14-19.

Schneider, A., Thiel, C., Rindermann, J., DeRossi, C., Popovici, D., Hoffmann, G.F., Grone, H.J., and Korner, C. (2012). Successful prenatal mannose treatment for congenital disorder of glycosylation-Ia in mice. Nature Medicine *18*, 71-73.

Schwarz, K., Iolascon, A., Verissimo, F., Trede, N.S., Horsley, W., Chen, W., Paw, B.H., Hopfner, K.P., Holzmann, K., Russo, R*., et al.* (2009). Mutations affecting the secretory COPII coat component SEC23B cause congenital dyserythropoietic anemia type II. Nat Genet *41*, 936-940.

Schwarzkopf, M., Knobeloch, K.P., Rohde, E., Hinderlich, S., Wiechens, N., Lucka, L., Horak, I., Reutter, W., and Horstkorte, R. (2002). Sialylation is essential for early

development in mice. Proc Natl Acad Sci U S A *99*, 5267-5270.

Senderek, J., Muller, J.S., Dusl, M., Strom, T.M., Guergueltcheva, V., Diepolder, I., Laval, S.H., Maxwell, S., Cossins, J., Krause, S.*, et al.* (2011). Hexosamine biosynthetic pathway mutations cause neuromuscular transmission defect. Am J Hum Genet *88*, 162-172.

Shao, L., Luo, Y., Moloney, D.J., and Haltiwanger, R. (2002). O-glycosylation of EGF repeats: identification and initial characterization of a UDP-glucose: protein O-glucosyltransferase. Glycobiology *12*, 763-770.

Stanley, P. (2007). Regulation of Notch signaling by glycosylation. Curr Opin Struct Biol *17*, 530-535.

Stevens, E., Carss, K.J., Cirak, S., Foley, A.R., Torelli, S., Willer, T., Tambunan, D.E., Yau, S., Brodd, L., Sewry, C.A.*, et al.* (2013). Mutations in B3GALNT2 cause congenital muscular dystrophy and hypoglycosylation of alpha-dystroglycan. Am J Hum Genet *92*, 354-365.

Takamiya, K., Yamamoto, A., Furukawa, K., Yamashiro, S., Shin, M., Okada, M., Fukumoto, S., Haraguchi, M., Takeda, N., Fujimura, K.*, et al.* (1996). Mice with disrupted GM2/GD2 synthase gene lack complex gangliosides but exhibit only subtle defects in their nervous system. Proc Natl Acad Sci U S A *93*, 10662-10667.

Varki, A. (2017). Essentials of glycobiology, Third edition. (Cold Spring Harbor, New York: Cold Spring Harbor Laboratory Press).

Vincent, T., Molina, L., Espert, L., and Mechti, N. (2003). Hyaluronan, a major non-protein glycosaminoglycan component of the extracellular matrix in human bone marrow, mediates dexamethasone resistance in multiple myeloma. Br J Haematol *121*, 259-269.

Willer, T., Prados, B., Falcon-Perez, J.M., Renner-Muller, I., Przemeck, G.K., Lommel, M., Coloma, A., Valero, M.C., de Angelis, M.H., Tanner, W.*, et al.* (2004). Targeted disruption of the Walker-Warburg syndrome gene Pomt1 in mouse results in embryonic lethality. Proc Natl Acad Sci U S A *101*, 14126-14131.

Yakubenia, S., Frommhold, D., Scholch, D., Hellbusch, C.C., Korner, C., Petri, B., Jones, C., Ipe, U., Bixel, M.G., Krempien, R.*, et al.* (2008). Leukocyte trafficking in a mouse model for leukocyte adhesion deficiency II/congenital disorder of glycosylation IIc. Blood *112*, 1472-1481.

Yamashita, T., Hashiramoto, A., Haluzik, M., Mizukami, H., Beck, S., Norton, A., Kono, M., Tsuji, S., Daniotti, J.L., Werth, N.*, et al.* (2003). Enhanced insulin sensitivity in mice lacking ganglioside GM3. Proc Natl Acad Sci U S A *100*, 3445-3449.

Yan, D., and Lin, X. (2009). Shaping morphogen gradients by proteoglycans. Cold Spring Harb Perspect Biol *1*, a002493.

Yoshikawa, M., Go, S., Takasaki, K., Kakazu, Y., Ohashi, M., Nagafuku, M., Kabayama, K., Sekimoto, J., Suzuki, S., Takaiwa, K.*, et al.* (2009). Mice lacking ganglioside

GM3 synthase exhibit complete hearing loss due to selective degeneration of the organ of Corti. Proc Natl Acad Sci U S A *106*, 9483-9488.

Zhang, N., and Gridley, T. (1998). Defects in somite formation in lunatic fringe-deficient mice. Nature *394*, 374-377.

Zuchner, S., Dallman, J., Wen, R., Beecham, G., Naj, A., Farooq, A., Kohli, M.A., Whitehead, P.L., Hulme, W., Konidari, I.*, et al.* (2011). Whole-exome sequencing links a variant in DHDDS to retinitis pigmentosa. Am J Hum Genet *88*, 201-206.

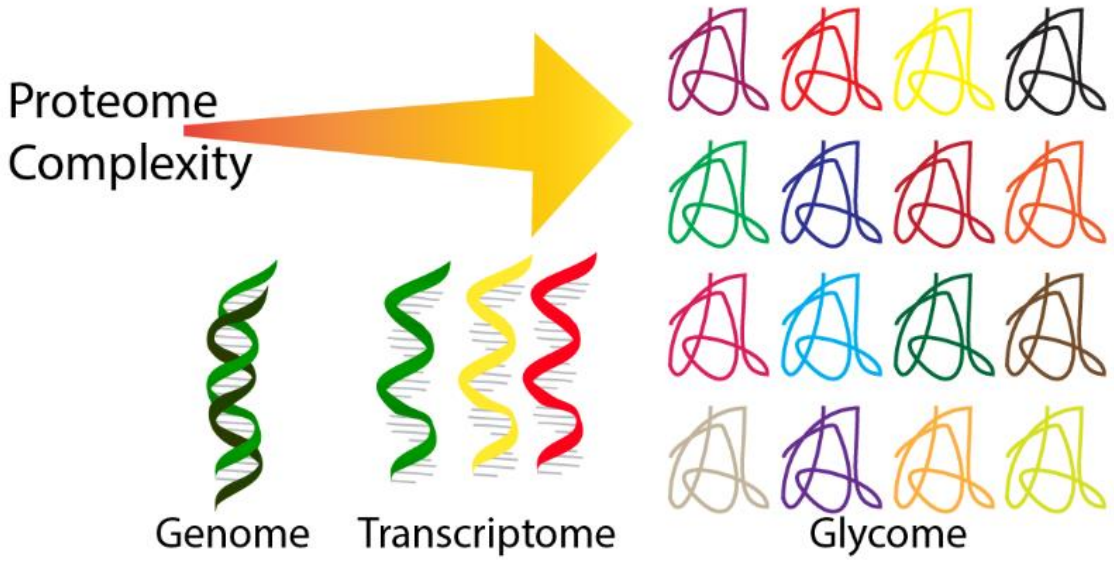

Fig. 1.1 Glycosylation confers great complexity on the proteome. Immense proteome complexity can be achieved by alternative splicing and post-translational modification of proteins. Glycosylation occurs in many varied ways providing a multiplicity of varieties of proteins in the glycome compared to the much smaller subset of proteins encoded by the genome alone.

Table 1.1 Models of human congenital disorders of glycosylation (as reported by OMIM)

Dis. Gene	Disease	MIM no.	Model	Refs
Disorders of N-glycosylation				
PMM2	CDG Type Ia	212065	Mouse	Schneider et al., 2012
MPI	CDG Type Ib	602579	None	
ALG6	CDG Type Ic	603147	None	
ALG3	CDG Type Id	601110	None	
ALG12	CDG Type Ig	607143	None	
ALG8	CDG Type Ih	608104	None	
ALG1	CDG Type Ik	608540	None	
ALG9	CDG Type Il	608776	None	
RFT1	CDG Type In	612015	None	
MGAT2	CDG Type IIa	212066	None	
DPAGT1	CDG Type Ij	608093	Mouse	Marek et al., 1999
ALG13	CDG Type Is	300884	None	
ALG2	CDG Type Ii	607906	Mouse	Dickinson et al., 2016
ALG11	CDG Type Ip	613661	None	
DDOST	CDG Type Ir	614507	Mouse	Dickinson et al., 2016
STT3A	CDG Type Iw	615596	None	
STT3B	CDG Type Ix	615597	None	
SSR4	CDG Type Iy	300934	None	
MOGS	CDG Type IIb	606056	Mouse	Dickinson et al., 2016

Table 1.1 cont.

Disorders of O-glycosylation

EXT1/EXT2	Exostoses Type I/II	133700	None	
B4GALT7	Ehlers-Danlos synd.	130070	None	
GALNT3	Tumoral calcinosis	211900	None	
SLC35D1	Schneckenbecken dysplasia	269250	Mouse	Hiraoka et al., 2007
B3GALTL	Peters' Plus synd.	261540	None	
LFNG	Spondylocostal Dysostosis 3	609813	Mouse	Zhan & Gridley, 1998 Evrard et al., 1998
POMT1	Musc. dystr., A1	236670	Mouse	Willer et al., 2004
	Musc. dystr., B1	613155	Mouse	Willer et al., 2004
	Musc. dystr., C1	609308	Mouse	Willer et al., 2004
POMT2	Musc. dystr., A2	613150	None	
	Musc. dystr., B2	613156	None	
	Musc. dystr., C2	613158	None	
POMGNT1	Musc. dystr., A3	253280	None	
	Musc. dystr., B3	613151	None	
	Musc. dystr., C3	613157	None	
EOGT	Adams-Oliver synd.	615297	Drosophila	Sakaidani et al., 2012
B3GALT6	Ehlers-Danlos synd.	615349	None	
CHSY1	Temtamy preaxial brachydactyly synd.	605282	C. elegans Zebrafish	Mizuguchi et al. 2003 Li et al., 2010
B3GALNT2	Musc. dystr. A11	615181	Zebrafish	Stevens et al., 2013
POFUT1	Dowling-Degos dis. 2	615327	Zebrafish	Li et al., 2013
POGLUT1	Musc. dystr. 2Z	617232	None	
	Dowling-Degos dis. 4	615696	None	

Disorders of glycosphingolipid and GPI-anchor glycosylation

ST3GAL5	Salt & pepper dev. regression synd.	609056	Mouse	Yamasita et al., 2003 Yosikawa et al., 2009

Table 1.1 cont.

Disorders of glycosphingolipid and GPI-anchor glycosylation				
PIGM	GPI deficiency	610293	None	
PIGN	Mult. cong. anomalies hypotonia-seizures syndrome 1	614080	None	
PIGV	Hyperphosphatasia mental retardation syndrome	239300	None	
PIGA	Mult. cong. anomalies hypotonia-seizures syndrome 2	300868	Mouse	Keller et al., 1999
PIGL	CHIME syndrome	280000	Mouse	Dickinson et al., 2016
B4GALNT1	Spastic paraplegia 26	609195	Mouse	Takamiya et al., 1996
Defects of multiple glycosylation and other pathways				
DPM1	CDG Type Ie	608799	Mouse	Dickinson et al., 2016
MPDU1	CDG Type If	609180	None	
SLC35C1	CDG Type IIc	266265	Drosophila Mouse	Ishikawa et al., 2005 Hellbusch et al., 2007 Yakubnia et al., 2008
DOLK	CDG Type Im	610768	None	
SRD5A3	CDG Type Iq	612379	Mouse	Cantagrel et al., 2010
COG1	CDG Type IIg	611209	None	
COG3	CDG Type IIq	617395	None	
COG4	CDG Type IIj	613489	None	
COG5	CDG Type Iii	613612	None	
COG6	CDG Type III	614576	None	
COG7	CDG Type IIe	608779	None	
COG8	CDG Type IIh	611182	None	
ATP6V0A2	Cutis laxa Type IIA	219200	None	

Table 1.1 cont.

Defects of multiple glycosylation and other pathways

SEC23B	Cowden syndrome 7	616858	Zebrafish	Schwarz et al., 2009
GFPT1	Myasthenia, cong.,12	610542	Zebrafish	Senderek et al., 2011
DPM2	CDG Type Iu	615042	Mouse	Dickinson et al., 2016
DPM3	CDG Type Io	612937	None	
B4GALT1	CDG Type IId	607091	Mouse Mouse Mouse	Lo et al., 1998 Asano et al., 1997 Kotani et al., 2001
GNE	Nonaka myopathy	605820	Mouse Mouse Mouse	Schwarzkopf et al., 2002 Galeano et al, 2007 Malicdan et al., 2007
SLC35A1	CDG Type IIf	603585	None	
SLC35A2	CDG Type IIm	300896	None	
SLC35A3	Arthrogryposis, mental retardation, and seizures	61553	None	
SRD5A3	CDG Type Iq	612379	Mouse	Cantagrel et al., 2010
DHDDS	Retinitis pigmentosa 59	613861	Zebrafish	Zuchner et al., 2011
TMEM165	CDG Type IIk	614727	None	
PGM1	CDG Type It	614921	None	
PGM3	Immunodeficiency 23	615816	None	

Abbreviations used:

Dis.: disease
CDG: congenital disorder of glycosylation
GPI: glycosylphosphatidylinositol
Cong.: congenital
Mult.: multiple
Dev.: development(al)
Synd.: syndrome
Musc. dystr.: Muscular dystrophy

CHAPTER 2

DPP SIGNALING IS MODULATED BY O-LINKED GLYCOSYLATION

Abstract

Embryogenesis in metazoans requires input from diverse signaling pathways to coordinate proper placement and organization of body structures, tissues, and organs. Activation and deactivation of signaling pathways at the right time and place are essential for embryogenesis, with defects in signaling often leading to congenital defects and disease. However, much remains to be understood about the regulation of interactions between ligands and their receptors. BMP/Dpp signaling regulators, acting on the pathway at all steps of signal transduction (extracellularly, at the membrane, in the cytoplasm, and in the nucleus) have been studied extensively. The Letsou lab has previously demonstrated that protein glycosylation, using UDP-*N*-acetylglucosamine (GlcNAc) as a substrate, regulates Dpp signaling in the *Drosophila* epidermis. With intact GlcNAc biosynthetic pathways, Dpp functions are tightly regulated. However, when GlcNAc production or utilization is disrupted, Dpp signaling range is extended with respect to both space and time. Here I describe the identification of the *super sex combs* (*sxc*)-encoded O-GlcNAc transferase in an RNAi screen for transferases functioning downstream of GlcNAc biosynthesis to regulate Dpp signaling. With intact O-GlcNAcylation (sxc^{+}), Dpp signals only in the most dorsal regions of the epidermis and in its absence (sxc^{-}), the signaling range expands. As expected for a modulator of the Dpp signal in *Drosophila*, I found that signaling in *sxc* mutants requires both Dpp and its

canonical type II receptor Punt. However, in an unexpected but revealing twist, I found that Dpp signals independently of its canonical type I receptor Tkv in *sxc* mutants. Signaling in this context depends instead on the type I receptor Sax, which is itself a target of O-GlcNAcylation. Taken together, this study demonstrates that both Tkv and Sax function as Dpp receptors and that despite their association with the same R-Smad, the Tkv and Sax responses to Dpp are substantively different, with spatial and temporal output properties distinguishing the two. This study also shows that *sxc* functions as a genetic on-off switch that modulates Dpp/Sax pathway output, with Sax being an O-GlcNAc modified target of Sxc. Moreover, I provide evidence that Dpp signaling is sensitive to dietary glucose and demonstrate that *sxc* embryonic phenotypes can be recapitulated by elimination of dietary sugar from parental diets. This study is the first to demonstrate a role for Sxc in embryogenesis to modulate Dpp.

Introduction

Coordinated cell movements and cell fate decisions during metazoan embryogenesis require diverse input from varied signaling pathways. Aberrations in these signaling cascades, both in terms of loss and gain of signaling, can result in congenital anomalies and termination of embryonic development. The Letsou lab seeks to understand how signaling in the *Drosophila* embryonic epidermis by Decapentaplegic (Dpp), one of the three fly bone morphogenic proteins (BMPs), is regulated to ensure proper development. Dpp, like other BMPs, is required for a host of biological processes including embryonic patterning and morphogenesis, and cell growth and proliferation (Derynck and Feng, 1997; Klinedinst and Bodmer, 2003; Muller et al., 2003; Xiao et al., 2007). Dpp signaling initiates as the Dpp ligand binds to a heteromeric receptor complex composed of type I and II receptors. The constitutively active type II receptor, Punt (Put), activates the type I receptor, Thickveins (Tkv), via phosphorylation and

initiates target gene expression changes via phosphorylation and activation of the Smad family transcription factor, Mothers against Dpp (Mad). Mutations that cause either too much or too little Dpp signaling lead to failures in Dpp-dependent processes, including dorsal closure (Byars et al., 1999; Humphreys et al., 2013; Muller et al., 2003; Xia and Karin, 2004; Xiao et al., 2007). Although it is thought that each BMP ligand in *Drosophila* has a unique and dedicated receptor complex, in vertebrates the number of BMP ligands exceeds the number of receptors complexes that could be formed to confer dedication of one complex for each ligand (Herpin and Cunningham, 2007). It is, therefore, of great importance to understand the complex regulation required to restrict BMP signaling through proper ligand/receptor interactions.

The Letsou lab uses the *Drosophila* process of dorsal closure (DC) as an experimental platform to study BMP/Dpp signaling. Dpp loss midway in embryogenesis (8-12 hrs. AEL) results in a well-characterized and easily identified DC defect (Byars et al., 1999; Humphreys et al., 2013; Scuderi and Letsou, 2005; VanHook and Letsou, 2008). At the molecular level, DC initiates with Jun-N-terminal kinase (JNK)-dependent *dpp* expression in the dorsal-most row of cells in the lateral epidermal sheet, termed the leading edge (LE) (Hou et al., 1997; Riesgo-Escovar and Hafen, 1997). Precise control of Dpp signaling is vital for all processes, and DC is not an exception to this rule; both loss- and gain-of-function Dpp signaling mutants disrupt the process, with each producing a distinctive embryonic phenotype (Humphreys et al., 2013). Loss of function of Dpp antagonists results in ectopic Dpp signaling and a distinguishing cuticle phenotype, characterized by hypotrophy of ventral denticle belts and puckering of the dorsal midline. The Letsou lab and others have used this signature loss-of-function cuticle phenotype to identify mutants with hyperactive Dpp signaling (*raw*, *ribbon* [*rib*], *puckered* [*puc*], and *mummy* [*mmy*]). *raw*, *rib* and *puc* all mediate their effects on Dpp signaling via modulation of JNK signaling, which is required to initiate *dpp* expression in

the epidermis, whereas *mmy* functions to antagonize the Dpp signaling pathway directly (Humphreys et al., 2013). Loss of *mummy* (*mmy*), which encodes an enzyme required for the production of UDP-*N*-acetylglucosamine (GlcNAc), leads to ectopic Dpp signaling in the epidermis (Araujo et al., 2005; Humphreys et al., 2013).

GlcNAc is utilized by glycosyltransferase to perform a wide variety of cellular functions including post-translational modification of proteins through N- and O-linked attachments and to synthesize glycosyl-phosphatidylinositol, chondroitin sulfate, and heparin sulfate molecules (Tonning et al., 2006). We targeted each of the GlcNAc transferases in the *Drosophila* genome by targeted RNAi in order to identify how GlcNAc is utilized to antagonize Dpp signaling. From this screen, we found that embryos expressing RNAi targeting *super sex combs* (*sxc*) share a loss-of-function patterning defect with *mmy* mutants (Sinclair et al., 2009). Although no embryonic phenotypes associated with loss of *sxc* have been reported, results from our RNAi screen suggest that there is a previously unappreciated role for *sxc* in embryonic development.

In *Drosophila*, there is a single OGT, *sxc*, and mutations of *sxc* were identified originally based on the presence of ectopic sex combs present on 2nd and sometimes 3rd leg pairs of deceased pharate adult male flies (Ingham, 1983; Sinclair et al., 2009). Sxc, like mammalian O-GlcNAc transferases (OGTs), is an enzyme that carries out O-linked glycosylation of serine/threonine residues of intracellular proteins. In contrast with the complex and oftentimes branched sugar chains found on proteins that have been N-glycosylated while transitioning through the Golgi or ER, O-GlcNAcylation occurs as a reversible addition of a single GlcNAc residue to a protein. Complete loss of *OGT* in mice is embryonic lethal (O'Donnell, et al., 2004), but no embryonic phenotypes associated with complete loss of *sxc* have been reported. Rather hypomorphic mutations in human *OGT* result in X-linked intellectual disability (Willems et al., 2017).

Here I report my characterization of the molecular underpinnings of how O-linked

glycosyl modifications carried out by Sxc antagonize Dpp signaling in the *Drosophila* embryonic epidermis. I demonstrate that loss of *sxc* results in partial embryonic lethality along with cuticle defects indicative of ectopic Dpp signaling. I report that Dpp signaling is ectopically activated in *sxc* embryos through the type I BMP receptor Saxophone (Sax), and that Sxc normally functions to repress Sax-mediated Dpp signaling activity via glycosylation. I also demonstrate that Dpp signaling is responsive to dietary glucose by altering O-GlcNAcylation of Sax by Sxc.

Results

sxc *functions downstream of mummy as a Dpp signaling antagonist*

The Letsou lab identified the *super sex combs* (*sxc*)-encoded O-GlcNAc transferase (OGT) in an RNAi screen for transferases functioning downstream of *mmy* and UDP-GlcNAc in regulating Dpp signaling. Targeted elimination of *sxc* via Tubulin:Gal4>UAS:sxc^{RNAi} during embryogenesis resulted in embryonic lethality and patterning defects similar to *mmy* mutant embryos (Fig. 2.1 A-C, Humphreys et al., 2013) and completely eliminated detectable zygotic transcripts (Fig. 2.2 A-F). In an extension of RNAi studies, I assessed embryonic lethality in animals homozygous for publically available and independently derived *sxc* alleles, ranging in strength from hypomorphic to null (Fig. 2.1 F). For all alleles, I observed an incompletely penetrant embryonic lethality in homozygotes ranging from 19% to 35%, with the highest measures of lethality observed in animals harboring the amorphic alleles (sxc^{1} and sxc^{6}, Fig. 2.1G). Analysis of cuticle from inviable mutant embryos confirmed RNAi studies and revealed an invariably expressed loss-of-function cuticle phenotype shared with *mmy* mutants and suggestive of hyperactive Dpp signaling, namely a dorsal pucker and hypotrophy of ventral denticle belts (Fig. 2.1D). The observed phenotype was not worsened when the null allele sxc^{1} was put in trans to a deficiency uncovering *sxc,*

demonstrating that *sxc*^{1} is indeed a null (Fig. 2.1E).

Given that *sxc*-dependent lethality is incompletely penetrant, I tested whether maternally derived sxc might be providing some function to rescue the embryonic lethality and cuticle defects I observed. Consistent with this idea I demonstrated that *sxc* is maternally deposited and ubiquitously expressed at least through dorsal closure stages of embryogenesis (Fig. 2.2 A-C). To test maternal function genetically, I generated animals with either maternal or maternal zygotic loss of *sxc* by expressing RNAi targeting *sxc* using the UAS-Gal4 system to drive RNAi during oogenesis and during embryogenesis. Loss of maternal *sxc* had no effect on embryonic viability compared to wild-type and no obvious cuticle phenotype (Fig. 2.2 J, L). In contrast, depletion of maternal RNA in a *sxc*^{1} mutant background resulted in 31% embryonic lethality and cuticle defects indistinguishable from those observed in *sxc*^{1} mutants alone. (Fig. 2.2 K-L). Thus, loss of zygotically-derived *sxc* is sufficient to explain all embryonic lethality observed.

Although I observed no difference in *dpp* expression in *sxc* from wild-type embryos (Fig. 2.3 A, C, E), I examined Dpp activation in the epidermis of dorsal closure stage *Drosophila* embryos via immunohistochemistry using an antibody directed against the phosphorylated form of Mad (pMad). We have previously demonstrated that Dpp signaling is activated transiently in the dorso-lateral epidermis of wild-type embryos 3-5 cells from the LE and that this activation quickly wanes as dorsal closure proceeds (Humphreys et al., 2013; Fig. 2.3B). In *sxc*^{1} embryos, however, I detected pMad 8-12 cells from the LE and observed its persistence throughout dorsal closure. This signaling defect is expanded to the same extent we previously documented in *mmy*^{1} (Humphreys *et al.*, 2010; see also Fig. 2.3 D-G).

Mechanism of sxc*-mediated antagonism of Dpp signaling*

Ectopic epidermal Dpp signaling results either from ectopic activation of the JNK signaling pathway, as in *raw* (Byars et al., 1999; Humphreys et al., 2013), or from ectopic activation of the Dpp signaling pathway, as with *mmy* (Humphreys et al., 2013). Thus, I next tested whether Sxc acts as an antagonist of the JNK or Dpp signaling pathway. To this end, I performed an immunohistochemistry analysis of Jun localization in wild-type, Jra^{AI109}, and sxc^{1} mutant embryos in situ using an antibody directed against Jun (Fig. 2.4A-C,). Normally, Jun accumulates in LE cells (Fig. 2.4A Humphreys et al., 2013) and I observed its proper accumulation in *sxc* mutants (Fig. 2.4B), whereas it was absent in Jra^{IA109} embryos (Fig. 2.4C). Next, I tested whether the amount of total Jun protein was altered in *sxc* mutants in a quantitative analysis of Jun protein. Western blot analysis revealed no significant difference in Jun protein levels in *sxc* mutants compared to wild-type (Fig. 2.4D). Finally, I used the JNK reporter line, dpp^{151H}, to test for altered JNK activity. This reporter line is expressed in the LE of wild-type embryos but is expressed beyond the LE in mutants of JNK antagonists (Johnson et al., 2003). I observed no difference in the reporter expression in *sxc* from wild-type embryos (Fig. 2.4E). Taken together, these data indicate that JNK signaling is unaffected in the *sxc* mutant background. Thus, ectopic JNK is not responsible for ectopic Dpp, and Sxc functions to modulate the Dpp pathway directly.

In an initial exploration of this idea, I tested whether ectopic Dpp signaling is dependent upon LE Dpp. I used the Jra^{IA109} mutant to specifically remove LE Dpp (Humphreys et al., 2013), and then I tested whether Dpp signaling is ectopically activated in $sxc^{1}Jra^{IA109}$ double mutants. I observed no Dpp signaling in the epidermis of this $sxc^{1}Jra^{IA109}$ double mutants, thereby demonstrating that the Dpp signaling pathway antagonized by Sxc is dependent on/triggered by LE *dpp* (Fig. 2.4 F-G).

sxc *genetically interacts with saxophone*

Having established that: 1) pMAD persists broadly in the epidermis of dorsal closure stage *sxc* embryos, and 2) ectopic Dpp signaling is dependent on LE *dpp* expression (see Figs. 2.4 F-G), I next considered the necessity of the canonical transcription factor/receptor complex components in Sxc-dependent Dpp signaling. Punt (Put), Thickveins (Tkv), and Mothers Against Dpp (Mad) are thought to be obligate transducers of the epidermal Dpp signal and as such loss of any one of these leads to a fully penetrant embryonic lethality along with characteristic defects in dorsal closure (Figs. 2.5 A, C, E. Loss of both *mad* and *sxc* in *sxc mad* double mutants leads to no change in phenotype (Fig. 2.5 A-B). Similarly, loss of both *put* and *sxc* in a *put sxc* double mutant leads to no change in phenotype in comparison to *put* alone (Fig. 2.5 C-D). Both double mutant genotypes produce a dorsal-open Dpp signaling-deficient phenotype, indicating that Dpp signal transduction in *sxc* mutants requires the canonical type II receptor Put and the transcription factor Mad. Conversely, and somewhat to our surprise, I found that dysregulated Dpp signaling phenotype persists in the *tkv sxc* double mutant (Fig. 2.5 F) and ectopic Dpp signaling is observed in this background beyond the normal domain (Fig. 2.5 F', compare wild-type in Fig. 2.4G). Moreover, in contrast to the incomplete penetrance that I observe in *sxc* single mutants (~40%), Dpp hyperactivity is a fully penetrant phenotype in *tkv sxc* double mutants (>98%). Taken together, these data indicate that: 1) there is a type I receptor that transduces the Dpp signal via phosphorylation of Mad independently of Tkv, and 2) this type I receptor activity is regulated by Sxc (OGT).

In addition to Tkv, there are two other BMP type I receptors in *Drosophila: saxophone* (*sax*) and *baboon* (*babo*). One of these, Saxophone (Sax), is expressed broadly throughout embryogenesis (FlyBase, 2003), although to date its only recognized role is to augment Dpp/Tkv signaling in dorsoventral axis determination in early

embryos via activation by the BMP ligand, Screw (Scw) (Nguyen et al., 1998). I employed double mutants to test the requirement for *sax* in *sxc*-dependent dpp signaling. Loss of *sax* (Fig. 2.5 G-H) in a *sxc* mutant background rescues the *sxc* phenotype, restoring both normal cuticle pattern and pMad profiles to *sax sxc* embryos (Fig. 2.5 H'), presumably because the Dpp signal is now funneled exclusively through Tkv. Moreover, I tested this idea using a triple mutant of *sax*, *tkv*, and *sxc* and found that all Dpp signaling in the embryonic epidermis has been eliminated in this background. Specifically, *tkv sax sxc* triple mutant embryos secrete a dorsal-open cuticle indistinguishable from that of *tkv* and diagnostic of Dpp signaling loss (Fig. 2.5 I-J).

While Sax is expressed in the embryonic epidermis during dorsal closure stage embryos, the ligands thought capable of activating Sax, Gbb and Scw are not expressed during these stages, nor is *scw/gbb* expression altered in *sxc* (Fig. 2.6 A, B, E, F; FlyBase, 2003b). Loss of *scw* results in a weak ventralized embryonic phenotype, while loss of *gbb* results in a weak dorsal closure defect. Loss of *sxc* in either the *scw* or *gbb* backgrounds resulted in ectopic Dpp signaling phenotypes (Fig. 2.6 C-D, G-H, K-L) demonstrating independence from *scw* and *gbb* in the *sxc* ectopic signaling phenotype.

Sxc *antagonizes Saxophone function via O-linked glycosylation*

Serine/threonine kinases and OGT both function to modify serine/threonine residues within proteins. Although a single protein could act as a substrate for both phosphorylation and O-GlcNAcylation, these post-translational modifications are mutually exclusive at any given serine or threonine residue. Our genetic data suggest that Sax receptor activity, but not that of Tkv, is regulated by O-GlcNAc and thus I tested whether Sax is different from Tkv in its modification by Sxc via O-GlcNAcylation. Lysates were prepared from wild-type embryos and transgenic embryos containing

either UAS:Sax-Flag or UAS:Tkv-GFP which was expressed ubiquitously via a tubulin:Gal4 driver. Sax and Tkv were immunoprecipitated from lysates with anti-Flag and anti-GFP antibodies. I used an antibody specific for O-GlcNAc modifications to detect the presence of O-GlcNAc on immunopurified Sax or Tkv lysates. I observed the presence of a band in the immunoprecipitated fraction in embryos expressing Sax-Flag, but not in that from *sxc*^{RNAi} embryos expressing Sax-Flag or embryos expressing Tkv-GFP alone (Fig. 2.7 A) thus demonstrating that Sax is O-glycosylated by Sxc in embryos. In the Western blotting experiments, I confirmed expression of Sax-Flag and Tkv-GFP using anti-Flag and anti-GFP antibodies, respectively, and demonstrated that these proteins are expressed at detectable levels (Fig. 2.7A).

Dpp signaling is sensitive to glucose availability

In mammalian cells, addition of excess sugar to media culture induces an increase in O-glycosylated proteins (Bond and Hanover, 2015; Schwartz and Pirrotta, 2009). Additionally, excessive O-glycosylation has been observed in diabetic patients (Konrad and Kudlow, 2002; Majumdar et al., 2004). These data have led researchers to speculate that OGT can function as a nutrient sensor for the cell in that increased glucose uptake by the cell leads to a greater production of GlcNAc, the sugar substrate used by OGT (Zachara and Hart, 2004a, b). Our observation that O-GlcNAc suppresses Sax-mediated transduction of Dpp evokes the expectation that nutrient poor conditions will activate Sax-mediated transduction of Dpp. I tested whether Sxc acts as a nutrient sensitive regulator of Dpp signaling by depriving parent flies of all dietary sugar and analyzed lethality and cuticle defects in embryos derived from these adults. I observed ~40% lethality in embryos derived from parents fed no sugar (Fig. 2.7 B). Analysis of cuticles from inviable embryos revealed the signature defects of ectopic Dpp signaling (Fig. 2.7 D; Bayrs et al., 1999). I observed no change in lethality frequency or cuticle

pattern in *sxc* embryos derived from parents on the no sugar diet compared to those raised on standard lab food (Fig. 2.7 B, E; compare to Fig 2.1 E). Taken together, these data demonstrate that embryonic Dpp signaling is sensitive to maternal sugar intake, and that Sxc is the sugar sensor.

Discussion

Here, I have demonstrated a novel role for *sxc* in embryonic development and Dpp signal antagonism (Fig. 2.8 A-B). While *sxc* is expressed in the embryo, its role in embryogenesis has been unexplored to date. This may be due to the incomplete penetrance of embryonic lethality observed in *sxc* homozygotes, but our study has demonstrated that embryonic lethality in *sxc* is fully penetrant when in combination with loss of Tkv. I have demonstrated that embryonic lethality in *sxc* and *sxc Tkv* backgrounds is due to ectopic Dpp signaling through the Type I BMP receptor Sax. I demonstrated that signaling occurs through Sax and that loss of *sax* in either background ablates any gain of Dpp signaling phenotypes observed. Therefore, I conclude that Sxc functions to control the signaling receptor complexes used to transduce Dpp signaling in the *Drosophila* epidermis during DC; specifically, Sxc functions to repress Dpp signaling occurring through Sax under standard lab conditions. However, these data fail to fully explain why Dpp signaling through Sax leads to lethality in only ~40% of embryos. I propose that there must be some difference in the ability of Dpp to signal through Put/Tkv complexes versus Put/Sax complexes. This may be due to an increased affinity of Dpp for Tkv versus Sax or differences in expression levels of Sax such that it is not as abundant as Tkv in the epidermis and these questions warrant further exploration. Alternatively, Sxc-mediated glycosylation of Sax could prevent the Put/Sax complex from ever forming. If this complex were to form and bind Dpp, it could act as a sink for Dpp and we would predict that loss of Sax would increase the pool of

Dpp available for signaling to Tkv. However, given that loss of *sax* results in no embryonic lethality or cuticle defect, I favor the idea that O-glycosylation of Sax prevents a Put/Sax complex from ever forming.

Our data also beg the question as to why Dpp could signal through a receptor complex composed of Sax if activation through Sax is detrimental. I demonstrated that sugar deprivation in adults led to ~40% embryonic lethality with cuticle defects resembling ectopic Dpp signaling phenotypes. Therefore, I conclude that Dpp signaling normally occurs through a Put/Tkv receptor complex, but can respond to nutrient input and adjust signaling output accordingly by modifying Sax (or not) by O-GlcNAcylation, thus modulating Sax activity function. While it is not surprising that nutrition plays a critical role in proper embryonic development, this is the first time, to our knowledge, that anyone has demonstrated a role for sugar in Dpp signaling. It remains to be seen whether this role for sugar is generalizable for all contexts in which Dpp signaling occurs or whether this is specific to the epidermis at this time during development. I argue that O-GlcNAcylation of Sax be explored further in the epidermis and elsewhere.

Using an in silico approach (Gupta and Brunak, 2002), I identified potential sites of O-linked glycosylation that sometimes overlap with predicted sites of phosphorylation in Tkv, Sax, and their mammalian homologs (Fig. 2.8 C). Some of the sites are conserved between all Type I receptors while others were unique to the Sax or Tkv receptors. I predict that some or all of these sites could represent key residues of Sxc-mediated glycosylation and therefore deactivation of Sax function, although this remains to be tested.

Drosophila *sxc* mutants provide a platform on which to understand loss of OGT in human development and disease contexts. Additionally, this study has shed light into the strict requirement for repression of Sax during embryogenesis. Activating mutations of the human Sax homologue of, *ACVR1* (Alk2), lead to ectopic BMP signaling and give

rise to Fibrodysplasia Ossificans Progressiva (FOP; OMIM ID#135100), a devastating condition associated with ossification of soft tissue. FOP is inherited in an autosomal dominant fashion and, while symptoms at birth are absent, ossification occurs progressively throughout life often with most patients being confined to a wheelchair by their third decade (Petrie et al., 2009). The mutation responsible for most cases maps to an R206H amino acid substitution. This mutation has been demonstrated in cell culture to lead to increased and continuous ACVR1 phosphorylation in the absence of ligand and a failure to internalize and degrade the ACVR1 protein (de la Penna et al., 2005). In both humans and *Drosophila* tight regulation of ACVR1/Sax activity is required to maintain proper levels of signaling. In the case of *Drosophila*, this regulation is achieved by O-glycosylation. Modification of ACVR1 by O-GlcNAcylation at any site has never been reported to date. However, our data suggest that ACVR1 may be a target of O-GlcNAcylation in human cells as it is in *Drosophila* and, therefore, should be examined in detail.

Our use of genetic and biochemical approaches in the *Drosophila* embryo have led to the discovery of a novel mechanism of BMP signal antagonism by O-GlcNAc. As the identification of O-GlcNAcylated proteins has progressed, it is becoming clearer that O-GlcNAc is an abundant modification with tremendous implication on protein function and cell signaling. Moreover, I have developed a genetically tractable system in which I can readily assess Sax activity and serve as a model for BMP signaling diseases, such as FOP.

Methods

Fly strains

The Oregon R strain served as the wild-type in all experiments. *mmy*^{1}, *raw*^{lG}, and *Jra*^{lA109} stocks were used as described (Humphreys et al., 2013). The Tubulin:Gal4

stock was a gift of Mark Metzstein, and *sxc* stocks were a gift of John Hanover. Stocks of sax^{5}, *Df*(*sxc*), *Df*(*Mad*), scw^{5}, gbb^{D4}, $babo^{32}$, and the maternal-driving Gal4 were obtained from the BDSC (stock numbers 8785, 740, 9713, 7306, 63053, 5399, and 31777, respectively) and described previously (FlyBase, 2003, version FB2017_01, released February 14, 2017). *sxc* RNAi strain was obtained from the VDRC (stock number 18611) (Dietzl et al., 2007). The dpp^{151H} (Johnson et al., 2003), Tkv^{5} (Terracol and Lengyel, 1994), and put^{88} (Simin et al., 1998) stocks were as described previously. UAS:Sax-Flag line was a generous gift of Kristi Wharton, UAS:Tkv-GFP line was a generous gift Tom Kornberg.

Phenotypic analysis

Cuticle analysis was performed by dark field microscopy after embryos were incubated in one-step mounting media at 37°C for 18 hrs. Lethal stage analyses were performed by plating embryos on grape juice agar plate and recording observed proportion of dead embryos after 48 hrs. RNA in situ hybridization and immunohistochemistry staining procedures were all described previously (Humphreys et al., 2013). In brief, rabbit anti-phospho-Smad1,5 Ser463/465 (1:20, Cell Signaling Technology) antibody or digoxigenin-labeled anti-sense RNA probes were incubated overnight on fixed embryo clutches. After several washes, secondary antibodies targeting pMad, goat anti-rabbit alkaline phosphatase (Jackson ImmunoResearch) or goat anti-rabbit Alexa Fluor 488 (Invitrogen Molecular Probes), or digoxigenin-labeled RNA probes, mouse anti-digoxigenin alkaline phosphatase Fab fragments (Roche), were incubated with the embryos overnight. The following day, alkaline phosphatase detection was performed using nitro blue tetrazolium chloride and 5-Bromo-4-chloro-3-indolyl phosphate followed by dehydration in methanol and overnight incubation in 80% glycerol.

Protein studies

Western blot studies and pMad quantification analyses were performed as described previously (Humphreys et al., 2013). In brief, protein lysates were loaded onto a 12% Acryl-Bis polyacrylamide gel and subjected to electrophoresis at 100v for 3 hrs. The gel was transferred to a PVDF membrane (Millipore) and blocked using 5% milk or 5% BSA in TBS + 0.05% Tween for 2 hrs. Primary antibodies were used at 1:200 (anti-Jun) or 1:1,000 concentration (anti-O-GlcNAc [RL2] from Abcam and anti-Flag [M2] from Sigma-Aldrich). HRP-conjugated goat-anti-mouse IgG secondary was used at 1:100,000 for anti-O-GlcNAc and 1:15,000 for anti-Flag as well as HRP-conjugated goat anti-rabbit secondary at 1:5,000 for anti-Jun. Blot detection was performed by mixing equal volumes of ECL Luminol solutions A and B (Santa Cruz) and developed on a Mini-Medical Series machine (AFP Imaging).

Immunoprecipitation assays were performed on embryonic lysates isolated using nondenaturing lysis buffer. Three µg of anti-Flag or anti-GFP antibody was incubated with the lysates for 90 mins. followed by a 60-min. incubation with protein-G sepharose beads (Santa Cruz). Beads were pelleted by centrifugation at 8,000 x G for 7 mins. Supernatant was collected and pelleted beads were subsequently washed in 500 µl lysis buffer 3 times. 2X Laemelli Sample Buffer was added to pellet and supernatant fractions and subsequently used in Western blot studies using the aforementioned protocol.

References

Araujo, S.J., Aslam, H., Tear, G., and Casanova, J. (2005). mummy/cystic encodes an enzyme required for chitin and glycan synthesis, involved in trachea, embryonic cuticle and CNS development--analysis of its role in Drosophila tracheal morphogenesis. Dev Biol *288*, 179-193.

Bond, M.R., and Hanover, J.A. (2015). A little sugar goes a long way: the cell biology of O-GlcNAc. J Cell Biol *208*, 869-880.

Byars, C.L., Bates, K.L., and Letsou, A. (1999). The dorsal-open group gene raw is

required for restricted DJNK signaling during closure. Development *126*, 4913-4923.

de la Pena, L.S., Billings, P.C., Fiori, J.L., Ahn, J., Kaplan, F.S., and Shore, E.M. (2005). Fibrodysplasia ossificans progressiva (FOP), a disorder of ectopic osteogenesis, misregulates cell surface expression and trafficking of BMPRIA. J Bone Miner Res 20, 1168-1176.

Derynck, R., and Feng, X.H. (1997). TGF-beta receptor signaling. Biochim Biophys Acta *1333*, F105-150.

Dietzl, G., Chen, D., Schnorrer, F., Su, K.C., Barinova, Y., Fellner, M., Gasser, B., Kinsey, K., Oppel, S., Scheiblauer, S*., et al.* (2007). A genome-wide transgenic RNAi library for conditional gene inactivation in Drosophila. Nature *448*, 151-156.

FlyBase (2003). The Flybase database of the Drosophila genome projects and community literature. Nuc Acid Res *31*, 172-175.

Gupta, R., and Brunak, S. (2002). Prediction of glycosylation across the human proteome and the correlation to protein function. Pac Symp Biocomput, 310-322.

Herpin, A., and Cunningham, C. (2007). Cross-talk between the bone morphogenetic protein pathway and other major signaling pathways results in tightly regulated cell-specific outcomes. FEBS J 274, 2977-2985.

Hou, X.S., Goldstein, E.S., and Perrimon, N. (1997). Drosophila Jun relays the Jun amino-terminal kinase signal transduction pathway to the Decapentaplegic signal transduction pathway in regulating epithelial cell sheet movement. Genes Dev *11*, 1728-1737.

Humphreys, G.B., Jud, M.C., Monroe, K.M., Kimball, S.S., Higley, M., Shipley, D., Vrablik, M.C., Bates, K.L., and Letsou, A. (2013). Mummy, A UDP-N-acetylglucosamine pyrophosphorylase, modulates DPP signaling in the embryonic epidermis of Drosophila. Dev Biol *381*, 434-445.

Ingham, P.W. (1983). Differential expression of bithorax complex genes in the absence of the extra sex combs and trithorax genes. Nature *306*, 591-593.

Johnson, A.N., Bergman, C.M., Kreitman, M., and Newfeld, S.J. (2003). Embryonic enhancers in the dpp disk region regulate a second round of Dpp signaling from the dorsal ectoderm to the mesoderm that represses Zfh-1 expression in a subset of pericardial cells. Dev Biol *262*, 137-151.

Klinedinst, S.L., and Bodmer, R. (2003). Gata factor Pannier is required to establish competence for heart progenitor formation. Development *130*, 3027-3038.

Konrad, R.J., and Kudlow, J.E. (2002). The role of O-linked protein glycosylation in beta-cell dysfunction. Int J Mol Med *10*, 535-539.

Majumdar, G., Wright, J., Markowitz, P., Martinez-Hernandez, A., Raghow, R., and Solomon, S.S. (2004). Insulin stimulates and diabetes inhibits O-linked N-acetylglucosamine transferase and O-glycosylation of Sp1. Diabetes *53*, 3184-

3192.

Muller, B., Hartmann, B., Pyrowolakis, G., Affolter, M., and Basler, K. (2003). Conversion of an extracellular Dpp/BMP morphogen gradient into an inverse transcriptional gradient. Cell *113*, 221-233.

Nguyen, M., Park, S., Marques, G., and Arora, K. (1998). Interpretation of a BMP activity gradient in Drosophila embryos depends on synergistic signaling by two type I receptors, SAX and TKV. Cell *95*, 495-506.

O'Donnell, N., Zachara, N.E., Hart, G.W., Marth, J.D. (2004). *Ogt*-dependent X-chromosome-linked protein glycosylation Is a requisite modification in somatic cell function and embryo viability. Mol. Cell Biol. *24*, 1680-1690.

Petrie, K.A., Lee, W.H., Bullock, A.N., Pointon, J.J., Smith, R., Russell, R.G., Brown, M.A., Wordsworth, B.P., and Triffitt, J.T. (2009). Novel mutations in ACVR1 result in atypical features in two fibrodysplasia ossificans progressiva patients. PLoS One 4, e5005.

Riesgo-Escovar, J.R., and Hafen, E. (1997). Drosophila Jun kinase regulates expression of decapentaplegic via the ETS-domain protein Aop and the AP-1 transcription factor DJun during dorsal closure. Genes Dev *11*, 1717-1727.

Schwartz, Y.B., and Pirrotta, V. (2009). A little bit of sugar makes polycomb better. J Mol Cell Biol *1*, 11-12.

Scuderi, A., and Letsou, A. (2005). Amnioserosa is required for dorsal closure in Drosophila. Dev Dyn *232*, 791-800.

Simin, K., Bates, E.A., Horner, M.A., and Letsou, A. (1998). Genetic analysis of punt, a type II Dpp receptor that functions throughout the Drosophila melanogaster life cycle. Genetics *148*, 801-813.

Sinclair, D.A., Syrzycka, M., Macauley, M.S., Rastgardani, T., Komljenovic, I., Vocadlo, D.J., Brock, H.W., and Honda, B.M. (2009). Drosophila O-GlcNAc transferase (OGT) is encoded by the Polycomb group (PcG) gene, super sex combs (sxc). Proc Natl Acad Sci U S A *106*, 13427-13432.

Terracol, R., and Lengyel, J.A. (1994). The thick veins gene of Drosophila is required for dorsoventral polarity of the embryo. Genetics *138*, 165-178.

Tonning, A., Helms, S., Schwarz, H., Uv, A.E., and Moussian, B. (2006). Hormonal regulation of mummy is needed for apical extracellular matrix formation and epithelial morphogenesis in Drosophila. Development *133*, 331-341.

VanHook, A., and Letsou, A. (2008). Head involution in Drosophila: genetic and morphogenetic connections to dorsal closure. Dev Dyn *237*, 28-38.

Willems, A.P., Gundogdu, M., Kempers, M.J.E., Giltay, J.C., Pfundt, R., Elferink, M., Loza, B.F., Fuijkschot, J., Ferenbach, A.T., van Gassen, K.L.I., van Aalten, D.M.F., Lefeber, D.J. (2017). Mutations in *N*-acetylglucosamine (*O*-GlcNAc) transferase in

patients with X-linked intellectual disability. JBC M117.790097

Xia, Y., and Karin, M. (2004). The control of cell motility and epithelial morphogenesis by Jun kinases. Trends Cell Biol *14*, 94-101.

Xiao, Y.T., Xiang, L.X., and Shao, J.Z. (2007). Bone morphogenetic protein. Biochem Biophys Res Commun *362*, 550-553.

Zachara, N.E., and Hart, G.W. (2004a). O-GlcNAc a sensor of cellular state: the role of nucleocytoplasmic glycosylation in modulating cellular function in response to nutrition and stress. Biochim Biophys Acta *1673*, 13-28.

Zachara, N.E., and Hart, G.W. (2004b). O-GlcNAc modification: a nutritional sensor that modulates proteasome function. Trends Cell Biol *14*, 218-221.

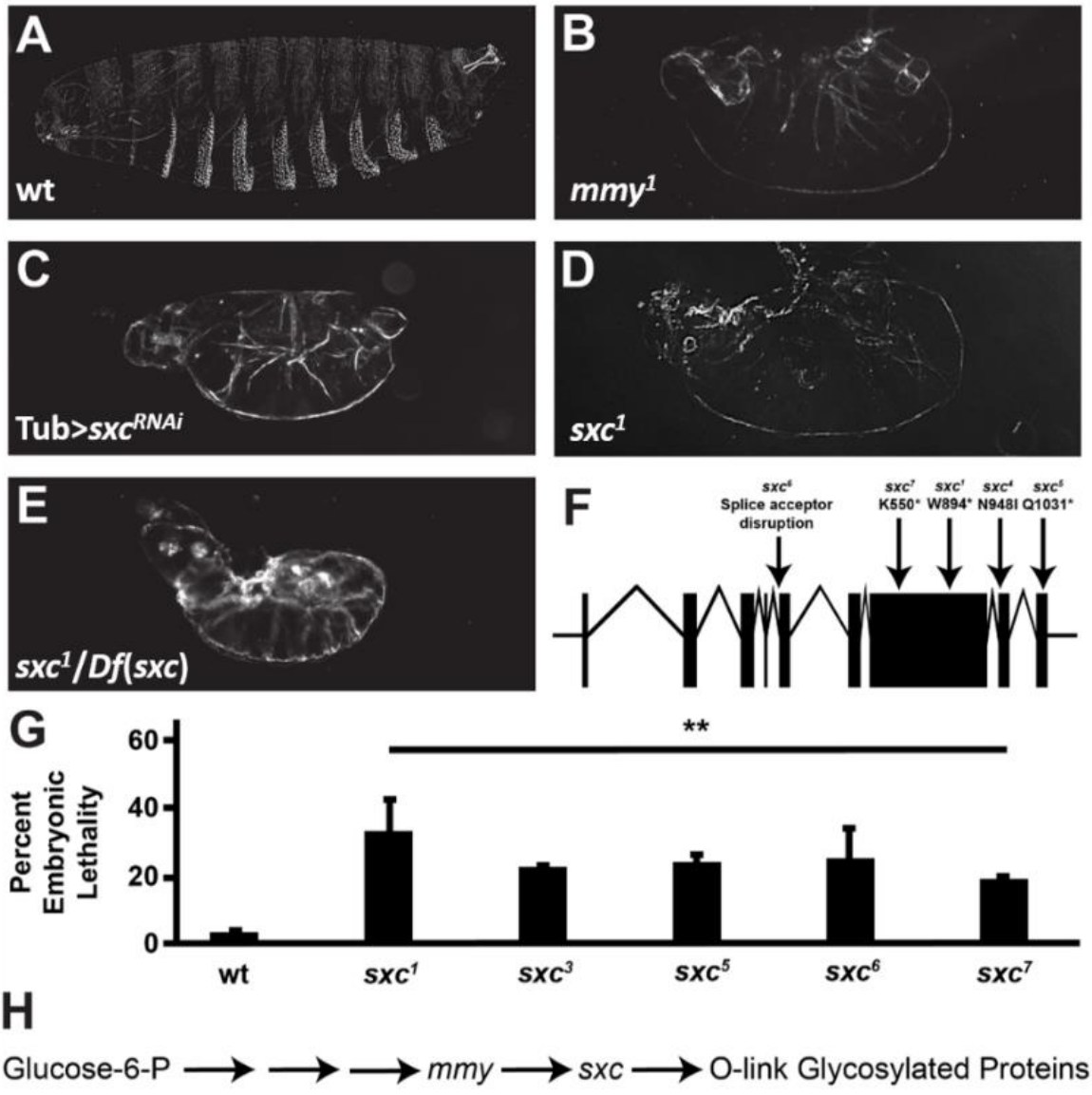

Fig. 2.1 *sxc* mutations result in embryonic lethality. Cuticle analysis of (A) wt, (B) *mmy*^{1}, (C) Tub>*sxc*^{RNAi}, (D) *sxc*^{1}, and (E) *sxc*^{1}/Df embryos. (F) *sxc* mutant allelic series map, *sxc*^{2} mutation is due to a 2:3 translocation, *sxc*^{3} aberration is not currently known. (G) *sxc* homozygotes from all lines exhibit partially penetrant embryonic lethality in all lines tested (**p<0.01). (H) Biochemical pathway in which *sxc* functions.

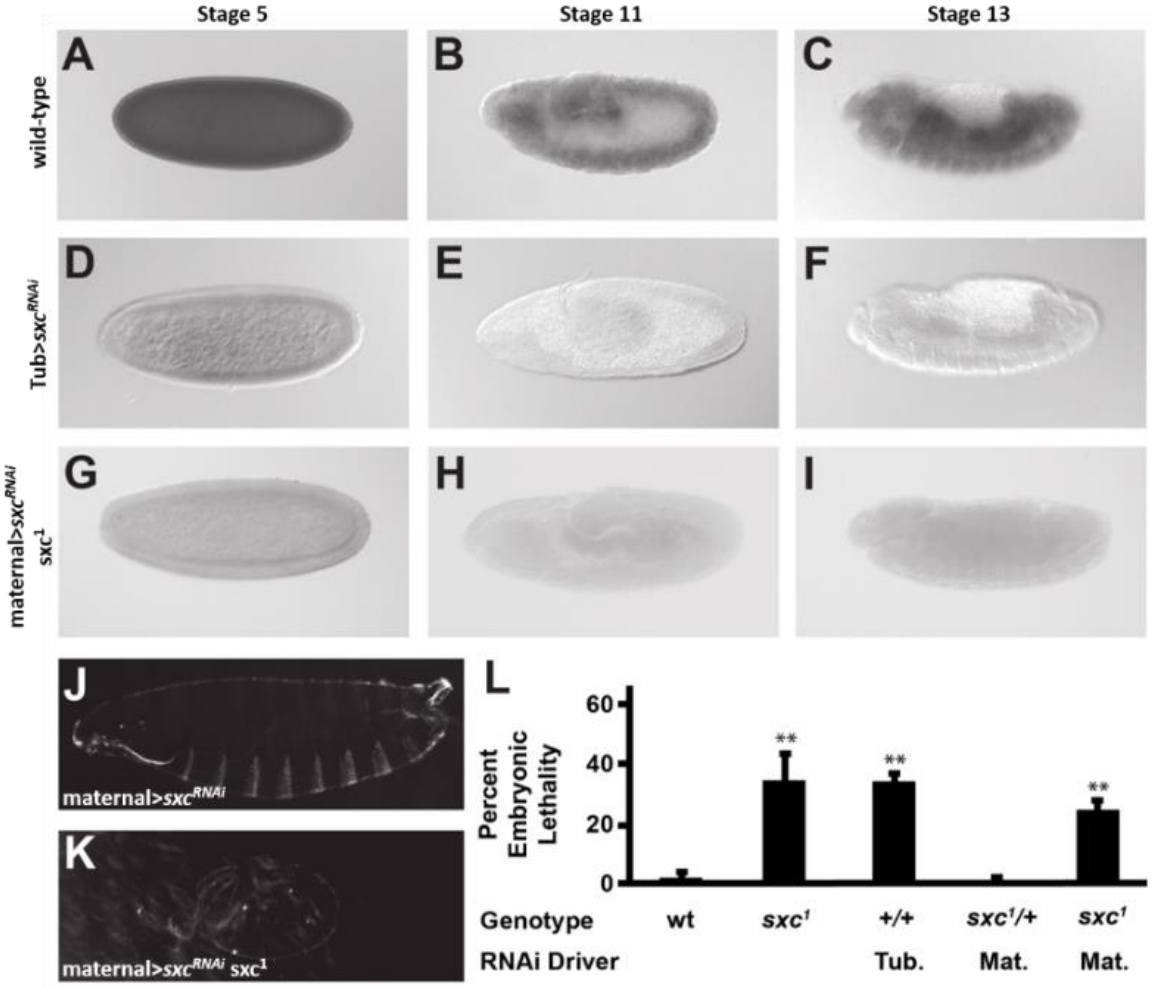

Fig. 2.2 Zygotically-derived *sxc* plays a critical role in development. *sxc* expression in (A-C) wild-type, (D-F) Tub>*sxc* shRNA and (G-I) Maternal Gal4>*sxc* shRNA sxc^1/sxc^1 embryos throughout embryogenesis (left to right: stage 5, stage 11, stage 13). Cuticle analysis of (J) Maternal Gal4>*sxc* shRNA $sxc^1/+$ and (K) Maternal Gal4>*sxc* shRNA sxc^1/sxc^1. (L) Quantification of embryonic lethality associated with maternal, zygotic, and maternal/zygotic loss of *sxc* (**p<0.01).

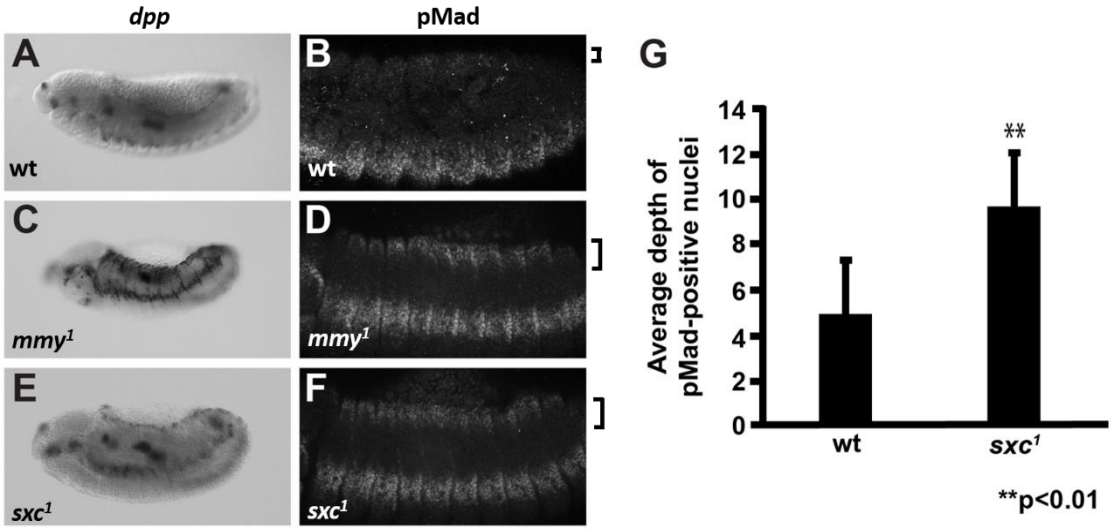

Fig. 2.3 Dpp signaling, but not *dpp* expression, is aberrant in *sxc*. d*pp* RNA is exclusively expressed from the leading edge cells in the dorsal epidermis of (A) wild-type embryos. This expression is expanded in (C) *mmy*^{1}, but not in (E) *sxc*^{1}. Mad is phosphorylated 4-6 cells deep within the epidermis of (B) wt embryos, but signaling is short lived during dorsal closure. Mad phosphorylation occurs at a greater distance from the leading edge in both (D) *mmy*^{1} and (F) *sxc*^{1} embryos and persists through dorsal closure. (G) Quantification of depth of pMad staining nuclei in wild-type and *sxc*^{1} embryos.

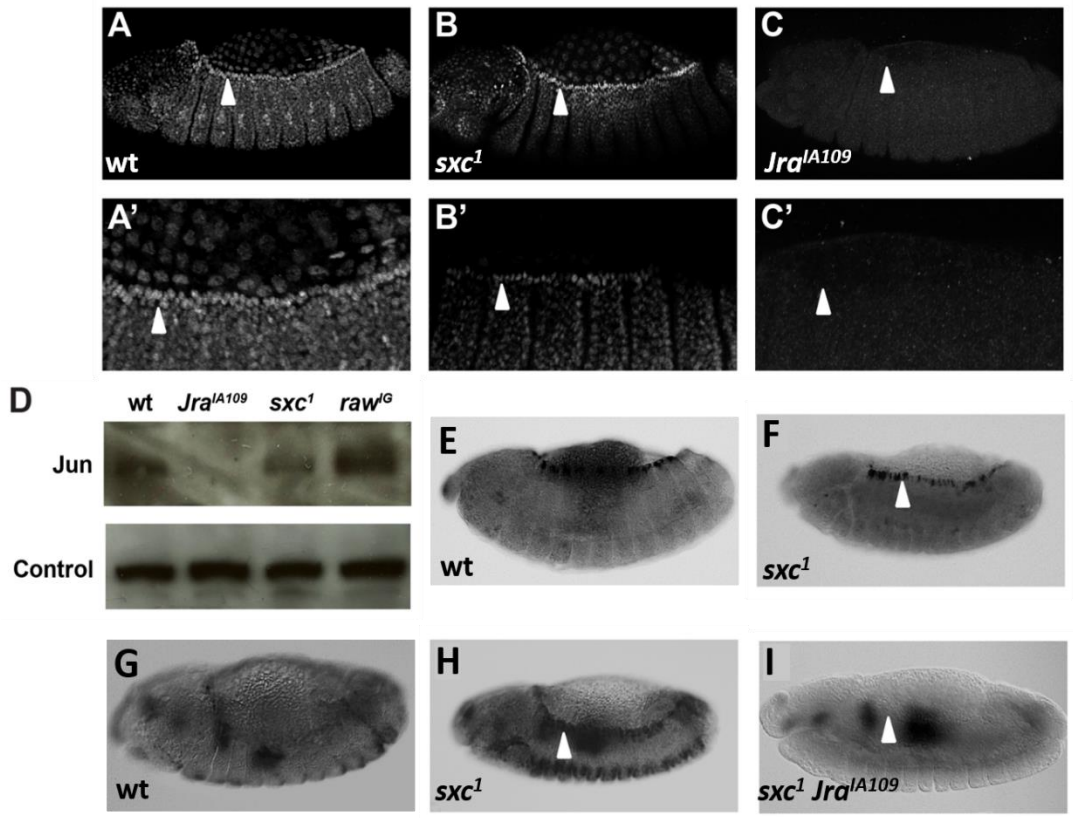

Fig. 2.4 *sxc* embryos do not exhibit JNK signaling defects. Jun protein is localized to leading edge cells (white arrowheads) in (A) wild-type embryos is indistinguishable from (C) *sxc*^{1} embryos and is completely absent in (B) *Jra*^{IA109} embryos. (D) Jun protein abundance is not increased in *sxc*^{1} embryonic lysates above wild-type embryonic lysates. This is in contrast to the previously described increase in Jun protein levels observed in embryonic lysates of a known JNK signaling antagonist, *raw*^{JG}. Also the JNK reporter is unaltered in (F) *sxc*^{1} embryos compared to wild-type embryos (E). The ectopic pMad phenotype in *sxc* requires Jun-dependent expression of *dpp* as no epidermal pMad is observed in (I) *sxc*^{1} *Jra*^{IA109} compared to (H) *sxc*^{1} alone; compare also (G) wild-type.

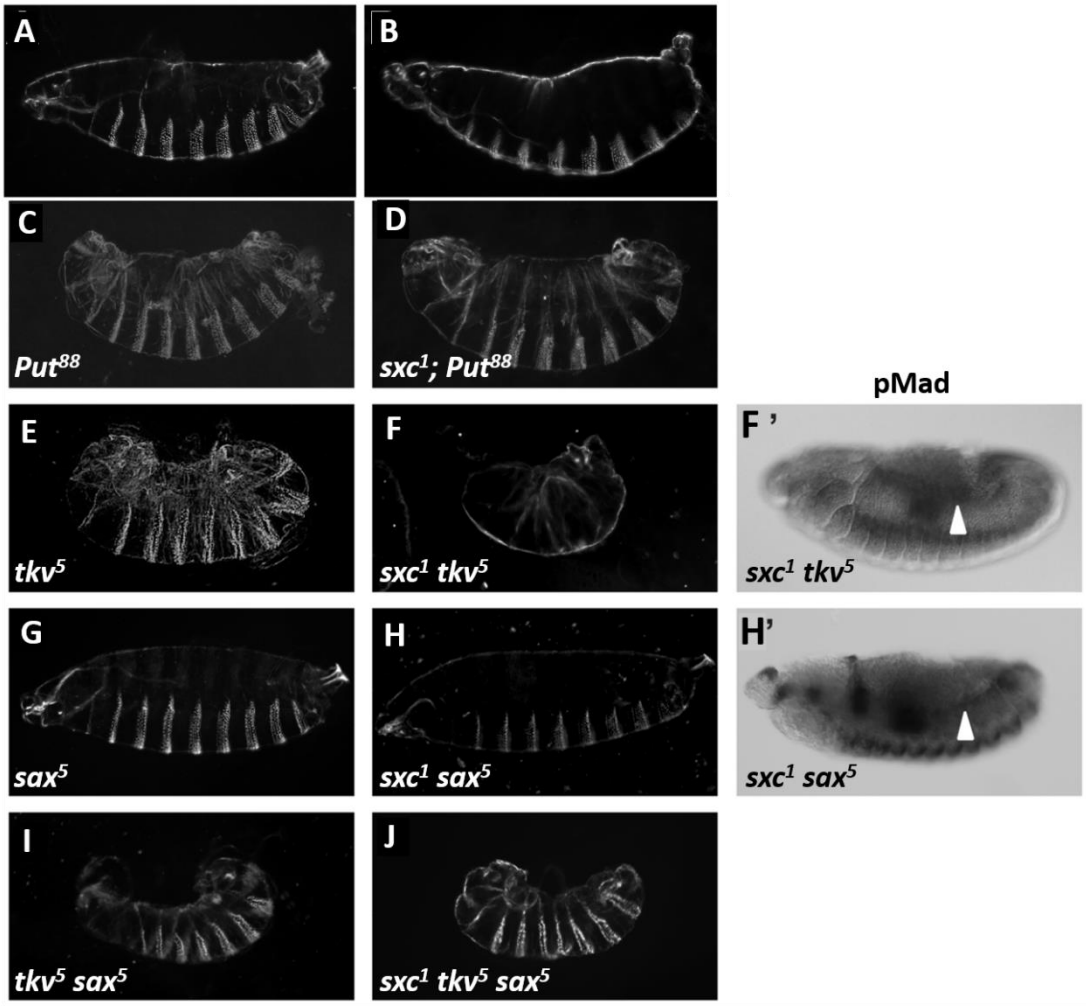

Fig. 2.5 Sxc interacts with the Dpp signaling pathway at the level of Sax. The *sxc* phenotype is lost in (B) *sxc*^{1} *Df*(*Mad*)/*sxc*^{1}; Tub>Mad^{RNAi}; compare (A) *Df*(*Mad*)/+; Tub>Mad^{RNAi}. No difference is observed between (C) *put*^{88} and (D) *sxc*^{1}; *put*^{88}. The *sxc* phenotype is observed in (F, F') *sxc*^{1} *tkv*^{5} compared with (E) *tkv*^{5}. The *sxc* phenotype is lost in (H, H') *sxc*^{1} *sax*^{5} compared to (G) *sax*^{5}. No difference is observed between (I) *sax*^{5} *tkv*^{5} and (J) *sxc*^{1} *sax*^{5} *tkv*^{5}.

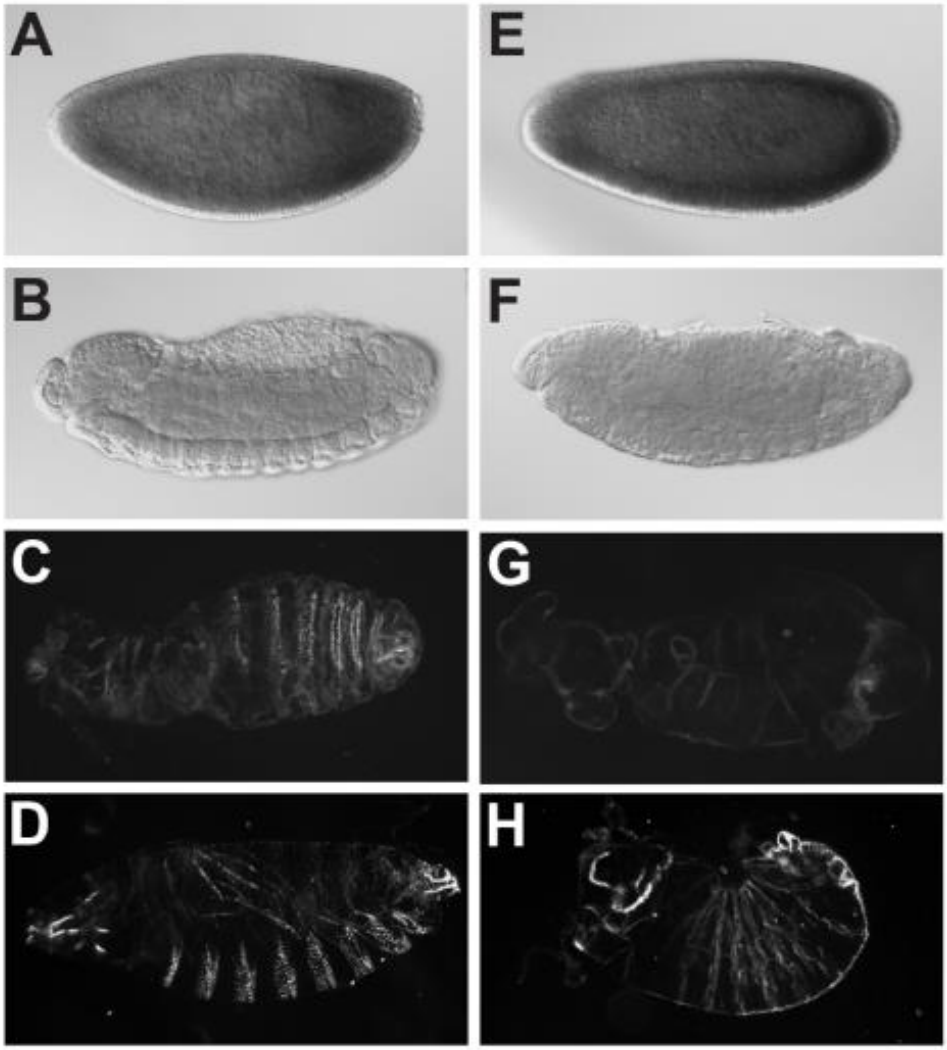

Fig. 2.6 *scw* and *gbb* is not expressed in the embryonic epidermis and plays no role in the *sxc* phenotype. *scw* is expressed in stage 5 embryos (A, E), but is absent in the epidermis of stage 12 embryos (B, F) in both wild-type (A-B) and sxc^{1} (E-F) embryos. Loss of *scw* in a *sxc* background (G) results in a phenotype with similarities to both *sxc* and *scw* (C) indicating that the *sxc* phenotype is independent of *scw* in the embryonic epidermis. The *sxc* phenotype also persists in sxc^{1} gbb^{D4} (H) double mutants compared to gbb^{D4} (D) mutants that exhibit weak dorsal closure defects.

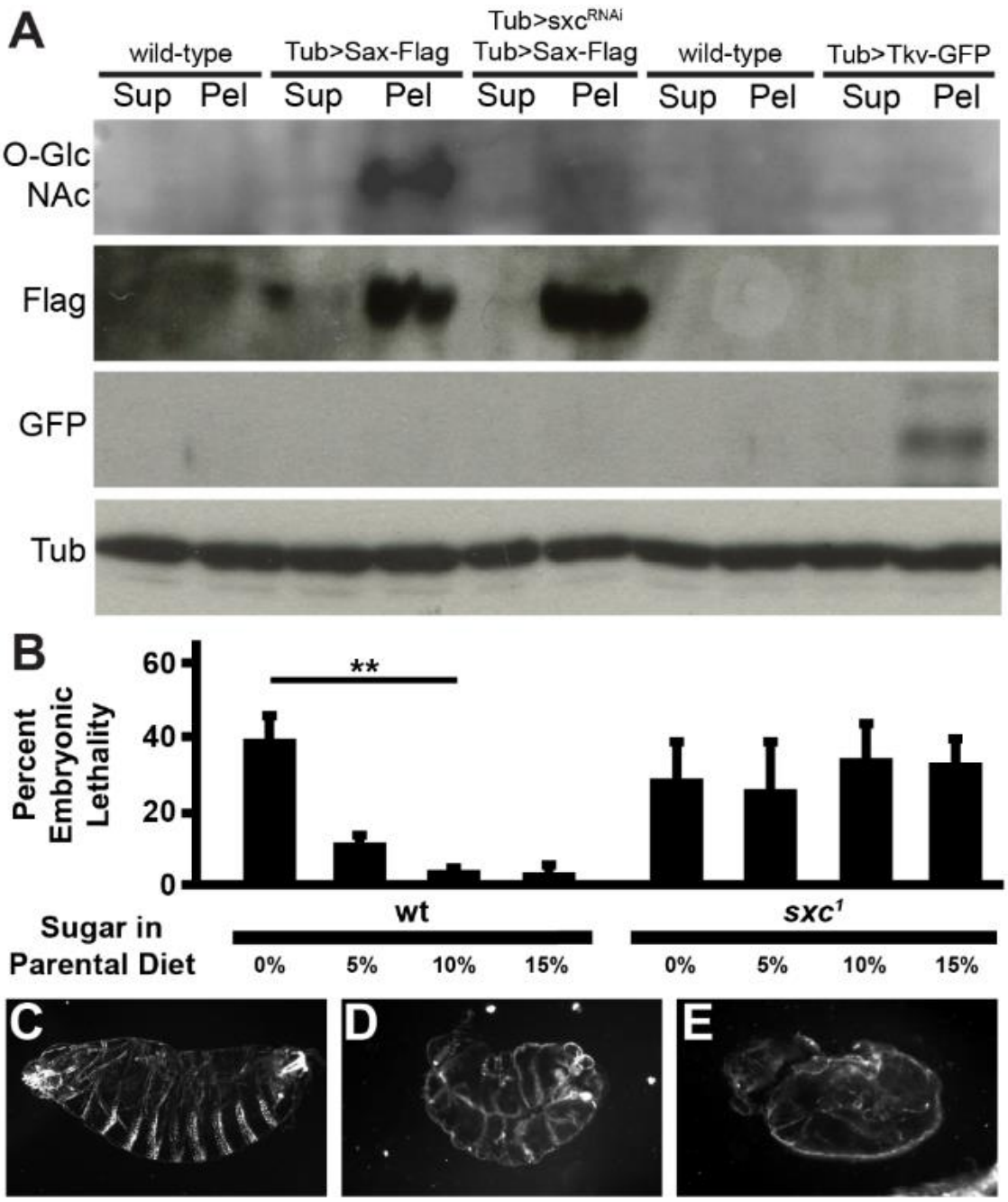

Fig. 2.7 Dpp signaling through Sax is modulated by O-linked glycosylation and dietary sugar. Sax-Flag and Tkv-GFP expressing embryonic lysates were subjected to immunoprecipitation and probed for the presence of O-GlcNAc via Western blot analysis (A). The presence of a band in the Sax-Flag expressing embryos compared to wild-type controls indicates that Sax is O-link glycosylated in vivo. No O-glycosylation is detected on Tkv. Forty percent of embryos derived from wild-type flies raised on no-sugar diets abort embryogenesis (B) and exhibit Dpp phenotypes (C-D). No change in phenotype is observed in lethality or cuticle phenotype in *sxc*^{1} embryos derived from flies raised on the no-sugar diet (E).

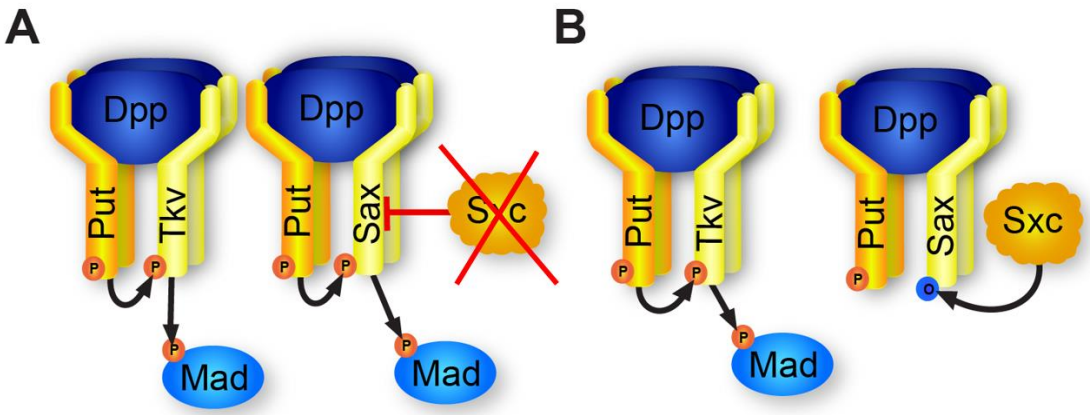

C

GS Domain

Sax	222	NDELLRATSAGDSTLREYLQHSVTSGSGSGLPLLVQRTLAKQVTL	266
ACVR1 (ALK2)	166	TIEGLITTNVGDSTLADLLDHSCTSGSGSGLPFLVQRTVARQITL	210
ACVRL1 (ALK1)	160	SSLILKASEQGDSMLGDLLDSDCTTGSGSGLPFLVQRIVARQVAL	204
Tkv	202	QPRLINSMCNSQLSPLSQLVE-QSSGSGSGLPLLVQRTIAKQIQM	245
BMPR1B (ALK6)	163	LEQDETYIPPGESLRDLIEQS-QSSGSGSGLPLLVQRTIAKQIQM	206

Fig. 2.8 Model of Sxc-mediated Dpp signal antagonism. Sxc functions to repress Dpp signal activation through Saxophone and limit all signaling through Tkv in the epidermis (A). We hypothesize that glycosylation of Sax either in the GS domain or in the kinase domain would abrogate its ability to interact with Put or its kinase function (B). There are several predicted sites of O-link glycosylation on Sax by Sxc (C). Yellow squares indicate sites of predicted glycosylation.

CHAPTER 3

THE DROSOPHILA B1,3-GALACTOSYLTRANSFERASE, IS REQUIRED FOR HYPERTROPHIC CELL GROWTH

Abstract

Glycans serve important developmental and homeostatic roles, and aberrations in glycan synthesis have been implicated in numerous diseases, both congenital and adult-onset. In an effort to characterize developmental roles for glycosyltransferases implicated in human congenital disease, we have generated several transferase mutants in the powerful genetic model, *Drosophila melanogaster*. Herein, we characterize phenotypes associated with the loss of the *Drosophila* ortholog of *B3GLCT*, *sugarcoated* (*sgct*), and demonstrate its utility as a model for Peters' Plus Syndrome, a congenital disorder of glycosylation associated with *B3GLCT* mutations. While many tissues exhibit hyperplastic growth (by mitosis), others, like bone, grow by hypertrophy (cell enlargement). We identified a role for *sgct* in cell hypertrophy during oogenesis and larval development. Our data point to the *sgct* fly as a unique and powerful genetic model of Peters' Plus Syndrome, providing insight into the etiology of growth and corneal defects observed in patients.

Introduction

Glycans, or polysaccharides, surround the surface of virtually every cell capable of differentiation and tissue formation in multicellular organisms (Haltiwanger and Lowe, 2004). Glycans facilitate communication between the cell and its environment and can

regulate cell-cell communication (Haerry et al., 1997; Haines and Irvine, 2003; Haltiwanger and Lowe, 2004; Varki, 2017). The presence of glycans in ordered arrays in diverse tissues throughout development has led researchers to speculate that they serve a critical role in development (Haltiwanger and Lowe, 2004; Varki, 2017). However, the complexity with which glycans are formed makes clarification of their specific developmental roles difficult to assess. This said, *Drosophila* has proven itself to be an invaluable model for elucidating glycan structure and for identifying how glycans are utilized, which in turn has provided insights into their function in other organisms as well (Haltiwanger and Lowe, 2004; Moulton and Letsou, 2016).

Protein glycosylation primarily occurs in the endoplasmic reticulum and Golgi apparatus, although the addition of a single O-GlcNAc residue is carried out by the O-GlcNAc transferase (OGT) on a subset of proteins that reside in the cytoplasm and nucleus (Varki, 2017). Glycosylated proteins, termed glycosaminoglycans (GAGs), are delineated based on where the protein is glycosylated and which sugars are used to glycosylate it. Sugars can be added to Ser/Thr residues via an oxygen group (O-linkage) or at Asn via a nitrogen side group (N-linkage). O-linked glycan chains are formed by the addition of single sugar residues in chains initiated by the addition of a GalNAc residue. Large glycoproteins that carry many clustered O-linked glycosyl chains are called mucins (Varki, 2017). Mucins are frequently found as transmembrane glycoproteins or in mucous secretions and function as facilitators of signal transduction, mediators of cell adhesion, and preventers of tissue desiccation. Mucins have been implicated in various diseases including cancer, with diverse malignancies promoting their own growth and survival by enhancing the expression of mucins on their cell surfaces, and eye diseases, with mucins functioning to lubricate and protect the eye (Jass and Walsh, 2001; Kufe, 2009; Mantelli and Argüeso, 2008).

Peters' Plus Syndrome, a rare anomaly associated with Peters' anomaly (corneal

opacity due to failure of the cornea to detach from the lens or iris), and growth defects have been demonstrated to be caused by a glycosyltransferase important in mucin formation (Maillette de Buy Wenniger-Prick and Hennekam, 2002). Specifically, Peters' Plus Syndrome is caused by mutations in *B3GLCT* (OMIM) but the precise role mucins play in the etiology of this disease remain unexplored.

We are leveraging the genetic toolkit available in *Drosophila melanogaster* to interrogate the role of mucins in Peters' Plus Syndrome with the specific goal to understand the etiology of Peters' Plus associated growth and corneal defects. To this end, we mutated the *Drosophila* ortholog of *B3GLCT*, *CG9109,* which we have named *sugarcoated* (*sgct*). *sgct* shares 37.3% amino acid identity across the entire protein length with the human *B3GLCT* gene (Fig. 3.1) along with complete conservation of transferase domains. Herein, we demonstrate that loss of *sgct* in *Drosophila* results in failure of developing fly larvae to grow and molt. Furthermore, targeted loss of *sgct* in oocytes results in termination of oocyte development and sterility. Both larval and oogenetic phenotypes are due to the failures of cells to enlarge during development. Tissues typically grow by employing cell division, whereas some postmitotic tissues can grow only by increasing cell size (hypertrophy). One tissue that grows primarily by hypertrophy is bone (Burdan et al., 2009). In the growth plate, chondrocyte populations initially expand mitotically, but as individual chondrocytes mature, they become postmitotic and enlarge only by cell hypertrophy. We provide evidence that mucins generated by the *Drosophila* homolog of *B3GLCT*, *sgct*, are required for hypertrophic cell growth in the developing *Drosophila* larva. Findings from this study lend new insight into the etiology of growth defects associated with Peters' Plus Syndrome.

Materials and methods

Fly strains

The Oregon R strain served as the wild-type in all experiments. The Tubulin:Gal4 stock was a gift of Mark Metzstein, and the maternal-driving Gal4 were obtained from the BDSC (stock number 31777) and described previously (FlyBase, 2003, version FB2017_01, released February 14, 2017). *CG9107* RNAi strain was obtained from the BDSC (stock number 43547).

Phenotypic analysis

Cuticle analysis was performed by dark field microscopy after embryos were incubated in one-step mounting media at 37°C for 18 hrs. Lethal stage analyses were performed by plating embryos on grape juice agar plate and recording observed proportion of dead embryos after 48 hrs. RNA in situ hybridization and immunohistochemistry staining procedures were all described previously (Humphreys et al., 2013). In brief, rabbit anti-phospho-Smad1,5 Ser463/465 (1:20, Cell Signaling Technology) antibody or digoxigenin-labeled anti-sense RNA probes were incubated overnight on fixed embryo clutches. After several washes, secondary antibodies targeting pMad, goat anti-rabbit alkaline phosphatase (Jackson ImmunoResearch) or goat anti-rabbit Alexa Fluor 488 (Invitrogen Molecular Probes), or digoxigenin-labeled RNA probes, mouse anti-digoxigenin alkaline phosphatase Fab fragments (Roche), were incubated with the embryos overnight. The following day, alkaline phosphatase detection was performed using nitro blue tetrazolium chloride and 5-Bromo-4-chloro-3-indolyl phosphate followed by dehydration in methanol and overnight incubation in 80% glycerol. Fluorescein-conjugated chitin-binding probe (New England BioLabs) was used to examine embryonic trachea by incubating embryos in the probe solution overnight and examining the trachea using darkfield microscopy on a Zeiss Axioskop. All larval

measurements were made by imaging live larvae on a Zeiss Axioskop and quantifying area in Image J. Fluorescently stained embryos were mounted in Vectashield Mounting Media with DAPI (H-1200; Vector Laboratories) and imaged with a FV1000 Olympus confocal microscope (Fluorescence Microscopy Core Facility at the University Of Utah School Of Medicine).

Feeding assay

Larval feeding was monitored by allowing larvae to feed on yeast paste containing Bromophenol Blue. Later, larvae were collected, washed thoroughly in PBS, and their guts examined under DIC imaging on a Zeiss Axioskop for the presence of blue dye. Larvae were also switched between feeding on dyed food for 24 hrs. and non-dyed food for 24 hrs. and examined using the same method to examine gut clearance over time.

Cryo EM studies

Larvae were collected and aged to the indicated time and high-pressure freezing/fixation were performed as described previously (Watanabe et al., 2013). All freezing and EM imaging were carried out by the technicians at the EM core at the University of Utah.

Results

We employ reverse genetic approaches to characterize roles of glycosyltransferases implicated in human diseases for which there are currently no good genetic models. One such disease, Peters' Plus Syndrome, results from mutations in the *B3GLCT* gene for which there is a single ortholog in the fly, *CG9109*, which we have named *sugarcoated* (*sgct*). *sgct* is maternally deposited (Fig. 3.2 A) and ubiquitously

expressed during embryogenesis (Fig. 3.2 B) suggestive of a role for *sgct* in development and pointing to the potential value of the *sgct* fly as an animal model of Peter's Plus. As a first step in creating this model, we generated a null allele of *sgct* by P-element mobilization (Fig. 3.2 D), designated $sgct^{11c}$. We confirmed that *sgct* expression is eliminated in $sgct^{11c}$ homozygotes by RNA hybridization *in situ* (Fig. 3.2 C). Although this allele disrupted the neighboring gene, *CG9107*, targeted disruption of this gene by RNAi resulted in no embryonic lethality or cuticle defects (Fig. 3.2 E, compare wild-type in D). We examined the requirements of both maternal and zygotic *sgct* transcripts on development.

Maternal sgct *is required for oocyte enlargement*

We recombined the *sgct* allele onto an FRT containing chromosome and obtained females which were heterozygous for this (*sgct* FRT) and a female sterile allele in cis to an FRT at the same chromosomal position (Ovo^D FRT). We also crossed in an ovarium-specific expressing FLPase transgene to generate females producing oocytes completely lacking *sgct*. We discovered that females lacking *sgct* expression in the germline are sterile. In an analysis of hundreds of *sgct* flies, we recovered only two eggs (Fig. 3.3 B), both of which were misshapen and harbored fused dorsal appendages (Fig. 3.3 A). Next, we used phase microscopy to assess *sgct* ovaries. We dissected individual ovarioles, stained them using DAPI, and examined them using a confocal microscope using darkfield and phase contrast microscopy techniques. Ovarioles obtained from *sgct* mosaic flies contained egg chambers that failed to elongate or grow throughout oogenesis (Fig. 3.3 E, E') in contrast to wild-type egg chambers (Fig. 3.3 C, C'). Furthermore, egg chamber development failed to complete, similar to egg chambers in the female sterile Ovo^D background (Fig. 3.3 D, D'). This defect in egg chamber growth and development is not due to a failure to specify an oocyte as a single

cell within each egg chamber properly expresses the oocyte maker *orb* in ovarioles derived from wild-type and *sgct* mosaic females (Fig. 3.3 F-G). Oocyte growth is a non-mitotic event and occurs by cell hypertrophy via endocytic take-up of vitelogenin (Schonbaum et al., 2000).

Zygotic sgct *is required for larval cell enlargement*

sgct^{11c} embryos are fully viable, hatch into larvae, and exhibit no obvious cuticle defects (data not shown). Rather, *sgct*^{11c} homozygotes exhibit lethality and growth defects during larval stages. Although *sgct*^{11c} larvae are no smaller than their wild-type counterparts at 24 hrs. after egg lay (AEL) (Fig. 3.4 A), they fail to grow in size and are significantly smaller than wild-type larvae by 5 hrs. after larval hatching (Fig. 3.4 A). Even though *sgct* larvae continue to eat throughout their lives (Fig. 3.4 D-E; compare wild-type in B-C), *sgct* larvae fail to molt at any point after 48 hrs. AEL and retain their signature L1 mouth hooks throughout their lives (Fig. 3.5 C-D; compare wild-type in A-B). *sgct* larvae suffer a fully penetrant larval lethality by 120 hrs. AEL, the time at which wild-type larvae transition into pupae.

Drosophila larval cells grow by hypertrophy and this is the primary contributor of organismal growth between L1 and L3. In order to determine the magnitude of growth failure, I measured cell size in *sgct* larvae compared to wild-type. Cell areas were the same in wild-type and *sgct*^{11c} homozygotes at the time of hatching (24 hrs. AEL), but while wild-type cells exhibit a significant three-fold expansion in size by 120 hrs. AEL, (3r larval instar stage) cell size in *sgct*^{11c} homozygotes remains unchanged (Fig. 3.6). These data demonstrate that *sgt*^{11c} larval cells like *sgt*^{11c} oocytes fail to hypertrophy during development and point to a previously unrecognized role for B3GLCT and mucins in this process.

sgct larvae fail to grow to any detectable degree (Fig. 3.7 A) and are fragile; even

the gentlest handling of *sgct* larvae resulted in cuticle rupture and death. Moreover, when *sgct* larvae were allowed to hatch on adhesive tape, their mere crawling across the tape led to their death by cuticle breakage (Fig. 3.7 B). These observations led us to speculate that *sgct* fragility is associated with failures in cuticle deposition. To test this idea, we examined wild-type and mutant larval cuticles at 24 and 120 hrs. AEL by cryo EM, first visualizing cuticle gross morphology and second measuring cuticle thickness. While there were no measurable differences in cuticle thickness or organization at early time points (Fig. 3. 7 G, I), cuticles from *sgct* larvae were thinner and morphologically disordered in comparison to wild-types at 120 hrs. AEL (corresponding to the L3 stage in a wild-type larva) (Fig. 3.7 H, J). Abnormal morphologies included cuticle inclusions (arrowhead), cuticle blebbing (asterisk), and improper layering of the cuticle (arrow) (Fig. 3.7 I-J). In terms of cuticle patterning, we observed disorganization of the cuticle layers and a loss of directionality of the stereotypic chevron-shaped wedges within each layer. In *sgct*, these wedges did not point in a consistent direction within or between cuticle layers. We suspect that these differences lead to the cuticle weakness observed and the ease with which the larvae are ruptured. Although cuticle defects were observed in dorsal trunk formation during late stages of embryogenesis (Fig. 3.7 F), these defects were detected only rarely (compare wild-type in C and mmy^{1} with stereotypic cuticle defects in D).

Discussion

Mucins are expressed in various tissues and perform diverse functions including regulating cell proliferation and cell secretion. Cell growth and proliferation are often correlated and occur concomitantly during tissue growth. However, in both vertebrates and invertebrates, there is a subset of nonmitotic tissues that undergo growth by cell hypertrophy rather than hyperplasia. In the case of *Drosophila*, larvae are mostly

composed of cells that grow in size and drive larval growth. These cells undergo endoreplication and duplicate their genome without completing cytokinesis (Edgar and Orr-Weaver, 2001) and, by our analysis grow by more than three-fold during larval development. Herein, we have described our discovery of a critical role for the glycosyltransferase, *sgct*, in hypertrophic growth of cells during *Drosophila* larval development and oogenesis and in the proper secretion of the larval cuticular exoskeleton.

Mutations in the human homolog of *sgct*, *B3GLCT*, result in a congenital disease called Peters' Plus Syndrome associated with congenital defects including growth defects and Peter's anomaly. We propose the *sgct* fly as a genetically tractable model for this disease which has proven useful in gaining insight into the etiology of the growth and corneal defects associated with this disorder which warrant further exploration. Specifically, failure in cells to grow by hypertrophy may be the primary defect in the bones of Peters' Plus patients. Additionally, the failure of cuticle secretion observed in *sgct* suggests that corneal cells of Peters' Plus patients may not be secreting mucins which could help the cornea detach from other cell layers in the eye. While insights gained from our exploration of *sgct* phenotypes in the fly, much remains unknown regarding the function of mucins in the Peters' Plus phenotypes. Undoubtedly, the fly will serve as an important springboard into exploration of the roles of mucins and provide a model in which to test hypotheses and identify therapeutic interventions for this and other human diseases.

References

Burdan, F., Szumilo, J., Korobowicz, A., Farooquee, R., Patel, S., Patel, A., Dave, A., Szumilo, M., Solecki, M., Klepacz, R.*, et al.* (2009). Morphology and physiology of the epiphyseal growth plate. Folia Histochem Cytobiol *47*, 5-16.

Edgar, B.A., and Orr-Weaver, T.L. (2001). Endoreplication cell cycles: more for less. Cell

105, 297-306.

Haerry, T.E., Heslip, T.R., Marsh, J.L., and O'Connor, M.B. (1997). Defects in glucuronate biosynthesis disrupt Wingless signaling in Drosophila. Development *124*, 3055-3064.

Haines, N., and Irvine, K.D. (2003). Glycosylation regulates Notch signalling. Nat Rev Mol Cell Biol *4*, 786-797.

Haltiwanger, R.S., and Lowe, J.B. (2004). Role of glycosylation in development. Annu Rev Biochem *73*, 491-537.

Jass, J.R., and Walsh, M.D. (2001). Altered mucin expression in the gastrointestinal tract: a review. J Cell Mol Med *5*, 327-351.

Kufe, D.W. (2009). Mucins in cancer: function, prognosis and therapy. Nat Rev Cancer *9*, 874-885.

Maillette de Buy Wenniger-Prick, L.J., and Hennekam, R.C. (2002). The Peters' Plus Syndrome: a review. Ann Genet *45*, 97-103.

Mantelli, F., and Argüeso, P. (2008). Functions of ocular surface mucins in health and disease. Curr Opin in Aller and Clin Immun *8*, 477-483.

Moulton, M.J., and Letsou, A. (2016). Modeling congenital disease and inborn errors of development in Drosophila melanogaster. Dis Model Mech *9*, 253-269.

Schonbaum, C.P., Perrino, J.J., and Mahowald, A.P. (2000). Regulation of the vitellogenin receptor during Drosophila melanogaster oogenesis. Mol Biol Cell 11, 511-521.

Syed, Z.A., Hard, T., Uv, A., and van Dijk-Hard, I.F. (2008). A potential role for Drosophila mucins in development and physiology. PLoS One *3*, e3041.

Varki, A. (2017). Essentials of glycobiology, Third edition. (Cold Spring Harbor, New York: Cold Spring Harbor Laboratory Press).

Watanabe, S., Liu, Q., Davis, M.W., Hollopeter, G., Thomas, N., Jorgensen, N.B., and Jorgensen, E.M. (2013). Ultrafast endocytosis at Caenorhabditis elegans neuromuscular junctions. Elife *2*, e00723.

```
HumanB3GLC    95 VLLLHQLAKQEGAWTILPLLPHFSV---TYSRNSSWIFFCEEETRIQ-IPKLLETLRRYD
Drosophila    69 VLKVHVMHELFNSWTMLDALPHLRAQARVLGARTEWIIWCQHNTRVSSLRGLLEQLRRQN
                 **  *        ** *  ***             **  *   **      *** ***

HumanB3GLC   151 PSKEWFLGKALHDEEATIIHHYAFSENPTVFKYPDFAAGWALSIPLVNKLTKRL----KS
Drosophila   129 PRELAFYGHALYDAEATIIHHFSNYKDPQRFPYPMLSAGVVFTGALLRRLADLVAPSGQN
                 *    * * ** * *******      *  * **   **      *   *

HumanB3GLC   207 ESLKSDFTIDLKHEIALYIWDKGGGPPLTPVP---EFCTNDVDFYCATTF---HSFLP--
Drosophila   189 ITVHSDFSIDASHELARFIFDNVSPDPHISTPISGGILLKSASYICSTPTSVPNRKLPCL
                     *** **  ** *  * *     *    *            * *        **

HumanB3GLC   259 LCRKPVKK--------------KDIFVAVKTCKKFHGDRIPIVKQTWESQASLIEYYSD
Drosophila   249 LHAQPEEPLTLGQRRNGCEHTTGSHIYFAIKTCAKFHKERIPIIERTWAADARNRRYYSD
                 *   *                    *  * *** ***  ****   **   *    ****

HumanB3GLC   304 YTENSIPTVDLGIPNTDRGHCGKTFAILERFLNR--SQDKTAWLVIVDDDTLIS------
Drosophila   309 VADVGIPAIGTGIPNVQTGHCAKTMAILQLSLKDIGKQLDIRWLMLVDDDTLLSLHLIHT
                      **    ****   *** ** ***   *     *    **  ****** *

HumanB3GLC   356 -----ISRLQHLLSCYDSGEPVFLGERYGYGL-GTGGYSYITGGGGMVFSREAVRRLLAS
Drosophila   369 HLPTSVPRVSALLCRHNATELVYLGQRYGYRLHAPDGFNYHTGGAGIVLSLPLVR-LIVQ
                        *   **      * * ** **** *    *  * *** * * *   ** *

HumanB3GLC   410 KCRCYSNDAPDDMVLGMCFSGLGIPVTHSPLFHQARPVDYPKDYLSHQVPISFHKHWNID
Drosophila   428 RCSCPSASAPDDMILGYCLQALGVPAIHVAGMHQARPQDYAGELLQLHAPLTFHKFWNTD
                  * * *  ***** ** *   ** *  *    ***** **    *    *  *** ** *

HumanB3GLC   470 PVKVYFTWLAPS
Drosophila   488 PEHTYRRWLGGS
                 *   *  **  *
```

Fig. 3.1 Alignment of *B3GLCT* and *sgct*. Human *B3GLCT* and *Drosophila sgct* share 37.3% amino acid identity and are predicted homologs.

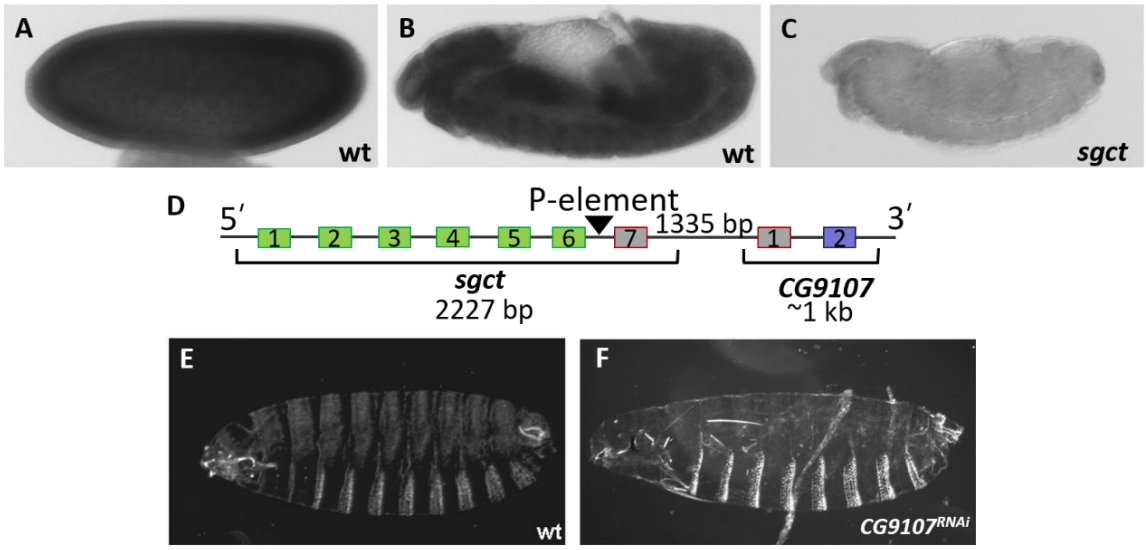

Fig. 3.2 *sgct* is maternally-deposited and zygotically expressed. *sgct* RNA transcripts can be detected in early blastoderm embryos (A), demonstrating maternal deposition of *sgct*, and ubiquitously in dorsal-closure stage embryos (B). Removal of the last exon of *sgct* by imprecise P-element excision (*sgct*^{11c}) ablates all detectable *sgct* expression by RNA *in situ* analysis (C). No embryonic phenotypes are observed in embryos expressing RNAi targeting the *CG9107* locus (F) compared to wild-type (E).

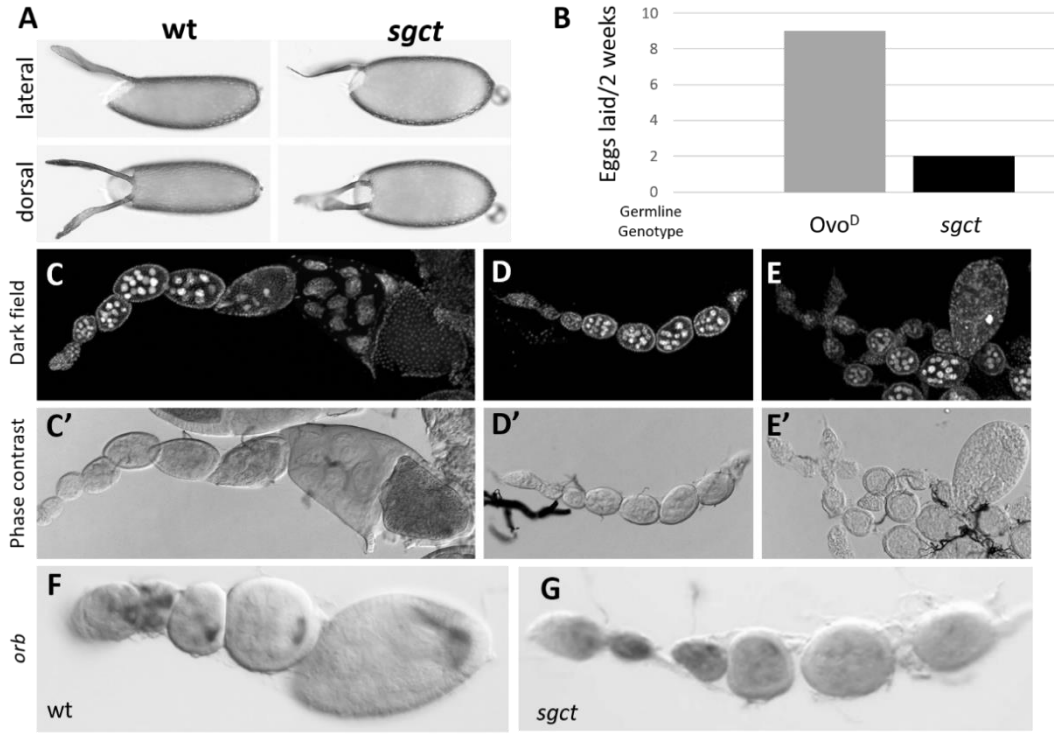

Fig. 3.3 *sgct* female germline fail to produce viable eggs and to elongate egg chambers. *sgct*^{11c} homozygous female germline result in a nearly complete ablation of fecundity and a failure of egg chambers to elongate during oogenesis. This failure occurs despite the ability of the oocyte to be specified during oogenesis.

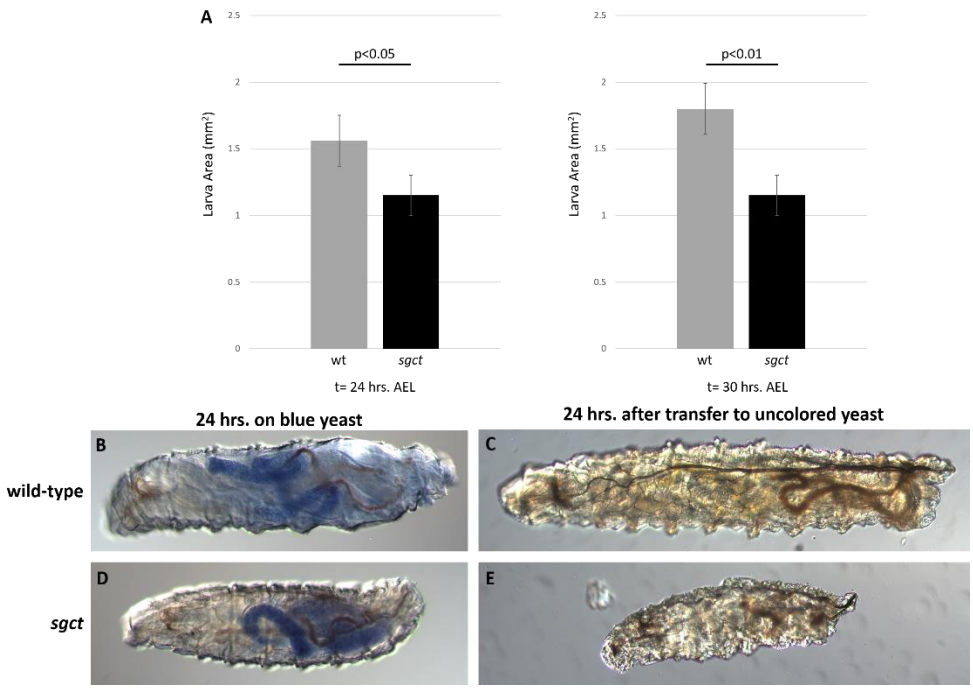

Fig. 3.4 *sgct* larvae fail to grow with age. *sgct*^{11c} homozygous larvae are viable but fail to grow compared to wild-type, despite their ability to eat and clear gut contents.

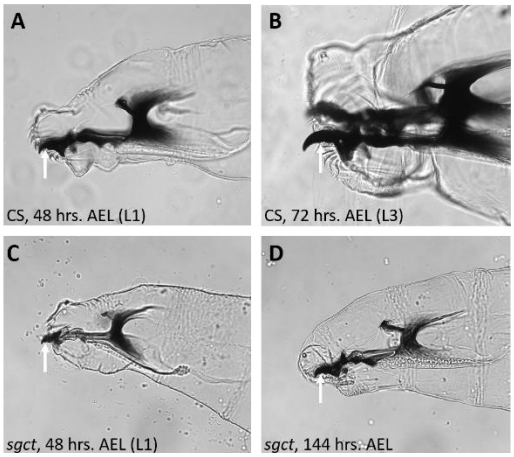

Fig. 3.5 *sgct* larvae fail to molt. *sgct*^{11c} homozygous larvae retain mouthooks indistinguishable from wild-type L1 larvae demonstrating an inability to molt and shed their exoskeleton.

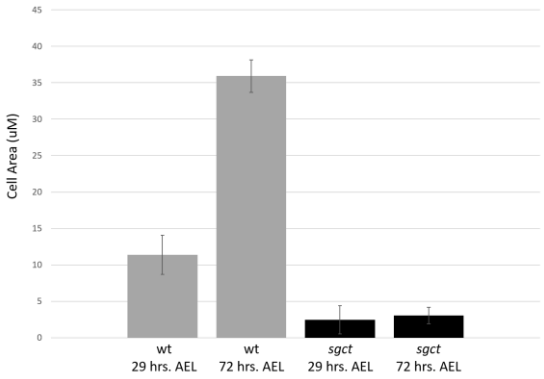

Fig. 3.6 *sgct* larvae fail to expand cell area during development. *sgct*^{11c} homozygous larvae fail to expand cell area during larval development compared to an over 300% in growth in cell area in wild-type during the same time course.

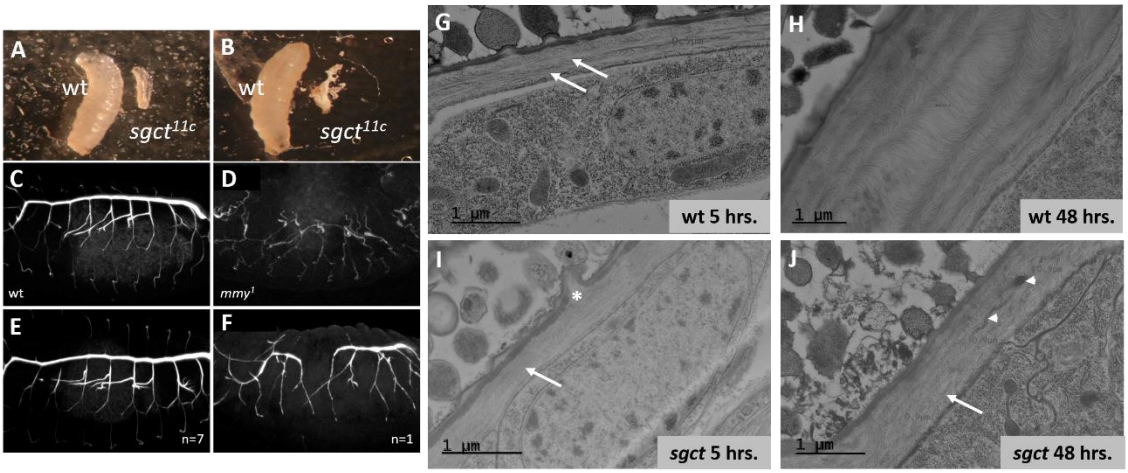

Fig. 3.7 *sgct* larvae exhibit cuticle defects. *sgct*^{11c} homozygous larvae exhibit a fragile cuticle phenotype and burst easily upon handling. Although *sgct*^{11c} exhibit embryonic tracheal defects, they occur at low frequency. *sgct*^{11c} larvae also exhibit completely penetrant cuticle deposition and patterning defects. Although cuticle is deposited normally at early larval stages, over time, this cuticle fails to expand and develops structural abnormalities such as inclusions (arrowheads), belbbing (asterisk) and disorganization of cuticle directionality (arrows).

CHAPTER 4

DPP SIGNALING IS ANTAGONIZED BY A CHONDROITIN-SULFATE SINK

The contents of this chapter is a manuscript that I am co-authoring which is currently being prepared for submission. I contributed to the writing of this manuscript and carried out the experiments and imaging to generate Figure 4.7.

Abstract

Decapentaplegic (Dpp) signaling simultaneously regulates epidermal and mesodermal processes in early *Drosophila* development. In the epidermis, Dpp directs the changes in cell shape and position underling the morphogenetic process of dorsal closure, while in the adjacent mesoderm it promotes organogenesis of the heart. The Dpp source for both processes is the epidermal leading edge (LE). Here we show that proper signal propagation in both tissues relies on a mesodermally-derived chondroitin-modified signaling sink. Loss of chondroitin by mutation of the gene encoding either the GalNAc epimerase Gale or the GalNAc transferase Wanderlust increases Dpp activity in both the epidermis and the mesoderm, providing the first in vivo evidence for the long-theorized sink. Moreover, our demonstration that the Dpp sink resides in cells immediately adjacent to the Dpp source, and in a neighboring tissue, underscores the importance of highly coordinated tissue functions in signal propagation – both with respect to signal production and elimination.

Introduction

Critical to the development of all multicellular organisms is the ability to transform equipotent embryonic cells into distinct tissues and organs. One way this cellular diversity is achieved is via morphogen signaling. Morphogens were first defined by Alan Turing in his 1952 landmark paper (Turing, 1952) as diffusible chemicals that form signaling gradients and by which different chemical concentrations determine different cellular reactions. In 1969, Lewis Wolpert refined our understanding of morphogen gradients with the French Flag model (Wolpert, 1969). In this revised model, a diffusible ligand forms a gradient across a signaling field (or between a source and distant cells), and cells within the signaling field act in accordance with the level of signal observed. Among others researching cellular signaling it was quickly noted that generation of a stable continuous gradient requires a "sink", a signal-destroying component located at a distance from the source (Crick, 1970). Without a sink, signal is expected to accumulate at uniform levels across the field but, until now, the genetic and molecular nature of a signaling sink, working either locally or at a distance, has not been identified. We have shown previously that Dpp gradient formation is modulated by UDP-glucose (Humphreys *et al.*, 2013), and here we extend our study to mechanism, showing that chondroitin sulfate (CS), a proteoglycan formed from UDP-glucose, functions as the Dpp sink in the embryonic mesoderm. These results are notable as they provide evidence for the first-ever localized signaling sink functioning *in vivo* and thus also provide the capstone piece to a long-held seminal theory in developmental biology.

Dpp belongs to the Bone Morphogenic Protein (BMP) group of evolutionarily-important signaling molecules conserved in vertebrates and invertebrates, with evidence suggesting a common ancestor at least 600 million years ago (Padgett *et al.*, 1993). BMPs were first identified and named for their ability to induce bone development (Urist, 1965). Since their discovery, BMPs have been shown to play roles in diverse

developmental and morphological processes, including organogenesis, wound healing, and stem cell maintenance (Frasch, 1995; Lyons *et al.*, 1990; Mandel *et al.*, 2010; Winnier *et al.*, 1995; Kawase *et al.*, 2004; Shivdasani and Ingham, 2003; Song *et al.*, 2004; Ying *et al.*, 2003). BMPs are diffusible ligands that form signaling gradients within and between tissues and signal through binding to a dimeric receptor complex containing type I and type II subunits; varying the components of the receptor affects specificity to specific BMP ligands. When the ligand-receptor complex is formed, the type I receptor subunit is activated by phosphorylation. In its turn, the activated type I receptor phosphorylates a Smad signal transducer; upon entering the nucleus, Smads binds to BMP-responsive targets to activate and enhance transcription (Massagué, 1998).

While several molecules that refine signaling range have been characterized (e.g., Thickveins [Tkv], Syndecan [Sdc], and others), the long-sought sink has eluded detection and characterization. The problem is made only more complex by the regulators' shared participation in multiple signaling pathways (Nishihara, 2010).

Mummy (Mmy), a UDP-N-acetylglucosamine pyrophosphorylase that synthesizes UDP-GlcNAc, functions in the epidermis to limit Dpp/BMP signaling (Humphreys *et al.*, 2013). UDP-GlcNAc is essential for the synthesis of heparin sulfate proteoglycans (HSPGs), which have been shown in *Drosophila* and other eukaryotes to play essential roles in modulating the effects of morphogens (Dpp/BMP, Wingless (Wg)/WNT, and Hedgehog (Hh)), usually as a facilitator of long-range signaling (Akiyama *et al*., 2008; Beckett *et al.*, 2008; Belenkaya *et al*., 2004; Capurro *et al*., 2008; Gallet *et al*., 2008; Gumienny *et al*., 2007). This said, we have not found any effect of loss of the HSPG, Syndecan, on epidermal Dpp/BMP signaling (not shown), and thus we speculated that there must be another requirement for UDP-GlcNAc in regulating epidermal Dpp/BMP signaling. Here we report our identification of two components of the chondroitin sulfate

(CS) synthesis pathway, *wanderlust* (*wand*), a gene with homology to the evolutionarily-conserved *Chondroitin sulfate synthase 2*, and its upstream partner *UDP-galactose 4'-epimerase* (*Gale*), as antagonists of Dpp/BMP signaling in the embryonic *Drosophila* epidermis and in the underlying mesoderm. Notably, the transcripts corresponding to both *wand* and *Gale* are expressed in a single row of mesodermal cells underlying the Dpp-secreting leading edge cells (LE) of the epidermis. Taken together, our data point to CS as an important developmental regulator, one which fulfills the requirements of a signaling sink and converts a potentially long-range signaling molecule into a shorter-range signaling molecule.

Results

mmy mutants are defective in glycosylation

mmy codes for the single *Drosophila* UDP-N-acetylglucosamine pyrophosphorylase, an enzyme catalyzing the final step of UDP-GlcNAc biosynthesis (Araújo *et al*., 2005). Certain *mmy* hypomorphs, such as mmy^{1}, exhibit defects in dorsal closure yet have intact chitin, indicating that the mmy^{1} dorsal closure defect stems from an alternative requirement for UDP-GlcNAc (Humphreys *et al*., 2013; Tonning *et al*., 2006). Aside from chitin synthesis, UDP-GlcNAc is utilized for a variety of functions including N- and O-linked glycosylation as well as synthesis of glycosyl-phospatidylinostiol (GPI), heparin sulfate (HS), and chondroitin sulfate (CS) (Breitling and Aebi, 2013; Hardingham and Fosang, 1992; Low, 1989; Wells *et al*., 2001). To determine whether *mmy* hypomorphs have a loss in UDP-GlcNAc synthesis that is sufficient to produce glycosylation defects, we used Western blot analysis to probe shifts in the molecular weight of Dally-like protein (Dlp), an HS proteoglycan consisting of a protein core of 85 kDa weight and attached HS chains of variable lengths (Fig. 4.1). In wild-type embryonic lysates, HS-modified Dlp appears as a broad band in the 130–160

kDa range of the blot, whereas in two independently generated *mmy* hypomorphs the Dlp band shifts to average 100 kDa; these data indicate that HS chains are truncated in *mmy* mutants and confirm that animals harboring hypomorphic alleles of *mmy* and exhibiting Dpp signaling abnormalities have insufficient UDP-GlcNAc levels to carry out full glycosylation.

Epidermal BMP/Dpp signaling is regulated by the chondroitin biosynthetic pathway

More than two dozen transferases function downstream of Mmy to effect glycosylation. To identify the transferase(s) functioning downstream of Mmy in regulating Dpp/BMP signaling, we disrupted each of the predicted *Drosophila* β-1,3 glycosyltransferases (Correia *et al*., 2003) by RNAi. To this end, we used the *tubulin Gal4* (*tub-Gal4*) driver to mediate ubiquitous expression of UAS-RNAi's targeting each of the transferases. Analysis of cuticle phenotypes revealed that loss of only one β-1,3 glycosyltransferase (CG43313) results in embryonic lethality and a loss-of-function cuticle phenotype that is shared with *mmy* and indicative of hyperactive Dpp signaling (Fig. 4.2 B,C,E). The *CG43313*-encoded transferase, which we have named Wanderlust (Wand), is homologous to human Chondroitin sulfate synthase 2 and catalyzes the elongation of chondroitin sulfate (Yada *et al*., 2003) (Fig. 4.2). Two previously described alleles of *wand* (*CG43313*^{PL61} and *CG43313*^{PL69}) are likely hypomorphic; they were generated by P-element insertion into the gene region (Bourbon *et al.*, 2002) and when homozygosed yield a fully penetrant larval lethality (data not shown).

Chondroitin synthesis lies downstream of Mmy in a linear biochemical pathway (Fig. 4.3 A). To confirm that the effects of *wand* RNAi are due to a loss of chondroitin, we turned to the gene functioning directly upstream of *wand* in the chondroitin biosynthetic pathway. The *Drosophila* gene *UDP-galactose 4'-epimerase* (*Gale*) is

required to convert UDP-GlcNAc into UDP-GalNAc (Sanders *et al*., 2010), the substrate of chondroitin sulfate synthases. Given this function, genetic and biochemical models predict that *Gale* embryos will suffer an embryonic lethality and share a loss-of-function cuticle phenotype with *mmy* and *wand* mutants. In examining cuticles from animals homozygous for two publically available amorphic alleles of *Gale*, we found that this prediction holds true (Fig. 4.3 D). The shared loss-of function phenotype of genes encoding three sequentially acting enzymes in the CS biosynthetic pathway (*mmy*, *Gale*, and *wand*) indicates that CS is an important protein modification enacting Dpp antagonism.

The dorsal-open, ventral-hypotrophic cuticle phenotypes observed in *Gale* and *wand* mutants are well-characterized signatures of ectopic epidermal Dpp/BMP signaling (Humphreys 2013; Bates *et al*., 2008; Byars *et al*., 1999; Riesgo-Escovar *et al*., 1997). To directly test the hypothesis that Gale and Wand are required (like Mmy) to limit Dpp signaling in the embryonic epidermis of *Drosophila*, we compared epidermal Dpp activity in wild-type, *Gale*, and $wand^{RNAi}$ (null) embryos. To do this, we used immunostains with antibodies directed against pMAD (the phosphorylated [activated] form of the Dpp signal transducer Mothers against dpp) and hybridizations in situ with *dpp* (a transcriptionally regulated target of the pathway).

In previous studies of epidermal MAD activity, we showed that pMAD is broadly distributed in the epidermis of wild-type embryos undergoing germ band extension, while later in development (in dorsal closure stages of embryogenesis), pMAD immunoreactivity disappears (Humphreys *et al*. 2013). Here, when we examined the epidermal Dpp signaling domain in *Gale* and *wand* mutant embryos, we found that although early pMAD profiles are similar in wild-type and mutant embryos (data not shown), differences are very clear later in development. Dpp signaling, which is normally attenuated during dorsal closure in wild-type embryos, persists temporally and

extends to greater depths in the epidermis of mutant embryos. Specifically, we observed that P-Mad-positive Dpp signaling fields are expanded in *Gale* and *wand*^{RNAi} mutants in a manner that is analogous to that observed in *mmy* mutants (Fig. 4.3 J-M, J'-M').

Results from hybridization studies in whole mount embryos in situ are consistent with those from immunostains. We observed LE-restricted epidermal *dpp* expression in wild-type embryos, from germ band extended to germ band retracted stages of development (Fig. 4.3 F). In contrast, in similarly staged *mmy, Gale, and wand* mutant embryos, we observed broad ectopic epidermal *dpp* expression (Fig. 4.3 G-I).

Integration of epidermal and mesodermal regulators of BMP/Dpp signaling

With the expectation that spatial patterns of *Gale* and/or *wand* expression might suggest a mechanism for CS-mediated Dpp signal antagonism, we next examined the genes' expression in hybridization studies of whole mount embryos in situ. While *Gale* is not maternally deposited, it is expressed in a single row of mesodermal cells underlying the epidermal LE (Fig. 4.4 A-B).

Unlike *Gale, wand* is maternally deposited in the early syncytial blastoderm; more notable, however, is our observation that as for *Gale,* the zygotic *wand* transcript is first visible in a single row of mesodermal cells underlying the LE epidermis (Fig. 4.4 D-E). The quantities and timing of *Gale* and *wand* expression are consistent with measures reported in the modENCODE database (Graveley *et a*l., 2011), and while Gale expression diminishes in stage 13 embryos, *wand* expression appears to become stronger (Fig. 4.4 C,F). To ascertain whether *Gale* and *wand* are expressed in cardiac or pericardial cells (the two dorsal-most rows of mesoderm in stage 13 embryos), we compared *wand* expression to that of a cardiac cell marker (*tinman*; [*tin*]) and a pericardial cell marker (*zfh1*) (Lockwood and Bodmer, 2002; Su *et al*., 1999). *wand* and *tin* are expressed in the same cells (Figs. 4.4 G-I, G'-I'), placing *wand* in the cardiac cells of the developing *Drosophila* heart, a tissue that in fact contacts the epidermal leading

edge and requires Dpp for its specification (Frasch, 1995).

Intriguingly, *wand* is also expressed in tissues that rely upon Dpp signaling for patterning and growth such as the gastric cecae and wing imaginal disc (Fig. 4.5 A-B). However, it is the co-expression of w*and* and the archetypal *dpp* reporter *tin* (Frasch, 1995; Xu *et al*., 1998; Yin and Frasch, 1998) in cardiac cells that led to our speculation that *wand* might be a transcriptionally-regulated target of Dpp that functions in a negative feedback loop. To test this idea, we examined *wand* expression in wild-type embryos, and in embryos either lacking Dpp signaling (Jra^{IA109}) or ectopically expressing Dpp signaling (mmy^{1}, and raw^{JG}). While *tin* expression is either absent or reduced in cardiac cells in Jra^{IA109} mutants and expanded in the mesoderm in raw^{JG} mutants (Lockwood and Bodmer, 2002; Yang and Su, 2011), *wand* expression in embryos with perturbed epidermal Dpp signaling is indistinguishable from that of wild-type (Figs. 4.5 C-E). These data show that *wand* expression is independent of Dpp and thus not part of a negative feedback loop.

CS functions as a signaling sink

Chondroitin sulfated proteoglycans are extracellular proteins that are found almost ubiquitously on cell surfaces and in extracellular matrix. As such, the expression of the CS proteoglycan biosynthetic genes *wand* and *gale* in cardiac cells underlying the LE, coupled with their genetic loss-of-function epidermal phenotypes, point to two possibilities for mesodermal CS function. First, CS might function as a canonical DPP sink, limiting an essential Dpp activity in both tissues: in the epidermis for dorsal closure and in the mesoderm for dorsal vessel (*Drosophila* heart) formation. Alternatively, a CS-modified extracellular matrix protein might be required for vectorial signaling: drawing signal to the mesoderm to promote dorsal vessel formation at the same time that it limits Dpp signaling activity in the epidermis. Genetic tests were used to distinguish between

sink and vectorial signaling roles for CS. In this regard loss of a CS sink is expected to lead to Dpp gain-of function phenotypes in both tissues, while loss of a vectorial signal facilitator is expected to lead to a Dpp gain-of-function phenotype in the epidermis, but to a loss-of-function phenotype in the mesoderm. Knowing that both *wand* and *gale* lead to Dpp gain-of-function phenotypes in the epidermis, we next tested for mesodermal phenotypes in mutants. To do this, we used the *B2-3-20* enhancer trap to monitor Dpp-dependent specification of embryonic cardiac cells (Fig. 4.6 A) (Bier *et al.*, 1989). *wand*^{RNAi} embryos exhibit a striking Dpp gain-of-function phenotype (Fig. 4.6 E), with even a greater excess of cardiac cells than has been reported previously for *raw* nulls (Fig. 4.6 C) (Klinedinst and Bodmer, 2003; Yang and Su, 2011). Thus, as depletion of CS leads to Dpp gain-of-function phenotypes in both the epidermis and the mesoderm, the molecule fulfills the criteria for sink function. In contrast mutations in *sdc* (which encodes an HS proteoglycan) and mmy (which is required for both HS and CS synthesis) lead to Dpp loss-of-function phenotypes – evidenced as a failure to specify cardiac cells in embryonic hemisegments (Fig. 4.6 B, D) (Knox *et al*., 2011).

We were somewhat surprised to see that the gain of Dpp in raw and wand mesodermal phenotypes were so different, with the wand phenotype appearing significantly stronger. While it is clear that Dpp is ectopically produced in both *raw* and *wand*, the use of a previously described Dpp reporter (Johnson *et al*., 2003) suggests that the differences observed between these genotypes can be explained by the difference in this reporter expression. In *raw*, the reporter is expressed broadly in the epidermis (Fig. 4.7 C) whereas in wild-type and *mmy* embryos (Fig. 4.7 A-B), there is no detectable difference in the reporter expression and staining is only present in the LE. This suggests that the Dpp produced in *raw* must not be an efficient source for function in the mesoderm. In *wand* on the other hand, the failure of the sink allows for excess dpp to be immediately available to its target cells in the dorsal most region of the

epidermis and underlying mesoderm. These data are consistent with the difference in JNK activation in the epidermis between *raw* and *mmy* where JNK is activated broadly in *raw* mutants but unchanged from wild-type in *mmy*. Therefore, we conclude that the Dpp reporter serves as a readout of JNK-dependent *dpp* expression.

Finally, having identified CS as an important modification in Dpp signal regulation, we tested whether the known cardiac CS proteoglycans *sdc* and *trol* either singly or together are sufficient to define the mesodermal sink. The role of *sdc* in mesodermal Dpp signaling plus its expression in cardiac cells makes it an attractive candidate as the mesoderm-expressed Dpp sink. However, *sdc* mutant embryos do not have cuticle defects associated with ectopic *dpp* transcription, nor do they exhibit ectopic epidermal *dpp* transcript *in situ* (data not shown). Thus, while *sdc* is an important effector of mesodermal Dpp signaling, it is not the Dpp sink. Similarly, *trol* mutant embryos did not exhibit cuticle defects associated with ectopic Dpp signaling, nor did we observe ectopic expression of *dpp* in the epidermis (data not shown). Last, we tested if the signal antagonist may not be tied to any particular protein, but is due to a combination of CS-modified proteins; thus, the overlapping cardiac expression domains of *sdc* and *trol* could compensate for the loss of one or the other. To test this model, we examined cuticle phenotypes and dpp expression in *trol sdc* double mutant embryos. While nearly 50% of double mutant animals failed to deposit a cuticle, we did not observe *mmy*-like cuticles or *dpp* expansion in *trol* mutants, *sdc* mutants, or *trol sdc* double mutants in excess of background levels (data not shown). We did not study the effects of *kon-tiki* or *multiplexin* loss of function, so one of these CS proteoglycans might still have a role in Dpp signal antagonism. The exact CS-modified protein(s) that enable the sink has yet to be identified.

Discussion

Embryonic cells differentiate, migrate, and divide in coordinated and repeatable patterns during development, and this reproducible execution is due in part to morphogen signaling. Morphogens as first defined by Alan Turing in his landmark paper, "The Chemical Basis of Morphogenesis," are diffusible chemicals that can self-organize to form a signaling gradient, wherein differential signal concentrations determine cellular reaction (Reviewed in Rogers and Schier, 2011; Turing, 1952). In 1969, Lewis Wolpert refined our understanding of morphogen gradients with the French Flag model, wherein a diffusible ligand forms a gradient between a source and distant cells, and cells produce a response that is dictated by the local concentration of morphogen the cell perceives (Wolpert, 1969). Shortly afterwards, Francis Crick realized that signal production and spreading will eventually lead to an even distribution of signal across all cells and noted that generation of a stable continuous gradient requires a "sink," a signaling component located at a distance from the source that destroys the signal (Crick, 1970). Morphogen gradients could most easily be explained by rapid, free diffusion in a closed system with constant destruction of the signaling ligand by a signaling sink. In time the model would be refined, in that in order to form a stable gradient, a sink need not be localized, and the effect of ligands binding to their receptors could in fact be sufficient to form a stable signaling gradient (Yu *et al*., 2009); overexpression studies indicated that receptors can serve as a sink for their ligands, as indicated by decreased signaling of *Drosophila* BMP homologue Decapentaplegic (Dpp) in cells adjacent to where the receptor Thickveins (Tkv) is ectopically increased (Lander *et al*., 2009; Mizutani *et al*., 2005). Additionally, not all morphogens establish gradients through the classical source-sink mechanism; the shape of the Bicoid gradient is primarily established through mRNA diffusion and distribution *(Lipshitz, 2009; Spirov et al*., 2009).

Despite the fact that a localized sink, either near or distant from the signaling source, has never been successfully identified in vivo, there is compelling evidence that one might exist. Several molecules have been shown to have the ability to bind to extracellular ligands and in some cases remove them from the system. With respect to BMP/Dpp signaling, there is evidence that the proteoglycan Perlecan serves as a sink for growth factors in the mammalian growth plate (Aviezer *et al*., 1994; Deguchi *et al*., 2002; Mongiat *et al.*, 2000; Smith *et al.*, 2007). In *Drosophila*, artificial BMP/Dpp sinks can be created through overexpression of heparan sulfate (HS) proteoglycans Dally and Dally-like (Belenkaya *et al*., 2004b) or overexpression of signaling receptors *(Lander et al.*, 2009; Mizutani *et al*., 2005). In *Drosophila* Decapentaplegic (Dpp) signaling, for instance, a localized sink could be functioning to restrict Dpp to the hub cells of *Drosophila* adult testes and ovaries, as well as the leading edge of the mesoderm and epidermis during embryonic dorsal closure (Humphreys *et al*., 2013; Kawase *et al*., 2004; Shivdasani and Ingham, 2003; Song *et al.*, 2004; Yang and Su, 2011)

In this study, we have shown evidence of the first genetically-defined localized signaling sink that converts a long-range signaling molecule into a short range one (Fig. 4.8). Our identification of *wand* and *Gale* as Dpp signaling antagonists points to CS as an important molecule functioning in shaping Dpp gradients in *Drosophila* development. Consistent with this idea is that *Drosophila* are reported to have high chondroitin-4-sulfate expression in ovaries (Pinto *et al.*, 2004), but little *de novo* heparan sulfate synthesis in embryos until about 10–12 hrs. AEL; there is a significant component of CS present in the embryo at this point, though whether it is maternally deposited or made *de novo* is unknown (Pinto *et al*., 2004). CS-C is only detected in trace amounts in *Drosophila* larvae, and chondroitin during embryonic and adult life is 4-sulfated or unsulfated (Pinto *et al*., 2004). CS is more prevalent than heparan sulfate at all stages in *Drosophila* development, having nearly equal levels in embryos, and approximately

20:1 and 10:1 ratios of CS to HS in 3rd instar larvae and adults, respectively *(Toyoda et al*., 2000).

We have previously noted in wild-type embryos that Mad phosphorylation rapidly decays in the epidermis during dorsal closure in a *mmy*-dependent fashion (Humphreys *et al*., 2013). Interestingly, the onset of expression of *wand* in the mesoderm adjacent to the leading edge coincides with this decay; further work will determine if CS synthesis might be the critical step in transitioning epidermal Dpp from a long-range to a short-range signal during dorsal closure. Experimental evidence has suggested that altering the heparan/chondroitin balance may be important in transitioning CS from a signaling mediator to a signaling sink. Mammalian Perlecan is involved in FGF delivery, and it can be modified by CS and HS. However, FGF is not released to its receptor if Perlecan is highly CS-modified; thus, CS may mark the change between a signaling effector and a sink in this protein (Smith *et al*., 2007). Unlike in the dorsolateral epidermis, the wing disc is an area of long-range Dpp signaling (Lecuit *et al*., 1996; Nellen *et al*., 1996; Schwank *et al.*, 2011). Though *wand* expression would likely lead to CS synthesis in the wing disc, this does not transition Dpp to a short-range signal in this context; thus the presence of CS does not strictly define short-range signaling. Context is very important in determining the interactions between CS proteoglycans and extracellular signaling molecules, and timing, dosage, sulfation, and other factors can determine whether the effect of a proteoglycan is positive, negative, or neutral on extracellular signals (Bai *et al*., 1999; Li *et al*., 2010; Mizumoto *et al*., 2013; Olivares *et al*., 2009; Shintani *et al*., 2006).

The embryonic epidermis is not the only tissue where Dpp signal is restricted to a short range. A similar restriction of Dpp signaling is seen in the stem cell niche of the testis, where Dpp expressed in somatic cells of the testes maintains the germline stem cells (Kawase *et al*., 2004; Michel *et al*., 2011; Song *et al*., 2004). It has also been

demonstrated that BMP signaling is, at least in part, modulated by an extracellular matrix containing type IV collagen in the *Drosophila* ovaries by sequestration of the ligand, Dpp (Wang, *et al*., 2008). Whether signaling range in these contexts is also restricted by chondroitin sulfate is unknown.

It may at first be surprising that *Gale* and *wand* mutants were not generated in the Heidelberg screens for mutants affecting the embryonic pattern of cuticle (Jürgens *et al*., 1984). After all, this was the screen that generated alleles of *dpp* antagonists, including *mmy* and *raw* (Bates *et al*., 2008; Byars *et al*., 1999; Humphreys *et al*., 2013). This could be due to the fact that *wand* is maternally deposited, and this maternal transcript may be sufficient to complete embryonic patterning in the absence of zygotic-encoded *wand*. In fact, the two alleles of *wand* that we tested failed to reproduce the *mmy* mutant phenotype. The phenotypes of *Gale* and *mmy* mutant embryos might be less severe than those seen in *wand* RNAi embryos for a few different reasons. First, there is a salvage pathway for hexosamines (including GalNAc) that allows them to reenter the pathway downstream of *mmy* and *Gale* (Vocadlo *et al*., 2003). As *wand* functions downstream of salvage, GalNAc recovered in the salvage pathway would still be blocked from being polymerized into CS in the RNAi embryos.

A second factor could be enzymatic redundancy. It is notable that *wand* is not the only predicted chondroitin synthase in the Drosophila genome. *CG9220* is predicted to encode an enzyme with similar function to *wand* (Wilson, 2002). Protein domain prediction identifies a chondroitin N-acetylgalactosaminyltransferase domain. Further study will determine if the expression patterns of *CG9220* and *wand* are complimentary or overlapping. Mice null for *wand* homologue *Css2* have no obvious phenotypic or morphological changes, perhaps due to redundancy of CS synthesis enzymes (Ogawa *et al*., 2012). Indeed, loss-of-function of *Css2* decreases the quantity of CS chains exceeding 10 kDa in weight, but does not affect the total number of CS chains attached

to core proteins (Ogawa *et al*., 2012). Similarly, mutations in *Gale* may have partially penetrant effects due to potentially redundant enzymatic activities from the product of *CG5955*, a predicted UDP-glucose 4-epimerase (Flybase). However, *CG5955* is not found in embryos until 16 hrs. after egg lay, according to the modENCODE RNA expression database (Celniker *et al*., 2009).

Tangential to the goal of this study was the observation that Dlp levels are decreased when glycosylation is inhibited in *mmy* mutant embryos. In many cases, glycosylation has been demonstrated to be dispensable for the interaction of a proteoglycan and signaling ligands. The *C. elegans* glypican LON-2 is an antagonist of BMP signaling (Gumienny *et al*., 2007; Taneja-Bageshwar and Gumienny, 2012). LON-2 has two functional domains that are able to bind to BMP; the C-terminal domain contains heparan sulfate attachment sites, while the N-terminal domain has no attachments but is able to bind to BMP and inhibit signaling independent of the C-terminal. In *Drosophila* the protein Dally does not require HS attachment to complete its role in Dpp signaling, though HS does make it more efficient (Kirkpatrick *et al*., 2006b). Expression of a *dally* construct with all HS attachment sites removed was able to partially rescue some signaling defects in *dally* mutant animals, especially in wing formation (Kirkpatrick *et al.*, 2006b). These data are complicated by the fact that the authors were unable to determine how much Dally was generated by the rescue construct. As partial loss of HS chains may decrease glypican stability, future studies on the role of HS and CS modification on protein function and interaction should take care to ensure that alterations in HS and CS levels do not result in unintended reduction in protein stability. Overall, the data presented here indicate that CS production may be utilized to create an extremely sharp signaling gradient, and this mechanism may be used in other organisms and developmental systems toward the same end. Increasing CS production might even be explored as a potential therapy for diseases caused by an

overabundance of BMP signaling activity.

Loss of function of *raw*, an antagonist of JNK, the transcriptional activator of epidermal dpp expression in the epidermis (Bates *et al.*, 2008; Byars *et al*., 1999), leads to overspecification of cardiac cells (Fig. 4.6 C) (Yang and Su, 2011) (Klinedinst and Bodmer, 2003; Yang and Su, 2011). While the raw phenotype is modest, *wand*^{RNAi} embryos have a clearer excess of cardiac cells (Fig. 4.6 E). The differences in overspecification likely reflect the different origins of Dpp, which is produced by both the activation of JNK and by Dpp autoregulation in the leading edge. Specifically, JNK activity initiates Dpp production and Dpp signaling maintains its own production during dorsal closure. A tool developed by Newfeld (*dpp*^{151H}, Johnson *et al*., 2003) was reported to be activated by Dpp autoregulation. In our hands, however, even though Dpp is produced and maintained ectopically in the epidermis of *mmy* and *raw* mutants, this reporter construct is only activated ectopically in *raw* (Fig. 4.7 C) whereas *mmy* and wild-type embryos are indistinguishable (Fig. 4.7 A-B). We hypothesize that this reporter line is activated by JNK rather than dpp autoregulation and that whereas ectopic Dpp activity in raw mutant embryos results from derepression of Jun in the epidermis, ectopic Dpp activity in mutants in UDP-GlcNAc pathway results from direct derepression of Dpp. Thus, in the case of *raw*, where Dpp signals from a broad epidermal source to the underlying mesoderm, overspecification of cardiac cells is low. On the other hand, in the case of *mmy*, where there is too much Dpp signal emanating from a physiologically relevant source due to a failure in the sink, extensive overspecification of cardiac cells is observed. Taken together, these data suggest that Dpp produced in excess in and around the leading edge and maintained by autoregulation and not by JNK is responsible for ectopic cardiac cell specification in the mesoderm and also results in epidermal failures in dorsal closure and patterning (Fig. 4.8).

Materials and methods

Drosophila strains

Fly lines used for this study include w^{1118}, mmy^{1}, mmy^{P15133}, *Tub-Gal4* (Bloomington), $mmy^{l(2)03851}$ (M. Krasnow), $Gale^{F00624.4}$ and $Gale^{\Delta y}$ (J. Fridovich-Kiel), sdc^{23} and sdc^{97} (G. Vorbrüggen), *B2-3-20* (E. Bier), $CG43313^{PL61}$ and $CG43313^{PL69}$ (A. Vincent), and the Vienna *Drosophila* UAS-shRNA lines (Dietzl *et al*., 2007) v2598, v2601, v2826, v5027, v6176, v6177, v7262, v7263, v7394, v7427, v7949, v8107, v12079, v13474, v16981, v16982, v21761, v26517, v29084, v29085, v33366, v33368, v35572, v35573, v42781, v44939, v45194, v45457, v46419, v46421, v51977, v100016, v100185, v101307, v101417, v101660, v102288, v104256, v104281, v105791, v106134, v106605, v106839, and v107840 (VDRC).

Cuticle analyses

For embryonic cuticle analysis, animals were dechorionated in 50% bleach solution and incubated overnight at 60°C in One-Step Mounting Medium (30% CMCP-10, 13% lactic acid, 57% glacial acetic acid). In some cases embryos were devitellinized prior to One-Step Mounting Medium incubation by shaking for 1 min. in equal parts methanol and heptane. Cuticles were visualized with dark field microscopy.

RNA in situ hybridization

For in situ hybridization, we generated digoxigenin-labeled probes as described previously (Byars *et al*., 1999). Probes were detected with anti-digoxigenin-AP Fab fragments (Roche), and visualized with DIC optics.

Immunolocalization

Alkaline phosphase immunolocalization studies were performed as described (Sullivan *et al.*, 1999). Fluorescent Phospho-Mad visualization was performed as previously described (Humphreys *et al*., 2013) using confocal techniques. For immunolocalization studies, we used rabbit anti-Phospho-Smad1,5 Ser463/465 (1:20, Cell Signaling Technology), mouse anti-β-Gal (1:500, Promega), goat anti-mouse alkaline phosphatase (1:2000, Promega), goat anti-rabbit alkaline phosphatase (concentration) (Jackson ImmunoResearch), and goat anti-rabbit Alexa Fluor 488 antibodies (1:200, Invitrogen Molecular Probes).

Western blotting

For Western blotting studies, control and experimental protein lysates were made from embryos 5-17 hrs. after egg lay (AEL). Absence of a GFP-marked balancer chromosome was used to distinguish mutant homozygote embryos from wild-type siblings. Protein lysates were separated on SDS-acrylamide gel and analyzed by Western blotting using anti-Dally-like protein antibody (1:1000, Developmental Studies Hybridoma Bank) and anti-Tubulin control (1:50000, 1:10,000). HRP-conjugated rabbit-anti-mouse was used as the secondary antibody (Jackson). Blots were stripped using a mild stripping protocol (Abcam) prior to being re-probed for Tubulin control.

References

Akiyama, T., Kamimura, K., Firkus, C., Takeo, S., Shimmi, O., and Nakato, H. (2008). Dally regulates Dpp morphogen gradient formation by stabilizing Dpp on the cell surface. Dev Biol *313*, 408-419.

Alarmo, E.-L., Rauta, J., Kauraniemi, P., Karhu, R., Kuukasjärvi, T., and Kallioniemi, A. (2006). Bone morphogenetic protein 7 is widely overexpressed in primary breast cancer. Genes. Chromosomes Cancer *45*, 411–419.

Andrew, D.J., Baig, A., Bhanot, P., Smolik, S.M., and Henderson, K.D. (1997). The

Drosophila dCREB-A gene is required for dorsal/ventral patterning of the larval cuticle. Development *124*, 181–193.

Araújo, S.J., Aslam, H., Tear, G., and Casanova, J. (2005). mummy/cystic encodes an enzyme required for chitin and glycan synthesis, involved in trachea, embryonic cuticle and CNS development--analysis of its role in *Drosophila* tracheal morphogenesis. Dev. Biol. *288*, 179–193.

Aviezer, D., Hecht, D., Safran, M., Eisinger, M., David, G., and Yayon, A. (1994). Perlecan, basal lamina proteoglycan, promotes basic fibroblast growth factor-receptor binding, mitogenesis, and angiogenesis. Cell *79*, 1005–1013.

Bai, X., Wei, G., Sinha, A., and Esko, J.D. (1999). Chinese hamster ovary cell mutants defective in glycosaminoglycan assembly and glucuronosyltransferase I. J. Biol. Chem. *274*, 13017–13024.

Bates, K.L., Higley, M., and Letsou, A. (2008). Raw mediates antagonism of AP-1 activity in *Drosophila*. Genetics *178*, 1989–2002.

Beckett, K., Franch-Marro, X., and Vincent, J.P. (2008). Glypican-mediated endocytosis of Hedgehog has opposite effects in flies and mice. Trends Cell Biol *18*, 360-363.

Belenkaya, T.Y., Han, C., Yan, D., Opoka, R.J., Khodoun, M., Liu, H., and Lin, X. (2004). *Drosophila* Dpp morphogen movement is independent of dynamin-mediated endocytosis but regulated by the glypican members of heparan sulfate proteoglycans. Cell *119*, 231–244.

Bier, E., Vaessin, H., Shepherd, S., Lee, K., McCall, K., Barbel, S., Ackerman, L., Carretto, R., Uemura, T., and Grell, E. (1989). Searching for pattern and mutation in the *Drosophila* genome with a P-lacZ vector. Genes Dev. *3*, 1273–1287.

Bourbon, H.-M., Gonzy-Treboul, G., Peronnet, F., Alin, M.-F., Ardourel, C., Benassayag, C., Cribbs, D., Deutsch, J., Ferrer, P., Haenlin, M., *et al.* (2002). A P-insertion screen identifying novel X-linked essential genes in *Drosophila*. Mech. Dev. *110*, 71–83.

Breitling, J., and Aebi, M. (2013). N-linked protein glycosylation in the endoplasmic reticulum. Cold Spring Harb. Perspect. Biol. *5*, a013359.

Brummel, T.J., Twombly, V., Marqués, G., Wrana, J.L., Newfeld, S.J., Attisano, L., Massagué, J., O'Connor, M.B., and Gelbart, W.M. (1994). Characterization and relationship of dpp receptors encoded by the saxophone and thick veins genes in *Drosophila*. Cell *78*, 251–261.

Byars, C.L., Bates, K.L., and Letsou, A. (1999). The dorsal-open group gene raw is required for restricted DJNK signaling during closure. Development *126*, 4913–4923.

Capurro, M.I., Xu, P., Shi, W., Li, F., Jia, A., and Filmus, J. (2008). Glypican-3 inhibits Hedgehog signaling during development by competing with patched for Hedgehog binding. Dev Cell *14*, 700-711.

Celniker, S.E., Dillon, L.A.L., Gerstein, M.B., Gunsalus, K.C., Henikoff, S., Karpen, G.H., Kellis, M., Lai, E.C., Lieb, J.D., MacAlpine, D.M., *et al*. (2009). Unlocking the secrets of the genome. Nature *459*, 927–930.

Correia, T., Papayannopoulos, V., Panin, V., Woronoff, P., Jiang, J., Vogt, T.F., and Irvine, K.D. (2003). Molecular genetic analysis of the glycosyltransferase Fringe in *Drosophila*. Proc. Natl. Acad. Sci. U. S. A. *100*, 6404–6409.

Crick, F. (1970). Diffusion in embryogenesis. Nature *225*, 420–422.

Deguchi, Y., Okutsu, H., Okura, T., Yamada, S., Kimura, R., Yuge, T., Furukawa, A., Morimoto, K., Tachikawa, M., Ohtsuki, S., *et al*. (2002). Internalization of basic fibroblast growth factor at the mouse blood-brain barrier involves perlecan, a heparan sulfate proteoglycan. J. Neurochem. *83*, 381–389.

Dietzl, G., Chen, D., Schnorrer, F., Su, K.-C., Barinova, Y., Fellner, M., Gasser, B., Kinsey, K., Oppel, S., Scheiblauer, S., *et a*l. (2007). A genome-wide transgenic RNAi library for conditional gene inactivation in *Drosophila*. Nature *448*, 151–156.

Fan, H., Oro, A.E., Scott, M.P., and Khavari, P.A. (1997). Induction of basal cell carcinoma features in transgenic human skin expressing Sonic Hedgehog. Nat. Med. *3*, 788–792.

Fisher, M.C., Li, Y., Seghatoleslami, M.R., Dealy, C.N., and Kosher, R.A. (2006). Heparan sulfate proteoglycans including syndecan-3 modulate BMP activity during limb cartilage differentiation. Matrix Biol. J. Int. Soc. Matrix Biol. *25*, 27–39.

Frasch, M. (1995). Induction of visceral and cardiac mesoderm by ectodermal Dpp in the early *Drosophila* embryo. Nature *374*, 464–467.

Friedrich, M.V., Schneider, M., Timpl, R., and Baumgartner, S. (2000). Perlecan domain V of *Drosophila* melanogaster. Sequence, recombinant analysis and tissue expression. Eur. J. Biochem. FEBS *267*, 3149–3159.

Gallet, A., Staccini-Lavenant, L., and Therond, P.P. (2008). Cellular trafficking of the glypican Dally-like is required for full-strength Hedgehog signaling and wingless transcytosis. Dev Cell *14*, 712-725.

Gobbi, G., Sangiorgi, L., Lenzi, L., Casadei, R., Canaider, S., Strippoli, P., Lucarelli, E., Ghedini, I., Donati, D., Fabbri, N., *et al*. (2002). Seven BMPs and all their receptors are simultaneously expressed in osteosarcoma cells. Int. J. Oncol. *20*, 143–147.

Graveley, B.R., Brooks, A.N., Carlson, J.W., Duff, M.O., Landolin, J.M., Yang, L., Artieri, C.G., van Baren, M.J., Boley, N., Booth, B.W., *et al*. (2011). The developmental transcriptome of *Drosophila* melanogaster. Nature *471*, 473–479.

Gumienny, T.L., MacNeil, L.T., Wang, H., de Bono, M., Wrana, J.L., and Padgett, R.W. (2007). Glypican LON-2 is a conserved negative regulator of BMP-like signaling in Caenorhabditis elegans. Curr. Biol. CB *17*, 159–164.

Hammonds, A.S., Bristow, C.A., Fisher, W.W., Weiszmann, R., Wu, S., Hartenstein, V.,

Kellis, M., Yu, B., Frise, E., and Celniker, S.E. (2013). Spatial expression of transcription factors in *Drosophila* embryonic organ development. Genome Biol. *14*, R140.

Hardingham, T.E., and Fosang, A.J. (1992). Proteoglycans: many forms and many functions. FASEB J. *6*, 861–870.

Hoodless, P.A., Haerry, T., Abdollah, S., Stapleton, M., O'Connor, M.B., Attisano, L., and Wrana, J.L. (1996). MADR1, a MAD-related protein that functions in BMP2 signaling pathways. Cell *85*, 489–500.

Humphreys, G.B., Jud, M.C., Monroe, K.M., Kimball, S.S., Higley, M., Shipley, D., Vrablik, M.C., Bates, K.L., and Letsou, A. (2013). Mummy, A UDP-N-acetylglucosamine pyrophosphorylase, modulates DPP signaling in the embryonic epidermis of *Drosophila*. Dev. Biol. *381*, 434–445.

Jack, J., and Myette, G. (1997). The genes raw and ribbon are required for proper shape of tubular epithelial tissues in *Drosophila*. Genetics *147*, 243–253.

Jaźwińska, A., Kirov, N., Wieschaus, E., Roth, S., and Rushlow, C. (1999). The *Drosophila* gene *brinker* reveals a novel mechanism of Dpp target gene regulation. Cell *96*, 563–573.

Jin, Y., Tipoe, G.L., Liong, E.C., Lau, T.Y., Fung, P.C., and Leung, K.M. (2001). Overexpression of BMP-2/4, -5 and BMPR-IA associated with malignancy of oral epithelium. Oral Oncol. *37*, 225–233.

Johnson, A.., Bergman, C.., Kreitman, M., and Newfeld, S. (2003). Embryonic enhancers in the dpp disk region regulate a second round of Dpp signaling from the dorsal ectoderm to the mesoderm that represses Zfh-1 expression in a subset of pericardial cells. Dev. Biol. *262*, 137–151.

Jürgens, G., Wieschaus, E., Nüsslein-Volhard, C., and Kluding, H. (1984). Mutations affecting the pattern of the larval cuticle in *Drosophila* melanogaster. Dev. Genes Evol. *193*, 283–295.

Kaplan, F.S., Fiori, J., DE LA Peña, L.S., Ahn, J., Billings, P.C., and Shore, E.M. (2006). Dysregulation of the BMP-4 signaling pathway in fibrodysplasia ossificans progressiva. Ann. N. Y. Acad. Sci. *1068*, 54–65.

Katoh, M., and Terada, M. (1996). Overexpression of bone morphogenic protein (BMP)-4 mRNA in gastric cancer cell lines of poorly differentiated type. J. Gastroenterol. *31*, 137–139.

Kawase, E., Wong, M.D., Ding, B.C., and Xie, T. (2004). Gbb/Bmp signaling is essential for maintaining germline stem cells and for repressing bam transcription in the *Drosophila* testis. Development *131*, 1365–1375.

Kirkpatrick, C.A., Knox, S.M., Staatz, W.D., Fox, B., Lercher, D.M., and Selleck, S.B. (2006). The function of a *Drosophila* glypican does not depend entirely on heparan sulfate modification. Dev. Biol. *300*, 570–582.

Klinedinst, S.L., and Bodmer, R. (2003). Gata factor Pannier is required to establish competence for heart progenitor formation. Development *130*, 3027–3038.

Knox, J., Moyer, K., Yacoub, N., Soldaat, C., Komosa, M., Vassilieva, K., Wilk, R., Hu, J., Vazquez Paz, L. de L., Syed, Q., *et al*. (2011). Syndecan contributes to heart cell specification and lumen formation during *Drosophila* cardiogenesis. Dev. Biol. *356*, 279–290.

Lander, A.D., Nie, Q., Wan, F.Y.M., and Zhang, Y.-T. (2009). Localized ectopic expression of Dpp receptors in a *Drosophila* embryo. Stud. Appl. Math. Camb. Mass *123*, 175–214.

Larkin, M.A., Blackshields, G., Brown, N.P., Chenna, R., McGettigan, P.A., McWilliam, H., Valentin, F., Wallace, I.M., Wilm, A., Lopez, R., *et al*. (2007). Clustal W and Clustal X version 2.0. Bioinforma. Oxf. Engl. *23*, 2947–2948.

Lecuit, T., Brook, W.J., Ng, M., Calleja, M., Sun, H., and Cohen, S.M. (1996). Two distinct mechanisms for long-range patterning by Decapentaplegic in the *Drosophila* wing. Nature *381*, 387–393.

Letsou, A., Arora, K., Wrana, J.L., Simin, K., Twombly, V., Jamal, J., Staehling-Hampton, K., Hoffmann, F.M., Gelbart, W.M., Massagué, J., *et al*. (1995). *Drosophila* Dpp signaling is mediated by the punt gene product: A dual ligand-binding type II receptor of the TGFβ receptor family. Cell *80*, 899–908.

Li, Y., Laue, K., Temtamy, S., Aglan, M., Kotan, L.D., Yigit, G., Canan, H., Pawlik, B., Nürnberg, G., Wakeling, E.L., *et al*. (2010). Temtamy preaxial brachydactyly syndrome Is caused by loss-of-function mutations in chondroitin synthase 1, a potential target of BMP signaling. Am. J. Hum. Genet. *87*, 757–767.

Lindner, J.R., Hillman, P.R., Barrett, A.L., Jackson, M.C., Perry, T.L., Park, Y., and Datta, S. (2007). The *Drosophila* Perlecan gene trol regulates multiple signaling pathways in different developmental contexts. BMC Dev. Biol. *7*, 121.

Lipshitz, H.D. (2009). Follow the mRNA: a new model for Bicoid gradient formation. Nat. Rev. Mol. Cell Biol. *10*, 509–512.

Lockwood, W.K., and Bodmer, R. (2002). The patterns of wingless, decapentaplegic, and tinman position the *Drosophila* heart. Mech. Dev. *114*, 13–26.

Low, M.G. (1989). Glycosyl-phosphatidylinositol: a versatile anchor for cell surface proteins. FASEB J. *3*, 1600–1608.

Lyons, K.M., Pelton, R.W., and Hogan, B.L. (1990). Organogenesis and pattern formation in the mouse: RNA distribution patterns suggest a role for bone morphogenetic protein-2A (BMP-2A). Dev. Camb. Engl. *109*, 833–844.

Mandel, E.M., Kaltenbrun, E., Callis, T.E., Zeng, X.-X.I., Marques, S.R., Yelon, D., Wang, D.-Z., and Conlon, F.L. (2010). The BMP pathway acts to directly regulate Tbx20 in the developing heart. Dev. Camb. Engl. *137*, 1919–1929.

Massagué, J. (1998). TGF-β signal transduction. Annu. Rev. Biochem. *67*, 753–791.

Medioni, C., Astier, M., Zmojdzian, M., Jagla, K., and Sémériva, M. (2008). Genetic control of cell morphogenesis during *Drosophila* melanogaster cardiac tube formation. J. Cell Biol. *182*, 249–261.

Michel, M., Raabe, I., Kupinski, A.P., Pérez-Palencia, R., and Bökel, C. (2011). Local BMP receptor activation at adherens junctions in the *Drosophila* germline stem cell niche. Nat. Commun. *2*, 415.

Mizumoto, S., Fongmoon, D., and Sugahara, K. (2013). Interaction of chondroitin sulfate and dermatan sulfate from various biological sources with heparin-binding growth factors and cytokines. Glycoconj. J. *30*, 619–632.

Mizutani, C.M., Nie, Q., Wan, F.Y.M., Zhang, Y.-T., Vilmos, P., Sousa-Neves, R., Bier, E., Marsh, J.L., and Lander, A.D. (2005). Formation of the BMP Activity Gradient in the *Drosophila* Embryo. Dev. Cell *8*, 915–924.

Momota, R., Naito, I., Ninomiya, Y., and Ohtsuka, A. (2011). *Drosophila* type XV/XVIII collagen, Mp, is involved in Wingless distribution. Matrix Biol. *30*, 258–266.

Mongiat, M., Taylor, K., Otto, J., Aho, S., Uitto, J., Whitelock, J.M., and Iozzo, R.V. (2000). The protein core of the proteoglycan perlecan binds specifically to fibroblast growth factor-7. J. Biol. Chem. *275*, 7095–7100.

Nellen, D., Burke, R., Struhl, G., and Basler, K. (1996). Direct and long-range action of a DPP morphogen gradient. Cell *85*, 357–368.

Nishihara, S. (2010). Glycosyltransferases and transporters that contribute to proteoglycan synthesis in *Drosophila*: Identification and functional analyses using the heritable and inducible RNAi system. Methods Enzymol. *480*, 323-351.

Nishisho, I., Nakamura, Y., Miyoshi, Y., Miki, Y., Ando, H., Horii, A., Koyama, K., Utsunomiya, J., Baba, S., and Hedge, P. (1991). Mutations of chromosome 5q21 genes in FAP and colorectal cancer patients. Science *253*, 665–669.

Nüsslein-Volhard, C., Wieschaus, E., and Kluding, H. (1984). Mutations affecting the pattern of the larval cuticle in *Drosophila* melanogaster. Wilhelm Rouxs Arch. Dev. Biol. *193*, 267–282.

Ogawa, H., Hatano, S., Sugiura, N., Nagai, N., Sato, T., Shimizu, K., Kimata, K., Narimatsu, H., and Watanabe, H. (2012). Chondroitin sulfate synthase-2 is necessary for chain extension of chondroitin sulfate but not critical for skeletal development. PloS One *7*, e43806.

Olivares, G.H., Carrasco, H., Aroca, F., Carvallo, L., Segovia, F., and Larraín, J. (2009). Syndecan-1 regulates BMP signaling and dorso-ventral patterning of the ectoderm during early Xenopus development. Dev. Biol. *329*, 338–349.

Padgett, R.W., Wozney, J.M., and Gelbart, W.M. (1993). Human BMP sequences can confer normal dorsal-ventral patterning in the *Drosophila* embryo. Proc. Natl. Acad.

Sci. U. S. A. *90*, 2905–2909.

Pinto, D.O., Ferreira, P.L., Andrade, L.R., Petrs-Silva, H., Linden, R., Abdelhay, E., Araújo, H.M.M., Alonso, C.-E.V., and Pavão, M.S.G. (2004). Biosynthesis and metabolism of sulfated glycosaminoglycans during *Drosophila* melanogaster development. Glycobiology *14*, 529–536.

Polakis, P. (2012). Wnt signaling in cancer. Cold Spring Harb. Perspect. Biol. *4*.

Ring, J.M., and Martinez Arias, A. (1993). Puckered, a gene involved in position-specific cell differentiation in the dorsal epidermis of the *Drosophila* larva. Dev. Camb. Engl. Suppl. 251–259.

Rogers, K.W., and Schier, A.F. (2011). Morphogen gradients: from generation to interpretation. Annu. Rev. Cell Dev. Biol. *27*, 377–407.

Sanders, R.D., Sefton, J.M.I., Moberg, K.H., and Fridovich-Keil, J.L. (2010). UDP-galactose 4' epimerase (GALE) is essential for development of *Drosophila* melanogaster. Dis. Model. Mech. *3*, 628–638.

Schwank, G., Dalessi, S., Yang, S.-F., Yagi, R., de Lachapelle, A.M., Affolter, M., Bergmann, S., and Basler, K. (2011). Formation of the long range Dpp morphogen gradient. PLoS Biol. *9*.

Shintani, Y., Takashima, S., Asano, Y., Kato, H., Liao, Y., Yamazaki, S., Tsukamoto, O., Seguchi, O., Yamamoto, H., Fukushima, T., *et al*. (2006). Glycosaminoglycan modification of neuropilin-1 modulates VEGFR2 signaling. EMBO J. *25*, 3045–3055.

Shivdasani, A.A., and Ingham, P.W. (2003). Regulation of stem cell maintenance and transit amplifying cell proliferation by TGF-β signaling in *Drosophila* spermatogenesis. Curr. Biol. *13*, 2065–2072.

Singh, A., and Morris, R.J. (2010). The Yin and Yang of bone morphogenetic proteins in cancer. Cytokine Growth Factor Rev. *21*, 299–313.

Smith, S.M.-L., West, L.A., Govindraj, P., Zhang, X., Ornitz, D.M., and Hassell, J.R. (2007). Heparan and chondroitin sulfate on growth plate perlecan mediate binding and delivery of FGF-2 to FGF receptors. Matrix Biol. J. Int. Soc. Matrix Biol. *26*, 175–184.

Song, X., Wong, M.D., Kawase, E., Xi, R., Ding, B.C., McCarthy, J.J., and Xie, T. (2004). Bmp signals from niche cells directly repress transcription of a differentiation-promoting gene, bag of marbles, in germline stem cells in the *Drosophila* ovary. Development *131*, 1353–1364.

Spirov, A., Fahmy, K., Schneider, M., Frei, E., Noll, M., and Baumgartner, S. (2009). Formation of the bicoid morphogen gradient: an mRNA gradient dictates the protein gradient. Dev. Camb. Engl. *136*, 605–614.

Su, M.T., Fujioka, M., Goto, T., and Bodmer, R. (1999). The *Drosophila* homeobox

genes zfh-1 and even-skipped are required for cardiac-specific differentiation of a numb-dependent lineage decision. Development *126*, 3241–3251.

Sullivan, W., Ashburner, M., and Hawley, R.S. (2000). *Drosophila* protocols, Ch. 9 (CSHL Press).

Taneja-Bageshwar, S., and Gumienny, T.L. (2012). Two functional domains in C. elegans glypican LON-2 can independently inhibit BMP-like signaling. Dev. Biol. *371*, 66–76.

Tomancak, P., Berman, B.P., Beaton, A., Weiszmann, R., Kwan, E., Hartenstein, V., Celniker, S.E., and Rubin, G.M. (2007). Global analysis of patterns of gene expression during *Drosophila* embryogenesis. Genome Biol. *8*, R145.

Tonning, A., Helms, S., Schwarz, H., Uv, A.E., and Moussian, B. (2006). Hormonal regulation of mummy is needed for apical extracellular matrix formation and epithelial morphogenesis in *Drosophila*. Dev. Camb. Engl. *133*, 331–341.

Toyoda, H., Kinoshita-Toyoda, A., and Selleck, S.B. (2000). Structural analysis of glycosaminoglycans in *Drosophila* and *Caenorhabditis elegans* and demonstration that tout-velu, a *Drosophila* gene related to EXT tumor suppressors, affects heparan sulfate in vivo. J. Biol. Chem. *275*, 2269–2275.

Turing, A.M. (1952). The chemical basis of morphogenesis. Philos. Trans. R. Soc. Lond. B. Biol. Sci. *237*, 37–72.

Urist, M.R. (1965). Bone: formation by autoinduction. Science *150*, 893–899.

Vocadlo, D.J., Hang, H.C., Kim, E.-J., Hanover, J.A., and Bertozzi, C.R. (2003). A chemical approach for identifying O-GlcNAc-modified proteins in cells. Proc. Natl. Acad. Sci. *100*, 9116–9121.

Wang, X., Harris, R.E., Bayston, L.J., Ashe, H.L. (2008). Type IV collagens regulate BMP signaling in *Drosophila*. Nature *455*, 72-77.

Waterhouse, A.M., Procter, J.B., Martin, D.M.A., Clamp, M., and Barton, G.J. (2009). Jalview Version 2—a multiple sequence alignment editor and analysis workbench. Bioinformatics *25*, 1189–1191.

Wells, L., Vosseller, K., and Hart, G.W. (2001). Glycosylation of nucleocytoplasmic proteins: signal transduction and O-GlcNAc. Science *291*, 2376–2378.

Wilson, I.B.H. (2002). Glycosylation of proteins in plants and invertebrates. Curr. Opin. Struct. Biol. *12*, 569–577.

Winnier, G., Blessing, M., Labosky, P.A., and Hogan, B.L. (1995). Bone morphogenetic protein-4 is required for mesoderm formation and patterning in the mouse. Genes Dev. *9*, 2105–2116.

Wolpert, L. (1969). Positional information and the spatial pattern of cellular differentiation. J. Theor. Biol. *25*, 1–47.

Xia, Y., and Karin, M. (2004). The control of cell motility and epithelial morphogenesis by Jun kinases. Trends Cell Biol. *14*, 94–101.

Xu, X., Yin, Z., Hudson, J.B., Ferguson, E.L., and Frasch, M. (1998). Smad proteins act in combination with synergistic and antagonistic regulators to target Dpp responses to the *Drosophila* mesoderm. Genes Dev. *12*, 2354–2370.

Yada, T., Gotoh, M., Sato, T., Shionyu, M., Go, M., Kaseyama, H., Iwasaki, H., Kikuchi, N., Kwon, Y.-D., Togayachi, A., *et al*. (2003). Chondroitin sulfate synthase-2. Molecular cloning and characterization of a novel human glycosyltransferase homologous to chondroitin sulfate glucuronyltransferase, which has dual enzymatic activities. J. Biol. Chem. *278*, 30235–30247.

Yang, S.-A., and Su, M.-T. (2011). Excessive Dpp signaling induces cardial apoptosis through dTAK1 and dJNK during late embryogenesis of *Drosophila*. J. Biomed. Sci. *18*, 85.

Yin, Z., and Frasch, M. (1998). Regulation and function of tinman during dorsal mesoderm induction and heart specification in *Drosophila*. Dev. Genet. *22*, 187–200.

Ying, Q.-L., Nichols, J., Chambers, I., and Smith, A. (2003). BMP induction of Id proteins suppresses differentiation and sustains embryonic stem cell self-renewal in collaboration with STAT3. Cell *115*, 281–292.

Yu, S.R., Burkhardt, M., Nowak, M., Ries, J., Petrášek, Z., Scholpp, S., Schwille, P., and Brand, M. (2009). Fgf8 morphogen gradient forms by a source-sink mechanism with freely diffusing molecules. Nature *461*, 533–536.

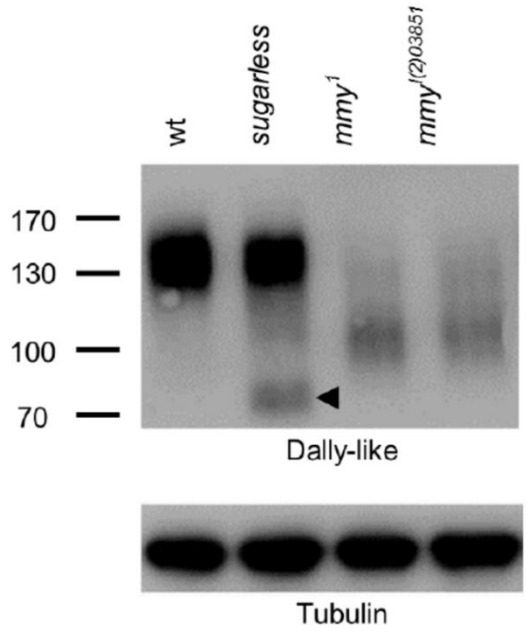

Fig. 4.1 *mmy* hypomorphs have defective glycosylation. A Western blot analysis of Dally-like protein (Dlp). Dlp consists of a core protein with molecular weight 85 kDa, which is post-translationally modified by glycosylation with heparin sulfate chains of variable length. The glycosylated protein appears as a smear of products of approximate molecular weight 13-160 kDa. The core protein is denoted by the black arrow in the *sugarless* lane, as *sugarless*, is required to initiate heparin sulfate attachment; the presence of glycosylated Dlp, is likely the product of enzyme translated from maternal mRNA. A reduction in Dlp molecular weight is observed in two independently generated hypomorphic *mmy* mutants, suggesting decreased availability of UDP-GlcNAc for post-translational glycosyl modifications; there is also a generalized decrease of band intensity in *mmy* mutant lysates, suggesting a decrease of Dlp protein in these genetic backgrounds.

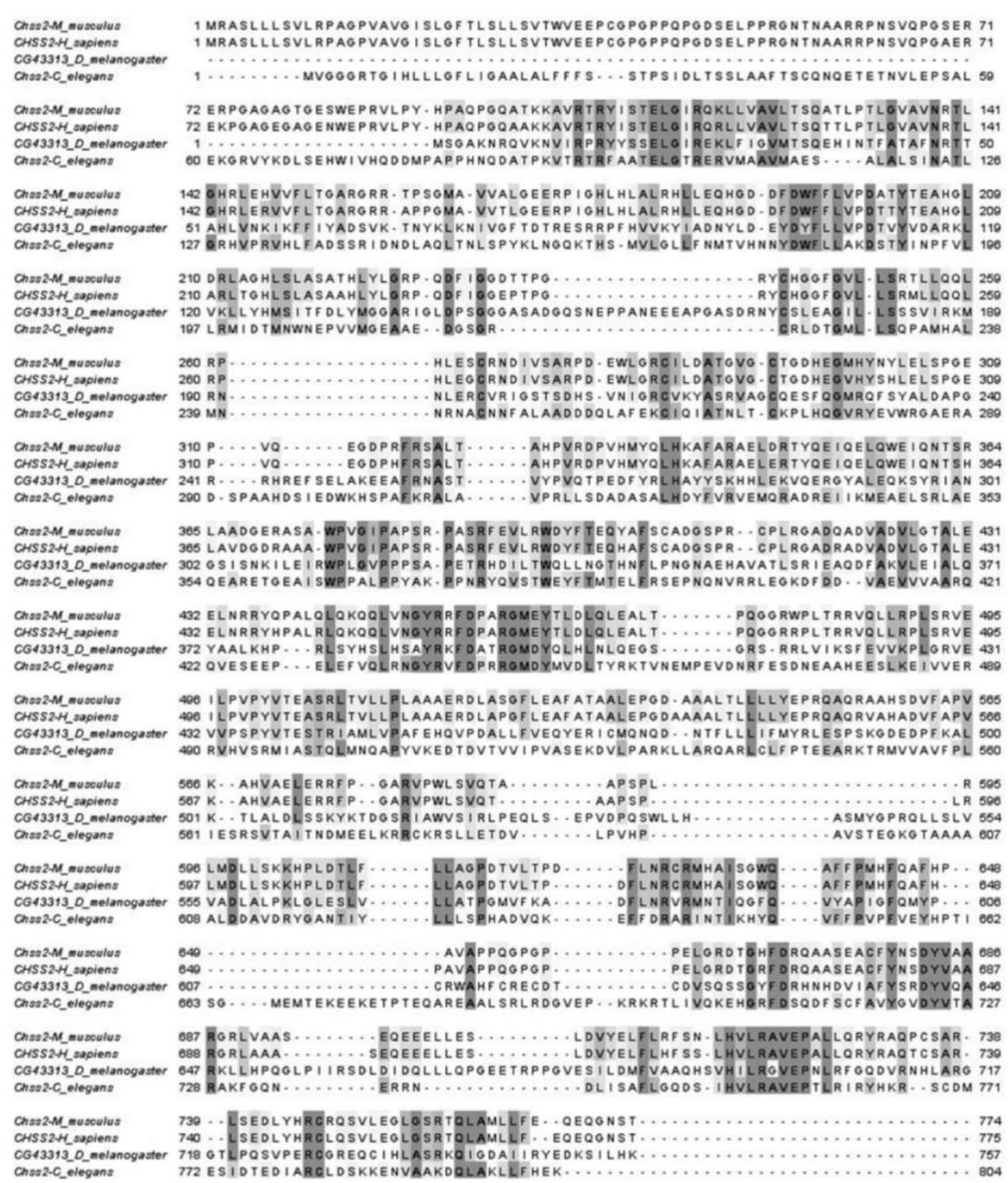

Fig. 4.2 *wand* is homologous to Chondroitin sulfate synthase 2. Multiple sequence alignment between Chondroitin sulfate synthase 2 (M. musculus), Chondroitin sulfate synthase 2 (H. sapiens), CG43313 (D. melanogaster), and Chondroitin sulfate synthase 2 (C. elegans). Sequences were aligned using ClustalX 2.1 (Larkin *et al*., 2007) and the alignment was shaded according to BLOSSUM62 scores using Jalview 2.8.1 (Waterhouse *et al*., 2009).

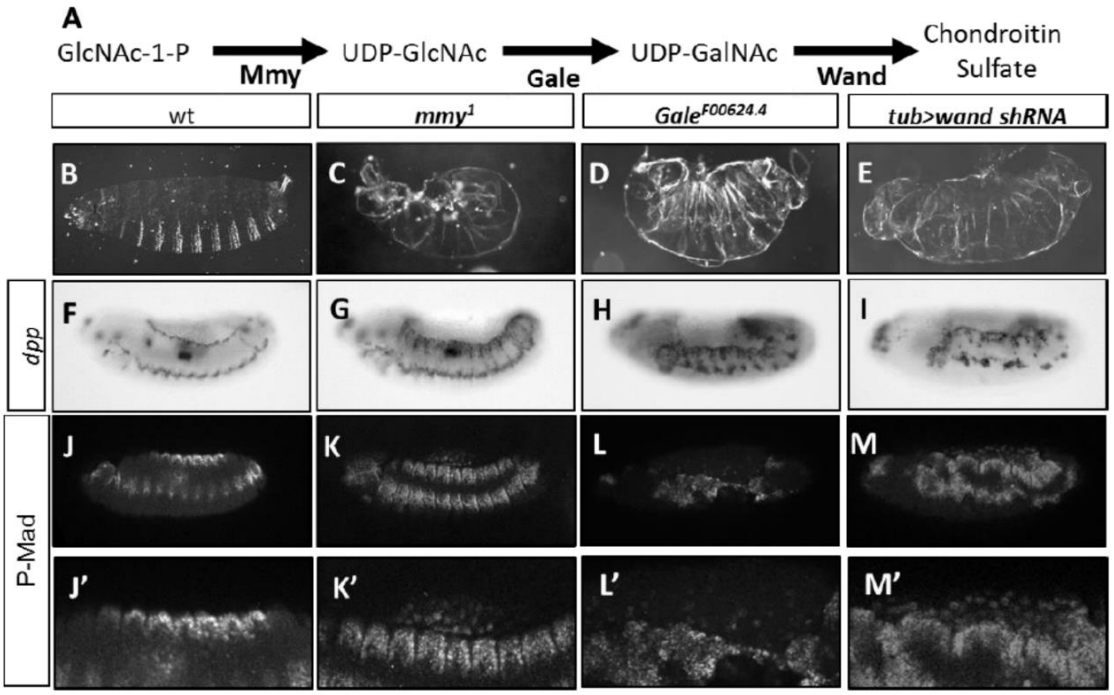

Fig. 4.3 Chondroitin sulfate synthesis is required for Dpp antagonism. (A). Biochemical pathway for converting GlcNAc-1-P to chondroitin. (B) A wild-type cuticle. (C) A *mmy*^{1} mutant cuticle has dorsal pucker, germband retraction and head involution defects, and hypotrophy of the ventral denticle belts. These phenotypes are shared by loss-of-function of downstream genes (D) *Galactose epimerase* (*Gale*), which converts UDP-GlcNAc to UDP-GalNAc, and (E) *wand*, which encodes a putative chondroitin sulfate synthase. This shared cuticle phenotype is indicative of ectopic *dpp* in the epidermis (F-I) *dpp* in situ in stage 13 embryos. (F) Lateral view of a wild-type embryo, *dpp* expression is restricted to the single row of leading edge epidermal cells during dorsal closure. Expansion of *dpp* transcription into the dorsolateral epidermis is observed in (G) *mmy*^{1}, (H) *Gale*$^{F00624.4}$, and (I) *CG43313* embryos (J-M) pMad in the epidermis of *Drosophila* embryos, single slices. (K) *mmy*^{1}, (L) *Gale*$^{F00624.4}$, mutants, and (M) *wand* RNAi embryos have an expansion of Dpp signaling activity in the epidermis beyond what is observed in (J) wild-type embryos.

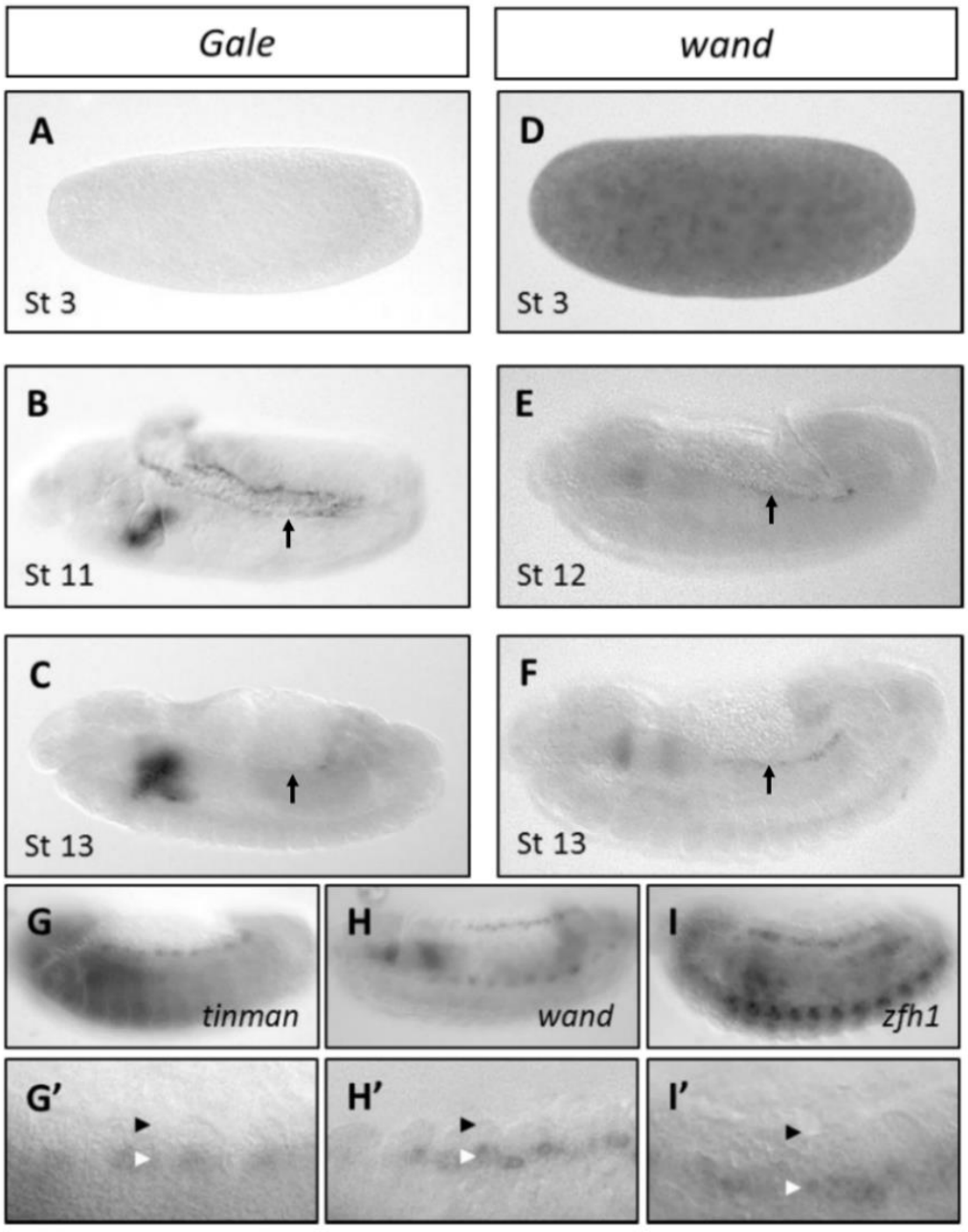

Fig. 4.4 Embryonic expression patterns of *Gale* and *wand*. *Gale* mRNA (A) is not maternally deposited. (B) Expression behind the epidermal leading edge initiates during embryonic stage 11, (C) but diminishes by stage 13. *wand* RNA (D) is maternally deposited. (E) Cardiac expression of *wand* initiates during stage 12 and continues through (F) stage 13 of embryogenesis. (G-I) A comparison of tissue expression of three transcripts, (G) *tinman*, a cardiac marker; (H) *wand*; and (I) *zfh1*, a pericardial cell marker. (G'-I') Black arrows denote the epidermal leading edge, whereas the white arrow depicts the location of mRNA transcript in situ. The gap distance between the two arrows is similar in *tinman* and *wand* RNA localization studies, suggesting that *wand* is expressed in cardiac cells, and not pericardial cells.

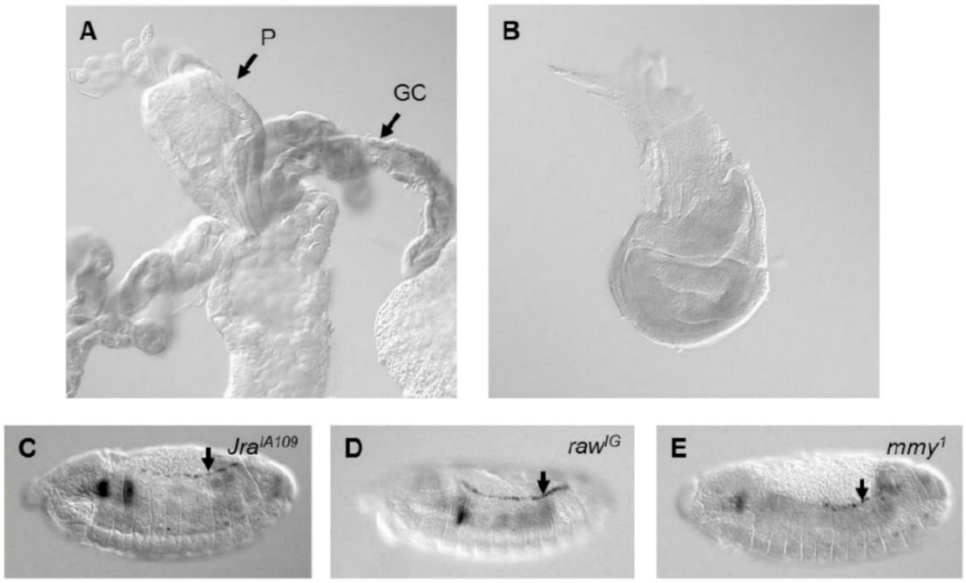

Fig. 4.5 Expression of *wand* in 3rd instar larvae and transcriptional control of *wand* in embryos. (A) *wand* mRNA is expressed in the gastric cecae (GC), but is absent from the rest of the foregut and midgut, including the proventriculus (P). (B) *wand* mRNA is also present in imaginal discs, such as this wing disc. *wand* remains restricted to the cardiac cells and its expression is not ablated in (C) Jra^{IA109}, (D) raw^{IG}, and (E) mmy^{1} mutant embryos.

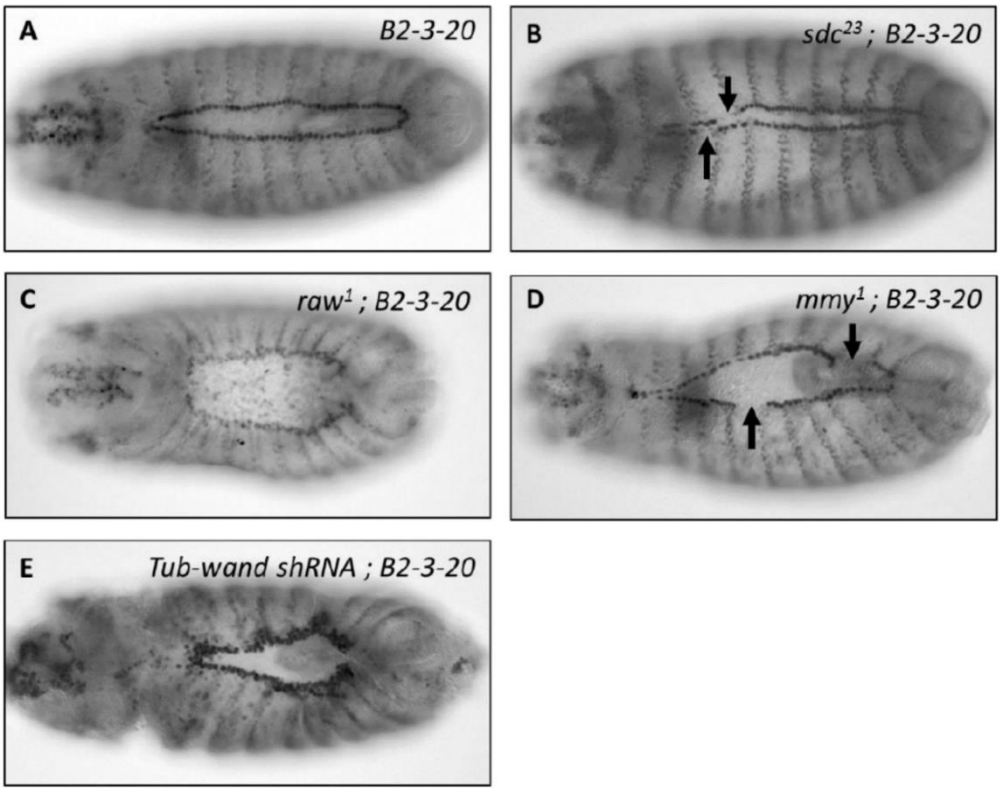

Fig. 4.6 Cardiac cells, visualized with anti-β-galactosidase. (A) Cardiac cells in a wild-type embryo; these cells lie directly underneath the LE epidermis. (B) Hemisegment loss of cardiac cells occurs in *sdc*^{23} mutants. Genetic interactions between *sdc* and *dpp* mutants suggest that *sdc*, possibly in concert with Dpp signaling, is required for cardiac specification. (C) *raw*^{1} mutants exhibit overspecification of cardiac cells, due to ectopic Dpp signaling. (D) *mmy*^{1} mutants have hemisegment loss of cardiac cells, similar to *sdc* mutants. This may be a result of *mmy* mutants having defective *sdc* function. (E) *Tub-wand shRNA* embryos have overspecification of cardiac cells. The differences in *mmy*^{1} and *wand shRNA* phenotypes may be due to the fact that *mmy* mutants have disrupted *sdc* function due to loss of both CS and HS. Sdc in *Tub-wand shRNA* embryos would have decreased CS attachment, but would retain HS and be capable of participating in Dpp signaling.

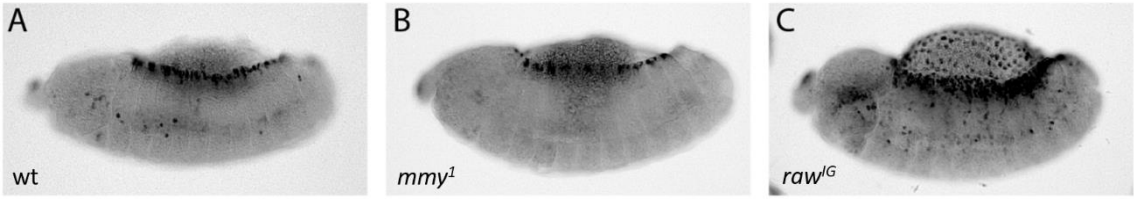

Fig. 4.7 The reporter *dpp*^{151H} is a JNK activity reporter, not a *dpp* expression reporter. We fail to observe expanded reporter expression in the epidermis of *mmy*^{1} (B) even though *dpp* is ectopically expressed beyond the LE; this is indistinguishable from wild-type (A). In contrast, in *raw*^{IG} (C), where JNK signaling and *dpp* expression are expanded beyond the LE, *dpp*^{151H} reporter expression is present beyond the LE.

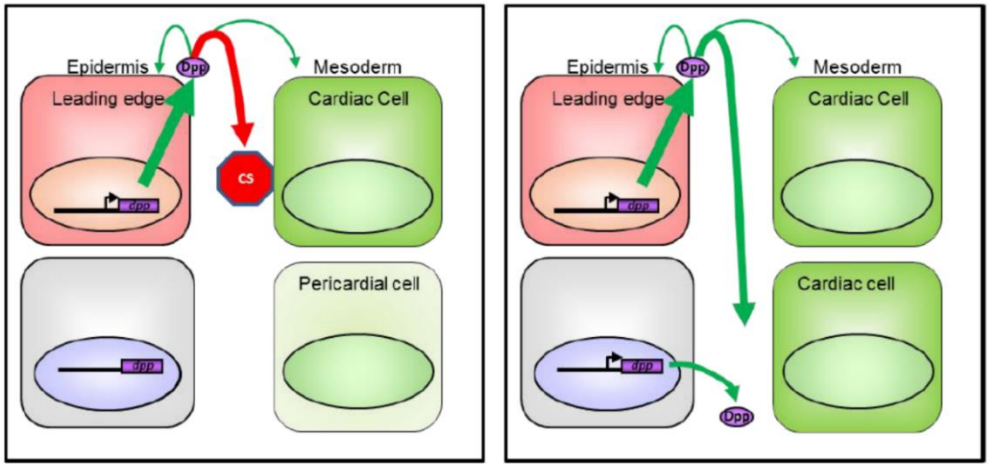

Fig. 4.8 Model for CS-mediated embryonic Dpp antagonism. (A) Dpp secreted from the LE of the epidermis. It signals back to the LE to promote further *dpp* transcription, and to the mesoderm to specify cardiac cell fate. Chondroitin sulfate, synthesized in the mesoderm, prevents excess Dpp signal from reaching the dorsolateral epidermis and mesoderm. (B) If the chondroitin sulfate sink is lost, Dpp access to dorsolateral epidermis and mesoderm is unrestricted; excess signaling results in ectopic *dpp* transcription and ectopic specification of cardiac cells.

CHAPTER 5

MODELING CONGENITAL DISEASE AND INBORN ERRORS OF DEVELOPMENT IN *DROSOPHILA MELANOGASTER*

Disease Models & Mechanisms (2016) 9: 253-269. Modeling congenital disease and inborn errors of development in *Drosophila melanogaster*. M. J. Moulton and A. Letsou.

© 2016. Published by The Company of Biologists Ltd | Disease Models & Mechanisms (2016) 9, 253-269 doi:10.1242/dmm.023564

REVIEW

SUBJECT COLLECTION: TRANSLATIONAL IMPACT OF *DROSOPHILA*

Modeling congenital disease and inborn errors of development in *Drosophila melanogaster*

Matthew J. Moulton and Anthea Letsou*

ABSTRACT

Fly models that faithfully recapitulate various aspects of human disease and human health-related biology are being used for research into disease diagnosis and prevention. Established and new genetic strategies in *Drosophila* have yielded numerous substantial successes in modeling congenital disorders or inborn errors of human development, as well as neurodegenerative disease and cancer. Moreover, although our ability to generate sequence datasets continues to outpace our ability to analyze these datasets, the development of high-throughput analysis platforms in *Drosophila* has provided access through the bottleneck in the identification of disease gene candidates. In this Review, we describe both the traditional and newer methods that are facilitating the incorporation of *Drosophila* into the human disease discovery process, with a focus on the models that have enhanced our understanding of human developmental disorders and congenital disease. Enviable features of the *Drosophila* experimental system, which make it particularly useful in facilitating the much anticipated move from genotype to phenotype (understanding and predicting phenotypes directly from the primary DNA sequence), include its genetic tractability, the low cost for high-throughput discovery, and a genome and underlying biology that are highly evolutionarily conserved. In embracing the fly in the human disease-gene discovery process, we can expect to speed up and reduce the cost of this process, allowing experimental scales that are not feasible and/or would be too costly in higher eukaryotes.

KEY WORDS: *Drosophila*, Congenital disorders, Inborn errors of development, Fly models, Forward genetics, Reverse genetics

Introduction

Congenital anomalies, or conditions that are manifest at or before birth, affect 3% of newborns in the USA (Kochanek et al., 2012; CDC, 2008) and 6% of newborns worldwide (Christianson et al., 2006). Many of these conditions are caused by heritable mutations, although environmental factors can also cause and/or contribute to the incidence and severity of congenital anomalies. In far too many cases, congenital disorders cannot be fully abrogated, accounting for 7% of all deaths among children under age 5 worldwide – more than the mortality due to HIV/AIDS and measles in this age group combined (Mathews et al., 2015). This percentage is much higher in the USA (20%) and in Europe (25%) (CDC, 2008; Kochanek et al., 2012; Liu et al., 2015). Syndromic congenital disorders, which manifest numerous simultaneous defects and account for about half of all cases of congenital anomaly at birth (Winter, 1996), are particularly difficult to manage clinically {e.g. CHARGE syndrome manifesting **coloboma** [emboldened words and phrases are defined in the glossary (see Box 1)], heart defects, **choanal atresia**, growth retardation, genitourinary malformation and ear abnormalities (Hsu et al., 2014), and velocardiofacial or Shprinstzens syndrome manifesting cardiac anomaly, **velopharyngeal insufficiency**, aberrant calcium metabolism and immune dysfunction (Chinnadurai and Goudy, 2012)}. Estimates suggest that the cause of at least 50% of congenital abnormalities remains unknown (Lobo and Zhaurova, 2008). It is vital that we understand the etiology of congenital anomalies because this knowledge provides a foundation for improved diagnostics as well as the design of preventatives and therapeutics that can effectively alleviate or abolish the effects of disease.

One of the most fruitful ways to understand human congenital anomalies and to discover prophylactic treatments is to study them in animal models. The high degree of conservation of fundamental biological processes between humans and the fruit fly *Drosophila melanogaster*, coupled with the broad repertoire of genetic approaches to which *Drosophila* is amenable, make this organism a uniquely powerful model system for understanding the basic biological etiology of human disease and development (Bier, 2005; Pandey and Nichols, 2011; Ugur et al., 2016). Comparisons of the *Drosophila* and human genomes reveal a very high level of conservation (Adams et al., 2000; Lander et al., 2001; Venter et al., 2001). Overall, homologous fly and human proteins share about 40% sequence identity; this increases to 80-90% or higher in conserved functional domains (Rubin et al., 2000). Importantly, 75% of human disease-related genes are thought to have a functional homolog in *Drosophila* (Chien et al., 2002; Reiter et al., 2001).

Detailed analysis has revealed the *Drosophila* genome to be far less complex than the human genome (Hartl, 2000). Indeed, it is the simplicity of this genome that in large part accounts for the fly's genetic tractability. *Drosophila* has about 14,000 genes on four chromosomes; three of these chromosomes account for 96% of the animal's genome (Adams et al., 2000). In comparison to humans, the fly has about 1/20 as much DNA, 1/8 as many chromosomes and 1/2 as many genes (Lander et al., 2001; Venter et al., 2001). The fly also has fewer gene duplications, with those in the human genome resulting from large-scale DNA duplications in an early chordate ancestor 350- to 650-million years ago (Bell et al., 2009; McLysaght et al., 2002). These characteristics make the fly a highly genetically tractable organism. Additional features of the fly that make it an accessible model to work with include: its rapid generation time (8.5 days under ideal conditions at 25°C); large family size (a single mating fly pair produces hundreds of genetically identical progeny within days); and small size (hundreds of flies can be housed in a single 6 oz polyethylene bottle) (Ashburner et al., 2011; Ashburner and Thompson, 1978). Each of these features contributes to a substantially lower cost for fly husbandry in comparison to other animal models, permitting experimental scales not feasible in most other experimental models.

Department of Human Genetics, University of Utah, 15 North 2030 East, Room 5100, Salt Lake City, UT 84112-5330, USA.

*Author for correspondence (aletsou@genetics.utah.edu)

REVIEW Disease Models & Mechanisms (2016) 9, 253-269 doi:10.1242/dmm.023564

Box 1. Glossary

Amorphic/hypomorphic allele: an allele with complete (amorphic) or partial (hypomorphic) loss of function of a gene.
Anophthalmia/microphthalmia: a condition in which formation of the eye is completely (anophthalmia) or severely (microphthalmia) abrogated.
Bicuspid aortic valve disease: a congenital condition in which two of the leaflets of the aortic valve are fused, forming a bicuspid valve instead of a tricuspid valve.
Brachydactyly: a condition characterized by shortening of the digits.
Cerebral autosomal-dominant arteriopathy with subcortical infarcts and leukoencephalopathy (CADASIL): a hereditary disorder that affects blood flow in blood vessels (often in the brain), resulting in strokes, migraine, recurrent seizures and white-matter deterioration.
Choanal atresia: a congenital disorder in which the back of the nasal cavity (choana) is blocked by tissue remaining after incomplete recanalization of the nasal fossae.
Coloboma: a congenital defect resulting in a hole in an eye structure (especially the iris).
Epifluorescence: visualization of an object in an optical microscope by excitation of a fluorophore incorporated into the sample. Light radiation given off from the viewing side excites the fluor and reflected light is captured as the image.
Epistasis: genetic interaction of non-allelic mutations that mask the phenotype of other mutations.
Gene regulatory network (GRN): a set of interacting genes working in coordination to alter gene expression.
Genetic redundancy: genetically distinct but functionally similar gene duplicates usually arising from paralogous gene duplication. Loss of any gene might not result in an overt phenotype if similar genes with redundant function can function in place of the lost gene.
Homeodomain transcription factor: a protein containing a domain that physically interacts with a DNA molecule and activates transcription nearby.
Imaginal disc: any portion of the *Drosophila* larval epidermis that will give rise to a particular organ after metamorphosis. There are 15 imaginal discs in the fly, which give rise to the wing, eye, leg, etc.
Infantile myofibromatosis-2 (IMF2): a congenital disorder characterized by aberrant mesenchymal cell proliferation resulting in benign skin, muscle, bone and visceral tumors.
Lateral meningocele syndrome (LMNS): a congenital disorder manifest as distinctive facial features, hypotonia, hyperextensibility, and neurological dysfunction due to protrusion of the meninges of the brain or spinal cord resulting from a defect in the cranium or spinal column.
Leukodystrophy: a disease characterized by degeneration of the white matter of the brain.
Orphan human disease: a disease that affects a relatively small population (generally <200,000 affected people in the USA), for which there is little or no therapeutic intervention available.
RAS/MAPK pathway: signaling pathway in which an extracellular signal peptide binds to a membrane-bound receptor and activates an intracellular signaling cascade involving RAS protein, which activates MAP kinases (MAPKs). The signaling cascade culminates in the activation of a transcription factor, which initiates transcription of a set of target genes.
RASopathy: family of diseases caused by mutations in RAS/MAPK signaling pathway components.
Spondylocostal dysostosis: a group of disorders of the axial skeleton characterized by a reduced rib number as well as defects in vertebra alignment and rib alignment.
Velopharyngeal insufficiency (VPI): a congenital disorder associated with an improper closing of the soft palate muscle (velopharyngeal sphincter) resulting in air escape through the nose instead of the mouth during speech.

At the organismal level, the adult fly is complex and not unlike humans. The fly has structures equivalent to the human heart, lung, liver, kidney, gut, reproductive tract and brain (Behr, 2010; Jeibmann and Paulus, 2009; Lesch and Page, 2012; Roeder et al., 2012; Wolf and Rockman, 2008; Ugur et al., 2016). The fly brain consists of more than 100,000 neurons, which form elaborate circuits governing insect behavioral processes such as locomotion, circadian rhythms, mating, aggression and feeding (Simpson, 2009). The visual system of the adult provides an exceptionally rich experimental system, yielding key information about vision as well as development (Baker et al., 2014; Borst and Helmstaedter, 2015; Paulk et al., 2013; Wernet et al., 2014). A landmark study by the late Walter Gehring revealed the fly and human eyes to be homologous structures (Halder et al., 1995). Products of divergent (rather than, as long thought, convergent) evolution, both the fly and human eye are dependent upon *Pax6* for their development (Gehring and Ikeo, 1999), and the two share an evolutionary ancestor – a marine rag-worm, *Platynereis* (Arendt et al., 2004).

Here, we explore the methods that have proven successful in generating *Drosophila* models for human congenital disorders. We discuss both forward and reverse genetic approaches (Fig. 1, Box 2), noting that, when the first genetic screens were undertaken in experimental systems such as *Drosophila* and *C. elegans*, the depth of the genetic homology shared between these organisms and humans was not yet evident. We highlight how outcomes from these screens yielded mechanistic details of signal transduction and shed light on the etiology of human congenital disorders affected by these pathways. Later, with the emergence of universal rules for metazoan development, forward genetic methods were employed to enhance our understanding of developmental programs in tissues and organs dependent upon conserved core regulatory networks for their growth and elaboration. Now, with the advent of the post-genomic age, investigators have turned to reverse genetic methods to directly assess roles of human disease gene candidates via gene knockdown/knockout and transgenesis, as described in the final section. Throughout, we focus on examples of *Drosophila* models of human inborn errors of development that have led to insights into etiology and which have informed the design of preventative and therapeutic treatment strategies.

Models of human congenital disorders and inborn errors of development

Drosophila has a rich experimental history in genetics and development, beginning with the observation that genes are organized on chromosomes and leading to Thomas Hunt Morgan's 1933 Nobel Prize in Medicine (http://www.nobelprize.org/nobel_prizes/medicine/laureates/1933/). Later in the 20th century, burgeoning molecular genetic analyses thrust *Drosophila* into a new age of discovery by enabling systematic spatiotemporal control of transgenes (Rubin and Spradling, 1983), initially through the use of the UAS:GAL4 (Brand and Perrimon, 1993) and FLP:FRT (Golic, 1994) gene regulatory systems, and most recently through gene-knockout and gene-editing strategies (Beumer and Carroll, 2014; Boutros and Ahringer, 2008; Gong and Golic, 2003). Together, these methodological breakthroughs, along with their second-generation reinventions [e.g. MARCM (Wu and Luo, 2006), TARGET (McGuire et al., 2003), GeneSwitch (Nicholson et al., 2008; Osterwalder et al., 2001) and ΦC31-mediated

Disease Models & Mechanisms (2016) 9, 253-269 doi:10.1242/dmm.023564

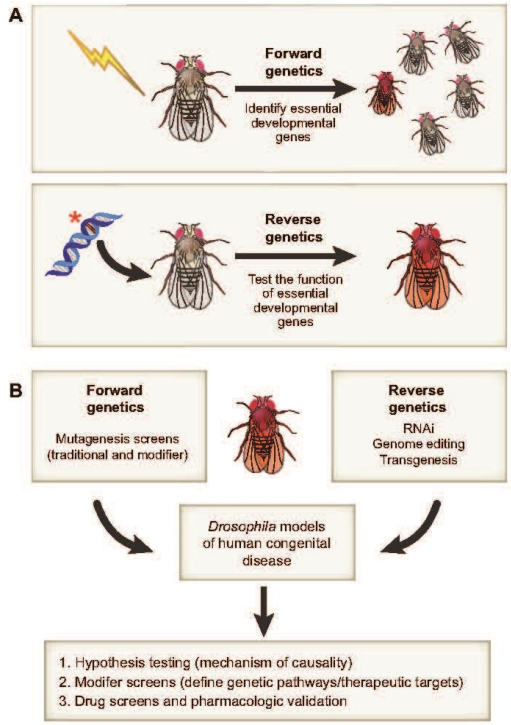

Fig. 1. Forward and reverse genetic approaches in *Drosophila*.
(A) Forward genetics uncovers the genetic basis of phenotype. Mutagenesis by any means (e.g. X-rays, chemicals or transposons; indicated by a lightning bolt) is used to generate mutant flies with aberrant phenotypes (indicated by the red fly), which are used as a starting point for gene discovery. Reverse genetics refers to the discovery of gene function through the targeted disruption of genes (here indicated by an asterisk showing a mutation in a gene sequence) and the analysis of the resulting phenotype(s). (B) Both forward and reverse genetic strategies are useful for the creation of animal models of disease that can be used as platforms to test hypotheses, perform modifier screens and identify new therapeutics. (A,B) In both panels, wild-type flies are shown in brown, mutant flies in red.

transgenesis (Groth et al., 2004); Box 2], have yielded a richness of information that illuminates the principles and rules by which gene products and cells interact with one another to control development, with implications for understanding disease.

Forward genetics – defining pathways and associated dysmorphologies

Forward genetic analysis (see Fig. 1) is an unbiased method for identifying gene function and is one of the most powerful approaches for understanding the genetic basis of human development and disease. Its impact on understanding the genetic basis of human development was first illustrated by the Nobel-Prize-winning screen pioneered by *Drosophila* geneticists Christiane Nusslein-Volhard and Eric Wieschaus (Roush, 1995). Their genome-wide screens for mutations that affect the pattern of the *Drosophila* cuticle led to the discovery of hundreds of loci that have essential and conserved roles in development (e.g. Nusslein-Volhard and Wieschaus, 1980). Complementing these elegant yet traditional screening endeavors were a subsequent generation of modifier screens (both enhancer and suppressor; e.g. Rogge et al., 1995; Box 2) that revealed not only genes encoding products that function as essential components of signaling pathways but also those that play modulatory roles. Most of the loci identified in these screens are conserved and encode comparable functions throughout metazoan lineages, including that

Box 2. Genetic methodologies

ΦC31-mediated transgenesis: method of inducing integration of an injected plasmid at a specific site in the genome. An integrase protein, ΦC31, induces recombination between the bacterial attachment site (*attB*) in the injected plasmid and the phage attachment site (*attP*) in the genome.

CRISPR/Cas9: method of inducing targeted double-stranded breaks in the genome. CAS9 binds to RNA (termed guide RNA) that pairs with genomic DNA and induces a double-stranded DNA break. Improper repair at these breakpoints in cells that give rise to the germline can lead to mutations that can be isolated in the next generation. Additionally, double-stranded DNA breaks can induce the incorporation of foreign DNA containing homology arms surrounding the break point. This system has been utilized to generate novel mutations in genes as well as facilitate targeted knock-in strategies.

Forward genetic screen: random, genome-wide mutagenesis to generate progeny with an aberrant phenotype(s). Identification of individual mutated genes leads to the discovery of genes involved in any given process. Identification of different genes with shared loss-of-function phenotypes leads to the discovery of genetic pathways. Traditional forward genetic screens in *Drosophila* using X-ray, chemical and transposon mutagenesis have uncovered numerous genetic pathways involved in development. These pathways and their function in development are often conserved in humans.

GeneSwitch: method to control induction of gene expression spatially and temporally. This method utilizes a GAL4–progesterone-receptor chimera protein that can be activated by the hormone progesterone.

Modifier screen: random mutagenesis performed in a mutant background (usually hypomorphic) to identify mutations that enhance or suppress a mutant phenotype. Modifier screens yield additional genes involved in a given process/pathway, including both integral and modulatory pathway components.

Mosaic analysis with a repressible cell marker (MARCM): system to generate labeled mutant mitotic clones within a field of wild-type cells. This system requires the use of: (1) the inducible gene expression system in which GAL4 protein activates transcription at upstream activation sites (UAS), (2) the repressor of GAL4 induction, GAL80, (3) spatiotemporally controlled expression of the DNA recombinase Flipase (FLP), and (4) a marker (usually fluorescent) downstream of the UAS. The mutant allele of interest and the *GAL80* transgene are recombined onto homologous chromosome arms containing FRT sites (the site at which FLP-mediated recombination will occur). FLP-induced mitotic recombination in cells heterozygous for the *GAL80* transgene and the mutant allele of interest yields recombinant daughter cells that inherit either two copies of the mutant allele or two copies of the *GAL80* transgene. Daughter cells lacking GAL80 and harboring the homozygous mutant allele will express the marker in a field of unmarked cells that did not undergo recombination or are homozygous for GAL80.

Reverse genetic screen: targeted mutagenesis of any given gene designed to understand the gene's biological function. Mutagenesis can be accomplished via numerous mechanisms, such as RNAi or CRISPR/Cas9.

RNA interference (RNAi): method of depleting a cell of a specific target mRNA. This is typically accomplished by expressing cytoplasmic double-stranded RNA that is subsequently processed by the cell into small single-stranded RNA molecules that are then used as templates to target and degrade complementary mRNA in the cell.

Temporal and regional gene expression targeting (TARGET): method to control induction of gene expression spatially and temporally. This method utilizes the UAS/GAL4 system in conjunction with a temperature-sensitive GAL80 to repress GAL4 activity at permissive temperatures.

Disease Models & Mechanisms (2016) 9, 253-269 doi:10.1242/dmm.023564

of humans (Rubin et al., 2000). Indeed, the Heidelberg screens, which relied on female sterility and cuticle phenotypes for high-throughput screening, successfully yielded key components of several essential developmental signaling pathways, such as the Toll (Tl), Decapentaplegic (Dpp), Hedgehog (Hh), Notch (N), Fibroblast growth factor (FGF), Wingless (Wg), Engrailed (En) and Hippo (Hpo) pathways. The use of forward genetic screens in *Drosophila* has led to substantial insights into the cellular and molecular basis of processes that can go awry in development (Table 1), a few examples of which are highlighted below.

The Toll pathway

Although perhaps best recognized for its conserved role in innate immunity, the Toll pathway, along with the CREB-binding protein (CBP) cofactor (called Nejire in *Drosophila*), modulates the activity of the Twist transcription factor via activation of NFκB [Nuclear factor κB; a transcription factor called Dorsal (Dl) in *Drosophila*] in early development in both flies and humans (Akimaru et al., 1997; Petrij et al., 2008; Wasserman, 2000). Reduced expression of Twist disrupts embryonic mesoderm differentiation in all metazoa (Castanon and Baylies, 2002). In humans, reduced expression of Twist (caused either by loss of a single copy of *CBP* or by hemizygosity for *Twist* itself) manifests as genetically related autosomal dominant developmental syndromes, either the rare syndrome Rubinstein-Taybi (1:100,000-1:125,000 live births) (Hennekam, 2006) or the more common syndrome Saethre-Chotzen/acrocephalosyndactyly type III (1:25,000-1:50,000 live births) (Rubinstein and Taybi, 1963; von Gernet et al., 1996). These two syndromes are difficult to distinguish because both are caused by reductions in either CBP or Twist function, and both are characterized by craniofacial and digit dysmorphologies. Importantly, the identification of the molecular underpinnings of these developmental abnormalities illustrates how the search for defects in specific developmental genes has become a vital and quickly evolving field in medical genetics (Harper, 2010).

The decapentaplegic/bone morphogenetic protein signaling pathway

The transforming growth factor β (TGF-β) superfamily comprises a large group of structurally related secreted signaling molecules that belong – based on similarities in sequence and function – to three subfamilies: the bone morphogenetic proteins (BMPs), the activin/inhibins, and the TGF-β proteins (Attisano and Wrana, 2002). TGF-β superfamily members signal through conserved transmembrane serine/threonine kinase receptor complexes, with signals transduced intracellularly via phosphorylation and activation of Smad transcription factors (Massague, 2012). TGF-β superfamily members play essential roles in embryonic patterning and tissue morphogenesis that are conserved among metazoans (Wu and Hill, 2009). As an example, bone morphogenetic protein 4 [BMP4; called Decapentaplegic (Dpp) in *Drosophila*] has numerous conserved roles during embryonic patterning and development: in the dorsoventral (DV) axis, and in the eye, heart and otic vesicle (Chen et al., 2004; Pujades et al., 2006; Slavotinek, 2011; Wall and Hogan, 1994). Given this conservation in function, it is not surprising that the phenotypic consequences of abnormal Dpp signaling in *Drosophila* bear similarities to human developmental disorders in which the orthologous BMP pathway is disrupted.

Flies provide an important experimental model in which to discern the mechanism and etiology of BMP4-associated human developmental disorders. These include **anophthalmia/microphthalmia**, microphthalmia syndromic 6 orofacial cleft 11, and **brachydactyly** type A2 (Bakrania et al., 2008; Lehmann et al., 2006; Suzuki et al., 2009). Eye, palate and digit defects, respectively, feature prominently in the clinical manifestation of these syndromes, and thus it is clear that BMP4 signaling deficiencies in humans are associated with an array of developmental defects identical to those already well-documented for Dpp in *Drosophila* (Simin et al., 1998; Spencer et al., 1982). Moreover, at the level of biological process, *Drosophila* Dpp signaling patterns the early embryo and **imaginal discs** (O'Connor et al., 2006), and regulates actin rearrangements that underlie the zippering of epithelial sheets during the essential embryonic process of dorsal closure in *Drosophila* (Glise and Noselli, 1997; Martin and Wood, 2002). Thus, as Twist transcriptional activity is required for proper mesoderm differentiation in both flies and humans, so also is Dpp/BMP signaling activity required for conserved developmental processes in flies and humans. Dpp/BMP conservation extends from the molecular level to that of biological process, demonstrating that mechanistic insights into developmental events made in flies can be extended to humans.

The identification of Dpp pathway antagonists in flies (Campbell and Tomlinson, 1999; Francois et al., 1994; Humphreys et al., 2013; Shimell et al., 1991) has revealed that increased levels of Dpp/BMP signaling also have lethal developmental consequences, contributing substantially to our understanding of the rare, but devastating, autosomal dominant ectopic bone formation disorder fibrodysplasia ossificans progressiva (FOP; 1:2,000,000 live births) (Pignolo et al., 2013). The most common mutation underlying this condition is R206H in the glycine-serine (GS) activation domain of the BMP type 1 receptor ACVR1 [called Saxophone (Sax) in *Drosophila*] (Shore et al., 2006). This missense mutation leads to constitutive ACVR1 activation and increased phosphorylation of downstream targets, including the transcription factor Smad1 (van Dinther et al., 2010). Discoveries made in *Drosophila* concerning the architecture of this pathway have provided a foundation for drug studies into kinase inhibitors as potential therapeutics for treating FOP (Kaplan et al., 2013, 1990; Le and Wharton, 2012; Twombly et al., 2009). Excessive TGFβ signaling also provides the foundation for our understanding of osteogenesis imperfecta, a heritable disease in which altered TGF-β signaling is thought to affect bone quantity and quality and thus result in bone fragility (Grafe et al., 2014).

The Hedgehog/Sonic hedgehog signaling pathway

Our understanding of the Hedgehog (Hh) signaling pathway [called Sonic hedgehog (SHH) in mammals], and how it contributes to congenital conditions, also has its foundations in *Drosophila* genetics. The Hh receptor, encoded by the gene *patched* (*ptc*; *PTCH1* in humans), was first identified in the Heidelberg screens for lethal patterning defects (Nusslein-Volhard and Wieschaus, 1980) and was subsequently cloned (Hooper and Scott, 1989; Nakano et al., 1989). Many other components of the Hh pathway were also identified in *Drosophila*, based on their similar loss-of-function embryonic phenotypes, well before their mouse orthologs were identified and cloned (Goodrich et al., 1996; Hahn et al., 1996). The observation that animals (both flies and mice) homozygous for loss-of-function Hh/SHH pathway mutations die in embryogenesis provides strong evidence that this signaling pathway fulfills conserved developmental roles. Decreased SHH signaling (either through haploinsufficiency for *SHH* or by increasing the repressive activity of PTCH1) has severe developmental consequences that mirror human holoprosencephaly (HPE), a common forebrain defect resulting from the failure of the cerebral hemispheres to separate. Few HPE fetuses survive to birth, but

Disease Models & Mechanisms (2016) 9, 253-269 doi:10.1242/dmm.023564

Table 1. Pathways associated with human congenital disorders

Pathway[1]	Disease	Phenotype MIM no.[2]	Human causal gene	*Drosophila* ortholog[3]
BMP	Brachydactyly, type A2	112600	*BMP2*	*dpp*
			NOG	*sog*
			BMPR1B	*put*
	Fibrodysplasia ossificans progressiva	135100	*ACVR1*	*sax*
			ACVR2	*tkv*
	Loeys-Dietz syndrome, type 1	609192	*SMAD3*	*mad*
	Loeys-Dietz syndrome, type 2	610168	*TGFBR2*	*put*
	Loeys-Dietz syndrome, type 3	613795	*TGFB2*	*Actβ*
	Loeys-Dietz syndrome, type 4	614816	*TGFBR1*	*tkv*
	Loeys-Dietz syndrome, type 5	615582	*TGFB3*	*Actβ*
	Chrondrodysplasia, acromesomelic, with genital anomalies	609441	*BMPR1B*	*put*
	Multiple synostoses syndrome 1	186500	*NOG*	*sog*
	Stapes ankylosis with broad thumb and toes	184460	*NOG*	*sog*
	Symphalangism, proximal	185800	*NOG*	*sog*
	Tarsal-carpal coalition syndrome	186570	*NOG*	*sog*
	Myhre syndrome	139210	*SMAD4*	*med*
	Renal hypodysplasia	191830	*BMP4*	*dpp*
	Microphthalmia syndromic 6	607932	*BMP4*	*dpp*
	Orofacial cleft 11	600625	*BMP4*	*dpp*
FGF	Hypogonadotropic hypogonadism	612702	*FGF8*	*bnl, pyr, ths*
			FGF17	*bnl, pyr, ths*
			FGFR1	*btl, htl*
	Lacrimo-auriculo-dento-digital (LADD) syndrome	149730	*FGF10*	*bnl, pyr, ths*
			FGFR2	*btl, htl*
			FGFR3	*btl, htl*
	Crouzon syndrome	123500	*FGFR2/3*	*btl, htl*
	Saethre-Chotzen-like syndrome	101400	*FGFR2/3*	*btl, htl*
	Congenital deafness with inner ear agenesis, microtia and microdontia	610706	*FGF3*	*bnl, pyr, ths*
	Trichomegaly	190330	*FGF5*	*bnl, pyr, ths*
	Multiple synostoses syndrome 3	612961	*FGF9*	*bnl, pyr, ths*
	Aplasia of lacrimal and salivary glands	180920	*FGF10*	*bnl, pyr, ths*
	Metacarpal 4-5 fusion	309630	*FGF16*	*bnl, pyr, ths*
	Renal hypodysplasia/aplasia 2	615721	*FGF20*	*bnl, pyr, ths*
	Hypophosphatemic rickets, autosomal dominant	193100	*FGF23*	*bnl, pyr, ths*
	Jackson-Weiss syndrome	123150	*FGFR1*	*btl, htl*
	Pfeiffer syndrome	101600	*FGFR2*	*btl, htl*
	Achondroplasia	100800	*FGFR3*	*btl, htl*
	Hypochondroplasia	146000	*FGFR3*	*btl, htl*
	Thanatophoric dysplasia I/II	187600/1	*FGFR3*	*btl, htl*
	Camptodactyly, tall stature and hearing loss (CATSHL) syndrome	610474	*FGFR3*	*btl, htl*
	Nevus, epidermal, somatic	162900	*FGFR3*	*btl, htl*
	Severe achondroplasia with developmental delay and acanthosis nigricans (SADDAN)	616482	*FGFR3*	*btl, htl*
	Muenke syndrome	602849	*FGFR3*	*btl, htl*
	Hartsfield syndrome	615465	*FGFR1*	*btl, htl*
	Osteoglophonic dysplasia	166250	*FGFR1*	*btl, htl*
	Trigonocephaly 1	190440	*FGFR1*	*btl, htl*
	Apert syndrome	101200	*FGFR2*	*btl, htl*
	Beare-Stevenson cutis gyrata syndrome	123790	*FGFR2*	*btl, htl*
	Bent bone dysplasia syndrome	614592	*FGFR2*	*btl, htl*
	Craniofacial-skeletal-dermatologic dysplasia	101600	*FGFR2*	*btl, htl*
	Scaphocephaly, maxillary retrusion and mental retardation	609579	*FGFR2*	*btl, htl*
	Antley-Bixler syndrome without genital anomalies or disordered steroidogenesis	207410	*FGFR2*	*btl, htl*
Hippo	Coloboma, ocular, with or without hearing impairment, cleft lip/palate, and/or mental retardation	120433	*YAP1*	*yki*
	Barth syndrome	302060	*TAZ*	*taz*
	Holt-Oram syndrome	142900	*TBX5*	*H15*
HOX	Bosley-Salih-Alorainy syndrome	601536	*HOXA1*	*lab*
	Athabascan brainstem dysgenesis syndrome	601536	*HOXA1*	*lab*
	Microtia, hearing impairment and cleft palate	612290	*HOXA2*	*pb*
	Radioulnar synostosis with amegakaryocytic thrombocytopenia	605432	*HOXA11*	*Abd-B*

Continued

Table 1. Continued

Pathway[1]	Disease	Phenotype MIM no.[2]	Human causal gene	*Drosophila* ortholog[3]
	Hand-foot-genital syndrome	140000	*HOXA13*	*Abd-B*
	Guttmacher syndrome	176305	*HOXA13*	*Abd-B*
	Hereditary congenital facial paresis, 3	614744	*HOXB1*	*lab*
	Ectodermal dysplasia, hereditary congenital, 3	602032	*HOXC13*	*Abd-B*
	Congenital vertical talus and Charcot-Marie-Tooth disease/Vertical talus, congenital	192950	*HOXD10*	*Abd-B*
	Synpolydactyly type II	186000	*HOXD13*	*Abd-B*
	Brachydactyly type D	113200	*HOXD13*	*Abd-B*
	Brachydactyly type E	113300	*HOXD13*	*Abd-B*
	Syndactyly type V	186300	*HOXD13*	*Abd-B*
	Brachydactyly-syndactyly	610713	*HOXD13*	*Abd-B*
JAK/STAT	Growth hormone insensitivity with immunodeficiency	245590	*STAT5B*	*Stat92E*
	Polycythemia vera	263300	*JAK2*	*hop*
	Thrombocythemia 3	614521	*JAK2*	*hop*
	Budd-Chiari syndrome	600800	*JAK2*	*hop*
NHR	Alopecia universalis	203655	*HR*	Unknown
	Hypotrichosis 4	146550	*HR*	Unknown
	Atrichia with papular lesions	209500	*HR*	Unknown
	Hypothyroidism, congenital, nongoitrous, 1	275200	*TSHR*	*Lgr1*
Notch	Alagille syndrome	610205	*NOTCH2*	*N*
			JAG1	*Ser*
	Congenital heart disease	600001	*JAG1*	*Ser*
	Tetralogy of Fallot	187500	*JAG1*	*Ser*
	Adams-Oliver syndrome 5	616028	*NOTCH1*	*N*
	Hajdu-Cheney syndrome	102500	*NOTCH2*	*N*
	Myofibromatosis, infantile 2	615293	*NOTCH3*	*N*
	Lateral meningocele syndrome	130720	*NOTCH3*	*N*
	Spondylocostal dysostosis 1	277300	*DLL3*	*dl*
SHH	Holoprosencephaly-3	142945	*SHH*	*hh*
			GLI2	*ci*
			PTCH1	*ptc*
	Basal cell nevus syndrome	109400	*PTCH1/2*	*ptc*
			SUFU	*Su(fu)*
	Holoprosencephaly-7	610828	*PTCH1*	*ptc*
	Greig cephalopolysyndactyly	175700	*GLI3*	*ci*
	Pallister-Hall syndrome	146510	*GLI3*	*ci*
	Postaxial polydactyly type A	174200	*GLI3*	*ci*
	Hirschsprung disease	142623	*RET*	*ret*
	Multiple endocrine neoplasia type 2	171400	*RET*	*ret*
TNF	Pediatric fever, familial	142680	*TNFRSF1A*	*PGRP-LC*
	Lymphoproliferative syndrome 2	615122	*TNFRSF7*	*PGRP-LC*
	Congenital heart defects, nonsyndromic, 2	614980	*TAB2*	*tab2*
	Ectodermal, dysplasia, anhidrotic, immunodeficiency, with or without lymphedema	300291/300301	*IKBKG*	*Ird5*
	Incontinentia pigmenti	308300	*IKBKG*	*Ird5*
Toll & Twist	Rubinstein-Taybi syndrome	180849	*CREBBP*	*nej*
	Saethre-Chotzen syndrome	101400	*TWIST1*	*twi*
Wnt/PCP	Van Maldergem syndrome	615546	*DCHS1*	*ds*
			FAT4	*ft*
	Exudative vitreoretinopathy 1	133780	*LRP5*	*arr*
			FZD4	*fzd*
			NDP	Unknown
	Hennekam lymphangiectasia-lymphedema syndrome 2	616006	*FAT4*	*ft*
	Robinow syndrome, autosomal dominant 2	616331	*DVL1*	*dsh*
	Mental retardation, autosomal dominant 19	615075	*CTNNB1*	*arm*
	Tetra-amelia syndrome	273395	*WNT3*	*wg*
	Mullerian aplasia and hyperandrogenism	158330	*WNT4*	*wg*
	SERKAL syndrome	611812	*WNT4*	*wg*
	Fuhrmann syndrome	228930	*WNT7A*	*wg*
	Odontoonychodermal dysplasia	257980	*WNT10A*	*wg*
	Split-hand/foot malformation 6	225300	*WNT10B*	*wg*
	Caudal duplication anomaly	607864	*AXIN1*	*axn*
	Tooth agenesis, selective, 4	150400	*AXIN2*	*axn*

Continued

REVIEW Disease Models & Mechanisms (2016) 9, 253-269 doi:10.1242/dmm.023564

Table 1. Continued

Pathway[1]	Disease	Phenotype MIM no.[2]	Human causal gene	*Drosophila* ortholog[3]
			WNT10A	*wg*
	Focal dermal hypoplasia	305600	*PORCN*	*por*
	Anonychia congenita	206800	*RSPO4*	Unknown
	Caudal regression syndrome	600145	*VANGL1*	*vang*
	Neural tube defects	182940	*VANGL1*	*vang*

[1]BMP, bone morphogenic protein; FGF, fibroblast growth factor; JAK, Janus kinase; PCP, planar cell polarity; SHH, Sonic hedgehog; STAT, signal transducer and activator of transcription; TNF, tumor necrosis factor.
[2]Mendelian Inheritance in Man (MIM) number and human disease causal gene from omim.org.
[3]flybase.org.

nonetheless the disorder is diagnosed in 1:20,000 live births (Edison and Muenke, 2003).

Although most HPE cases are considered sporadic, familial cases have also been described (Heussler et al., 2002). The most commonly mutated gene in both sporadic and familial forms of the disease is *SHH*, but mutation of other pathway components (for example, in the receptor *PTCH1*, and in a SHH target gene, the transcription factor *GLI2*) have also been causally linked to the disorder (Ming et al., 2002; Ming and Muenke, 2002; Roessler et al., 2003). The pathway has long been known to be essential for forebrain patterning (Hebert and Fishell, 2008). The lack of clear genotype-to-phenotype correlations associated with HPE (Traiffort et al., 2004) underscores our recognition that most genetic diseases, including HPE, are complex. This complexity is usually interpreted to mean that genes do not act in isolation, but rather in concert with their individual genetic backgrounds and/or environments. In cases like this, *in vivo* modifier screens and quantitative (high-throughput) functional genomic assays in cell culture are invaluable for a comprehensive understanding of pathways as well as for a fuller understanding of loci contributing to dysmorphic disease susceptibility in the long term (St Johnston, 2002). Indeed, both types of second-generation screens have yielded conserved modulators of Hh/Shh pathway activity, including the phosphoprotein phosphatase Microtubule star (Mts) and the cell-surface glypican Dally-like (Dlp) (Casso et al., 2008; Lum et al., 2003).

Interestingly, many genes associated with developmental defects are also linked to neoplasia. For example, mutations in SHH signaling pathway genes cause autosomal dominant basal cell nevus syndrome (BSNS) (Hahn et al., 1996; Johnson et al., 1996), a condition defined by a wide range of clinical manifestations, including the development of postnatal skin tumors in association with malformations of the ribs (duplicated, fused, splayed or misshapen) and skull (especially its enlargement) (Gorlin and Goltz, 1960). Such overgrowth phenotypes are now better understood in light of discoveries made in *Drosophila* on the role of Hh as a negative regulator of cell growth and proliferation (Ingham, 1998; Neumann, 2005).

The Notch signaling pathway

Several human congenital disorders are associated with mutation of the Notch pathway. John Dexter and Thomas Hunt Morgan described the first *Notch* alleles (in flies with notched wings) almost 100 years ago (Morgan, 1917). The Artavanis-Tsakonis and Young labs independently cloned and sequenced the *Drosophila* gene (Kidd et al., 1986; Wharton et al., 1985), paving the way for additional mechanistic studies in flies and worms. The *Notch* gene encodes a transmembrane receptor that is proteolytically cleaved upon ligand binding, with the cleaved intracellular domain entering the nucleus to regulate gene expression (Greenwald, 2012; Lieber et al., 1993; Struhl and Adachi, 1998; Struhl et al., 1993; Struhl and Greenwald, 2001). The conserved Notch pathway is one of the most widely used mechanisms of intercellular communication in all metazoan organisms, and a century of work deciphering the developmental roles of Notch signaling in *Drosophila* has provided the basis for more recent insights into the central role of the Notch pathway in human development (Yamamoto et al., 2014).

In humans, loss of function of the Notch2 receptor or of its ligand Jagged leads to Alagille syndrome, an autosomal dominant condition that is moderately prevalent, with an occurrence of 1 in 20,000 live births (Kamath et al., 2003). The syndrome is distinguished by bile duct paucity; in addition, abnormalities of the heart, eye and skeleton often occur in association with distinctive facial features (Kamath et al., 2003). Importantly, bile duct epithelial morphogenesis defects displayed by individuals with Alagille syndrome and $Notch^{A/+}$; $Jagged^{A/+}$ double-heterozygous mice are reminiscent of the epithelial morphogenesis defects observed in Notch pathway *Drosophila* mutants (Hartenstein et al., 1992).

More generally, the Notch signaling pathway plays a conserved role in organ development in all metazoa – ranging from insect to nematode to echinoderm to human; effects of pathway mutation are pleiotropic and dependent on dose and context (Gridley, 2003). Additional congenital disorders associated with defects in Notch signaling include **spondylocostal dysostosis** (a skeletal disorder), **lateral meningocele syndrome** (LMNS; a disorder distinguished by craniofacial dimorphism), **CADASIL** (a vascular disorder) and **bicuspid aortic valve disease** (a malformation of the aorta) (Chapman et al., 2011; Garg et al., 2005; Gripp et al., 2015; Rutten et al., 2014). Hyperactivation of the pathway can also lead to developmental abnormalities, e.g. **infantile myofibromatosis-2** (IMF2; a disorder of mesenchymal proliferation) (Martignetti et al., 2013). The Notch pathway loss-of-function phenotypes that are shared between flies and humans, e.g. epithelial morphogenesis (described above) and embryonic neurogenesis (de la Pompa et al., 1997), highlight the conserved roles for Notch signaling in development and further emphasize the power of insect models for probing mechanisms of human development.

Forward genetics – gleaning insights into tissue morphogenesis

In accordance with their developmental roles in *Drosophila*, mutations in several human genes cause predictable, analogous defects. For example, in both flies and humans, mutations in HOX genes and Hox family members alter spatial identities: mutations in the Hox family member *Pax6* [called *eyeless* (*ey*) in *Drosophila*] eliminates eyes; mutations in *SALL1* [which has two homologs in *Drosophila*, called *spalt major* (*salm*) and *spalt-related* (*salr*)] disrupt eye and auditory elements (respectively); and mutations in *Nkx2-5* [called *tinman* (*tin*) in *Drosophila*] lead to heart defects. In all cases, these genes encode transcription factors that are components of conserved **gene regulatory networks** (GRNs; genomic subsystems that coordinate inputs from transcriptional

Disease Models & Mechanisms (2016) 9, 253-269 doi:10.1242/dmm.023564

activators and repressors during differentiation and development). Importantly, GRNs are evolutionarily conserved in their transcriptional regulation of similar sets of effector genes. Thus, the organ and tissue systems that flies share with humans are not only functionally analogous but also constructed from similar building blocks. The depth of this homology validates the use of fly models to provide detailed portraits of human tissue and organ development.

Below we discuss three model *Drosophila* biological systems (eye, heart and lung) that illustrate how forward genetic methods have been useful not only for organizing human developmental disorders on the basis of signal transduction pathways, but also for validating models of development on the basis of conserved complex GRNs.

Eye development

Although long thought to exemplify convergent evolution, the *Drosophila* compound and mammalian camera eyes have actually diverged in evolution (Gehring, 2014). In both flies and mammals, the eye is the product of the Pax6 (Ey in the fly) master regulator, a **homeodomain transcription factor** conserved in evolution (Quiring et al., 1994). *ey* is both necessary and sufficient to specify eye development in flies, and the human homolog functions heterologously to direct the making of an eye in flies (Halder et al., 1995). Moreover, loss of *Pax6* or additional components of the eye GRN produces aniridia (iris hypoplasia) not only in flies and humans, but also in zebrafish, frogs, chicks and mice (Bhatia et al., 2013; Kaufman et al., 1995; Nakayama et al., 2015; Takamiya et al., 2015; Treisman, 1999). In line with this, Gehring and colleagues demonstrated that the transcription factors encoded by *Pax2* (called *D-Pax2* or *shaven* in *Drosophila*) and *Sox2* (called *SoxN* in *Drosophila*), along with the lens-specific DC5 enhancer (defined in chick), form a conserved regulatory circuit responsible for secretion of crystalline, an essential lens protein (Blanco et al., 2005). Thus, conserved downstream effectors of GRNs function in specialized cells of the eye, and the effects of master regulators are properly parsed. There is a wide-ranging literature focused on Pax6 function in eye development (Gehring, 2002; Gehring and Ikeo, 1999; and references therein), and it is clear that the *Drosophila* genetic system has provided a particularly informative model in which to study the development of visual systems in compound and camera eyes alike (Pennisi, 2002; Pichaud and Desplan, 2002).

The eye is one the best-studied tissues in *Drosophila*, with a wealth of knowledge coming from high-throughput studies of genes with loss-of-function phenotypes in the eye that are easily visualized using reflected light and/or scanning electron microscopy (Baker et al., 2014). Several standard forward genetic screens have been performed to identify genes required for eye development (e.g. Janody et al., 2004; Moberg et al., 2001; Tapon et al., 2001), whereas modifier screens (Box 2), dependent upon dose-sensitive perturbations of development, have been used in especially elegant ways to study the fundamentals of receptor tyrosine kinase and Ras signaling (e.g. Karim et al., 1996; Rogge et al., 1991; Simon et al., 1991).

Heart development

The heart, like the eye, is ancient in origin, with its development controlled by an evolutionarily conserved GRN. In *Drosophila*, the heart is known as the dorsal vessel and it functions as a linear peristaltic pump. Each of the core GRN elements required to enact the cardiac genetic program in humans is also expressed in the *Drosophila* heart. All core GRN elements are transcription factors: NKX2 (at least two in humans; Tinman in *Drosophila*); MEF2 and Hand (both known by the same name in *Drosophila*, with two and four homologs, respectively, in humans), GATA (three homologs in humans; Pannier in *Drosophila*); and Tbx (at least seven homologs in humans: Midline and H15 in *Drosophila*) (Azpiazu and Frasch, 1993; Bodmer, 1993; Han et al., 2006; Kolsch and Paululat, 2002; Miskolczi-McCallum et al., 2005; Reim et al., 2005; Sorrentino et al., 2005). *MEF2*, which is conserved from yeast to humans, encodes the most ancient myogenic transcription factor on record (Potthoff and Olson, 2007). It is expressed in the cardiac structures of flies and humans, as well as in all organisms lying between them in the evolutionary spectrum (Black and Olson, 1998).

In humans and flies, mutations in any component of the heart GRN lead to congenital heart disease, the most common birth defect in humans (Global Burden of Disease Study 2013 Collaborators, 2015). Notably, mutations of the human NK2 family member NKX2 homeobox 5 (*NKX2-5*) are associated with cardiac conduction abnormalities, as well as ventricular and atrial septal defects (Elliott et al., 2003); in the fly, *tinman* mutants lack the dorsal vessel. The mechanisms by which the loss of GRN transcription factors TBX5 and TBX1 can lead to inborn errors of development (Holt Oram syndrome and cardiac outflow tract abnormalities, respectively), has been particularly well studied in model systems, including *Drosophila* (e.g. Fink et al., 2009; Porsch et al., 1998; Schaub et al., 2015).

A lack of **genetic redundancy** in the fly has been particularly important for advancing our understanding of heart development because it allows phenotypes to be seen in single mutants that would not otherwise be detectable in higher eukaryotes, which have greater redundancy (Olson, 2006). Several moderate- to high-throughput tools have been developed that allow investigators to probe models of heart disease in the fly (Ugur et al., 2016). First, we are equipped to view the *Drosophila* larval and pupal beating hearts using a standard dissection microscope for analysis (Cooper et al., 2009; Wessells and Bodmer, 2004). Second, a more sensitive, but lower throughput, methodology to assess heart function in fixed samples is optical coherence tomography (OCT), a 3D subsurface imaging technique (Bradu et al., 2009). Finally, relying on genetic methods of analysis, we can employ heart-specific *GAL4* drivers (like *tinman:GAL4*) to express GFP in the hearts of mutants, and conventional **epifluorescence** (or confocal microscopy as a backup) for real-time observation of heart function (Lo and Frasch, 2001; Qian et al., 2008).

Lung development and branching morphogenesis

Insights into the genetic control of lung epithelial outgrowth (also known as branching morphogenesis) have their foundation in traditional loss-of-function studies of *Drosophila* (Baer et al., 2007; Chanut-Delalande et al., 2007; Ghabrial et al., 2011). The *Drosophila* tracheal system comprises a network of tubes that lead from openings on the surface of the animal and subdivide into smaller and smaller tubes that deliver oxygen to internal tissues (Behr, 2010). The primary branches of the tracheal system are set down during embryonic development, deploying genetic programs similar to those functioning in human lung development (Liu et al., 2003). The simple structure of the *Drosophila* respiratory system makes it particularly appealing as a prototypical model for studying branching morphogenesis. Respiratory development begins with the formation of small bud-like sacs, a process dependent on two genes [*trachealess* (*trh*) and *tango* (*tgo*)] that each encode a basic helix-loop-helix (bHLH) protein (for which vertebrate counterparts remain unidentified). The subsequent elongation (in both flies and humans) of these branches depends on the Sprouty and FGF proteins, with Sprouty negatively regulating FGF10 [called Branchless (Bnl)

Disease Models & Mechanisms (2016) 9, 253-269 doi:10.1242/dmm.023564

in *Drosophila*] (Hacohen et al., 1998; Warburton et al., 2001). *Drosophila bnl* mutants have airways that are wider and shorter than normal (Jarecki et al., 1999); in mammals, loss of the FGF10 receptor FGFr2b [Breathless (Btl) in *Drosophila*] is incompatible with viability, producing undifferentiated epithelial tubes (Gredler et al., 2015; Mailleux et al., 2002).

At the end of *Drosophila* embryonic development, specialized cells within the tracheal system, called terminal cells, undergo dramatic morphogenetic changes by extending numerous thinly branched cytoplasmic projections (Ghabrial et al., 2003). Terminal cell branching is exquisitely sensitive to oxygen physiology, both in target tissues and in the terminal cells themselves (Jarecki et al., 1999). In addition, terminal cell branching is readily quantifiable. Assessment of the effects of genetic mutations on terminal cell development has revealed terminal-cell-autonomous and non-autonomous requirements for oxygen (Ghabrial et al., 2011). *Drosophila* models have also been used to test for genes associated with congenital lung disease such as asthma (e.g. *Tl*; Roeder et al., 2012), and congenital lung defects such as airway remodeling (e.g. *rhomboid*; Affolter et al., 2003) and tubulogenesis (e.g. *unpaired*; Maruyama and Andrew, 2012).

Reverse genetics – genotype-to-phenotype considerations

Developmental pathways are deeply conserved, indeed to the extent that they are considered universal (Halder et al., 1995); thus, our understanding of developmental processes in humans can be informed by an understanding of orthologous gene functions in model organisms. Recent improvements to and wide applicability of reverse genetic strategies to systematically target gene inactivation (Hardy et al., 2010) now makes it possible to expeditiously assess the roles of orthologs of human disease gene candidates in models systems such as the fly (see Fig. 1).

The Human Genome Project was a landmark endeavor, undertaken with a clear imperative to galvanize the field of medical genetics by supporting the diagnosis and management of hereditary disorders. With the sequence of the human genome now available, we must now consider how to link DNA sequences to the emergent properties of that genome. However, although genome annotation challenges have been embraced and automated, we have fallen behind in our ability to analyze at the functional level the tremendous amount of available genomic data. This is the genotype-to-phenotype bottleneck. Put another way, the speed of discovery of rare disease-causing genes has outpaced our ability to understand mechanistically how mutant alleles lead to clinical symptoms and disease. Addressing this challenge requires the development, characterization and sharing of new animal models of human disease.

The OMIM (Online Mendelian Inheritance in Man) database is a valuable resource that can point the translational scientist to rare congenital disease candidate genes that have likely orthologs in *Drosophila*, with the expectation that these orthologs can be interrogated in insect models, even without prior assignment to a biological pathway. As a starting point, Hu and colleagues (2011) used MeSH (Medical Subject Heading) terms to identify 2283 *Drosophila* genes that share at least one functional annotation with a human ortholog associated with a disease. Their analysis confirms our expectations that genes conserved functionally at the biochemical level are frequently also conserved at the biological level, and illustrates how the identification of orthologs can be an important first step to using a *Drosophila* model (or indeed any animal model) to study human congenital disease (Fig. 2). Conserved genotype-phenotype relationships in flies and humans are vital to the success of reverse genetic strategies, allowing us to make accurate predictions about loss-of-function phenotypes in *Drosophila* for orthologs of human disease candidate genes, the obligatory first step in human disease modeling. In line with this, FlyBase recently introduced Human Disease Model Reports, an integration of disease-related information from different databases (including OMIM). These reports provide a universal/less-specialized entry point for both *Drosophila* and non-*Drosophila* researchers interested in fly models of disease (Millburn et al., 2016).

Our ability to manipulate the fly genome has progressed in line with advances in discovering disease-causing mutations. These technological developments have allowed us to interrogate human disease candidate gene functions in *Drosophila* using reverse genetic approaches. One expedient way to do this is through the use of temporally and spatially controlled RNA interference (RNAi) using the UAS:GAL4 system (Box 2). This combinatorial approach makes it possible to disrupt gene activity at a level of resolution that was difficult to achieve when only classical genetic loss-of-function methods were available. Current state-of-the-art methodology exploits a set of double-stranded RNAs (dsRNAs) to achieve genome-wide RNAi knockdown. By fusing an inverted tandem repeat DNA sequence to the yeast-derived *UAS* promoter, dsRNA expression can be controlled in trans through the temporal- and/or tissue-specific expression of yeast *GAL4*. CRISPR/Cas9 genome-editing techniques (Box 2) offer unique opportunities to precisely

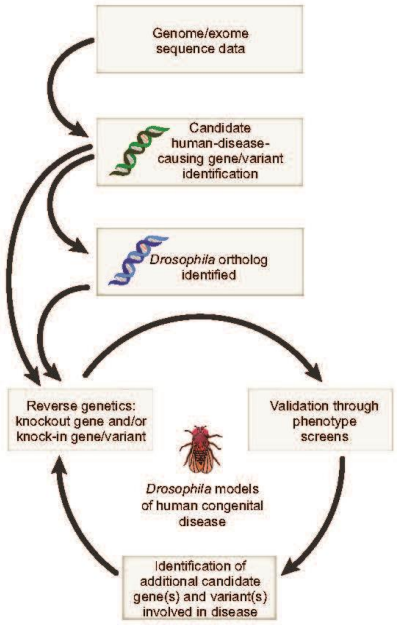

Fig. 2. The *Drosophila* pipeline for modeling human disease. Candidate disease-causing mutations are identified using variant sequence data obtained from patient sources, including whole-genome and exome sequence datasets. When *Drosophila* orthologs of candidate disease-causing genes are identified, they can be targeted for disruption and/or a human gene variant can be introduced into the fly genome; phenotypic studies are used to assess validity of the model. Upon validation, fly models of human disease and development can be used as screening platforms for the identification of additional genes and variants involved in the conserved disease/development process, and for the identification of drugs and therapies.

REVIEW Disease Models & Mechanisms (2016) 9, 253-269 doi:10.1242/dmm.023564

Table 2. Resources for generating *Drosophila* models of human congenital disease

Name	URL	Description
Databases		
FlyBase	flybase.org	Catalog of published *Drosophila* genomic data including: aberrations (deficiencies, inversions, translocations), cytologically mapped features, expression data, mutant phenotype data, references
FlyReactome	fly.reactome.org	A curated repository for *Drosophila melanogaster* signaling pathways
modENCODE	modencode.org	model organism ENCyclopedia Of DNA Elements: comprehensive compilation of genomic functional elements in the model organisms *C. elegans* and *D. melanogaster*
OMIM	omim.org	Online Mendelian Inheritance in Man: compilation of human genes and genetic disorders
Stock collections and centers		
BDGP	fruitfly.org	Berkley *Drosophila* Genome Project: resource center providing the sequence and annotation of the *Drosophila melanogaster* genome; produces gene disruptions using P-element-mediated mutagenesis and characterizes the sequence and expression of cDNAs
BDSC	flystocks.bio.indiana.edu	Bloomington *Drosophila* Stock Center: located at Indiana University (Bloomington, IN); maintains over 50,000 *Drosophila* stocks; distributed over 200,000 stocks in 2014
DGRC	dgrc.bio.indiana.edu	*Drosophila* Genome Resource Center: resource center collecting and distributing DNA clones, vectors and cell lines; also develops and tests genomics technologies for use in *Drosophila*
Drosdel Isogenic	drosdel.org.uk	An isogenic deficiency kit for *Drosophila*
Exelixis collection	drosophila.med.harvard.edu	Collection of piggyBac insertion and deficiency strains generated by Exelixis Inc. and donated to the Harvard Medical School for distribution
FlyORF	flyorf.ch	Fly Open Reading Frame: collection of 2400 transgenic *Drosophila melanogaster* UAS-ORF lines generated using the ΦC31 integrase method
GDP	flypush.imgen.bcm.tmc.edu/pscreen	Gene Disruption Project: collection of 12,000 non-targeted transposon-insertion mutant lines distributed through the BDSC, including the MiMIC (Minos-mediated integration cassette) collection
Kyoto	kyotofly.kit.jp/~flydb/cgi-bin/index.cgi	Located at the Kyoto Institute of Technology (Kyoto, Japan), the Kyoto stock center collects, maintains and distributes *Drosophila* stocks
NIG-Fly	shigen.nig.ac.jp/fly/nigfly	National Institute of Genomics-Fly: located in Mishima, Japan; maintains about 13,000 *Drosophila* mutant stocks for distribution
TRiP	flyrnai.org	Transgenic RNAi Project: collection of RNAi transgenic fly lines capable of disrupting the activity of single genes with a spatial and temporal resolution that is impossible or exceedingly difficult to achieve using classical genetic methods
VDRC	stockcenter.vdrc.at	Vienna *Drosophila* RNAi Center: located in Vienna; maintains and distributes transgenic *Drosophila* stocks and DNA resources

recreate loss-of-function mutations *in situ* (Gratz et al., 2015a,b); however, there are no current reports of disease models that take advantage of this genome-editing technique in the fly.

The *Drosophila* RNAi Screening Center (DRSC) at Harvard University has undertaken an effort to generate and utilize RNAi constructs for various research applications. With the aim of understanding the function of genes suspected of causing **orphan human diseases**, the DRSC has generated more than 9000 UAS: RNAi transgenic fly lines (designated TRiP for Transgenic RNAi Project), 1575 of which target the *Drosophila* orthologs of human genes linked to disease (Hu et al., 2011). Notably, the TRiP RNA collection provides 85% coverage for 670 high-confidence disease-associated human genes with similarly high-confidence *Drosophila* orthologs (http://www.flyrnai.org/HuDis). TRiP lines are readily available (from DRSC and Bloomington Stock Center). The Vienna *Drosophila* RNAi Collection (VDRC) currently boasts a set of almost 32,000 *Drosophila* transgenic RNAi lines, corresponding to an estimated 90% of the entire fly genome (Dietzl et al., 2007). Although the VDRC collection is larger than the TRiP collection, fewer of the RNAi lines that it contains are the product of targeted integration, and evidence suggests that validated phenotypes are more readily obtained with the use of TRiP lines (Green et al., 2014). Taken together, though, these resources ensure a human congenital disease validation pipeline in *Drosophila* (with some examples briefly described here) that is less costly and less time consuming than reverse genetic validation strategies in vertebrate model systems (Bell et al., 2009; Giacomotto and Segalat, 2010). Although these and other genetic tools (Table 2) are unmatched in any other model system, invertebrates might not always provide exact models of human development and there are known human disease genes for which there is no fly ortholog (Chien et al., 2002; Reiter et al., 2001). In these cases, a vertebrate model system might be better suited for analysis.

Human and *Drosophila* sequence databases, in combination with emerging compilations of phenotype annotations in both species, are the large 21st century datasets that serve as a starting point for reverse genetic strategies to generate *Drosophila* models of human congenital disorders, some of which are described below.

Hypoparathyroidism-retardation-dysmorphism syndrome

Hypoparathyroidism-retardation-dysmorphism (HRD) syndrome, which is also diagnosed as Sanjad-Sakati or Richardson-Kirk syndrome, is a rare, autosomal recessive inherited condition characterized by congenital hypothyroidism, mental retardation, and growth failure associated with facial dysmorphia (Abdel-Al et al., 1989; Richardson and Kirk, 1990; Sanjad et al., 1991). HRD results from mutations in the *TBCE* (tubulin-specific chaperone E) gene, which encodes a protein that is required for the proper folding of alpha-tubulin subunits and thus for the formation of alpha-beta-tubulin heterodimers (Parvari et al., 2002). The mechanism by which mutated *TBCE* causes HRD is not well understood. *Drosophila* geneticists seeking to generate a fly model of HRD identified by bioinformatics analysis one high-scoring *Drosophila TBCE* ortholog, *tbce*, for which they generated RNAi targeting constructs, as well as classic **amorphic alleles** (Jin et al., 2009). *Drosophila tbce* mutants exhibit a range of phenotypes, including

Disease Models & Mechanisms (2016) 9, 253-269 doi:10.1242/dmm.023564

abnormalities in microtubule distribution that are reminiscent of human HRD phenotypes and which are shared by individuals with related conditions, including fragile X syndrome (FXS) and hereditary spastic paraplegia (Sherwood et al., 2004; Trotta et al., 2004; Zhang and Broadie, 2005). The *Drosophila* model has proven especially useful for studying the molecular pathogenesis of HRD: genetic tests of **epistasis** have led to the identification of spastin (itself linked to hereditary spastic paraplegia) as a TBCE partner in microtubule regulation (Jin et al., 2009), providing translational scientists with new insights into TBCE's mechanism of action.

CHARGE syndrome

RNAi silencing and targeted gene-disruption approaches in *Drosophila* are also being used to model CHARGE syndrome, a common autosomal dominant disorder (1:10,000 live births) associated with wide-ranging congenital dysmorphologies, including malformations of the nasal cavity, heart, inner ear and retina (Blake et al., 1998). Two thirds of CHARGE syndrome cases are caused by mutations in the chromatin-organizing protein chromodomain helicase DNA-binding gene 7 (*CHD7*; called *Kismet* in *Drosophila*) (Sanlaville and Verloes, 2007). However, the role of CHD7 in generating the array of congenital anomalies seen in individuals with CHARGE syndrome remains unclear. The *Drosophila* model recapitulates several important aspects of the human disease (Ghosh et al., 2014; Melicharek et al., 2010), but a greater understanding of how the animal model might be best exploited to understand CHARGE syndrome perhaps comes from studies of loss-of-function mutants in *Drosophila* chromatin-organizing proteins belonging to the Polycomb group (Duncan and Lewis, 1982). In these mutants, loss of chromatin organization leads to the dysregulation of homeotic gene targets and results, not surprisingly, in wide-ranging developmental deficiencies.

Treacher Collins syndrome

Treacher Collins syndrome (1/50,000 live births) is an autosomal dominant craniofacial dysmorphology disorder caused by mutations affecting the protein TCOF1 (Treacher Collins-Franceschetti syndrome 1; Nopp140 in *Drosophila*). 60% of cases occur in infants with no previous family history of the disease, and are thus thought to arise *de novo*. Treacher Collins syndrome has been successfully modeled in flies through the disruption of *Nopp140*, which encodes a 140-kDa nucleolar and Cajal body phosphoprotein that is thought to be a ribosome assembly factor, although its specific function remains unknown (Waggener and DiMario, 2002). Whereas complete loss of *Nopp140* function is incompatible with viability, a 30% gene disruption produces dysmorphologies in the wing, leg and tergite (Cui and DiMario, 2007). In addition, the *Nopp140*^{RNAi} fly model has revealed how incomplete disruptions of Nopp140/TCOF1-dependent processes of nucleolar stress and cell death can lead to developmental dysmorphologies (He et al., 2015; James et al., 2013).

Congenital disorder of glycosylation, type IIc

Another example of the power of RNAi for generating *Drosophila* models of human congenital disease comes from studies of *Drosophila* Gfr (GDP-fucose transporter 1). In humans, mutations in *SLC35c1*, the human *Gfr* ortholog, cause the rare autosomal recessive congenital disorder of glycosylation, type IIc (CDG). Affected individuals exhibit severe mental retardation, short stature and characteristic facial dysmorphia, in addition to immune dysfunction (Frydman et al., 1992); oral administration of fucose alleviates postnatal immune deficiencies (Luhn et al., 2001). *Drosophila* geneticists, using RNAi-based knockdown strategies, discovered that flies exhibit Notch-like phenotypes when they lack Gfr and that Gfr is responsible for Notch *O*-fucosylation (Ishikawa et al., 2005). Given the previous association of the Notch pathway with Alagille syndrome, another congenital disorder associated with mental retardation, slow growth and facial dysmorphism (see earlier discussion of the Notch pathway), Ishikawa and colleagues interpreted their findings to mean that defective Notch signaling is responsible for the developmental defects associated with both CDG and Alagille syndrome. This study highlights how shared loss-of-function phenotypes generated by reverse genetic strategies can identify functional links between proteins, thereby advancing our understanding of human disease etiology and pointing us to improved diagnostic methods.

Townes-Brocks' syndrome

Townes-Brocks' syndrome (TBS) is a rare autosomal dominant inherited malformation syndrome that is characterized by anal, renal, limb and ear abnormalities, and is uniquely associated with mutations in the *SALL1* gene, which encodes a transcription factor called Spalt-like 1 [Spalt major (Salm) in flies]. Flies null for *salm*, a target of the Dpp and Hh signaling pathways, suffer embryonic lethality (Jurgens, 1988). However, an analysis of the tissue-specific functions of *salm* and *spalt-related* (*salr*) in mosaic flies that carry both wild-type and mutant cells revealed that these flies manifest antennae and genitalia defects. In addition, electrophysiological assays confirm that these flies are also deaf (Dong et al., 2003). Thus, auditory and genital abnormalities in mutant flies are reminiscent of those seen in individuals with TBS, and our comprehensive genetic and molecular understanding of Sal regulatory circuits in flies can inform our understanding of the biological abnormalities associated with TBS in humans. In this regard, most disease-causing TBS alleles produce a truncated protein that, although able to correctly interact with other Spalt proteins (there are four in humans), is unable to function properly (de Celis and Barrio, 2009).

Reverse genetics – humanized models

In addition to loss-of-function experiments dependent on forward and reverse genetic strategies, the versatile *Drosophila* experimental system also allows researchers to 'knock-in' genes of interest (usually gain-of-function alleles) using traditional transgenesis protocols. Most examples of the technique's utility for disease modeling in the fly comes from the analyses of neurodegenerative conditions, perhaps because these disorders share a common pathological denominator, protein misfolding. The subsequent formation of aberrant protein aggregates with toxic conformers selectively damage neuronal populations. In the case of Alexander disease, the autosomal dominantly inherited **leukodystrophy** is caused by mutations of *GFAP* (glial fibrillary acidic protein) for which there is no ortholog in flies. Nonetheless, glial expression of human mutant *GFAP* in transgenic flies induces the formation of Rosenthal fibers (inclusions that serve as markers of the human condition) and promotes glial-mediated neurodegeneration (Wang et al., 2011). Humanized *Drosophila* strains are used most widely to model neurological disorders (Bonini and Fortini, 2003; Jaiswal et al., 2012; Muqit and Feany, 2002), but also to study inborn errors of development, as we discuss below.

Noonan and LEOPARD syndromes

Mutation of *PTPN11*, which codes for the protein tyrosine phosphatase SHP2, is associated with two clinically related pleomorphic **RASopathies** (Noonan syndrome and LEOPARD syndrome), both of which are characterized by cardiovascular,

Disease Models & Mechanisms (2016) 9, 253-269 doi:10.1242/dmm.023564

craniofacial and skeletal malformations (Aoki et al., 2016). In the case of Noonan syndrome, gain-of-function missense mutations in *PTPN11* account for 50% of all cases, whereas mutations in other components of the **Ras/MAPK pathway** (*KRAS*, *SOS1* and *RAF1*) cause the remainder (Tidyman and Rauen, 2009). In all cases, gain-of-function missense mutations are thought to increase signaling through the Ras/MAPK pathway (Niihori et al., 2005). Noonan syndrome is inherited as an autosomal dominant disorder, but, for many affected individuals, there is no family history and cases are thought to result from *de novo* mutation. LEOPARD syndrome, which is also inherited in an autosomal dominant fashion and is distinguished from Noonan syndrome by the presence of multiple lentigines (café-au-lait spots), results only from a small set of *PTPN11* missense mutations, which are believed to be associated with the loss, rather than with the gain, of SHP2 function (Digilio et al., 2002).

In order to investigate how loss- and gain-of-function alleles of the same locus might lead to analogous phenotypes, *Drosophila* geneticists created transgenic flies that harbor the mutations found in the majority of individuals with LEOPARD syndrome {Y279C and T468M of the *PTPN11* gene [*corkscrew* (*csw*) in *Drosophila*]} to create humanized models of LEOPARD syndrome. Ubiquitous expression of either allele leads to ectopic wing venation and, in the case of Y279C, to rough eyes and increased numbers of the R7 photoreceptor – all readouts of increased RAS/MAPK signaling (Oishi et al., 2009). Recognition that LEOPARD syndrome mutations, despite their reduced src homology 2 (SH2) phosphatase activity, have gain-of-function developmental defects provided the first satisfying rationale for how *PTPN11* mutations with opposite effects on phosphatase activity might produce analogous phenotypes.

Drosophila transgenic models that harbor the gain-of-function *PTPN11/csw* mutations associated with either Noonan syndrome 1 (A72S and N308D) or juvenile myelomonocytic leukemia (E76K) (Oishi et al., 2006) have also been created; each mutation increases RAS/MAPK signaling, with A72S and E76K being the most active. Whereas ubiquitous expression of the two strongest alleles leads to embryonic lethality, expression of the Noonan-associated mutation N308D causes the formation of ectopic veins similar to those seen in the LEOPARD model.

The value of humanized allele models such as these should not be underestimated. They can be used to generate hypotheses that can then be tested in mammalian models, and provide a foundation for sensitized screens, which probe for mechanism through the identification of previously unknown interacting genes and/or therapeutic compounds. In recent years, *Drosophila* has gained traction as a repurposed tool to investigate congenital disorders of metabolism, such as diabetes (Jaiswal et al., 2012; Padmanabha and Baker, 2014), as well as syndromes caused by dominant mutations, such as the disorder epidermolysis bullosa simplex, a blistering skin disorder caused by dominant mutations in the keratin proteins keratin 5 or keratin 14 (Bohnekamp et al., 2015).

Conclusions

The *Drosophila* embryo has been mined extensively, through classic genetic loss-of-function approaches, to advance our understanding of the fundamentals of development, including pattern formation, cell fate determination, morphogenesis and organogenesis. Indeed, as discussed in this Review, elegant combinations of genetics, molecular biology and biochemistry in the *Drosophila* embryo have been used to identify and characterize virtually every important signal transduction pathway in eukaryotes, from flies to humans. Now, when we identify *Drosophila* genes that have human orthologs suspected of having developmental roles, their specific functions can be assessed in high-throughput, embryonic-lethal-stage studies in *Drosophila*.

Some consider *Drosophila* to be multiple models rolled into one, with each of its life stages (embryo, larva, pupa and adult) offering unique opportunities to model human disease and development: the embryo is useful for the study of development; *Drosophila* larvae are useful for studying physiological processes and some simple behaviors (e.g. foraging); studies in pupae have been instrumental in investigating hormonal processes (e.g. Durisko et al., 2014; Huang et al., 2014; Nassel et al., 2013; Sokolowski, 2003; Weitkunat and Schnorrer, 2014) and the adult stage of the *Drosophila* life cycle can provide us with insights into neurodegenerative disease (Alzheimer's, Parkinson's, Huntington's, FXS), and sleep and seizure disorders, as well as into cognitive/psychosis and affective disorders, cancer, cardiovascular disease, inflammation and infectious disease, and metabolic diseases, including diabetes (for review see Pandey and Nichols, 2011; Alfa and Kim, 2016). Overall, the fly offers substantial opportunities for modeling human disease well beyond the congenital disorders we discuss here.

Of note too is our recognition that the fly response to drugs is oftentimes similar to that in mammals (Andretic et al., 2008; Satta et al., 2003; Wolf and Heberlein, 2003). One of the most important advances in model-systems drug discovery was centered on an analysis of small-molecule rescue of the fragile X phenotype in the *Drosophila* model of FXS (Chang et al., 2008). FXS, an X-linked dominant neurodevelopmental syndrome characterized by moderate to severe mental retardation, macroorchidism and distinctive facial anomalies, is caused by loss of the protein-synthesis inhibitor *FMR1* (fragile X mental retardation). *FMR1* mutation results from expansion of its CGG triplet, of which there are five to 40 repeats in wild-type alleles and 55 to 200 repeats in mutant alleles, and consequent silencing of the *FMR1* gene (Santoro et al., 2012). Both the neuronal and behavioral aspects of human FXS are recapitulated in flies, either through the targeted inactivation of the *Drosophila Fmr* gene or by overexpression of mutant alleles with various repeat lengths (Wan et al., 2000). Importantly, this fly model has been used successfully for drug discovery, with mGluR (a presumed FMR1 target) antagonists rescuing behavioral phenotypes in compound screens (Chang et al., 2008). mGluR studies have been extended successfully to mouse models of FXS (Dolen et al., 2010, 2007), although so far two different mGlu5 inhibitors have failed to benefit FXS patients in clinical trials (Scharf et al., 2015).

The fruit fly, with its genetic tractability and conserved genome, offers attractive and proven opportunities for gene validation and modeling of human developmental abnormalities, leading in the long term to 21st century precision medicine encompassing diagnostics and therapies. The many success stories highlighted in this Review provide compelling justification for expansion of methodologies in flies (as well as extension whenever possible to other models, including zebrafish and mice) to assess function of the candidate disease genes that are frequently identified in neonate whole-genome sequencing studies (Petrikin et al., 2015). The models that we discuss also highlight deep conservation in flies and humans that extends from genome sequence to biological process, providing a compelling argument for more frequent use of fly models in the drug discovery process. Although there are clear indications of success based on mechanistic insight for FOP (Kaplan et al., 2013; Le and Wharton, 2012) as well as compound screening for FXS (Chang et al., 2008), it is also clear that the fly represents an underutilized model in the drug discovery process.

This article is part of a subject collection on Spotlight on *Drosophila*: Translational Impact. See related articles in this collection at http://dmm.biologists.org/collection/drosophila-disease-model.

Acknowledgements
The authors thank Diana Lim for figure preparation, and Molly Jud and Sandy Kazuko for helpful comments on the manuscript.

Competing interests
The authors declare no competing or financial interests.

Funding
A.L. acknowledges support from the NSF (IOS – 1558010).

References

Abdel-Al, Y. K., Auger, L. T. and el-Gharbawy, F. (1989). Kenny-Caffey syndrome: case report and literature review. *Clin. Pediatr.* **28**, 175-179.
Adams, M. D., Celniker, S. E., Holt, R. A., Evans, C. A., Gocayne, J. D., Amanatides, P. G., Scherer, S. E., Li, P. W., Hoskins, R. A., Galle, R. F. et al. (2000). The genome sequence of Drosophila melanogaster. *Science* **287**, 2185-2195.
Affolter, M., Bellusci, S., Itoh, N., Shilo, B., Thiery, J.-P. and Werb, Z. (2003). Tube or not tube: remodeling epithelial tissues by branching morphogenesis. *Dev. Cell* **4**, 11-18.
Akimaru, H., Hou, D.-X. and Ishii, S. (1997). Drosophila CBP is required for dorsal-dependent twist gene expression. *Nat. Genet.* **17**, 211-214.
Alfa, R. W. and Kim, S. K. (2016). Using Drosophila to discover mechanisms underlying type 2 diabetes. *Dis. Model. Mech.* **9**, doi:10.1242/dmm.023887 (in press).
Andretic, R., Kim, Y.-C., Jones, F. S., Han, K.-A. and Greenspan, R. J. (2008). Drosophila D1 dopamine receptor mediates caffeine-induced arousal. *Proc. Natl. Acad. Sci. USA* **105**, 20392-20397.
Aoki, Y., Niihori, T., Inoue, S.-I. and Matsubara, Y. (2016). Recent advances in RASopathies. *J. Hum. Genet.* **61**, 33-39.
Arendt, D., Tessmar-Raible, K., Snyman, H., Dorresteijn, A. W. and Wittbrodt, J. (2004). Ciliary photoreceptors with a vertebrate-type opsin in an invertebrate brain. *Science* **306**, 869-871.
Ashburner, M. and Thompson, J. (1978). The laboratory culture of Drosophila. In *The Genetics and Biology of Drosophila*, Vol. 2A (ed. M. Ashburner and T. Wright), pp. 1-81. London and New York: Academic Press.
Ashburner, M., Golic, K. G. and Hawley, R. S. (2011). *Drosophila: A Laboratory Handbook*. Cold Spring Harbor, NY: Cold Spring Harbor Laboratory Press.
Attisano, L. and Wrana, J. L. (2002). Signal transduction by the TGF-beta superfamily. *Science* **296**, 1646-1647.
Azpiazu, N. and Frasch, M. (1993). tinman and bagpipe: two homeo box genes that determine cell fates in the dorsal mesoderm of Drosophila. *Genes Dev.* **7**, 1325-1340.
Baer, M. M., Bilstein, A. and Leptin, M. (2007). A clonal genetic screen for mutants causing defects in larval tracheal morphogenesis in Drosophila. *Genetics* **176**, 2279-2291.
Baker, N. E., Li, K., Quiquand, M., Ruggiero, R. and Wang, L.-H. (2014). Eye development. *Methods* **68**, 252-259.
Bakrania, P., Efthymiou, M., Klein, J. C., Salt, A., Bunyan, D. J., Wyatt, A., Ponting, C. P., Martin, A., Williams, S., Lindley, V. et al. (2008). Mutations in BMP4 cause eye, brain, and digit developmental anomalies: overlap between the BMP4 and hedgehog signaling pathways. *Am. J. Hum. Genet.* **82**, 304-319.
Behr, M. (2010). Molecular aspects of respiratory and vascular tube development. *Respir. Physiol. Neurobiol.* **173** Suppl., S33-S36.
Bell, A. J., McBride, S. M. J. and Dockendorff, T. C. (2009). Flies as the ointment: Drosophila modeling to enhance drug discovery. *Fly* **3**, 39-49.
Beumer, K. J. and Carroll, D. (2014). Targeted genome engineering techniques in Drosophila. *Methods* **68**, 29-37.
Bhatia, S., Bengani, H., Fish, M., Brown, A., Divizia, M. T., de Marco, R., Damante, G., Grainger, R., van Heyningen, V. and Kleinjan, D. A. (2013). Disruption of autoregulatory feedback by a mutation in a remote, ultraconserved PAX6 enhancer causes aniridia. *Am. J. Hum. Genet.* **93**, 1126-1134.
Bier, E. (2005). Drosophila, the golden bug, emerges as a tool for human genetics. *Nat. Rev. Genet.* **6**, 9-23.
Black, B. L. and Olson, E. N. (1998). Transcriptional control of muscle development by myocyte enhancer factor-2 (MEF2) proteins. *Annu. Rev. Cell Dev. Biol.* **14**, 167-196.
Blake, K. D., Davenport, S. L. H., Hall, B. D., Hefner, M. A., Pagon, R. A., Williams, M. S., Lin, A. E. and Graham, J. M., Jr (1998). CHARGE association: an update and review for the primary pediatrician. *Clin. Pediatr.* **37**, 159-173.
Blanco, J., Girard, F., Kamachi, Y., Kondoh, H. and Gehring, W. J. (2005). Functional analysis of the chicken delta1-crystallin enhancer activity in Drosophila reveals remarkable evolutionary conservation between chicken and fly. *Development* **132**, 1895-1905.
Bodmer, R. (1993). The gene tinman is required for specification of the heart and visceral muscles in Drosophila. *Development* **118**, 719-729.
Bohnekamp, J., Cryderman, D. E., Paululat, A., Baccam, G. C., Wallrath, L. L. and Magin, T. M. (2015). A Drosophila model of epidermolysis bullosa simplex. *J. Invest. Dermatol.* **135**, 2031-2039.
Bonini, N. M. and Fortini, M. E. (2003). Human neurodegenerative disease modeling using Drosophila. *Annu. Rev. Neurosci.* **26**, 627-656.
Borst, A. and Helmstaedter, M. (2015). Common circuit design in fly and mammalian motion vision. *Nat. Neurosci.* **18**, 1067-1076.
Boutros, M. and Ahringer, J. (2008). The art and design of genetic screens: RNA interference. *Nat. Rev. Genet.* **9**, 554-566.
Bradu, A., Ma, L., Bloor, J. W. and Podoleanu, A. (2009). Dual optical coherence tomography/fluorescence microscopy for monitoring of Drosophila melanogaster larval heart. *J. Biophotonics* **2**, 380-388.
Brand, A. and Perrimon, N. (1993). Targeted gene expression as a means of altering cell fates and generating dominant phenotypes. *Development* **118**, 401-415.
Campbell, G. and Tomlinson, A. (1999). Transducing the Dpp morphogen gradient in the wing of Drosophila: regulation of Dpp targets by brinker. *Cell* **96**, 553-562.
Casso, D. J., Liu, S., Iwaki, D. D., Ogden, S. K. and Kornberg, T. B. (2008). A screen for modifiers of hedgehog signaling in Drosophila melanogaster identifies swm and mts. *Genetics* **178**, 1399-1413.
Castanon, I. and Baylies, M. K. (2002). A Twist in fate: evolutionary comparison of Twist structure and function. *Gene* **287**, 11-22.
CDC. (2008). Update on overall prevalence of major birth defects–Atlanta, Georgia, 1978-2005. *Morb. Mortal Wkly. Rep.* **57**, 1-5.
Chang, S., Bray, S. M., Li, Z., Zarnescu, D. C., He, C., Jin, P. and Warren, S. T. (2008). Identification of small molecules rescuing fragile X syndrome phenotypes in Drosophila. *Nat. Chem. Biol.* **4**, 256-263.
Chanut-Delalande, H., Jung, A. C., Lin, L., Baer, M. M., Bilstein, A., Cabernard, C., Leptin, M. and Affolter, M. (2007). A genetic mosaic analysis with a repressible cell marker screen to identify genes involved in tracheal cell migration during Drosophila air sac morphogenesis. *Genetics* **176**, 2177-2187.
Chapman, G., Sparrow, D. B., Kremmer, E. and Dunwoodie, S. L. (2011). Notch inhibition by the ligand DELTA-LIKE 3 defines the mechanism of abnormal vertebral segmentation in spondylocostal dysostosis. *Hum. Mol. Genet.* **20**, 905-916.
Chen, D., Zhao, M., Harris, S. E. and Mi, Z. (2004). Signal transduction and biological functions of bone morphogenetic proteins. *Front. Biosci.* **9**, 349-358.
Chien, S., Reiter, L. T., Bier, E. and Gribskov, M. (2002). Homophila: human disease gene cognates in Drosophila. *Nucleic Acids Res.* **30**, 149-151.
Chinnadurai, S. and Goudy, S. (2012). Understanding velocardiofacial syndrome: how recent discoveries can help you improve your patient outcomes. *Curr. Opin. Otolaryngol. Head Neck Surg.* **20**, 502-506.
Christianson, A., Howson, C. P. and Modell, B. (2006). *The hidden toll of dying and disabled children. March of Dimes Global Report on Birth Defects*. http://www.marchofdimes.org/materials/global-report-on-birth-defects-the-hidden-toll-of-dying-and-disabled-children-full-report.pdf
Cooper, A. S., Rymond, K. E., Ward, M. A., Bocook, E. L. and Cooper, R. L. (2009). Monitoring heart function in larval Drosophila melanogaster for physiological studies. *J. Vis. Exp.* e1596.
Cui, Z. and DiMario, P. J. (2007). RNAi knockdown of Nopp140 induces minute-like phenotypes in Drosophila. *Mol. Biol. Cell* **18**, 2179-2191.
de Celis, J. F. and Barrio, R. (2009). Regulation and function of Spalt proteins during animal development. *Int. J. Dev. Biol.* **53**, 1385-1398.
de la Pompa, J. L., Wakeham, A., Correia, K. M., Samper, E., Brown, S., Aguilera, R. J., Nakano, T., Honjo, T., Mak, T. W., Rossant, J. et al. (1997). Conservation of the Notch signalling pathway in mammalian neurogenesis. *Development* **124**, 1139-1148.
Dietzl, G., Chen, D., Schnorrer, F., Su, K. C., Barinova, Y., Fellner, M., Gasser, B., Kinsey, K., Oppel, S., Scheiblauer, S. et al. (2007). A genome-wide transgenic RNAi library for conditional gene inactivation in Drosophila. *Nature* **448**, 151-156.
Digilio, M. C., Conti, E., Sarkozy, A., Mingarelli, R., Dottorini, T., Marino, B., Pizzuti, A. and Dallapiccola, B. (2002). Grouping of multiple-lentigines/LEOPARD and Noonan syndromes on the PTPN11 gene. *Am. J. Hum. Genet.* **71**, 389-394.
Dolen, G., Osterweil, E., Rao, B. S. S., Smith, G. B., Auerbach, B. D., Chattarji, S. and Bear, M. F. (2007). Correction of fragile X syndrome in mice. *Neuron* **56**, 955-962.
Dolen, G., Carpenter, R. L., Ocain, T. D. and Bear, M. F. (2010). Mechanism-based approaches to treating fragile X. *Pharmacol. Ther.* **127**, 78-93.
Dong, P. D. S., Todi, S. V., Eberl, D. F. and Boekhoff-Falk, G. (2003). Drosophila spalt/spalt-related mutants exhibit Townes-Brocks' syndrome phenotypes. *Proc. Natl. Acad. Sci. USA* **100**, 10293-10298.

Duncan, I. and Lewis, E. B. (1982). Genetic control of body segment differentiation in *Drosophila*. In *Developmental Order: Its Origin and Regulation* (ed. S. Subtelny). pp. 533-554. New York: Liss.
Durisko, Z., Kemp, R., Mubasher, R. and Dukas, R. (2014). Dynamics of social behavior in fruit fly larvae. *PLoS ONE* **9**, e95495.
Edison, R. and Muenke, M. (2003). The interplay of genetic and environmental factors in craniofacial morphogenesis: holoprosencephaly and the role of cholesterol. *Congenit. Anom.* **43**, 1-21.
Elliott, D. A., Kirk, E. P., Yeoh, T., Chandar, S., McKenzie, F., Taylor, P., Grossfeld, P., Fatkin, D., Jones, O., Hayes, P. et al. (2003). Cardiac homeobox gene NKX2-5 mutations and congenital heart disease: associations with atrial septal defect and hypoplastic left heart syndrome. *J. Am. Coll. Cardiol.* **41**, 2072-2076.
Fink, M., Callol-Massot, C., Chu, A., Ruiz-Lozano, P., Izpisua Belmonte, J. C., Giles, W., Bodmer, R. and Ocorr, K. (2009). A new method for detection and quantification of heartbeat parameters in Drosophila, zebrafish, and embryonic mouse hearts. *Biotechniques* **46**, 101-113.
Francois, V., Solloway, M., O'Neill, J. W., Emery, J. and Bier, E. (1994). Dorsal-ventral patterning of the Drosophila embryo depends on a putative negative growth factor encoded by the short gastrulation gene. *Genes Dev.* **8**, 2602-2616.
Frydman, M., Etzioni, A., Eidlitz-Markus, T., Avidor, I., Varsano, I., Shechter, Y., Orlin, J. B. and Gershoni-Baruch, R. (1992). Rambam-Hasharon syndrome of psychomotor retardation, short stature, defective neutrophil motility, and Bombay phenotype. *Am. J. Med. Genet.* **44**, 297-302.
Garg, V., Muth, A. N., Ransom, J. F., Schluterman, M. K., Barnes, R., King, I. N., Grossfeld, P. D. and Srivastava, D. (2005). Mutations in NOTCH1 cause aortic valve disease. *Nature* **437**, 270-274.
Gehring, W. J. (2002). The genetic control of eye development and its implications for the evolution of the various eye-types. *Int. J. Dev. Biol.* **46**, 65-73.
Gehring, W. J. (2014). The evolution of vision. *Wiley Interdiscip. Rev. Dev. Biol.* **3**, 1-40.
Gehring, W. J. and Ikeo, K. (1999). Pax 6: mastering eye morphogenesis and eye evolution. *Trends Genet.* **15**, 371-377.
Ghabrial, A., Luschnig, S., Metzstein, M. M. and Krasnow, M. A. (2003). Branching morphogenesis of the Drosophila tracheal system. *Annu. Rev. Cell Dev. Biol.* **19**, 623-647.
Ghabrial, A. S., Levi, B. P. and Krasnow, M. A. (2011). A systematic screen for tube morphogenesis and branching genes in the Drosophila tracheal system. *PLoS Genet.* **7**, e1002087.
Ghosh, R., Vegesna, S., Safi, R., Bao, H., Zhang, B., Marenda, D. R. and Liebl, F. L. W. (2014). Kismet positively regulates glutamate receptor localization and synaptic transmission at the Drosophila neuromuscular junction. *PLoS ONE* **9**, e113494.
Giacomotto, J. and Segalat, L. (2010). High-throughput screening and small animal models, where are we? *Br. J. Pharmacol.* **160**, 204-216.
Glise, B. and Noselli, S. (1997). Coupling of Jun amino-terminal kinase and Decapentaplegic signaling pathways in Drosophila morphogenesis. *Genes Dev.* **11**, 1738-1747.
Global Burden of Disease Study 2013 Collaborators (2015). Global, regional, and national incidence, prevalence, and years lived with disability for 301 acute and chronic diseases and injuries in 188 countries, 1990–2013: a systematic analysis for the Global Burden of Disease Study 2013. *Lancet* **386**, 743-800.
Golic, K. G. (1994). Local transposition of P elements in Drosophila melanogaster and recombination between duplicated elements using a site-specific recombinase. *Genetics* **137**, 551-563.
Gong, W. J. and Golic, K. G. (2003). Ends-out, or replacement, gene targeting in Drosophila. *Proc. Natl. Acad. Sci. USA* **100**, 2556-2561.
Goodrich, L. V., Johnson, R. L., Milenkovic, L., McMahon, J. A. and Scott, M. P. (1996). Conservation of the hedgehog/patched signaling pathway from flies to mice: induction of a mouse patched gene by Hedgehog. *Genes Dev.* **10**, 301-312.
Gorlin, R. J. and Goltz, R. W. (1960). Multiple nevoid basal-cell epithelioma, jaw cysts and bifid rib. A syndrome. *N. Engl. J. Med.* **262**, 908-912.
Grafe, I., Yang, T., Alexander, S., Homan, E. P., Lietman, C., Jiang, M. M., Bertin, T., Munivez, E., Chen, Y., Dawson, B. et al. (2014). Excessive transforming growth factor-beta signaling is a common mechanism in osteogenesis imperfecta. *Nat. Med.* **20**, 670-675.
Gratz, S. J., Harrison, M. M., Wildonger, J. and O'Connor-Giles, K. M. (2015a). Precise genome editing of Drosophila with CRISPR RNA-guided Cas9. *Methods Mol. Biol.* **1311**, 335-348.
Gratz, S. J., Rubinstein, C. D., Harrison, M. M., Wildonger, J. and O'Connor-Giles, K. M. (2015b). CRISPR-Cas9 genome editing in Drosophila. *Curr. Protoc. Mol. Biol.* **111**, 31.2.1-31.2.20.
Gredler, M. L., Seifert, A. W. and Cohn, M. J. (2015). Tissue-specific roles of Fgfr2 in development of the external genitalia. *Development* **142**, 2203-2212.
Green, E. W., Fedele, G., Giorgini, F. and Kyriacou, C. P. (2014). A Drosophila RNAi collection is subject to dominant phenotypic effects. *Nat. Methods* **11**, 222-223.
Greenwald, I. (2012). Notch and the awesome power of genetics. *Genetics* **191**, 655-669.
Gridley, T. (2003). Notch signaling and inherited disease syndromes. *Hum. Mol. Genet.* **12** Suppl. 1, R9-R13.
Gripp, K. W., Robbins, K. M., Sobreira, N. L., Witmer, P. D., Bird, L. M., Avela, K., Makitie, O., Alves, D., Hogue, J. S., Zackai, E. H. et al. (2015). Truncating mutations in the last exon of NOTCH3 cause lateral meningocele syndrome. *Am. J. Med. Genet. A* **167A**, 271-281.
Groth, A. C., Fish, M., Nusse, R. and Calos, M. P. (2004). Construction of transgenic Drosophila by using the site-specific integrase from phage phiC31. *Genetics* **166**, 1775-1782.
Hacohen, N., Kramer, S., Sutherland, D., Hiromi, Y. and Krasnow, M. A. (1998). sprouty encodes a novel antagonist of FGF signaling that patterns apical branching of the Drosophila airways. *Cell* **92**, 253-263.
Hahn, H., Wicking, C., Zaphiropoulous, P. G., Gailani, M. R., Shanley, S., Chidambaram, A., Vorechovsky, I., Holmberg, E., Unden, A. B., Gillies, S. et al. (1996). Mutations of the human homolog of Drosophila patched in the nevoid basal cell carcinoma syndrome. *Cell* **85**, 841-851.
Halder, G., Callaerts, P. and Gehring, W. J. (1995). Induction of ectopic eyes by targeted expression of the eyeless gene in Drosophila. *Science* **267**, 1788-1792.
Han, Z., Yi, P., Li, X. and Olson, E. N. (2006). Hand, an evolutionarily conserved bHLH transcription factor required for Drosophila cardiogenesis and hematopoiesis. *Development* **133**, 1175-1182.
Hardy, S., Legagneux, V., Audic, Y. and Paillard, L. (2010). Reverse genetics in eukaryotes. *Biol. Cell* **102**, 561-580.
Harper, P. S. (2010). *Practical Genetic Counselling*. Boca Raton, FL: CRC Press.
Hartenstein, A. Y., Rugendorff, A., Tepass, U. and Hartenstein, V. (1992). The function of the neurogenic genes during epithelial development in the Drosophila embryo. *Development* **116**, 1203-1220.
Hartl, D. L. (2000). Molecular melodies in high and low C. *Nat. Rev. Genet.* **1**, 145-149.
He, F., James, A., Raje, H., Ghaffari, H. and DiMario, P. (2015). Deletion of Drosophila Nopp140 induces subcellular ribosomopathies. *Chromosoma* **124**, 191-208.
Hebert, J. M. and Fishell, G. (2008). The genetics of early telencephalon patterning: some assembly required. *Nat. Rev. Neurosci.* **9**, 678-685.
Hennekam, R. C. M. (2006). Rubinstein-Taybi syndrome. *Eur. J. Hum. Genet.* **14**, 981-985.
Heussler, H. S., Suri, M., Young, I. D. and Muenke, M. (2002). Extreme variability of expression of a Sonic Hedgehog mutation: attention difficulties and holoprosencephaly. *Arch. Dis. Child* **86**, 293-296.
Hooper, J. E. and Scott, M. P. (1989). The Drosophila patched gene encodes a putative membrane protein required for segmental patterning. *Cell* **59**, 751-765.
Hsu, P., Ma, A., Wilson, M., Williams, G., Curotta, J., Munns, C. F. and Mehr, S. (2014). CHARGE syndrome: a review. *J. Paediatr. Child Health* **50**, 504-511.
Hu, Y., Flockhart, I., Vinayagam, A., Bergwitz, C., Berger, B., Perrimon, N. and Mohr, S. E. (2011). An integrative approach to ortholog prediction for disease-focused and other functional studies. *BMC Bioinformatics* **12**, 357.
Huang, Y.-C., Lu, Y.-N., Wu, J.-T., Chien, C.-T. and Pi, H. (2014). The COP9 signalosome converts temporal hormone signaling to spatial restriction on neural competence. *PLoS Genet.* **10**, e1004760.
Humphreys, G. B., Jud, M. C., Monroe, K. M., Kimball, S. S., Higley, M., Shipley, D., Vrablik, M. C., Bates, K. L. and Letsou, A. (2013). Mummy, A UDP-N-acetylglucosamine pyrophosphorylase, modulates DPP signaling in the embryonic epidermis of Drosophila. *Dev. Biol.* **381**, 434-445.
Ingham, P. W. (1998). The patched gene in development and cancer. *Curr. Opin. Genet. Dev.* **8**, 88-94.
Ishikawa, H. O., Higashi, S., Ayukawa, T., Sasamura, T., Kitagawa, M., Harigaya, K., Aoki, K., Ishida, N., Sanai, Y. and Matsuno, K. (2005). Notch deficiency implicated in the pathogenesis of congenital disorder of glycosylation IIc. *Proc. Natl. Acad. Sci. USA* **102**, 18532-18537.
Jaiswal, M., Sandoval, H., Zhang, K., Bayat, V. and Bellen, H. J. (2012). Probing mechanisms that underlie human neurodegenerative diseases in Drosophila. *Annu. Rev. Genet.* **46**, 371-396.
James, A., Cindass, R., Jr, Mayer, D., Terhoeve, S., Mumphrey, C. and DiMario, P. (2013). Nucleolar stress in Drosophila melanogaster: RNAi-mediated depletion of Nopp140. *Nucleus* **4**, 123-133.
Janody, F., Lee, J. D., Jahren, N., Hazelett, D. J., Benlali, A., Miura, G. I., Draskovic, I. and Treisman, J. E. (2004). A mosaic genetic screen reveals distinct roles for trithorax and polycomb group genes in Drosophila eye development. *Genetics* **166**, 187-200.
Jarecki, J., Johnson, E. and Krasnow, M. A. (1999). Oxygen regulation of airway branching in Drosophila is mediated by branchless FGF. *Cell* **99**, 211-220.
Jeibmann, A. and Paulus, W. (2009). Drosophila melanogaster as a model organism of brain diseases. *Int. J. Mol. Sci.* **10**, 407-440.
Jurgens, G. (1988). Head and tail development of the *Drosophila* embryo involves *spalt*, a novel homeotic gene. *EMBO J.* **7**, 189-196.
Jin, S., Pan, L., Liu, Z., Wang, Q., Xu, Z. and Zhang, Y. Q. (2009). Drosophila Tubulin-specific chaperone E functions at neuromuscular synapses and is required for microtubule network formation. *Development* **136**, 1571-1581.
Johnson, R. L., Rothman, A. L., Xie, J., Goodrich, L. V., Bare, J. W., Bonifas, J. M., Quinn, A. G., Myers, R. M., Cox, D. R., Epstein, E. H., Jr et al. (1996).

Human homolog of patched, a candidate gene for the basal cell nevus syndrome. *Science* **272**, 1668-1671.
Kamath, B. M., Bason, L., Piccoli, D. A., Krantz, I. D. and Spinner, N. B. (2003). Consequences of JAG1 mutations. *J. Med. Genet.* **40**, 891-895.
Kaplan, F. S., Tabas, J. A. and Zasloff, M. A. (1990). Fibrodysplasia ossificans progressiva: a clue from the fly? *Calcif. Tissue Int.* **47**, 117-125.
Kaplan, F. S., Pignolo, R. J. and Shore, E. M. (2013). From mysteries to medicines: drug development for fibrodysplasia ossificans progressiva. *Expert Opin. Orphan. Drugs* **1**, 637-649.
Karim, F. D., Chang, H. C., Therrien, M., Wassarman, D. A., Laverty, T. and Rubin, G. M. (1996). A screen for genes that function downstream of Ras1 during Drosophila eye development. *Genetics* **143**, 315-329.
Kaufman, M. H., Chang, H. H. and Shaw, J. P. (1995). Craniofacial abnormalities in homozygous Small eye (Sey/Sey) embryos and newborn mice. *J. Anat.* **186**, 607-617.
Kidd, S., Kelley, M. R. and Young, M. W. (1986). Sequence of the notch locus of Drosophila melanogaster: relationship of the encoded protein to mammalian clotting and growth factors. *Mol. Cell. Biol.* **6**, 3094-3108.
Kochanek, K. D., Kirmeyer, S. E., Martin, J. A., Strobino, D. M. and Guyer, B. (2012). Annual summary of vital statistics: 2009. *Pediatrics* **129**, 338-348.
Kolsch, V. and Paululat, A. (2002). The highly conserved cardiogenic bHLH factor Hand is specifically expressed in circular visceral muscle progenitor cells and in all cell types of the dorsal vessel during Drosophila embryogenesis. *Dev. Genes Evol.* **212**, 473-485.
Lander, E. S. Linton, L. M. Birren, B. Nusbaum, C. Zody, M. C. Baldwin, J. Devon, K. Dewar, K. Doyle, M. FitzHugh, W. et al. (2001). Initial sequencing and analysis of the human genome. *Nature* **409**, 860-921.
Le, V. Q. and Wharton, K. A. (2012). Hyperactive BMP signaling induced by ALK2 (R206H) requires type II receptor function in a Drosophila model for classic fibrodysplasia ossificans progressiva. *Dev. Dyn.* **241**, 200-214.
Lehmann, K., Seemann, P., Boergermann, J., Morin, G., Reif, S., Knaus, P. and Mundlos, S. (2006). A novel R486Q mutation in BMPR1B resulting in either a brachydactyly type C/symphalangism-like phenotype or brachydactyly type A2. *Eur. J. Hum. Genet.* **14**, 1248-1254.
Lesch, B. J. and Page, D. C. (2012). Genetics of germ cell development. *Nat. Rev. Genet.* **13**, 781-794.
Lieber, T., Kidd, S., Alcamo, E., Corbin, V. and Young, M. W. (1993). Antineurogenic phenotypes induced by truncated Notch proteins indicate a role in signal transduction and may point to a novel function for Notch in nuclei. *Genes Dev.* **7**, 1949-1965.
Liu, L., Johnson, W. A. and Welsh, M. J. (2003). Drosophila DEG/ENaC pickpocket genes are expressed in the tracheal system, where they may be involved in liquid clearance. *Proc. Natl. Acad. Sci. USA* **100**, 2128-2133.
Liu, L., Oza, S., Hogan, D., Perin, J., Rudan, I., Lawn, J. E. Cousens, S., Mathers, C. and Black, R. E. (2015). Global, regional, and national causes of child mortality in 2000–13, with projections to inform post-2015 priorities: an updated systematic analysis. *Lancet* **385**, 430-440.
Lo, P. C. H. and Frasch, M. (2001). A role for the COUP-TF-related gene seven-up in the diversification of cardioblast identities in the dorsal vessel of Drosophila. *Mech. Dev.* **104**, 49-60.
Lobo, I. and Zhaurova, K. (2008). Birth defects: causes and statistics. *Nat. Educ.* **1**, 18.
Luhn, K., Marquardt, T., Harms, E. and Vestweber, D. (2001). Discontinuation of fucose therapy in LADII causes rapid loss of selectin ligands and rise of leukocyte counts. *Blood* **97**, 330-332.
Lum, L., Yao, S., Mozer, B., Rovescalli, A., Von Kessler, D., Nirenberg, M. and Beachy, P. A. (2003). Identification of Hedgehog pathway components by RNAi in Drosophila cultured cells. *Science* **299**, 2039-2045.
Mailleux, A. A., Spencer-Dene, B., Dillon, C., Ndiaye, D., Savona-Baron, C., Itoh, N., Kato, S., Dickson, C., Thiery, J. P. and Bellusci, S. (2002). Role of FGF10/FGFR2b signaling during mammary gland development in the mouse embryo. *Development* **129**, 53-60.
Martignetti, J. A., Tian, L., Li, D., Ramirez, M. C. M., Camacho-Vanegas, O., Camacho, S. C., Guo, Y., Zand, D. J., Bernstein, A. M., Masur, S. K. et al. (2013). Mutations in PDGFRB cause autosomal-dominant infantile myofibromatosis. *Am. J. Hum. Genet.* **92**, 1001-1007.
Martin, P. and Wood, W. (2002). Epithelial fusions in the embryo. *Curr. Opin. Cell Biol.* **14**, 569-574.
Maruyama, R. and Andrew, D. J. (2012). Drosophila as a model for epithelial tube formation. *Dev. Dyn.* **241**, 119-135.
Massague, J. (2012). TGFbeta signalling in context. *Nat. Rev. Mol. Cell Biol.* **13**, 616-630.
Mathews, T. J., MacDorman, M. F. and Thoma, M. E. (2015). Infant mortality statistics from the 2013 period linked birth/infant death data set. *Natl. Vital. Stat. Rep.* **64**, 1-30.
McGuire, S. E., Le, P. T., Osborn, A. J., Matsumoto, K. and Davis, R. L. (2003). Spatiotemporal rescue of memory dysfunction in Drosophila. *Science* **302**, 1765-1768.
McLysaght, A., Hokamp, K. and Wolfe, K. H. (2002). Extensive genomic duplication during early chordate evolution. *Nat. Genet.* **31**, 200-204.
Melicharek, D. J., Ramirez, L. C., Singh, S., Thompson, R. and Marenda, D. R. (2010). Kismet/CHD7 regulates axon morphology, memory and locomotion in a Drosophila model of CHARGE syndrome. *Hum. Mol. Genet.* **19**, 4253-4264.
Millburn, G. H., Crosby, M. A., Gramates, L. S., Tweedie, S. and the FlyBase Consortium (2016). FlyBase portals to human disease research using Drosophila models. *Dis. Model. Mech.* **9**, 245-252.
Ming, J. E. and Muenke, M. (2002). Multiple hits during early embryonic development: digenic diseases and holoprosencephaly. *Am. J. Hum. Genet.* **71**, 1017-1032.
Ming, J. E., Kaupas, M. E., Roessler, E., Brunner, H. G., Golabi, M., Tekin, M., Stratton, R. F., Sujansky, E., Bale, S. J. and Muenke, M. (2002). Mutations in PATCHED-1, the receptor for SONIC HEDGEHOG, are associated with holoprosencephaly. *Hum. Genet.* **110**, 297-301.
Miskolczi-McCallum, C. M., Scavetta, R. J., Svendsen, P. C., Soanes, K. H. and Brook, W. J. (2005). The Drosophila melanogaster T-box genes midline and H15 are conserved regulators of heart development. *Dev. Biol.* **278**, 459-472.
Moberg, K. H., Bell, D. W., Wahrer, D. C. R., Haber, D. A. and Hariharan, I. K. (2001). Archipelago regulates Cyclin E levels in Drosophila and is mutated in human cancer cell lines. *Nature* **413**, 311-316.
Morgan, T. H. (1917). The theory of the gene. *Am. Nat.* **51**, 513-544.
Muqit, M. M. K. and Feany, M. B. (2002). Modelling neurodegenerative diseases in Drosophila: a fruitful approach? *Nat. Rev. Neurosci.* **3**, 237-243.
Nakano, Y., Guerrero, I., Hidalgo, A., Taylor, A., Whittle, J. R. S. and Ingham, P. W. (1989). A protein with several possible membrane-spanning domains encoded by the Drosophila segment polarity gene patched. *Nature* **341**, 508-513.
Nakayama, T., Fisher, M., Nakajima, K., Odeleye, A. O., Zimmerman, K. B., Fish, M. B., Yaoita, Y., Chojnowski, J. L., Lauderdale, J. D., Netland, P. A. et al. (2015). Xenopus pax6 mutants affect eye development and other organ systems, and have phenotypic similarities to human aniridia patients. *Dev. Biol.* **408**, 328-344.
Nassel, D. R., Kubrak, O. I., Liu, Y., Luo, J. and Lushchak, O. V. (2013). Factors that regulate insulin producing cells and their output in Drosophila. *Front. Physiol.* **4**, 252.
Neumann, C. (2005). Hedgehogs as negative regulators of the cell cycle. *Cell Cycle* **4**, 1139-1140.
Nicholson, L., Singh, G. K., Osterwalder, T., Roman, G. W., Davis, R. L. and Keshishian, H. (2008). Spatial and temporal control of gene expression in Drosophila using the inducible GeneSwitch GAL4 system. I. Screen for larval nervous system drivers. *Genetics* **178**, 215-234.
Niihori, T., Aoki, Y., Ohashi, H., Kurosawa, K., Kondoh, T., Ishikiriyama, S., Kawame, H., Kamasaki, H., Yamanaka, T., Takada, F. et al. (2005). Functional analysis of PTPN11/SHP-2 mutants identified in Noonan syndrome and childhood leukemia. *J. Hum. Genet.* **50**, 192-202.
Nusslein-Volhard, C. and Wieschaus, E. (1980). Mutations affecting segment number and polarity in Drosophila. *Nature* **287**, 795-801.
O'Connor, M. B., Umulis, D., Othmer, H. G. and Blair, S. S. (2006). Shaping BMP morphogen gradients in the Drosophila embryo and pupal wing. *Development* **133**, 183-193.
Oishi, K., Gaengel, K., Krishnamoorthy, S., Kamiya, K., Kim, I.-K., Ying, H., Weber, U., Perkins, L. A., Tartaglia, M., Mlodzik, M. et al. (2006). Transgenic Drosophila models of Noonan syndrome causing PTPN11 gain-of-function mutations. *Hum. Mol. Genet.* **15**, 543-553.
Oishi, K., Zhang, H., Gault, W. J., Wang, C. J., Tan, C. C., Kim, I.-K., Ying, H., Rahman, T., Pica, N., Tartaglia, M. et al. (2009). Phosphatase-defective LEOPARD syndrome mutations in PTPN11 gene have gain-of-function effects during Drosophila development. *Hum. Mol. Genet.* **18**, 193-201.
Olson, E. N. (2006). Gene regulatory networks in the evolution and development of the heart. *Science* **313**, 1922-1927.
Osterwalder, T., Yoon, K. S., White, B. H. and Keshishian, H. (2001). A conditional tissue-specific transgene expression system using inducible GAL4. *Proc. Natl. Acad. Sci. USA* **98**, 12596-12601.
Padmanabha, D. and Baker, K. D. (2014). Drosophila gains traction as a repurposed tool to investigate metabolism. *Trends Endocrinol. Metab.* **25**, 518-527.
Pandey, U. B. and Nichols, C. D. (2011). Human disease models in Drosophila melanogaster and the role of the fly in therapeutic drug discovery. *Pharmacol. Rev.* **63**, 411-436.
Parvari, R., Hershkovitz, E., Grossman, N., Gorodischer, R., Loeys, B., Zecic, A., Mortier, G., Gregory, S., Sharony, R., Kambouris, M. et al. (2002). Mutation of TBCE causes hypoparathyroidism-retardation-dysmorphism and autosomal recessive Kenny-Caffey syndrome. *Nat. Genet.* **32**, 448-452.
Paulk, A., Millard, S. S. and van Swinderen, B. (2013). Vision in Drosophila: seeing the world through a model's eyes. *Annu. Rev. Entomol.* **58**, 313-332.
Pennisi, E. (2002). Evolution of developmental diversity: evo-devo devotees eye ocular origins and more. *Science* **296**, 1010-1011.
Petrij, F., Dorien, J. M. Peters, R. C. M. and Hennekam, R. G. (2008). *CBP* (*BREBP*) and the Rubinstein-Taybi Syndrome. In *Inborn Errors of Development: the Molecular Basis of Clinical Disorders of Morphogenesis* (ed. C. J. Epstein, R. P. Erickson and A. J. Wynshaw-Boris), pp. 925-942. New York: Oxford University Press.

Petrikin, J. E., Willig, L. K., Smith, L. D. and Kingsmore, S. F. (2015). Rapid whole genome sequencing and precision neonatology. *Semin. Perinatol.* **39**, 623-631.
Pichaud, F. and Desplan, C. (2002). Pax genes and eye organogenesis. *Curr. Opin. Genet. Dev.* **12**, 430-434.
Pignolo, R. J., Shore, E. M. and Kaplan, F. S. (2013). Fibrodysplasia ossificans progressiva: diagnosis, management, and therapeutic horizons. *Pediatr. Endocrinol. Rev.* **10** Suppl. 2, 437-448.
Porsch, M., Hofmeyer, K., Bausenwein, B. S., Grimm, S., Weber, B. H. F., Miassod, R. and Pflugfelder, G. O. (1998). Isolation of a Drosophila T-box gene closely related to human TBX1. *Gene* **212**, 237-248.
Potthoff, M. J. and Olson, E. N. (2007). MEF2: a central regulator of diverse developmental programs. *Development* **134**, 4131-4140.
Pujades, C., Kamaid, A., Alsina, B. and Giraldez, F. (2006). BMP-signaling regulates the generation of hair-cells. *Dev. Biol.* **292**, 55-67.
Qian, L., Mohapatra, B., Akasaka, T., Liu, J., Ocorr, K., Towbin, J. A. and Bodmer, R. (2008). Transcription factor neuromancer/TBX20 is required for cardiac function in Drosophila with implications for human heart disease. *Proc. Natl. Acad. Sci. USA* **105**, 19833-19838.
Quiring, R., Walldorf, U., Kloter, U. and Gehring, W. J. (1994). Homology of the eyeless gene of Drosophila to the Small eye gene in mice and Aniridia in humans. *Science* **265**, 785-789.
Reim, I., Mohler, J. P. and Frasch, M. (2005). Tbx20-related genes, mid and H15, are required for tinman expression, proper patterning, and normal differentiation of cardioblasts in Drosophila. *Mech. Dev.* **122**, 1056-1069.
Reiter, L. T., Potocki, L., Chien, S., Gribskov, M. and Bier, E. (2001). A systematic analysis of human disease-associated gene sequences in Drosophila melanogaster. *Genome Res.* **11**, 1114-1125.
Richardson, R. J. and Kirk, J. M. (1990). Short stature, mental retardation, and hypoparathyroidism: a new syndrome. *Arch. Dis. Child* **65**, 1113-1117.
Roeder, T., Isermann, K., Kallsen, K., Uliczka, K. and Wagner, C. (2012). A Drosophila asthma model - what the fly tells us about inflammatory diseases of the lung. *Adv. Exp. Med. Biol.* **710**, 37-47.
Roessler, E., Du, Y.-Z., Mullor, J. L., Casas, E., Allen, W. P., Gillessen-Kaesbach, G., Roeder, E. R., Ming, J. E., Ruiz i Altaba, A. and Muenke, M. (2003). Loss-of-function mutations in the human GLI2 gene are associated with pituitary anomalies and holoprosencephaly-like features. *Proc. Natl. Acad. Sci. USA* **100**, 13424-13429.
Rogge, R. D., Karlovich, C. A. and Banerjee, U. (1991). Genetic dissection of a neurodevelopmental pathway: son of sevenless functions downstream of the sevenless and EGF receptor tyrosine kinases. *Cell* **64**, 39-48.
Rogge, R., Green, P., Urano, J., Horn-Saban, S., Mlodzik, M., Shilo, B., Hartenstein, V. and Banerjee, U. (1995). The role of yan in mediating the choice between cell division and differentiation. *Development* **121**, 3947-3958.
Roush, W. (1995). Nobel prizes: fly development work bears prize-winning fruit. *Science* **270**, 380-381.
Rubin, G. M. and Spradling, A. (1983). Vectors for P element-mediated gene transfer in Drosophila. *Nucleic Acids Res.* **11**, 6341-6351.
Rubin, G. M., Yandell, M. D., Wortman, J. R., Gabor Miklos, G. L., Nelson, C. R., Hariharan, I. K., Fortini, M. E., Li, P. W., Apweiler, R., Fleischmann, W. et al. (2000). Comparative genomics of the eukaryotes. *Science* **287**, 2204-2215.
Rubinstein, J. H. and Taybi, H. (1963). Broad thumbs and toes and facial abnormalities. A possible mental retardation syndrome. *Am. J. Dis. Child.* **105**, 588-608.
Rutten, J. W., Haan, J., Terwindt, G. M., van Duinen, S. G., Boon, E. M. J. and Lesnik Oberstein, S. A. J. (2014). Interpretation of NOTCH3 mutations in the diagnosis of CADASIL. *Expert. Rev. Mol. Diagn.* **14**, 593-603.
Sanjad, S. A., Sakati, N. A., Abu-Osba, Y. K., Kaddoura, R. and Milner, R. D. (1991). A new syndrome of congenital hypoparathyroidism, severe growth failure, and dysmorphic features. *Arch. Dis. Child.* **66**, 193-196.
Sanlaville, D. and Verloes, A. (2007). CHARGE syndrome: an update. *Eur. J. Hum. Genet.* **15**, 389-399.
Santoro, M. R., Bray, S. M. and Warren, S. T. (2012). Molecular mechanisms of fragile X syndrome: a twenty-year perspective. *Annu. Rev. Pathol.* **7**, 219-245.
Satta, R., Dimitrijevic, N. and Manev, H. (2003). Drosophila metabolize 1,4-butanediol into gamma-hydroxybutyric acid in vivo. *Eur. J. Pharmacol.* **473**, 149-152.
Scharf, S. H., Jaeschke, G., Wettstein, J. G. and Lindemann, L. (2015). Metabotropic glutamate receptor 5 as drug target for Fragile X syndrome. *Curr. Opin. Pharmacol.* **20**, 124-134.
Schaub, C., Marz, J., Reim, I. and Frasch, M. (2015). Org-1-dependent lineage reprogramming generates the ventral longitudinal musculature of the Drosophila heart. *Curr. Biol.* **25**, 488-494.
Sherwood, N. T., Sun, Q., Xue, M., Zhang, B. and Zinn, K. (2004). Drosophila spastin regulates synaptic microtubule networks and is required for normal motor function. *PLoS Biol.* **2**, e429.
Shimell, M. J., Ferguson, E. L., Childs, S. R. and O'Connor, M. B. (1991). The Drosophila dorsal-ventral patterning gene tolloid is related to human bone morphogenetic protein 1. *Cell* **67**, 469-481.
Shore, E. M., Xu, M., Feldman, G. J., Fenstermacher, D. A., Cho, T.-J., Choi, I. H., Connor, J. M., Delai, P., Glaser, D. L., LeMerrer, M. et al. (2006). A recurrent mutation in the BMP type I receptor ACVR1 causes inherited and sporadic fibrodysplasia ossificans progressiva. *Nat. Genet.* **38**, 525-527.
Simin, K., Bates, E., Horner, M. and Letsou, A. (1998). Genetic analysis of punt, a type II Dpp receptor that functions throughout the Drosophila melanogaster life cycle. *Genetics* **148**, 801-813.
Simon, M. A., Bowtell, D. D. L., Dodson, G. S., Laverty, T. R. and Rubin, G. M. (1991). Ras1 and a putative guanine nucleotide exchange factor perform crucial steps in signaling by the sevenless protein tyrosine kinase. *Cell* **67**, 701-716.
Simpson, J. H. (2009). Mapping and manipulating neural circuits in the fly brain. *Adv. Genet.* **65**, 79-143.
Slavotinek, A. M. (2011). Eye development genes and known syndromes. *Mol. Genet. Metab.* **104**, 448-456.
Sokolowski, M. B. (2003). NPY and the regulation of behavioral development. *Neuron* **39**, 6-8.
Sorrentino, R. P., Gajewski, K. M. and Schulz, R. A. (2005). GATA factors in Drosophila heart and blood cell development. *Semin. Cell Dev. Biol.* **16**, 107-116.
Spencer, F. A., Hoffmann, F. M. and Gelbart, W. M. (1982). Decapentaplegic: a gene complex affecting morphogenesis in Drosophila melanogaster. *Cell* **28**, 451-461.
St Johnston, D. (2002). The art and design of genetic screens: Drosophila melanogaster. *Nat. Rev. Genet.* **3**, 176-188.
Struhl, G. and Adachi, A. (1998). Nuclear access and action of notch in vivo. *Cell* **93**, 649-660.
Struhl, G. and Greenwald, I. (2001). Presenilin-mediated transmembrane cleavage is required for Notch signal transduction in Drosophila. *Proc. Natl. Acad. Sci. USA* **98**, 229-234.
Struhl, G., Fitzgerald, K. and Greenwald, I. (1993). Intrinsic activity of the Lin-12 and Notch intracellular domains in vivo. *Cell* **74**, 331-345.
Suzuki, S., Marazita, M. L., Cooper, M. E., Miwa, N., Hing, A., Jugessur, A., Natsume, N., Shimozato, K., Ohbayashi, N., Suzuki, Y. et al. (2009). Mutations in BMP4 are associated with subepithelial, microform, and overt cleft lip. *Am. J. Hum. Genet.* **84**, 406-411.
Takamiya, M., Weger, B. D., Schindler, S., Beil, T., Yang, L., Armant, O., Ferg, M., Schlunck, G., Reinhard, T., Dickmeis, T. et al. (2015). Molecular description of eye defects in the zebrafish Pax6b mutant, sunrise, reveals a Pax6b-dependent genetic network in the developing anterior chamber. *PLoS ONE* **10**, e0117645.
Tapon, N., Ito, N., Dickson, B. J., Treisman, J. E. and Hariharan, I. K. (2001). The Drosophila tuberous sclerosis complex gene homologs restrict cell growth and cell proliferation. *Cell* **105**, 345-355.
Tidyman, W. E. and Rauen, K. A. (2009). The RASopathies: developmental syndromes of Ras/MAPK pathway dysregulation. *Curr. Opin. Genet. Dev.* **19**, 230-236.
Traiffort, E., Dubourg, C., Faure, H., Rognan, D., Odent, S., Durou, M.-R., David, V. and Ruat, M. (2004). Functional characterization of sonic hedgehog mutations associated with holoprosencephaly. *J. Biol. Chem.* **279**, 42889-42897.
Treisman, J. E. (1999). A conserved blueprint for the eye? *Bioessays* **21**, 843-850.
Trotta, N., Orso, G., Rossetto, M. G., Daga, A. and Broadie, K. (2004). The hereditary spastic paraplegia gene, spastin, regulates microtubule stability to modulate synaptic structure and function. *Curr. Biol.* **14**, 1135-1147.
Twombly, V., Bangi, E., Le, V., Malnic, B., Singer, M. A. and Wharton, K. A. (2009). Functional analysis of saxophone, the Drosophila gene encoding the BMP type I receptor ortholog of human ALK1/ACVRL1 and ACVR1/ALK2. *Genetics* **183**, 563-579, 1SI–8SI.
Ugur, B., Chen, K. and Bellen, H. J. (2016). Drosophila tools and assays for the study of human diseases. *Dis. Model. Mech.* **9**, 235-244.
van Dinther, M., Visser, N., de Gorter, D. J., Doorn, J., Goumans, M. J., de Boer, J. and ten Dijke, P. (2010). ALK2 R206H mutation linked to fibrodysplasia ossificans progressiva confers constitutive activity to the BMP type I receptor and sensitizes mesenchymal cells to BMP-induced osteoblast differentiation and bone formation. *J. Bone Miner. Res.* **25**, 1208-1215.
Venter, J. C., Adams, M. D., Myers, E. W., Li, P. W., Mural, R. J., Sutton, G. G., Smith, H. O., Yandell, M., Evans, C. A., Holt, R. A. et al. (2001). The sequence of the human genome. *Science* **291**, 1304-1351.
von Gernet, S., Schuffenhauer, S., Golla, A., Lichtner, P., Balg, S., Mühlbauer, W., Murken, J., Fairley, J. and Meitinger, T. (1996). Craniosynostosis suggestive of Saethre-Chotzen syndrome: clinical description of a large kindred and exclusion of candidate regions on 7p. *Am. J. Med. Genet.* **63**, 177-184.
Waggener, J. M. and DiMario, P. J. (2002). Two splice variants of Nopp140 in Drosophila melanogaster. *Mol. Biol. Cell* **13**, 362-381.
Wall, N. A. and Hogan, B. L. M. (1994). TGF-beta related genes in development. *Curr. Opin. Genet. Dev.* **4**, 517-522.
Wan, L., Dockendorff, T. C., Jongens, T. A. and Dreyfuss, G. (2000). Characterization of dFMR1, a Drosophila melanogaster homolog of the fragile X mental retardation protein. *Mol. Cell. Biol.* **20**, 8536-8547.

Wang, L., Colodner, K. J. and Feany, M. B. (2011). Protein misfolding and oxidative stress promote glial-mediated neurodegeneration in an Alexander disease model. *J. Neurosci.* **31**, 2868-2877.
Warburton, D., Tefft, D., Mailleux, A., Bellusci, S., Thiery, J.-P., Zhao, J., Buckley, S., Shi, W. and Driscoll, B. (2001). Do lung remodeling, repair, and regeneration recapitulate respiratory ontogeny? *Am. J. Respir. Crit. Care Med.* **164**, S59-S62.
Wasserman, S. A. (2000). Toll signaling: the enigma variations. *Curr. Opin. Genet. Dev.* **10**, 497-502.
Weitkunat, M. and Schnorrer, F. (2014). A guide to study Drosophila muscle biology. *Methods* **68**, 2-14.
Wernet, M. F., Huberman, A. D. and Desplan, C. (2014). So many pieces, one puzzle: cell type specification and visual circuitry in flies and mice. *Genes Dev.* **28**, 2565-2584.
Wessells, R. J. and Bodmer, R. (2004). Screening assays for heart function mutants in Drosophila. *Biotechniques* **37**, 58-60, 62, 64 passim.
Wharton, K. A., Johansen, K. M., Xu, T. and Artavanis-Tsakonas, S. (1985). Nucleotide sequence from the neurogenic locus notch implies a gene product that shares homology with proteins containing EGF-like repeats. *Cell* **43**, 567-581.
Winter, R. M. (1996). Analysing human developmental abnormalities. *Bioessays* **18**, 965-971.
Wolf, F. W. and Heberlein, U. (2003). Invertebrate models of drug abuse. *J. Neurobiol.* **54**, 161-178.
Wolf, M. J. and Rockman, H. A. (2008). Drosophila melanogaster as a model system for the genetics of postnatal cardiac function. *Drug Discov. Today Dis. Models* **5**, 117-123.
Wu, M. Y. and Hill, C. S. (2009). Tgf-beta superfamily signaling in embryonic development and homeostasis. *Dev. Cell* **16**, 329-343.
Wu, J. S. and Luo, L. (2006). A protocol for mosaic analysis with a repressible cell marker (MARCM) in Drosophila. *Nat. Protoc.* **1**, 2583-2589.
Yamamoto, S., Schulze, K. L. and Bellen, H. J. (2014). Introduction to Notch signaling. *Methods Mol. Biol.* **1187**, 1-14.
Zhang, Y. Q. and Broadie, K. (2005). Fathoming fragile X in fruit flies. *Trends Genet.* **21**, 37-45.

CHAPTER 6

FUTURE DIRECTIONS

The findings described in this dissertation provide mechanistic insight into the integral and diverse roles that glycans play in Dpp signaling, cell hypertophic growth, and mucin secretion. My studies have also lent insight into the way in which glycans can regulate complex developmental processes by integrating nutritional status. That being said, there is still much to discover in the field of glycobiology. It is clear that, even as we've been able to answer some questions, many more have come to light. It is anticipated that the work outlined here will provide a springboard for identifying important questions and will provide a platform with which to interrogate them.

While I have discovered a novel role for Sax in Dpp signal transduction and demonstrated that its function is repressed by Sxc-mediated O-glycosylation, the site(s) of O-glycosylation remains unprobed. We plan to exploit advances in both genome editing and mass spectrophotometry to identify the site(s) of Sax glycosylation. Specifically, numerous candidate sites for O-glycosylation are predicted by *in silico* algorithms, and these will be considered for targeted mutation and functional probes for effects on Dpp signaling. Additionally, Flag-Sax can be immunopurified from embryos and submitted to tandem mass spectrometry analysis to identify all O-glycosylation modification sites. This approach may also prove useful in testing whether reciprocity between O-glycosylation and phosphorylation is occurring on Sax. This said, reciprocity might also be tested via Western blot analysis, by probing immunopurified Sax for O-GlcNAc after phosphatase treatment. Altogether, these studies would confirm the

presence of O-GlcNAc on endogenous Sax and provide additional insight into the mechanism of Sxc-mediated Dpp antagonism during dorsal closure.

It also remains unclear whether Sxc functions broadly throughout development as a Dpp signaling antagonist. As described previously, maternal loss of *sxc* plays no role in embryonic development suggesting that at least during early embryogenesis when Dpp is required to specify dorsal fates, *sxc* is not acting as a signaling repressor. However, whether or not *sxc* functions to antagonize Dpp signaling in the larval wing imaginal disc, where Dpp signaling is required for proper growth and patterning of the wing disc, has not been probed. It is evident from modENCODE data that *sxc* is expressed in the wing disc, although I have demonstrated that *sxc* expression is not always correlated with its role as a Dpp signaling antagonist. It remains to be seen, even if *sxc* antagonizes Dpp signaling in the wing disc, whether it does so via inhibition of Sax-dependent Dpp signaling or via some other mechanism. Although Sax is also expressed in the wing disc, prediction of Sxc targets has proven difficult and therefore, it is unknown whether Sax would also be glycosylated in this context. Dpp signaling in the wing disc has been extensively studied and no role of Sax-dependent Dpp signaling has been reported to date. However, it is entirely possible that, like during dorsal closure, Dpp activity through Sax is inhibited by Sxc, and thus any Sax phenotype would be masked unless observed in a *sxc* mutant background.

Further interrogation into the conservation of Sax glycosylation is warranted, including an examination of whether the human ortholog of Sax, ACVR1 is also modified by glycosylation. The R260H mutation in human ACVR1 protein leads to ectopic activation of BMP signaling even in the absence of ligand and results in the disease, Fibrodysplasia Ossificans Progressiva, resulting in ossification of soft tissue. It remains to be seen whether this activating mutation could be antagonized by glycosylation of some other residue to repress ACVR1 activity. Experiments carried out in human cell

lines could begin to unravel the nascent glycosyl modifications on ACVR1 and explore any key differences in ACVR1 derived from FOP patients. Furthermore, the fly could be used to generate similar activating mutations in Sax to explore mechanism of ectopic BMP signal induction.

In addition to the role of O-glycans in Dpp signal antagonism, much remains unknown about the role of extracellular O-glycans, mucins, in development and the regulation of cell size. While *Drosophila* mucin core proteins have been identified and described previously (Syed et al., 2008), none of these have been assayed for cell growth phenotypes in either larvae or the female germline even though several are expressed in the right time and place to have a role, such as *Muc12Ea*, which is expressed in the ovary. Targeted mutagenesis by CRISPER/CAS9 or targeted knockdown via RNAi of these mucins could be utilized to identify which protein is modified by *sgct* to enact a cell growth pathway. Furthermore, a genome-wide approach to identify modifiers of the cell growth pathway could be utilized. Using this approach, mothers with *sgct* germlines could be mutagenized and mutant lines recovered that restore female fertility; or *sgct* larvae could be mutagenized and larvae that grow beyond L1 size could be selected for further analysis. These approaches have the ability to reveal a wide array of genes involved in this potentially complex cell growth pathway and would also provide the potential to recover an allelic series which would prove useful in follow-up analyses. Results from a screen would provide candidate interacting genes likely including mucin core proteins and/or genes involved in endoreplication. As candidate genes are discovered and validated, we can use our genetic model of Peters' Plus Syndrome to further probe mechanisms of mucins in cell growth and better our model to recapitulate additional phenotypes in Peters' Plus patients.

References

Syed, Z.A., Hard, T., Uv, A., and van Dijk-Hard, I.F. (2008). A potential role for Drosophila mucins in development and physiology. PLoS One 3, e3041.

APPENDIX A

WNT/LEF1-DEPENDENT HYPOTHALAMIC NEUROGENESIS MEDIATES ANXIETY

The following was submitted to PLoS Biology, May 2017.

Wnt/Lef1-dependent hypothalamic neurogenesis mediates anxiety

Yuanyuan Xie[1], Dan Kaufmann[2]†, Matthew J. Moulton[3]†, John A. Gaynes[1], Samin Panahi[1], Dingxi Zhou[1,7], Hai-Hui Xue[4], Camille M. Fung[5], Edward M. Levine[6]‡, Anthea Letsou[3], KC Brennan[2], Richard I. Dorsky[1]*

[1]Department of Neurobiology and Anatomy, University of Utah, Salt Lake City, UT 84112, USA.

[2]Department of Neurology, University of Utah, Salt Lake City, UT 84132, USA.

[3]Department of Human Genetics, University of Utah, Salt Lake City, UT 84112, USA.

[4]Department of Microbiology, Carver College of Medicine, University of Iowa, Iowa City, IA 52242, USA.

[5]Division of Neonatology, Department of Pediatrics, University of Utah School of Medicine, Salt Lake City, UT 84158, USA.

[6]Department of Ophthalmology and Visual Sciences, John A. Moran Eye Center, University of Utah, Salt Lake City, Utah 84132, USA.

[7]School of Life Sciences, Peking University, Beijing 100871, China.

†These authors contributed equally to this work.

‡Current address: Department of Ophthalmology and Visual Sciences, Vanderbilt University School of Medicine, Nashville, TN 37232, USA.

*Corresponding author. Email: richard.dorsky@neuro.utah.edu

Abstract

Homologous neuronal circuits mediate specific behaviors in diverse animal species, suggesting that the molecular mechanisms underlying circuit development may also be conserved. Here we demonstrate that the Wnt/ß-catenin mediator Lef1 is specifically required for the differentiation of hypothalamic neurons that regulate anxiety and growth rate in both zebrafish and mice, although the identity of Lef1-dependent neurons is different between the two species. We further show that zebrafish and *Drosophila* have common Lef1-dependent gene expression in their respective neuroendocrine organs, consistent with a shared molecular pathway that diverged in mammals. Together this work suggests that Lef1 regulates an ancient mechanism of circuit development that is fundamentally important for animal behavior.

Results

Individual transcription factors can regulate the development of neuronal subtypes involved in specific behaviors (*1*). However it is not clear whether they function similarly in diverse species, and the upstream signals have not been identified. Wnt/ß-catenin signaling represents an intriguing candidate pathway for coupling extracellular signals to the transcription of evolutionarily selected target genes. Our laboratory previously showed a conserved role for Wnt/ß-catenin activity mediated by Lef1 in hypothalamic neurogenesis (*2*), so we sought to determine whether Lef1-dependent neurons have a defined behavioral function.

In *lef1* null zebrafish mutants the caudal hypothalamus begins to be reduced in size between 3-4 days postfertilization (dpf) (Fig. A.1 A, A.5 A-C), and contains fewer Wnt-responsive cells (*3*) (Fig. A.1B-D). Mutants also have fewer serotonergic ependymal cells and fewer GABAergic HuC/D+ neurons (Fig. A.11 E-H, A.5 D-G), but not *th2*+ dopaminergic neurons (*4*) (Fig. A.5 H-J), indicating a loss of specific neuronal

populations. BLBP+ cells were not reduced (Fig. A.5 K-M), confirming that Wnt signaling is dispensable for the development of hypothalamic radial glia (*2*, *5*).

While cell proliferation in the caudal hypothalamus of *lef1* mutants was normal at 3 dpf and beyond (Fig. A.1 I-K, A.5 N-S), we observed an increase in apoptosis (Fig. A.1 L). Loss of *p53* rescued apoptosis, but not neurogenesis (Fig. A.1 L-N), suggesting a primary defect in progenitor differentiation, which we confirmed using BrdU labeling (Fig. A.5 T-V). Transplantation of cells during gastrulation (*6*) (Fig. A.1 O), rescued neurogenesis only in wild-type donor cells (Fig. A.1 P-S) demonstrating that Lef1 directly promotes the differentiation of hypothalamic neurons.

RNA-seq analysis of the 3 dpf hypothalamus identified 138 differentially expressed protein-coding genes with an adjusted P-value < 0.1, among which 129 were reduced in *lef1* mutants. QIAGEN Ingenuity Pathway Analysis identified significant association of these genes with anxiety and depression (Fig. A.2 A). Among 38 genes tested by *in situ* hybridization on 3 dpf offspring of *lef1+/-* incrosses, 26 showed predicted hypothalamic expression changes in approximately 25% of embryos (Fig. A.2 B-C, A.6 A-C), including several known Wnt targets (*7*) (Fig. A.2 B). We also observed expression in the adult caudal hypothalamus of 23 out of 24 genes tested (Fig. A.6 D), suggesting simultaneous presence of Wnt activity and Lef1-dependent neuronal populations throughout life.

lef1 mutants raised with siblings had decreased survival and were smaller (Fig. A.7 A, C). When separated at 15 dpf mutants survived normally (Fig. A.7 B, C) but were still smaller even at culture densities that maximize growth (*8*) (Fig. A.2 D) (Fig. A.7 D). We performed a novel tank diving test to measure exploratory behavior (*9*), and found that *lef1* mutant larvae had a longer latency to enter the upper half of a novel tank and spent less overall time in this zone (Fig. A.2 E-F, A.7 E), consistent with increased anxiety.

Other defects in zebrafish *lef1* mutants could affect behavior (*2*, *10*), so we next created a tissue-specific mouse model using *Nkx2.1*^{Cre} and *Lef1*^{flox} alleles (*11*, *12*). *Lef1* is expressed in the caudal mouse hypothalamus from embryonic (E) day 10.5 to adulthood (*13*, *14*), and while *Lef1* null mutants exhibit postnatal lethality and a smaller body size, no hypothalamic phenotypes have been reported (*15*). We confirmed loss of hypothalamic Lef1 and Wnt reporter expression (*16*) in mutant (*Lef1*^{CKO}) mice (Fig. A.8 C-H), which were viable, fertile, and morphologically indistinguishable from controls (*Lef1*^{CON}). However, both male and female *Lef1*^{CKO} mice gained weight more slowly after weaning (Fig. A.3 A-B).

Using an elevated plus maze test we found that male but not female *Lef1*^{CKO} mice spent significantly less time in the open arms and more time in the closed arms (Fig. A.3 C-D, A.9 A-M). In an open field test, male and estrous female *Lef1*^{CKO} mice spent significantly less time in the center zone than littermate controls. However there was no effect in diestrous females (Fig. A.3 E-G, A.9 N-P). These results are consistent with elevated anxiety in *Lef1*^{CKO} mice despite normal mobility (Fig. A.9 A, N, O), which may also contribute to their reduced growth rate (Fig. A.3 A, B) (*17*).

We performed RNA-seq at E14.5 with dissected hypothalami of male *Lef1*^{CON} and *Lef1*^{CKO} mice, and surprisingly identified only one affected protein-coding gene with an adjusted P-value < 0.1 and greater than a two-fold change, *Pro-melanin concentrating hormone* (*Pmch*). *Pmch* expression in the posterior periventricular hypothalamus normally overlaps with *Lef1*, and extends into the lateral hypothalamus (Fig. A.3 I-N) (*18*). We confirmed loss of *Pmch* expression by quantitative PCR (qPCR) and immunohistochemistry in E14.5 *Lef1*^{CKO} embryos, and loss of the Wnt/Lef1 target *Sp5* by qPCR (Fig. A.3 H, A.8 I-K).

RNA-seq analysis at P22, when *Lef1*^{CKO} mice begin to exhibit a growth defect (Fig. A.3 A-B) identified only 2 affected protein-coding genes with an adjusted P-value <

0.1: *Pmch* and *Tacr3*. We confirmed reduced expression of *Pmch* and *Tacr3*, as well as *Cartpt*, all of which are co-expressed in the same neurons (*19*), at P22 using qPCR and *in situ* hybridization (Fig. A.3 H, O-T, A.7 K). While ablation of *Pmch*+ neurons leads to reduced body weight, the underlying mechanism remains unclear (*20*, *21*). However characterization of their inputs and activity supports a role for these cells in mediating stress and anxiety (*22*).

Orthologs of several Lef1-dependent zebrafish genes such as *Corticotropin releasing hormone binding protein* (*Crhbp*) regulate anxiety and body growth in the mouse (*24*), and are also expressed with or adjacent to *Lef1* in the mouse hypothalamus (*18*, *23*). However we found that their expression, as well as expression of genes encoding peptide hormones such as *Pomc, Hcrt, Npy,* and *Agrp,* was unaffected in *Lef1*^{CKO} mice (Fig. A.3 H, A.8 K-M). In addition we confirmed that expression of zebrafish *pmch* orthologs does not depend on *lef1* (Fig. A.10 A-D) (*25*). Therefore, while the resulting behavioral function may be conserved, it is likely that the identity of *Lef1*-dependent neurons has changed between fish and mammals.

It is thus possible that Lef1-dependent neurons in zebrafish represent a more evolutionarily ancient pathway, whereas the anatomy and function of Lef1-dependent *Pmch*+ neurons in mice may be specific to mammals (*26*). Interestingly, anxiety pathways in *Drosophila* involve Corticotropin releasing hormone signaling (*27*), and we observed co-expression of the *lef1* ortholog *pan* and *crhbp* ortholog *CG15537* in the *Drosophila* neuroendocrine pars lateralis (PL) primordia at stage 16 (Fig. A.4 A-D) (*28*). We examined *CG15537* expression in *Drosophila pan* mutants (*29*) and found a specific loss of expression in the PL (Fig. A.4 E-F), consistent with regulation by Wnt activity.

Together this work supports an evolutionarily conserved role for Wnt signaling in the development of hypothalamic neurons that regulate anxiety. While the pathway has been associated with multiple behavioral disorders in other brain regions (*30*), our

findings may prove useful for the diagnosis and treatment of neuroendocrine-related anxiety disorders.

Materials and methods

Subjects: zebrafish

All experimental protocols were approved by the University of Utah Institutional Animal Care and Use Committee and were in accordance with the guidelines from the National Institutes of Health. Zebrafish (*Danio rerio*) were bred and maintained as previously described (*31*). Wild-type strains were *AB. The following mutant and transgenic strains were used: *lef1*^{zd11} (*32*), *Tg(top:GFP)*^{w25} (*33*), *Tg(dlx6a-1.4dlx5a-dlx6a:GFP)* ^{ot1} (*34*), *Tg(h2afv:GFP)*^{kca6} (*35*), *Tg(th2:GFP-Aequorin)*^{zd201} (*36*), *p53*^{e7} (*37*). *lef1*$^{-/-}$ homozygous mutants were identified between 3 dpf and 10 dpf by DASPEI staining as described previously (*38*) and at or after 15 dpf by loss of caudal fin (*32*); wild-type and heterozygous siblings were used as controls. Primers for genotyping are listed in Table A.2.

Subjects: mice

Male and female C57BL/6J mice were group-housed with 2-5 mice per cage in a reverse 12 h light/dark cycle with *ad libitum* access to food and water. All experimental protocols were approved by the University of Utah Institutional Animal Care and Use Committee and were in accordance with the guidelines from the National Institutes of Health. Mice were 19-20 and 15-20 weeks old at the time of behavioral tests for male and female animals, respectively. *Ai9* reporter *Rosa*^{tdTomato} (line 007905) (*39*), *Nkx2.1*^{Cre} (line 008661) (*40*) and *TCF/Lef:H2B-GFP* mice (line 013752) (*41*) were purchased from Jackson Laboratories. *Lef1*$^{flox/flox}$ mice were provided by H.H.X (*42*). All strains were maintained on a C57BL/6J background except *TCF/Lef:H2B-GFP* mice, which were

originally on a C57BL/6 × 129 background. Male *Nkx2.1*$^{Cre/Cre}$;*Lef1*$^{flox/+}$ and female *Lef1*$^{flox/flox}$;*Rosa*$^{tdTomato/tdTomato}$ mice were used to generate conditional knockout (*Lef1*^{CKO}: *Nkx2.1*$^{Cre/+}$;*Lef1*$^{flox/flox}$;*Rosa*$^{tdTomato/+}$) and control (*Lef1*^{CON}: *Nkx2.1*$^{Cre/+}$;*Lef1*$^{flox/+}$;*Rosa*$^{tdTomato/+}$) offspring. Females were maintained by inbreeding. Male breeders were maintained by interbreeding *Nkx2.1*$^{Cre/Cre}$;*Lef1*$^{+/+}$ and *Nkx2.1*$^{Cre/Cre}$;*Lef1*$^{flox/+}$ for less than 5 generations to avoid potential artifacts caused by Cre homozygous inbreeding (*43*). In approximately 10% of experimental animals, *Ai9* reporter expression was observed throughout the body consistent with published literature (*40*); such animals were not used for experiments. Sex at E14.5 was determined by genotyping by Jarid 1c (*44*). When generating experimental mice for measuring body weight and behavioral tests, each litter was culled to 8 pups at P0. Primers for genotyping are listed in Table A.2.

Subjects: Drosophila

Wild-type *Drosophila melanogaster* were Canton-S strain. *pan*+/- (w^{1118}; pan^{2}/P{ActGFP}unc-13^{GJ}) was purchased from Bloomington (BL4759).

Zebrafish transplantation experiments

At the sphere stage, 10–50 blastula cells from donor embryos were transplanted using a glass micropipette into the dorsal side of shield stage host embryos, 20-40 degrees from the animal pole, representing the hypothalamus anlage (*45*). Embryos were then raised to 5 dpf for immunohistochemistry. Donor and host embryos were retained for genotyping to identify *lef1* mutants.

BrdU labeling

Four dpf zebrafish embryos were incubated in E3 media containing 10 mM BrdU (Sigma) at 28.5 °C for the indicated time before being washed in E3 media at least 3 times.

Immunohistochemistry: zebrafish

Embryos and larvae were fixed in 4% paraformaldehyde (PFA) for 3 hrs. at room temperature (RT) or overnight (O/N) at 4 °C followed by brain dissection. Brains were either dehydrated in methanol and stored at -20 °C, or immediately processed for immunohistochemistry. For 3 dpf embryos, 5% sucrose was included in the fixative to ease dissection. Brains were treated with 0.5 U Dispase (Gibco #17105-041) in 2% PBST (PBS/2% Triton X-100) for 60 mins. at RT. For BrdU, PCNA, pH3 or Caspase-3 staining, brains were washed in water for 5 mins. twice, followed by incubation in 2 N HCl for 60 mins. at RT, followed by two more water washes. Brains were then blocked in 5-10% goat serum in 0.5% PBST for 60 mins. at RT. Embryos were incubated in primary antibodies in block O/N at 4 °C and secondary antibodies and Hoechst 33342 (Life Technologies, H3570) in block O/N at 4 °C before mounting in Fluoromount-G (SouthernBiotech) with the ventral hypothalamus facing the coverslip.

Primary antibodies were all used at 1:500 dilution except as noted: chicken anti-GFP (Aves Labs, GFP-1020), rabbit anti-GFP (Molecular Probes, A11122), mouse anti-HuC/D (Molecular Probes, A21271), rabbit anti-5-HT (ImmunoStar, 541016), rabbit anti-pH3 (1:400, Cell Signaling, 9713), rabbit anti-active Caspase-3 (BD Pharmingen, 559565), rabbit anti-BLBP (Abcam, ab32432), mouse anti-PCNA (Sigma, P8825) and chicken anti-BrdU (ICL, CBDU-65A-Z).

Secondary antibodies were all used at 1:500 dilution: goat anti-mouse Alexa Fluor 448 (Invitrogen, A11001), goat anti-rabbit Alexa Fluor 488 (Invitrogen, A11008), donkey

anti-chicken Alexa Fluor 488 (Jackson ImmunoResearch, 703-545- 155), goat anti-rabbit cy3 (Jackson ImmunoResearch, 111-165-003), goat anti-mouse cy3 (Jackson ImmunoResearch, 115-165-003), goat anti-mouse Alexa Fluor 647 (Invitrogen, A21235), goat anti-rabbit Alexa Fluor 647 (Invitrogen, A21244) and goat anti-chicken Alexa Fluor 647 (Invitrogen, A21449). Hoechst 33342 (1:10,000) was used to stain nuclei.

Immunohistochemistry: mice

E14.5 embryo heads were dissected in PBS and fixed in 4% PFA at RT for 1.5 hrs. or O/N at 4 °C. Brains were dissected and cryoprotected in 15% and then 30% sucrose, embedded in OCT, and stored at -80 °C. Brains were cryosectioned at a thickness of 16 µm, air dried and stored at -80 °C. Air-dried sections were then washed in PTW (PBS+0.1% Tween 20) for 3 times, followed by permeabilization in 0.25% PBST for 5 mins. and blocking in 10% goat serum in PTW for 60 mins. Sections were incubated in primary antibodies in blocking solution O/N at 4 °C and secondary antibodies in blocking solution for 2 hrs. at RT, followed by Hoechst 33342 stain for 10 mins. at RT before mounting in Fluoromount-G. Antibodies used were as described above except rabbit anti-LEF1 (1:200, Cell Signaling, 2230), goat anti-Pmch (1:500, Santa Cruz, sc14509) and donkey anti-goat Alexa Fluor 647 (1:400, Invitrogen, A21447).

Probes for in situ hybridization

In situ hybridization probes were made by a clone-free method as described previously (*46*, *47*), with DNA templates purified using Zymo Research DNA clean & concentrator^{TM}-5 kit. Primers were designed by Primer-BLAST (*48*) except for mouse genes with primer sequences available from the Allen Brain Atlas (ABA) (*49*) or Genepaint Atlas (*50*). A full list of primers used to make probes is in Table A.3. cDNA made from 3 dpf zebrafish embryos, P2 and P60 mouse hypothalamus and adult

Drosophila was used as the initial template for PCR to generate T7 promoter-containing DNA. RNA probes for zebrafish *lef1* (*51*) and *axin2* (*52*) were previously described. RNA probes for *Drosophila pan* were generated with a cDNA library.

Whole mount in situ hybridization: zebrafish

Zebrafish whole mount *in situ* hybridization was performed as described previously (*53*) except that adult zebrafish were fixed in 4% PFA O/N at 4 °C followed by washing in PBS and brain dissection. All tissues were treated for 30 mins. with 10 µg/ml Proteinase K. Pigmented embryos were bleached in 1% H_2O_2/5% Formamide/0.5× SSC O/N at RT. Embryos and adult brains were imaged in 100% glycerol and PBS, respectively.

For automated whole mount *in situ* hybridization, all steps following probe hybridization and before color reaction were performed using a BioLane HTI (Intavis).

Section in situ hybridization: mice

Twenty-five µm brain cryosections were collected and post-fixed as previously described (*54*) (http://developingmouse.brain-map.org/docs/Overview.pdf). *In situ* hybridization was then performed as described (*45*).

Whole mount in situ hybridization: Drosophila

Drosophila whole mount *in situ* hybridization was performed as described previously (*46*).

Body length: zebrafish

Zebrafish from a single home tank were anesthetized using Tricaine in shallow water. Images were acquired of immobilized, nonoverlapping fish with a ruler for scale. Body length was calculated by measuring the distance between the mouth and the

anterior edge of the tail fin, using ImageJ.

Novel tank diving test

Five fish from *lef1*+/- incrosses were raised per tank starting at 5 dpf. *lef1* mutants and controls were separated at 15 dpf. Novel tank diving tests were performed on 16 dpf larvae during the early afternoon of the same days. Novel rectangular tanks (16.6 cm × 9.5 cm × 12.3 cm) were illuminated by a centered white light, and videos were acquired with a mounted Nokia Lumia 640 phone 1080p camera. For each experiment, single mutant and control larvae were netted and then removed simultaneously from their home cages and transferred to novel tanks with identical water volume. Any larvae that were not immediately released from the net were excluded from analysis. The order of netting mutant and control fish was rotated between trials. Videos were then imported and analyzed using Ethovision XT v.11.5 (Noldus, Leesburg, VA), with a tracking period of 2 mins. beginning 1 min. after release into the novel tank to decrease water agitation resulting from netting. Tracks were analyzed for time in upper half of the tank and latency to enter the upper half of the tank.

Body weight: mice

All pups were weaned at P21 immediately following the first weighing. Pups weighing less than 6.5 g were excluded from analysis. All mice were weighed during the morning of the same days of the following weeks.

Behavior tests: mice

Group housed mice were allowed to acclimate to the animal facility for behavioral tests 9 days after an on-campus transfer. Each mouse was handled daily for 2 mins., during mid-morning for 7 days before commencement of behavioral testing using the

cupped hand method (*57*). A vaginal lavage procedure was done after daily handling for estrous phase evaluation for 7 days, as previously reported (*58*). Female mice in their proestrus or estrus phases were collectively grouped as “Estrus” and females in their metestrus and diestrus phases were collectively grouped as “Diestrus.” All mice were acclimated to the behavior room for 1 hr. under red light (69 lux) before commencement of tests. Open field and elevated plus maze behavioral tests were performed in order, once daily for two days, from 9 am to 5 pm. The experimenter was blinded to genotype.

Open field test

Each mouse was placed in a circular plexiglass chamber (4.5’’ diameter × 3’’ height) located inside an illuminated (330 lux) circular open field (OF) arena (110 cm diameter) and allowed to acclimate for 1 min to decrease movement bias resulting from experimenter handling. After 1 min the plexiglass chamber was manually removed from outside the arena, and the mouse was allowed to freely explore the OF arena for 10 mins. Movement was video recorded and analyzed using Ethovision v.9 (Noldus, Leesburg, VA). The center zone of the OF arena was defined as 4% center area of the total area.

Elevated plus maze

The elevated plus maze (EPM) apparatus was elevated 60 cm from the floor, having two open arms (35 cm × 5 cm) and two closed arms (35 cm × 16 cm) connected by a central platform (5 cm × 5 cm). The EPM was illuminated by a white light (205 lux) at the center platform. Each mouse was placed in a rectangular opaque white plexiglass chamber (2’’ × 3’’ × 5’’) located on the center platform, and allowed to acclimate for 1 min before commencement of the test. The white chamber was mechanically elevated from outside of the maze and the mouse was allowed to freely explore the EPM for 5

mins. Behavior was video recorded and analyzed using Ethovision v.9 (Noldus, Leesburg, VA).

RNA-seq: zebrafish

Embryos were fixed for 1.5 hrs. in 4% PFA/5% sucrose in PBS at RT, followed by hypothalamus dissection. For each biological replicate, 28-38 dissected hypothalami were pooled for *lef1* mutant and control samples. RNA was extracted using a RecoverAll™ Total Nucleic Acid Isolation Kit for FFPE (Ambion, AM1975) according to the manufacturer's instructions. Three biological replicates were obtained on different days. A total of 300 ng RNA per sample was submitted to the High Throughput Genomic Core at the University of Utah for: RNA quality control by High Sensitivity R6K ScreenTape, RNA concentration by vacuum drying, cDNA library prep by Illumina TruSeq Stranded RNA Kit with Ribo-Zero Gold and sequencing by HiSeq 50 Cycle Single-Read Sequencing version 3. RNA-seq reads were mapped to the GRCz10 zebrafish genome assembly and differential gene expression analysis was carried out by the Bioinformatics Core at the University of Utah using DESeq2.

RNA-seq: mice

E14.5 and P22 non-weaned male $Lef1^{CON}$ and $Lef1^{CKO}$ hypothalami were dissected using a fluorescent microscope in ice-cold PBS while tail tissue was retained for genotyping. E14.5 tissues were immediately immersed in RNAlater (Thermo Fisher) and stored at 4 °C. P22 tissues were immediately homogenized in TRIzol (Thermo Fisher) and stored at -80 °C. Three biological replicates were prepared from 5 pooled (E14.5) or single (P22) hypothalami pooled from $Lef1^{CON}$ and $Lef1^{CKO}$ mice, and RNA was extracted on the same day using TRIzol followed by an RNeasy Mini Kit (Qiagen) with on-column

DNase digestion (Sigma). One µg of RNA per sample was submitted to the High Throughput Genomic Core at the University of Utah for RNA quality control with Agilent RNA ScreenTape, cDNA library prep with Illumina TruSeq Stranded RNA Kit with Ribo-Zero Gold and sequencing using HiSeq 50 Cycle Single-Read Sequencing version 4. RNA-seq reads were mapped to GRCm38 and differential gene expression analysis was carried out using the same methods as for zebrafish RNA-seq.

qPCR

RNA from male and female mice was prepared as described above for RNA-seq. 2.5 µg of RNA was used for cDNA synthesis with a SuperScript III Reverse Transcriptase kit (Invitrogen). qPCR was performed using Platinum SYBR Green master mix (Invitrogen) on 96-well CFX Connect (Biorad) plates or 384-well QuantStudio 12K Flex (Life Technologies) plates at the Genomics Core at the University of Utah, according to manufacturer's instructions. *Gapdh* was used to normalize quantification, and reverse transcriptase was omitted for controls. qPCR primers were designed from PrimerBank (*59*) and are listed in Table A.4. qPCR analysis was performed with the $\Delta\Delta C_t$ method to determine relative expression change (*60*). Dissociation curve analysis was performed to confirm the specificity of amplicons.

Image analysis and cell counting

Fluorescent images of dissected zebrafish and mouse brains were obtained with an Olympus FV1000 confocal microscope at the Cell Imaging Core at the University of Utah. Z-stack images were all maximum intensity z-projections of 3 µm slices; single- or double-labeled cells were manually counted in FV1000 ASW 4.2 Viewer. All the zebrafish and mouse *in situ* hybridization images were obtained with an Olympus SZX16 dissecting microscope except those in Fig. S2C and Fig. 3O-T which were obtained with

an Olympus BX51WI compound microscope. Two months postfertilization (mpf) zebrafish images in Fig. S3A-B were acquired using a Leica MZ16 microscope. *Drosophila in situ* hybridization images were obtained with a Zeiss Axioskop.

Ingenuity Pathway Analysis (IPA)

Because IPA (QIAGEN, Redwood City, www.qiagen.com/ingenuity) did not support zebrafish genes at the time when tested, 129 mouse orthologous genes were identified corresponding to total 138 zebrafish protein-coding genes with adjusted P-value smaller than 0.1. IPA was performed according to QIAGEN's instruction and "diseases and functions" were extracted from the software.

Statistical analysis

No statistical methods were used to predetermine sample size. For behavioral assays, sample size was determined based on accepted practice. The experiments were not randomized. Due to visible phenotypes, the investigators were not blinded to outcome assessment except for whole mount *in situ* hybridization of zebrafish *lef1+/-* incrosses, *Drosophila pan+/-* incrosses, and mouse body weight and behavioral assays. Two-tailed unpaired Student's t tests were performed for all statistical analysis, except mouse body weight (two-way ANOVA with repeated measures), using GraphPad Prism software v6. Outliers were identified by Grubbs' test for mouse behavioral assays. Significance was assigned at $P < 0.05$.

References

1. K. Sokolowski *et al.*, Specification of Select Hypothalamic Circuits and Innate Behaviors by the Embryonic Patterning Gene Dbx1. *Neuron*. **86**, 1–14 (2015).

2. X. Wang *et al.*, Wnt signaling regulates postembryonic hypothalamic progenitor differentiation. *Dev. Cell*. **23**, 624–36 (2012).

3. R. I. Dorsky, L. C. Sheldahl, R. T. Moon, A transgenic Lef1/beta-catenin-dependent reporter is expressed in spatially restricted domains throughout zebrafish development. *Dev. Biol.* **241**, 229–37 (2002).

4. A. D. McPherson *et al.*, Motor Behavior Mediated by Continuously Generated Dopaminergic Neurons in the Zebrafish Hypothalamus Recovers after Cell Ablation. *Curr. Biol.* **26**, 263–269 (2015).

5. R. N. Duncan *et al.*, Hypothalamic radial glia function as self-renewing neural progenitors in the absence of Wnt/β-catenin signaling. *Development*. **143**, 45–53 (2016).

6. K. Woo, S. E. Fraser, Order and coherence in the fate map of the zebrafish nervous system. *Development*. **121**, 2595–609 (1995).

7. G. Weidinger, C. J. Thorpe, K. Wuennenberg-Stapleton, J. Ngai, R. T. Moon, The Sp1-related transcription factors sp5 and sp5-like act downstream of Wnt/beta-catenin signaling in mesoderm and neuroectoderm patterning. *Curr. Biol.* **15**, 489–500 (2005).

8. B. Reed, M. Jennings, Guidance on the housing and care of Zebrafish Danio rerio. *Res. Anim. Dep. Sci. Group, RSPCA, West Sussex, United Kingdom* (2010).

9. J. M. Cachat *et al.*, Video-Aided Analysis of Zebrafish Locomotion and Anxiety-Related Behavioral Responses. *Zebrafish Neurobehav. Protoc.* **51**, 1–14 (2010).

10. H. F. Mcgraw *et al.*, Lef1 is required for progenitor cell identity in the zebrafish lateral line primordium. *Development*. **138**, 3921–30 (2011).

11. Q. Xu, M. Tam, S. S. A. Anderson, Fate mapping Nkx2.1-lineage cells in the mouse telencephalon. *J. Comp. Neurol.* **29**, 16–29 (2008).

12. S. Yu *et al.*, The TCF-1 and LEF-1 transcription factors have cooperative and opposing roles in T cell development and malignancy. *Immunity*. **37**, 1–26 (2012).

13. M. Oosterwegel *et al.*, Differential expression of the HMG box factors TCF-1 and LEF-1 during murine embryogenesis. *Development*. **118**, 439–48 (1993).

14. T. Shimogori *et al.*, A genomic atlas of mouse hypothalamic development. *Nat. Neurosci.* **13**, 767–75 (2010).

15. C. van Genderen *et al.*, Development of several organs that require inductive epithelial-mesenchymal interactions is impaired in LEF-1-deficient mice. *Genes Dev.* **8**, 2691–703 (1994).

16. A. Ferrer-Vaquer *et al.*, A sensitive and bright single-cell resolution live imaging reporter of Wnt/ß-catenin signaling in the mouse. *BMC Dev. Biol.* **10**, 121 (2010).

17. J. a Carr, Stress, neuropeptides, and feeding behavior: a comparative perspective. *Integr. Comp. Biol.* **42**, 582–590 (2002).

18. A. Visel, C. Thaller, G. Eichele, GenePaint.org: an atlas of gene expression patterns in the mouse embryo. *Nucleic Acids Res.* **32**, D552-6 (2004).

19. F. Brischoux, D. Fellmann, P. Y. Risold, Ontogenetic development of the diencephalic MCH neurons: A hypothalamic “MCH area” hypothesis. *Eur. J. Neurosci.* **13**, 1733–1744 (2001).

20. T. Alon, J. M. Friedman, Late-Onset Leanness in Mice with Targeted Ablation of Melanin Concentrating Hormone Neurons. *J. Neurosci.* **26**, 389–397 (2006).

21. B. B. Whiddon, R. D. Palmiter, Ablation of Neurons Expressing Melanin-Concentrating Hormone (MCH) in Adult Mice Improves Glucose Tolerance Independent of MCH Signaling. *J. Neurosci.* **33**, 2009–2016 (2013).

22. J. A. González, P. Iordanidou, M. Strom, A. Adamantidis, D. Burdakov, Awake dynamics and brain-wide direct inputs of hypothalamic MCH and orexin networks. *Nat. Commun.* **7**, 11395 (2016).

23. L. Ng *et al.*, An anatomic gene expression atlas of the adult mouse brain. *Nat. Neurosci.* **12**, 356–362 (2009).

24. I. J. Karolyi *et al.*, Altered anxiety and weight gain in corticotropin-releasing hormone-binding protein-deficient mice. *Proc. Natl. Acad. Sci. U. S. A.* **96**, 11595–11600 (1999).

25. J. R. Berman, G. Skariah, G. S. Maro, E. Mignot, P. Mourrain, Characterization of two melanin-concentrating hormone genes in zebrafish reveals evolutionary and physiological links with the mammalian MCH system. *J. Comp. Neurol.* **517**, 695–710 (2009).

26. S. Croizier *et al.*, The vertebrate diencephalic MCH system: A versatile neuronal population in an evolving brain. *Front. Neuroendocrinol.* **34**, 65–87 (2013).

27. F. Mohammad *et al.*, Ancient Anxiety Pathways Influence Drosophila Defense Behaviors. *Curr. Biol.* **26**, 981–986 (2016).

28. V. Hartenstein, The neuroendocrine system of invertebrates: a developmental and evolutionary perspective. *J. Endocrinol.* **190**, 555–570 (2006).

29. M. Van de Wetering *et al.*, Armadillo coactivates transcription driven by the product of the Drosophila segment polarity gene dTCF. *Cell*. **88**, 789–799 (1997).

30. R. S. Duman, B. Voleti, Signaling pathways underlying the pathophysiology and treatment of depression: Novel mechanisms for rapid-acting agents. *Trends Neurosci.* **35**, 47–56 (2012).

31. J. E. Lee, S. Wu, L. M. Goering, R. I. Dorsky, Canonical Wnt signaling through Lef1 is required for hypothalamic neurogenesis. *Development*. **133**, 4451–61 (2006).

32. N. Ghanem *et al.*, Regulatory roles of conserved intergenic domains in vertebrate

Dlx bigene clusters. *Genome Res.* **13**, 533–43 (2003).

33. S. Pauls, B. Geldmacher-Voss, J. a Campos-Ortega, A zebrafish histone variant H2A.F/Z and a transgenic H2A.F/Z:GFP fusion protein for in vivo studies of embryonic development. *Dev. Genes Evol.* **211**, 603–10 (2001).

34. S. Berghmans *et al.*, tp53 mutant zebrafish develop malignant peripheral nerve sheath tumors. *Proc. Natl. Acad. Sci. U. S. A.* **102**, 407–12 (2005).

35. L. Madisen *et al.*, A robust and high-throughput Cre reporting and characterization system for the whole mouse brain. *Nat. Neurosci.* **13**, 133–40 (2010).

36. C. Gil-Sanz *et al.*, Lineage Tracing Using Cux2-Cre and Cux2-CreERT2 Mice. *Neuron*. **86**, 1091–1099 (2015).

37. S. J. Clapcote, J. C. Roder, Simplex PCR assay for sex determination in mice. *Biotechniques*. **38**, 702–706 (2005).

38. C. Thisse, B. Thisse, High-resolution in situ hybridization to whole-mount zebrafish embryos. *Nat. Protoc.* **3**, 59–69 (2008).

39. J. Logel, D. Dill, S. Leonard, Synthesis of cRNA probes from PCR-generated DNA. *Biotechniques*. **13**, 604–606+608 (1992).

40. J. Ye *et al.*, Primer-BLAST: a tool to design target-specific primers for polymerase chain reaction. *BMC Bioinformatics*. **13**, 134 (2012).

41. R. I. Dorsky *et al.*, Maternal and embryonic expression of zebrafish lef1. *Mech. Dev.* **86**, 147–150 (1999).

42. X. Wang, J. J. E. Lee, R. I. Dorsky, Identification of Wnt-responsive cells in the zebrafish hypothalamus. *Zebrafish*. **6**, 49–58 (2009).

43. E. Oxtoby, T. Jowett, Cloning of the zebrafish krox-20 gene (krx-20) and its expression during hindbrain development. *Nucleic Acids Res.* **21**, 1087–95 (1993).

44. C. L. Thompson *et al.*, A high-resolution spatiotemporal atlas of gene expression of the developing mouse brain. *Neuron*. **83**, 309–323 (2014).

45. N. Schaeren-Wiemers, A. Gerfin-Moser, A single protocol to detect transcripts of various types and expression levels in neural tissue and cultured cells: in situ hybridization using digoxigenin-labelled cRNA probes. *Histochemistry*. **100**, 431–40 (1993).

46. C. L. Byars, K. L. Bates, a Letsou, The dorsal-open group gene raw is required for restricted DJNK signaling during closure. *Development*. **126**, 4913–4923 (1999).

47. J. L. Hurst, R. S. West, Taming anxiety in laboratory mice. *Nat. Methods*. **7**, 825–6 (2010).

48. A. C. McLean, N. Valenzuela, S. Fai, S. A. L. Bennett, Performing vaginal lavage, crystal violet staining, and vaginal cytological evaluation for mouse estrous cycle staging identification. *J. Vis. Exp.*, e4389 (2012).

49. A. Spandidos, X. Wang, H. Wang, B. Seed, PrimerBank: a resource of human and mouse PCR primer pairs for gene expression detection and quantification. *Nucleic Acids Res.* **38**, D792-9 (2010).

50. T. D. Schmittgen, K. J. Livak, Analyzing real-time PCR data by the comparative CT method. *Nat. Protoc.* **3**, 1101–1108 (2008).

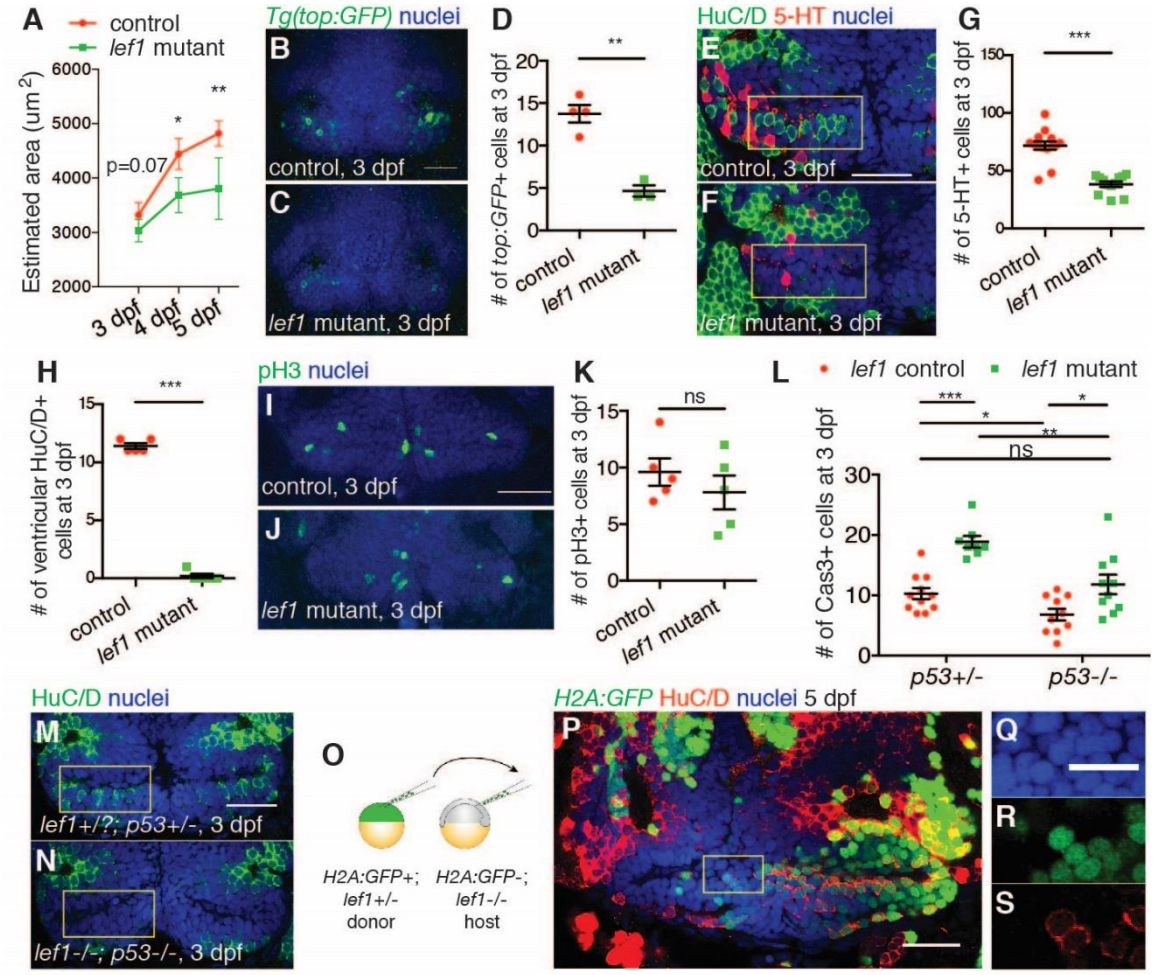

Fig. A.1. *lef1* promotes neurogenesis in the zebrafish caudal periventricular hypothalamus. (Hc). (**A**) Reduced Hc size in *lef1* mutants by 4 dpf. (**B**-**D**) Fewer Wnt-responsive cells in the Hc of 3 dpf *lef1* mutants. (**E**-**H**) Loss of 5-HT+ and ventricular HuC/D+ cells in the Hc of 3 dpf *lef1* mutants (yellow rectangles). (**I**-**K**) Normal mitosis in 3 dpf *lef1* mutants. (**L**) Increased Caspase3+ (Cas3+) cells in 3 dpf *lef1* mutants is rescued by loss of *p53*. (**M** and **N**) *lef1;p53* double mutants still lack ventricular HuC/D+ cells (yellow rectangles) at 3 dpf. (**O**-**S**) Rescue of ventricular HuC/D+ expression by transplanting labeled wild-type cells into a 5 dpf unlabeled *lef1-/-* host. Yellow rectangle in (**P**) depicts area in (**Q**-**S**). All images show ventral view of whole-mounted brain with anterior on top. Data are mean ± SEM, except mean ± SD in (**A**). ***P < 0.001, **P < 0.01, *P < 0.05, ns. P > 0.05 by two-tailed unpaired Student's t tests. All scale bars are 25 µm except 12.5 µm in (**Q**-**S**). See Table A.1 for description of confocal imaging, quantification and experimental n.

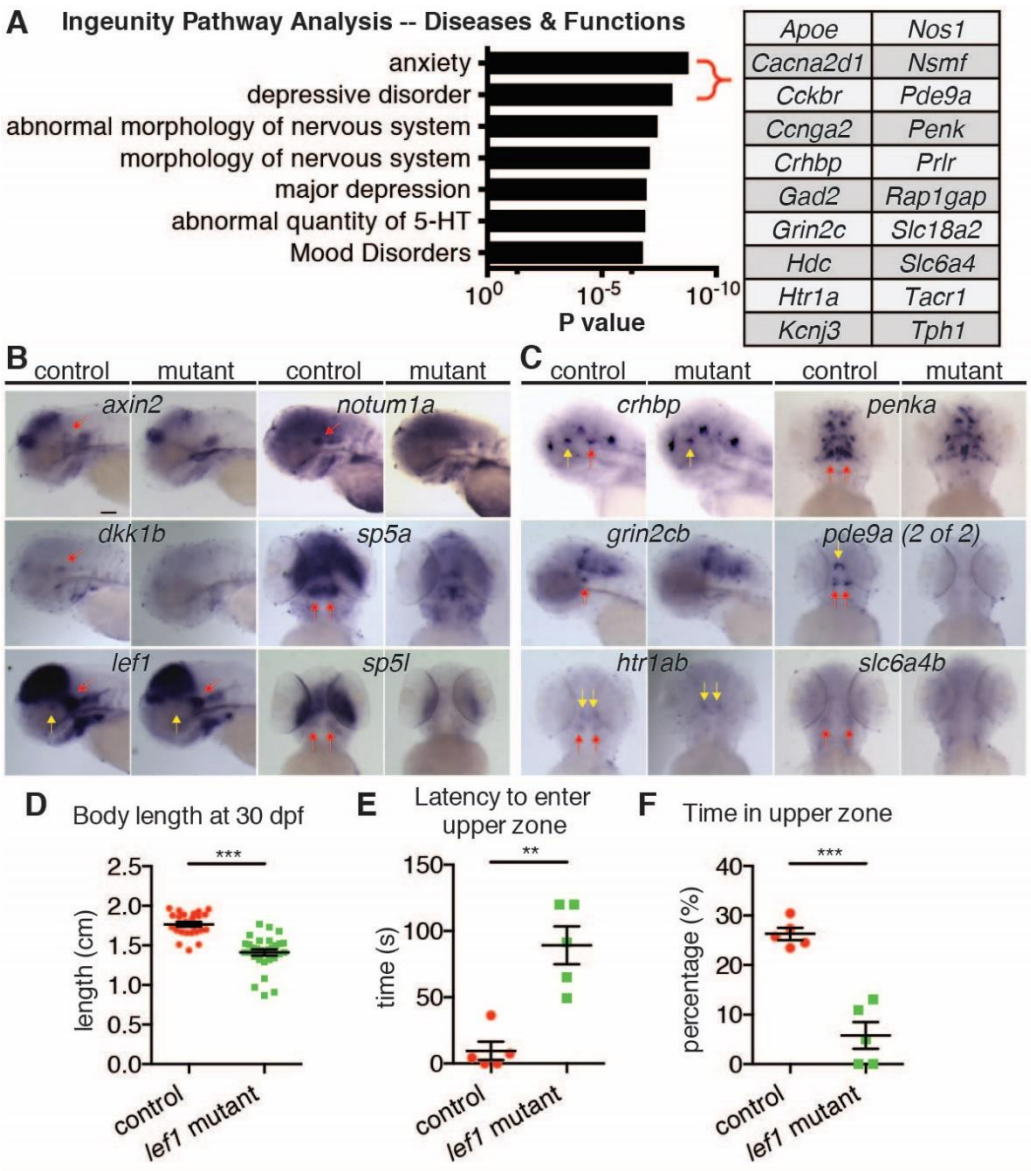

Fig. A.2. Lef1 activates zebrafish hypothalamic genes and regulates behaviors associated with anxiety. (**A**) Ingenuity Pathway Analysis for 129 mouse orthologs of 138 hypothalamic *lef1*-dependent genes revealed 20 genes associated with anxiety and depressive disorder. (**B** and **C**) Whole mount *in situ* hybridization of 3 dpf control and *lef1* mutant embryos for known Wnt targets (**B**) and genes associated with anxiety and depressive disorder (**C**) shows specific loss of expression in the caudal hypothalamus of *lef1* mutants. Red and yellow arrows indicate gene expression in caudal and rostral hypothalamus, respectively. Scale bar: 100 μm. (**D**) *lef1* mutants are smaller than controls at 30 dpf when raised at 5 fish per tank separated by genotype. n = 25, 30 for control and mutant, respectively. (**E** and **F**) *lef1* mutants display reduced exploratory behavior in a novel tank diving test, with a longer latency to enter (**E**) and less time spent in (**F**) the upper zone of a novel tank. Data are mean ± SEM. **P < 0.01, ***P < 0.001 by two-tailed unpaired Student's t tests.

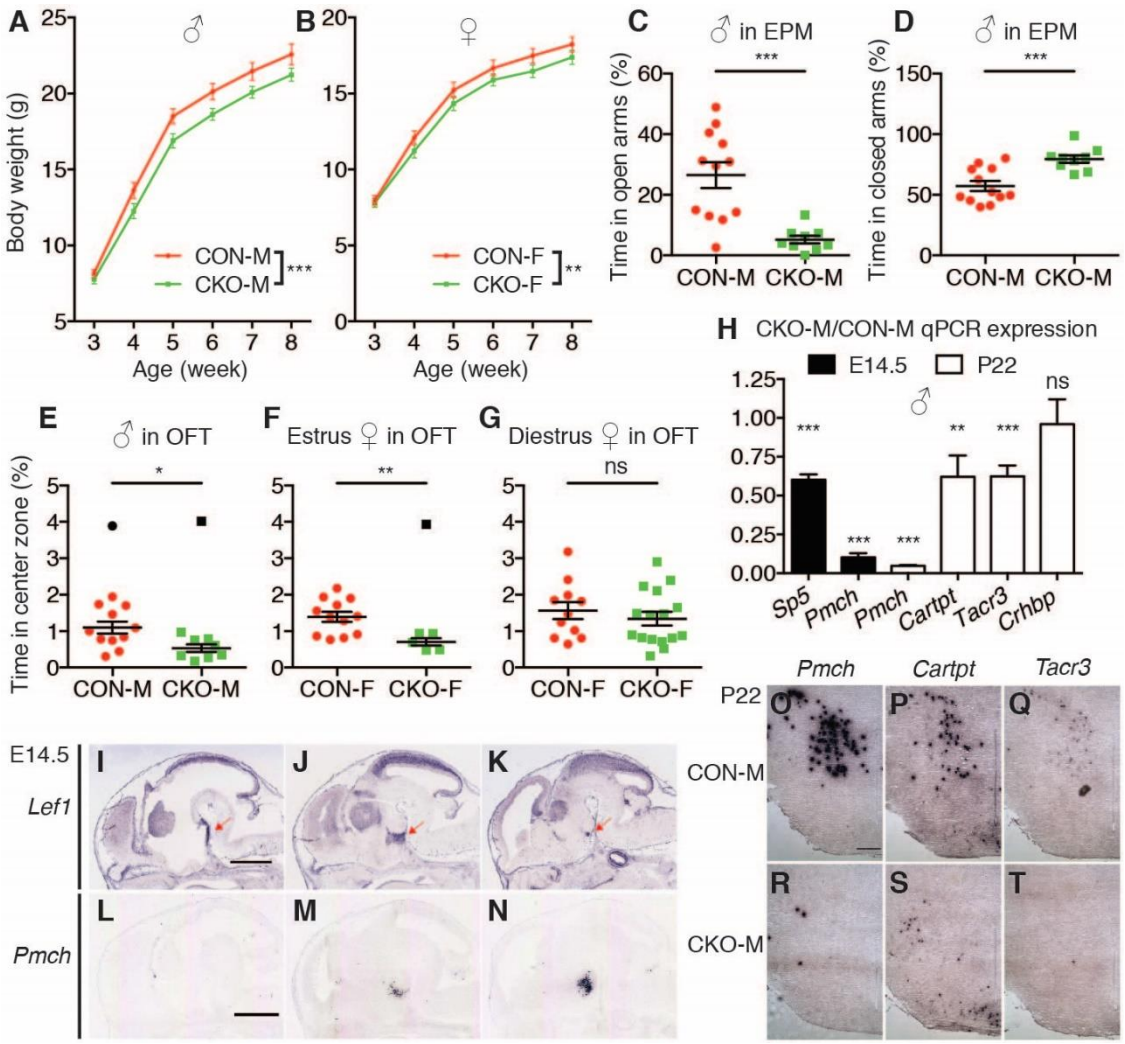

Fig. A.3. Hypothalamic Lef1 regulates growth, anxiety, and Pmch+ neuron formation in mice. (A and B) Male *Lef1*^{CKO} (CKO-M) (A, $F_{1,26}$ = 22.2) and female *Lef1*^{CKO} (CKO-F) (B, $F_{1,25}$ = 8.842) gained weight more slowly than controls (CON) after weaning. (C and D) Elevated plus maze (EPM). CKO-M spend less time in the open arms (C) and more time in the closed arms (D). (E-G) Open field test (OFT). CKO-M (E) and CKO-F in estrus (F), but not in diestrus (G), spend less time in the center zone. (H) qPCR analysis of hypothalamic gene expression in male E14.5 and P22 mice. (I-N) E14.5 sagittal images (www.genepaint.org) show co-expression of *Lef1* (I-K, red arrows) and *Pmch* (L-N) in the hypothalamus (*18*). (O-T) Reduced expression of *Pmch* (O and R), *Cartpt* (P and S) and *Tacr3* (Q and T) in the lateral hypothalamus of P22 CKO-M from 25 µm coronal sections. Data are mean ± 95% CI in (A and B), mean ± SEM in (C-G) and mean ± SD in (H). ***P < 0.001, **P < 0.01, *P < 0.05, ns. P > 0.05 by two-way ANOVA with repeated measures (A and B) and two-tailed unpaired Student's t tests (C-H). n = (A) 27, 27; (B) 26, 26 for CON and CKO, respectively. Outliers in (E and F) depicted in black were excluded using the Grubbs' test (P < 0.05). Scale bars: 400 µm in (I) and (L); 30 µm in (O).

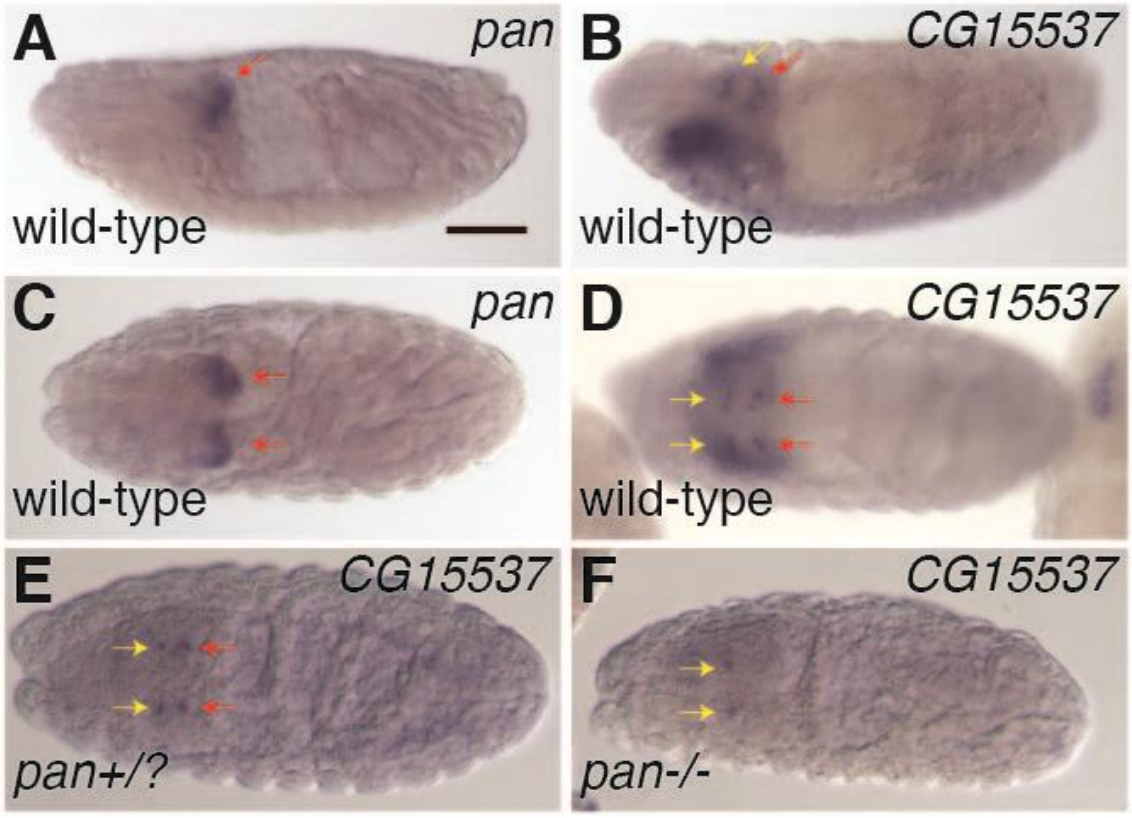

Fig. A.4. Loss of *Drosophila Crhbp* ortholog expression in *pan* mutants. Whole mount *in situ* hybridization images of stage 16 *Drosophila* embryos for the *Lef1* ortholog *pan* (A and C) and *Crhbp* ortholog *CG15537* (B, D, E and F). Yellow and red arrows indicate gene expression in the pars intercerebralis (PI) and pars lateralis (PL), respectively. Co-expression of *pan* (A and C) and *CG15537* (B and D) in the PL primordia of wild-type embryos. Expression of *CG15537* is specifically lost in the PL primordia of *pan-/-* (F, n = 32 (22.5%)) embryos compared to control siblings (E, n = 110 (77.5%)). Scale bar: 150 µm.

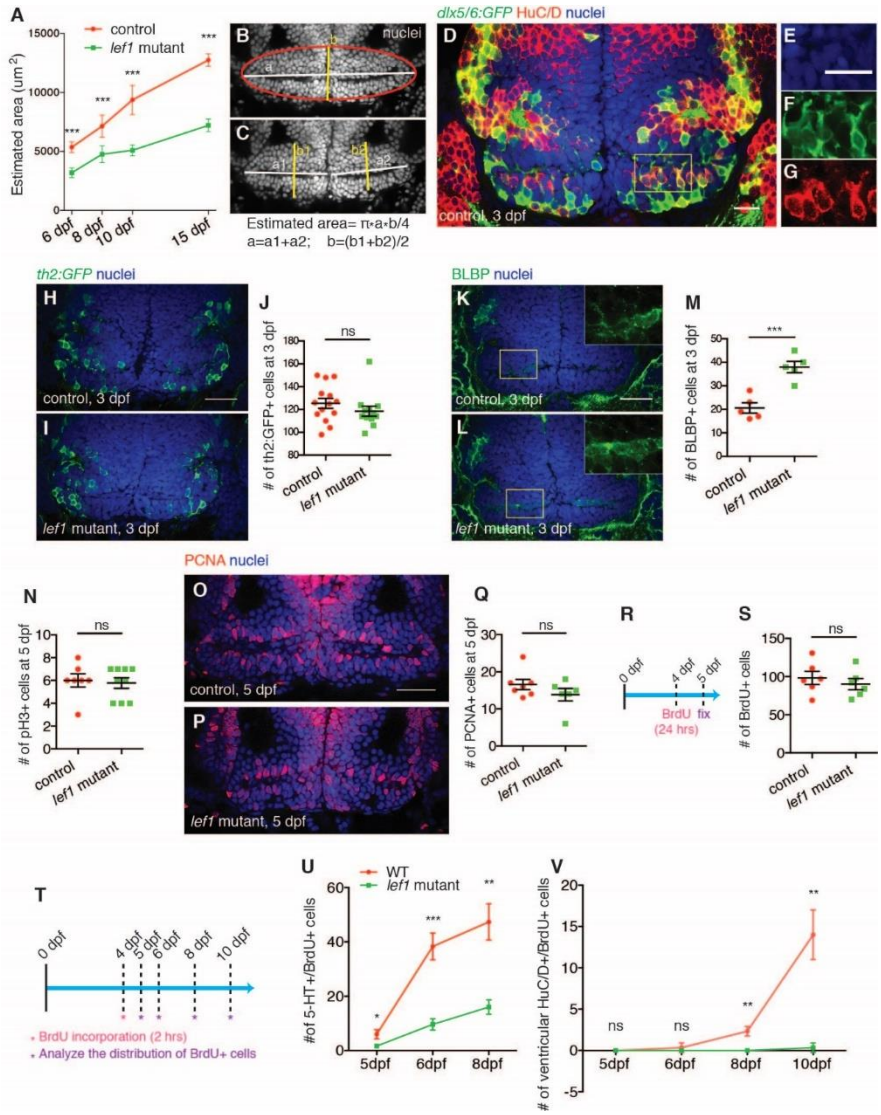

Fig. A.5. *lef1* regulates neurogenesis in the zebrafish caudal periventricular hypothalamus (Hc). (A-C) Progressive reduction of Hc size in *lef1* mutants compared to controls after 5 dpf calculated by area of confocal ventricular slices. Hc was defined as an oval indicated by red outline in (B). The area of the oval was calculated by the equations shown with lengths of a1, a2, b1, b2 measured by ImageJ in (C). (D-G) Ventricular HuC/D+ cells co-express GABAergic lineage marker *dlx5/6:GFP* in the 3 dpf Hc. Three confocal channel-split magnified images of the region depicted by the yellow rectangle in (D) are shown in (E-G). (H-J) Normal *th2:GFP*+ cells in the Hc of a 3 dpf *lef1* mutant. (K-M) Increased BLBP+ cells in the Hc of a 3 dpf *lef1* mutant. Higher magnification views of yellow rectangles in single channel are shown in the insets. (N-S) Normal proliferation in the Hc of a 5 dpf *lef1* mutant as shown by pH3+ (N) and PCNA+ (O-Q) cells, and 1 day BrdU labeling (R and S). (T-V) BrdU pulse-chase (T) to measure birth of 5-HT+ and HuC/D+ cells. *lef1* mutants have fewer 5-HT+/BrdU+ cells (U) and ventricular HuC/D+/BrdU+ cells (V). Data are mean ± SEM, except mean ± SD in (A, U, V). ***P < 0.001, **P < 0.01, *P < 0.05, ns. P > 0.05 by two-tailed unpaired Student's t tests. All images are confocal ventricular slices. All scale bars are 25 μm except 12.5 μm in (E) (see Table A.1 for information of quantification and more n numbers).

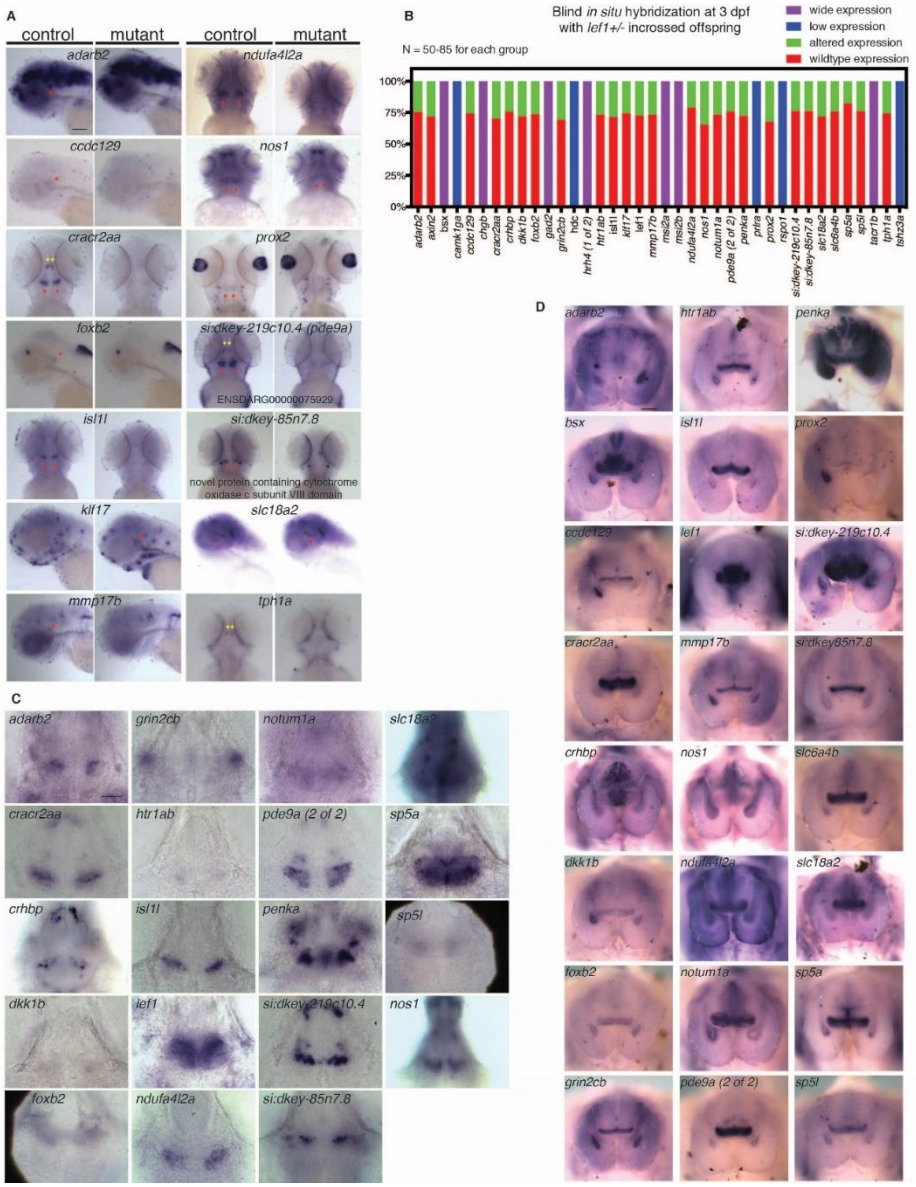

Fig. A.6. Whole mount *in situ* hybridization for zebrafish Lef1-dependent genes identified from RNA-seq. (A) 3 dpf control and *lef1* mutant embryos following *in situ* hybridization. Red and yellow arrows indicate gene expression in caudal and rostral hypothalamus, respectively. Lateral (*adarb2, ccdc129, foxb2, klf17, mmp17b* and *slc18a2*) or ventral (other genes) views were selected for optimal expression visualization. All genes have reduced expression in Hc of *lef1* mutants except *klf17,* which has ectopic expression in Hc. (B) Expression following *in situ* hybridization on 3 dpf offspring from *lef1*+/- incrosses. 50-85 embryos were analyzed per gene. (C) Images of 3 dpf wild-type brains centered on Hc from ventral view. (D) Gene expression in the hypothalamus of 4 mpf female wild-type zebrafish from ventral view. All genes tested showed strong expression in adult Hc except *prox2* with weak expression and *adarb2* with no expression. Images of ventral view have anterior on top; images of lateral view have anterior on the left. Scale bars: 0.1 mm in (A); 5 µm in (C); 0.2 mm in (D).

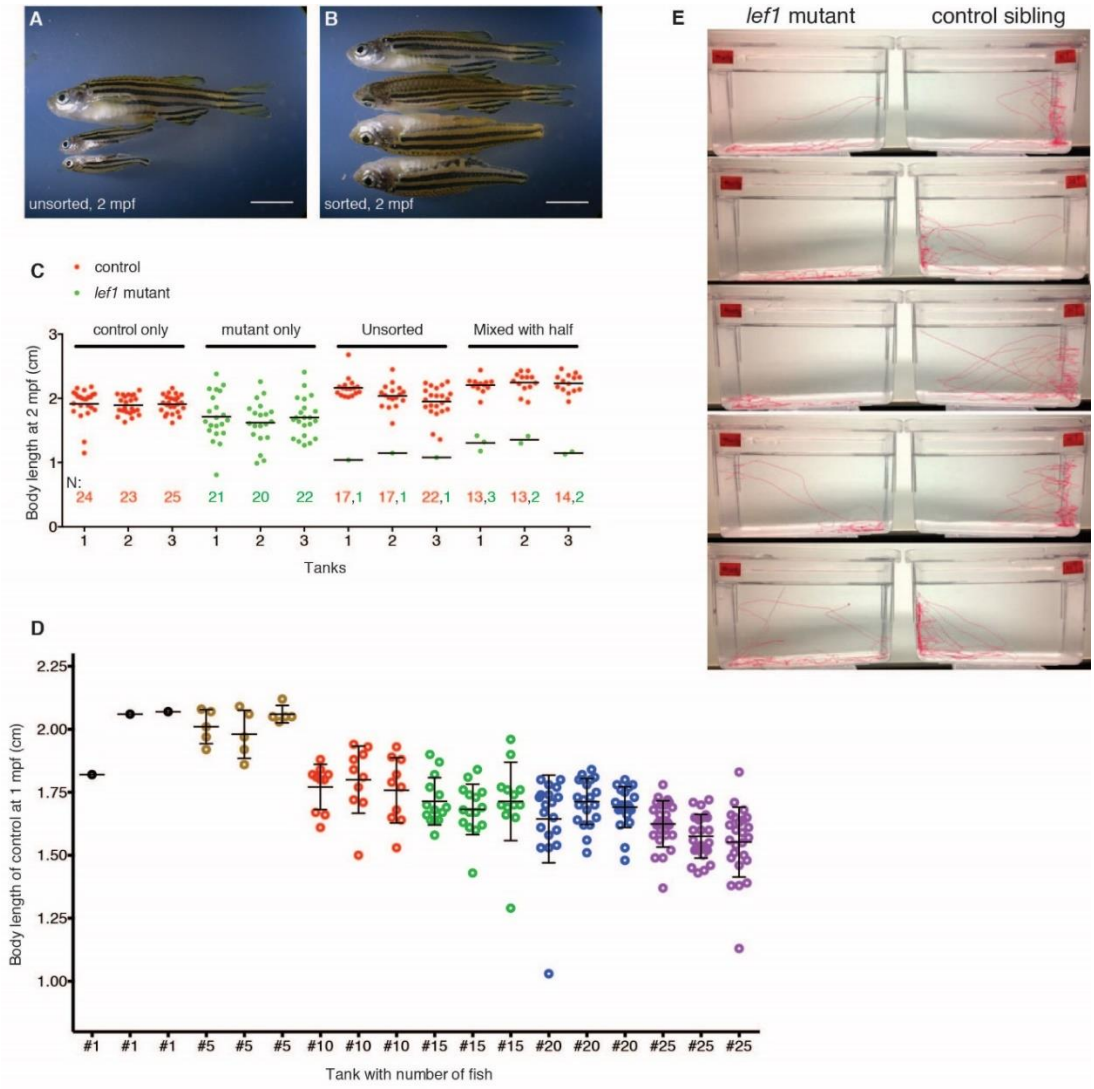

Fig. A.7. Physiological and behavioral analysis of zebrafish *lef1* mutants. (A-C) *lef1* mutants have a smaller body size and higher lethality rate when raised together with control siblings. Larvae were sorted by genotype from offspring of *lef1*+/- incrosses at 15 dpf and raised at 25 per tank. Body length and number of surviving fish at 2 months postfertilization (mpf) are shown in (C). (D) When raised at 1 or 5 per tank, wild-type fish had maximal growth. Data are mean ± SD. (E) 2 mins. swimming traces of 16 dpf control and *lef1* mutant siblings in the novel tank diving tests. Scale bars: 0.5 cm.

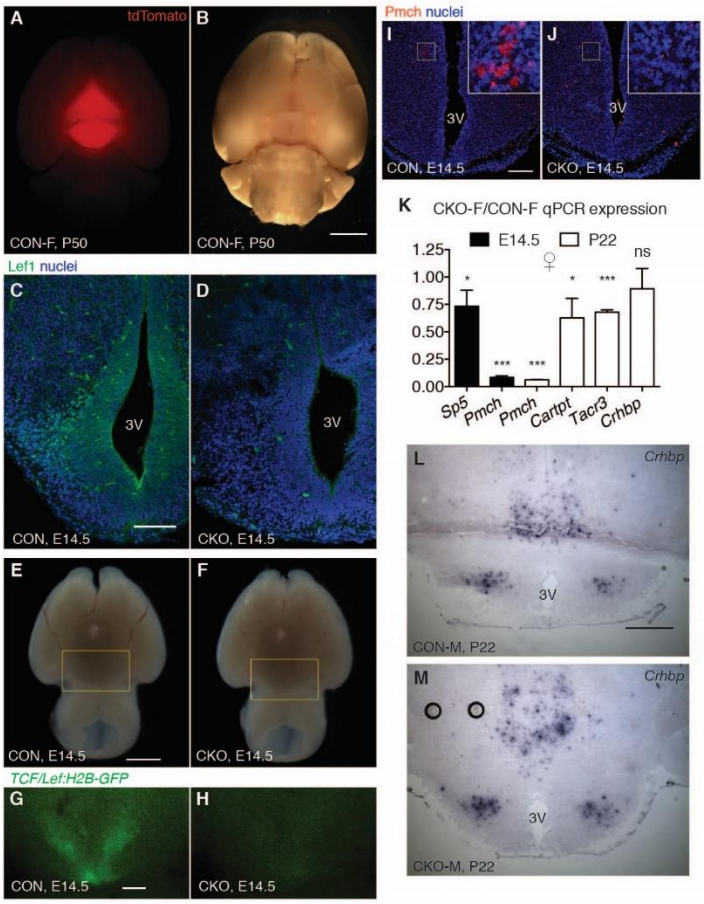

Fig. A.8. Cellular and molecular phenotypes in mouse *Lef1*^{CKO} hypothalamus. (A and B) P50 female *Nkx2.1*$^{Cre/+}$;*Lef1*$^{flox/+}$;*Rosa*$^{tdTomato/+}$ (CON-F) expresses tdTomato in the hypothalamus. Red fluorescence (A) and bright field (B) ventral view images of the same brain with anterior on top are shown. (C and D) Lef1 protein expression is lost in the hypothalamus of E14.5 *Lef1*^{CKO} (CKO-M) compared to *Lef1*^{CON} (CON-M) controls. Coronal images are Z-projections of 16 µm confocal optical sections, shown with dorsal side on top. (E-H) Wnt reporter *TCF/Lef:H2B-GFP* expression is reduced in the hypothalamus of CKO (H) compared to CON (G) at E14.5. Green fluorescence (G and H) views of yellow rectangles in bright field (E and F) view images of the same brain are shown, respectively. Images are ventral views with anterior side on top. (I and J) Loss of Pmch+ cells in the hypothalamus of E14.5 CKO. Higher magnification views of yellow rectangles are shown in the insets. Coronal images are Z-projections of 16 µm confocal optical slices, shown with dorsal side on top. (K) Real-time PCR (qPCR) analysis of hypothalamic gene expression in female mice. *Pmch* expression is reduced in hypothalami dissected from female *Lef1*^{CKO} (CKO-F) mice compared to female *Lef1*^{CON} (CON-F) mice at both E14.5 and P22. CKO-F also has reduced expression of the Wnt/Lef1 target *Sp5* at E14.5 and the *Pmch*+ neuron co-expressing genes *Cartpt* and *Tacr3* at P22, but normal expression of *Crhbp*. Data are mean ± SD. *P < 0.05, ***P < 0.001, ns. P > 0.05 by two-tailed unpaired Student's t tests. (L and M) Normal *Crhbp* expression in the hypothalamus of P22 CKO-M from 25 µm coronal section *in situ* hybridization, shown with dorsal side on top. 3V: 3rd ventricle. Scale bars: 100 µm in (B, C, E and I); 25 µm in (G); 500 µm in (L).

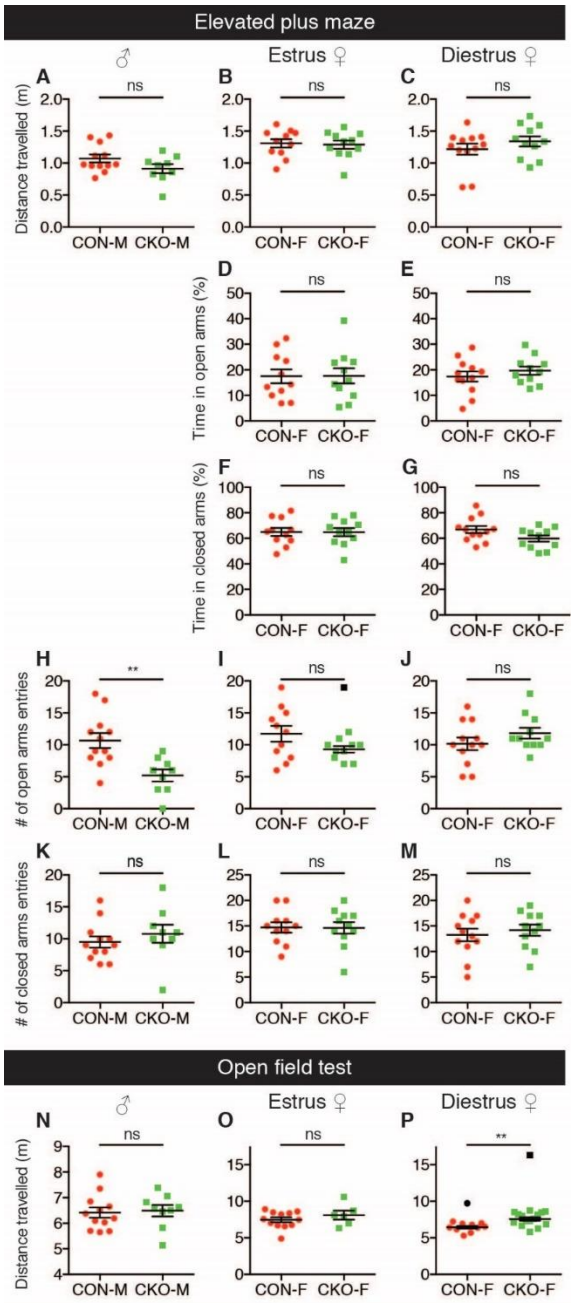

Fig. A.9. Mouse anxiety tests. Elevated plus maze (A-M). Distance travelled (A-C), percentage of time in the open arms (D and E) and closed arms (F and G), number of entries into the open arms (H-J) and closed arms (K-M) are shown for male mice (A, H and K), female mice in estrus (B, D, F, I and L) and female mice in diestrus (C, E, G, J and M). Open field test (N-P). Distance travelled is shown for male mice (N), female mice in estrus (O) and diestrus (P). n = 12, 9 for male CON, CKO; n = 12, 6 for female CON, CKO in estrus; n = 11, 16 for female CON, CKO in diestrus. Data are mean ± SEM. ***P < 0.001, **P < 0.01, ns. P > 0.05 by two-tailed unpaired Student's t tests. Outliers depicted in black were excluded from statistical analysis using the Grubbs' test (P < 0.05).

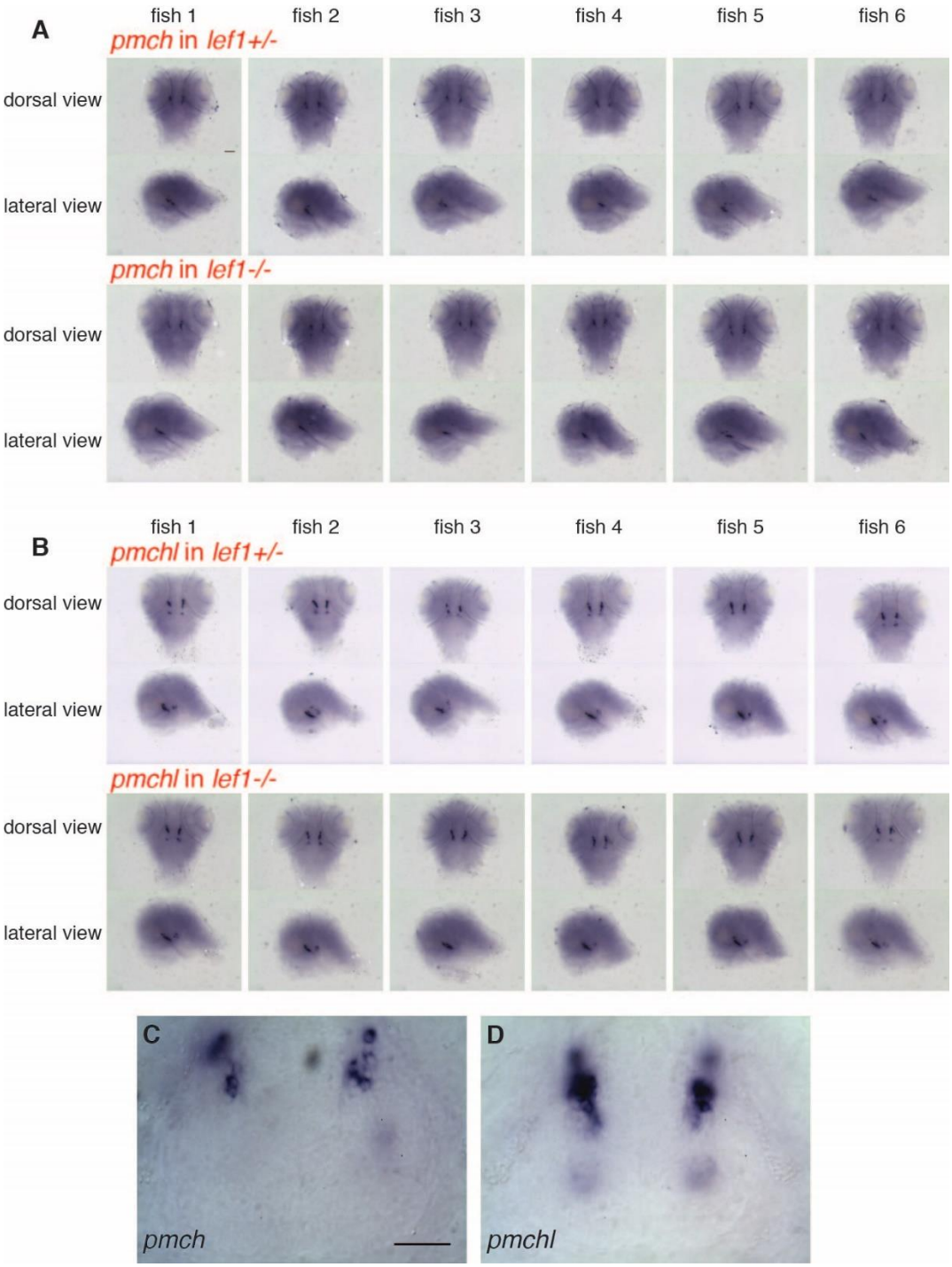

Fig. A.10. Normal expression of *pmch* and *pmchl* in zebrafish *lef1* mutants. (A and B) Whole mount *in situ* hybridization images for *pmch* (A) and *pmchl* (B) in the hypothalamus of 3 dpf zebrafish *lef1+/-* and *lef1-/-* embryos. (C and D) Images of 3 dpf wild-type brains centered on Hc from ventral view for *pmch* (C) and *pmchl* (D). Scale bar: 100 µm in (A); 5 µm in (C). Images of dorsal or ventral views have anterior on top; images of lateral views have anterior on the left.

Table A.1. Details of confocal images. Quantification and number of samples (n) for Fig. 1 and Fig. S1.

		Sample size		number of cells counted on	confocal picture
		control	mutant		
Figure 1					
A	3 dpf	n = 5	n = 5		
	4 dpf	n = 5	n = 3		
	5 dpf	n = 5	n = 4		
B, C					z-stack
D		n = 4	n = 3	left half of ventricular slice	
E, F					ventricular slice
G		n = 14	n = 12	left half of z-stack	
H		n = 5	n = 5	left half of ventricular slice	
I, J					z-stack
K		n = 5	n = 5	entire z-stack of hypothalamus	
L	p53+/-	n = 11	n = 8	entire z-stack of hypothalamus	
	p53-/-	n = 10	n = 10		
M, N					ventricular slice
P					ventricular slice
Figure S1					
A	6 dpf	n = 8	n = 7		
	8 dpf	n = 8	n = 6		
	10 dpf	n = 6	n = 6		
	15 dpf	n = 3	n = 4		
J		n = 14	n = 12	left half of z-stack	
M		n = 5	n = 5	left half of z-stack	
N		n = 7	n = 9	entire z-stack of hypothalamus	
Q		n = 7	n = 6	left half of ventricular slice adjacent to the ventricle	
S		n = 6	n = 6	entire z-stack of hypothalamus	
U, V		n = 3	n = 3	entire z-stack of hypothalamus	

Table A.2. Primer sequences for genotyping. Restriction enzyme BsaJI is used after PCR for *lef1*^{zd11}.

Gene	species		Primer Sequence
lef1^{zd11}	zebrafish	F	CACTCTCTCCAGCCCAACATT
		R	TGTTACTGTTGGGACTGATTTCTG
p53$^{e7/e7}$	zebrafish	F	GATAGCCTAGTGCGAGCACACTCTT
		R-wt	AGCTGCATGGGGGGGAT
		R-mut	AGCTGCATGGGGGGGAA
Lef1-flox	mouse	F	GCAGATATAGACACTAGCACC
		R	TCCACACAACTAACGGCTAC
Tcf7-flox	mouse	F	AGCTGAGCCCCTGTTGTAGA
		R	TTCTTTGACCCCTGACTTGG
Nkx2.1-Cre	mouse	F	ATGCTTCTGTCCGTTTGCCG
		R	CCTGTTTTGCACGTTCACCG
Jarid 1c	mouse	F	CTGAAGCTTTTGGCTTTGAG
		R	CCACTGCCAAATTCTTTGG
Rosa-TdTomato	mouse	F-wt	AAGGGAGCTGCAGTGGAGTA
		R-wt	CCGAAAATCTGTGGGAAGTC
		F-mut	CTGTTCCTGTACGGCATGG
		R-mut	GGCATTAAAGCAGCGTATCC
TCF/Lef1: H2B-GFP	mouse	F	ACAACAAGCGCTCGACCATCAC
		R	AGTCGATGCCCTTCAGCTCGAT

Table A.3. Primer sequences for synthesizing *in situ* hybridization probes. Reverse primers also included a T7 promoter-containing sequence "CCAAGCTTCTAATACGACTCACTATAGGGAGA" that was added 5' to the listed sequences above (*47*). All primers were designed by Primer-BLAST except mouse genes *Cartpt* (ABA experiment 72077479), *Crhbp* (ABA experiment 77455017), *Pmch* (Genepaint set MH227) and *Tacr3* (ABA experiment 80342167).

Zebrafish gene	Forward	Reverse
adarb2	TCGCAGTAAGAAGCAGGCAA	GACGGTAACAAGTGGGCAGA
bsx	ACCGACCAGAGTGATTTTGT	TCTTCATTGTCGTCCAGCGT
camk1ga	CGCCCTGAAGTGTGTGAAGA	GATGCATTGATGGCACGCTT
ccdc129	CGGGACATTTCCGTACTCGT	CTGCTGTACTTATTCCAGAGGGT
chgb	CCCGAGCTACGTCAACAAAA	CTTTTAACTCCTGTTGCGGGG
cracr2aa	AAGAGGTGCGGAGTCTTTGG	ATCCTGCGGAGCTGGTTTTT
crhbp	GCTGGGTGATGAAGGGTGAG	ACTTGTGCAGTACCCCTCATTT
dkk1b	TGCTCTCTACTGCATGCCTC	TAGTGTCTCTGGCATGTGTGC
foxb2	CGGCCAGGGAAGAACTCCTA	TCGGTGTAGGTTTGATGGGC
gad2	GCTGGAAACGGCAGTCAAAG	GGCACGTATCCCTTCTGCTT
grin2cb	GGGTGTTTGGGTCCCTCTCT	TGTATCCAGGCCCCAAAAGC
hdc	GTGTTCATAGTTTTACTGCGTCCT	ACAGTGTATAGCGTGAGGGA
hrh4 (1 of 2)	TCGACCTATACGCAGGGAGT	GCTACCAAGACCAAGGAGAGT
htr1ab	TGCCGATGGCTGCTCTTTAC	GCGAGTTTGAATAGCCGAGC
isl1l	GGTTGTGGGCTTGAGATCCT	TGATGTCCGTTGGACTTGCT
klf17	ACTAACCCAAGGGCTGGAGA	TGTACGTTTTCCCGCATCCA
mmp17b	GCAGTCGCCAAAATTCGAGG	AACATGCCCCCTTTGAGTCC
msi2a	AGAGGCTTCGGCTTCGTAAC	ACAGCAGTTGCGATGTTGGT
msi2b	TTTGAGAACGAGGATGTGGTGG	GGCCTTTACCTCAAATGAGATGG
ndufa4l2a	AAACACCCAGGACTGATCCC	CTGCGTCTTCTGTTGGCCTT
nos1	GCGTTTTCCCTGGCAACAAT	TTCTTTGGTCTTCCGGGCTC
notum1a	TATTTCTTGAGGGCGGCTGG	GTCTTGTAGACTGCGGTCCC
PDE9A (2 of 2)	GGAGGACGCGGAGATAATGG	ATGTGTTGCTCCAGACAGGG
penka	CCTGTCTCGTGCTCATGGTT	GGACGTGACCCAGAAATGGT
pmch	AGCTAGGTTCTGCAACCATCA	CATACATTTCTGCTCGTCATGTT
pmchl	AACCGCTAAAGCAAACGCTC	TTCAGATAAACAGCATCAAGTTGTA
prlra	AGTGGTTTTTCTCTCATCTCTGAC	CTTTGAGCATCCAGGTGAGGA
prox2	CTGAGCAGAACTGTGAGCGA	TGGAACCTGGAAGTCGTTGG
rspo1	TCGACCCCGACTCTTCATCT	GGACTTAACCGAGCCAGCAT
si:dkey-219c10.4	CCGTGTGACATTCGGGATCT	GTTGTTGTACCCCGGATGGT
si:dkey-85n7.8	TGCTGACCTTTCTGAGGGGA	ACACCAAAAGAGGTTTGGGAAG
slc18a2	TCAAACACCAGTCAAGCAACT	TAGCGTTTCCTCGTTCCTCG
slc6a4b	GAAGGAGACCAGCGTATGGG	CTCCGATGATGTAGCCGACC
sp5a	AGGAACGACACACTACAGGC	ACCGTAAACCTTCCCGCATC

Table A.3 cont.

Mouse gene		
sp5l	GTTTCCCAGCCACATGCAAC	ATGCTCCCATCGCAACCATT
tacr1b	TTCTGGTGTCGGTAGTGGGA	ACTGTGGTTTCCATTCGGCT
tph1a	CTGCGGTTGTGTTTTCCCTG	CCCAGTGAAGCCAGACCAAT
tshz3a	CTGTCAGCCCTCTAAGTGCC	CCTCTAGCTGGCGATACAGC
Cartpt	GCTACCTTTGCTGGGTGC	CAACAGGGAAAGAGCCCA
Crhbp	AAGGGGAGAGAGCCGCTA	TTTCCATTTGCTGCCCAT
Pmch	GCACTCTTGTTTGGCTTTATGC	GAGGTTTAATGCACACGTCAAGC
Tacr3	GAGGACCGTCACCAACTATTTC	AGCTCATCGTAGCTGGAGACTT
Drosophila gene		
CG15537	CCCAGTGTAAAGCGGTCCTT	GGTTCTGATAGCGACCGGAG

Table A.4. **Primer sequences for qPCR.**

Gene	**PrimerBank ID**		**Primer Sequence**	**amplicon size**
Sp5	11967967a1	F	TGGGTTCACCCTCCAGACTTT	195
		R	CCGGCGAGAACTCGTAAGG	
Pmch	12861395a1	F	GTCTGGCTGTAAAACCTTACCTC	161
		R	CCTGAGCATGTCAAAATCTCTCC	
Cartpt	7304945a1	F	CCCGAGCCCTGGACATCTA	103
		R	GCTTCGATCTGCAACATAGCG	
Tacr3	10946720a1	F	CTGGGCTTGCCAGTGACAT	173
		R	CGCTTGTGGGCCAAGATGAT	
Crhbp	162287189c2	F	CTTACCCTCGGACACTTGCAT	130
		R	GGTCTGCTAAGGGCATCATCT	

APPENDIX B

SHIFTING PARADIGMS: PHOSPHORYLATION OF JUN IS REQUIRED FOR STABILITY NOT ACTIVITY

Introduction

Multicellular organisms are built and sustained via a series of conserved biological processes requiring relay of extracellular stimuli to intracellular transducers (signal transduction). One key signal transduction pathway is the mitogen-activated protein kinase (MAPK) pathway, an evolutionarily conserved kinase cascade whose members are phosphorylated and activated in sequence, leading ultimately to the phosphorylation of target transcription factors. Our unexpected finding that an unphosphorylated target of the kinase cascade is active in vivo, leads us to postulate that phosphorylation is not (as previously thought) an on/off switch for transcription factor activation, but rather a modulator of transcription factor activity.

The MAPK family includes three subgroups: extracellular-signal regulated kinase (ERK), p38, and Jun N-terminal kinase (JNK). The JNK signaling pathway, which is the focus of the studies described here, is conserved in all eukaryotes from *Caenorhabditis elegans* to humans and evolved from the stress-activated kinase in yeast, known as HOG1 (Cobb and Goldsmith, 1995). Pathway members were initially discovered as UV-stress-responsive kinases that phosphorylate mammalian Jun (Adler et al., 1992; Derijard et al., 1994; Kyriakis et al., 1994). Notably, the list of stresses that activate JNK signaling has grown, primarily through studies in *Drosophila*, to include oxidative, immune, and wound stresses (Bidla et al., 2007; Bosch et al., 2005; Karkali and Panayotou, 2012; Riesgo-Escovar et al., 1996). Jun, the phosphorylation target of JNK, is a bZIP DNA-binding protein that is part of the AP-1 transcription factor important for gene regulation (Karin, 1995), and much has been construed regarding its post-translational regulation.

Studies in vitro have been instrumental in delimiting the transactivation domain of Jun; it contains four serines and threonines (S63/73, T91/93) in the N-terminus, and phosphorylation at these sites increases the DNA-binding and transcriptional activity of

the AP-1 transcription factor (Behrens et al., 1999; Papavassiliou et al., 1995; Pulverer et al., 1991), a heterodimer of Jun and Fos. While a central role for Jun phosphorylation in enhancing transcriptional activity of AP-1 is clear, our understanding of the mechanistic requirements for phosphorylation in vivo is surprisingly limited. Analysis of Jun post-translational regulation has been conducted almost exclusively using biochemical strategies in vitro, where studies reveal what a protein can do, not necessarily what it does do. Below, we describe our use of a powerful Jun assay system in vivo (*Drosophila* embryos) that complements decades of Jun studies in vitro.

Historically, the fruit fly *Drosophila melanogaster* has provided a powerful experimental platform for studying conserved signaling pathways. In this regard, disruption of the JNK pathway midway in embryogenesis results in a well-characterized and easily identified dorsal closure (DC) defect (Rios-Barrera and Riesgo-Escovar, 2013). DC is an essential embryonic process during which the laterally-positioned epidermal sheets extend to the dorsal midline where they fuse to enclose the entire embryo in epidermis. At the molecular level, DC initiates with JNK signaling and target gene expression (*dpp*) in the dorsal-most cells of the lateral epidermal sheet (the leading edge [LE]). Tight control of JNK signaling is vital, as not only do loss-of-function mutants disrupt DC, but so also do gain-of-function mutants (Bates et al., 2008). Indeed, these complementary phenotypes underscore the power of the DC system for studying JNK pathway architecture in vivo.

The Letsou lab uses the fruit fly, Drosophila melanogaster, to understand JNK signaling. Importantly, our breakthrough finding that unphosphorylated Jun is active in vivo is paradigm shifting. In this regard, our studies reveal a new role for phosphorylation in regulating JNK signaling. Since JNK signaling is involved in a host of processes integral to normal animal development and physiology, it is crucial that we understand if Jun phosphorylation functions as an on/off switch or instead as a more fluid regulator of

Jun activity (i.e. a dimmer switch). This distinction is important because the maintenance of tight control of JNK signaling, both spatially and temporally, is essential to organismal viability; dysregulated JNK signaling leads to developmental defects as well as devastating diseases such as cancer.

It has long been known that N-terminal phosphorylation of Jun increases target gene expression (Pulverer et al., 1991). Although N-terminal phosphorylation is considered to be synonymous with Jun activity and although phosphorylation of proteins has generally been considered to be an on/off switch for activity, this has never been unequivocally demonstrated for Jun. Indeed, current dogma largely ignores an almost 20-year-old report showing that Jun phosphorylation at its N-terminus stabilizes the protein in vitro such that phospho-Jun is resistant to degradation while unphosphorylated Jun is prone to rapid degradation (Musti et al., 1997). As a first test of whether Jun-N-terminal phosphorylation acts as an on/off switch in an in vivo system, we generated UAS-Jun transgenic flies where Jun is either wild-type (Jun^{+}; N-terminal serines and threonines remain intact) or nonphosphorylatable (Jun^{A}; N-terminal serines and threonines are replaced by alanines). In an analysis of transgene function (where cuticle phenotype correlates to signaling activity), we found that the nonphosphorylatable Jun^{A} transgene rescues the Jra mutant, just not as effectively as Jun^{+} (Jud & Letsou, unpublished). These data show that phosphorylation is not essential for Jun activity and that phosphorylation is not simply an on/off switch for Jun activity.

I tested whether Jun N-terminal phosphorylation stabilizes Jun and whether unphosphorylated Jun is preferentially degraded via the ubiquitin pathway. At the heart of this study is the postulated link connecting Jun phosphorylation state to Jun degradation. It is intriguing to speculate that graduated and quantitative regulation of JNK signaling (rheostasis) provides beneficial flexibility to an organism's response to internal and/or external developmental challenges (e.g., an ability to reset a threshold

activation response in answer to an environmental stress).

Materials and methods

Drosophila strains

Fly lines for this study include Oregon R for wild-type, *bsk*^{1}, *bsk*^{2}, *Jra*^{lA109}, *raw*^{lG}, *P(otu-GAL4::VP16.R, w*; P(GAL4-nos.NGT)40; P(GAL4::VP16-nos.UTR)CG6325*^{MVD1} (maternal GAL4 line), that are all available from the Bloomington Drosophila Stock Center at Indiana University. Additional lines generously gifted to our lab includes P(tubP-GAL4)LL7/TM3,P(Dfd-GMR-nvYFP)3 Sb^{1} (Mark Metzstein) and *ago*^{1} and *ago*^{3} (Kenneth Moberg). Double mutants were generated using standard mating protocols and/or recombination and were tested for the presence of the mutant alleles by standard complementation testing. For all assays, homozygous mutant embryos older than 6 hrs. after egg lay were identified by the absence of a balancer chromosome containing *twi-GAL4, UAS-GFP*.

Phenotypic analysis

Embryonic lethal cuticular phenotypes were viewed after mounting dechorionated and devitellinized samples in one-step mounting media (30% CMCP-10, 13% lactic acid, 57% glacial acetic acid). Hybridizations in situ were performed using digoxigenin-labeled RNA probes and 1:2000 α-DIG AP-conjugated Fab fragments (11093274910; Roche Diagnostics) as previously described (Byars et al., 1999). Cuticles were imaged using dark field optics on a Zeiss Axioskop microscope with AxioVision camera.

Protein studies

For immunoblot studies, proteins for control and experimental lysates were prepared from embryos collected over 2 hrs. and aged from 0-12 hrs. after egg lay (AEL)

or collected over 4 hrs. and aged to 8-12 hrs. AEL. Lysates were prepared as a 2:1 ratio (embryos: volume [µL]) under denaturing conditions with 1x Laemmli buffer (125mM Tris-base pH=6.8, 2% SDS, 10% glycerol, 5% 2-mercaptoethanol, 0.05% bromophenol blue). Protein lysates were separated on SDS-acrylamide gels, transferred to PVDF membranes (IPSN08132; Merck Millipore Ltd.) and analyzed by Western blotting with the rabbit α-Jun antibody (25763 1:200; Santa Cruz Biotechnology) and HRP-conjugated goat α-rabbit (1:1000; Chimicon) antibodies. Antibodies were diluted in TBS or TBST (0.05% Tween), each with 1x Western Blocking Reagent (11 921 673 001; Roche Diagnostics). Chemiluminescence was visualized by luminol (sc-2048; Santa Cruz Biotechnology), and the Amersham Hyperfilm ECL (28906835; GE Healthcare) was developed on the AFP Mini-Medical series developer.

Results

Previous reports of *raw* have demonstrated a clear increase in phosphorylated Jun protein (Humphreys et al., 2013), but the mechanism by which this accumulation occurs remains elusive. This could be due to genetic interactions between *raw* and June kinases, where Raw antagonizes a Jun kinase, or by stabilization of phospho-Jun protein where Raw antagonizes Jun degradation. Herein, I test both models of Jun accumulation and demonstrate that Raw does not antagonize a kinase, but rather influences the stability of Jun protein.

The Letsou lab has examined the role Jun kinases on the *raw* mutant phenotype, including *bsk*, *p38*, and *rolled* and found that none of these kinases play any role on the *raw* mutant phenotype (Jud & Letsou, unpublished). However, these experiments only probed Jun kinase activity using zygotic loss-of-function alleles. Therefore, I examined the role of the only maternally-derived Jun kinase, *bsk*, on the *raw* cuticle defects observed (Fig. B.1 A-B, Flybase, 2003). To this end I tested the function of maternal-*bsk*

on the *raw* cuticle phenotype, specifically the dorsal pucker and hypotrophy of the ventral denticle belts. I eliminated *bsk* expression in early wt and raw^{lG} embryos by driving expression of a UAS:bsk^{RNAi} transgene with a maternal set of Gal4 drivers (ref). (Fig. B.1 C-D). I observed no difference in cuticle phenotype (Fig. B.1 E) as compared to previously reported *raw* mutants (Byars et al., 1999) demonstrating that maternal *bsk* plays no role in the *raw* mutant phenotype and that Raw does not antagonize a Jun kinase.

Next, I examined whether Raw antagonizes Jun stabilization by testing for genetic interactions between *raw* and the ubiquitin proteasome pathway. It has been demonstrated that mammalian c-Jun is degraded by the ubiquitin proteasome pathway (reviewed in Davis et al., 2014). *Fbw7 (archipelago* (*ago*) in *Drosophila*) codes for the ubiquitin ligase targeting c-Jun for degradation (Davis et al., 2004; Wei et al., 2005). If the *raw*-dependent accumulation of Jun is due to failures in the ubiquitin proteasome pathway, I expect *ago* and *raw* to share loss-of-function phenotypes, specifically a dorsal pucker and hypotrophy of the ventral denticle belts. First, I examined cuticle phenotypes of ago^{1} null mutants and observed a loss-of-function phenotype similar to that of *raw* nulls (Fig. B.1 F). As expected for a null mutation, the phenotype observed in ago^{1} mutants was not enhanced when ago^{1} was placed in trans to a deficiency, thus confirming that it is a null for this phenotype (Fig. B.2 A).

Given the shared loss-of-function phenotypes observed in both *raw* and *ago*, I tested for genetic interactions between these two genes by examining the cuticle phenotype of ago^{1} homozygotes in a raw^{lG} heterozygous background. I observed enhancement of the *ago* phenotype demonstrating a role for *ago* in that the *raw* mutant phenotype (Fig. B.2 B). Last, I examined the cuticle phenotypes of maternal and zygotic loss of ago^{1} and ago^{3} mutants and observed a worsening of the phenotype compared to the zygotic loss alone (Fig. B.2 C-D). These data, taken together, demonstrate a role for

maternal and zygotic *ago* in the *raw* cuticle phenotype.

These genetic data demonstrating a role for *ago* in the *raw* cuticle phenotype suggest that the accumulation of Jun observed in *raw* is due to an inability for Jun to be degraded in *raw*. I, therefore, examined the role of *ago* on Jun protein accumulation in zygotic and maternal/zygotic *ago* mutants. I observed no change in Jun protein levels in the zygotic mutants alone, but a two-fold increase in protein in the maternal/zygotic mutants (Fig. B.3) demonstrating that Ago plays a critical role in Jun protein stability in vivo.

Discussion

While JNK signaling has been well-studied in diverse metazoans, much remains to be understood about how this pathway is antagonized to prevent or limit its activity in vivo. Herein, I characterized the role of *ago* in Jun stability and JNK signaling. I demonstrated that an ubiquitin ligase, *ago*, is responsible for maintaining biologically appropriate levels of Jun in the cell, but that, along with previous unpublished reports (Jud & Letsou, unpublished), a Jun kinase is not responsible for the elevated Jun levels we observe in *raw* mutants. I demonstrated a genetic interaction between *ago* and *raw* and postulate that Jun may be brought to Ago by Raw, in order that Jun may be degraded. Thus, phosphorylated Jun accumulates in *raw* due to alterations in its stability such that it remains unable to be degraded by the ubiquitin proteasome pathway. This is in contrast to the widely-held view that phosphorylated Jun is bioactive and that the unphosphorylated Jun protein is not. These data, together with unpublished data from the Letsou Lab (Jud & Letsou, unpublished), establish a new paradigm for Jun activity in vivo.

References

Adler, V., Polotskaya, A., Wagner, F., and Kraft, A.S. (1992). Affinity-purified c-Jun amino-terminal protein kinase requires serine/threonine phosphorylation for activity. The Journal of Biological Chemistry *267*, 17001-17005.

Bates, K.L., Higley, M., and Letsou, A. (2008). Raw mediates antagonism of AP-1 activity in *Drosophila*. Genetics *178*, 1989-2002.

Behrens, A., Sibilia, M., and Wagner, E.F. (1999). Amino-terminal phosphorylation of c-Jun regulates stress-induced apoptosis and cellular proliferation. Nature Genetics *21*, 326-329.

Bidla, G., Dushay, M.S., and Theopold, U. (2007). Crystal cell rupture after injury in Drosophila requires the JNK pathway, small GTPases and the TNF homolog Eiger. Journal of Cell Science *120*, 1209-1215.

Bosch, M., Serras, F., Martin-Blanco, E., and Baguna, J. (2005). JNK signaling pathway required for wound healing in regenerating Drosophila wing imaginal discs. Developmental Biology *280*, 73-86.

Byars, C.L., Bates, K.L., and Letsou, A. (1999). The dorsal-open group gene raw is required for restricted DJNK signaling during closure. Development *126*, 4913-4923.

Cobb, M.H., and Goldsmith, E.J. (1995). How MAP kinases are regulated. The Journal of Biological Chemistry *270*, 14843-14846.

Davis, R.J., 2000. Signal transduction by the JNK group of MAP kinases. Cell 103, 239-252.

Derijard, B., Hibi, M., Wu, I.H., Barrett, T., Su, B., Deng, T., Karin, M., and Davis, R.J. (1994). JNK1: a protein kinase stimulated by UV light and Ha-Ras that binds and phosphorylates the c-Jun activation domain. Cell *76*, 1025-1037.

FlyBase (2003). The Flybase database of the Drosophila genome projects and community literature. Nucleic Acid Research *31*, 172-175.

Karin, M. (1995). The regulation of AP-1 activity by mitogen-activated protein kinases. The Journal of Biological Chemistry *270*, 16483-16486.

Karkali, K., and Panayotou, G. (2012). The Drosophila DUSP puckered is phosphorylated by JNK and p38 in response to arsenite-induced oxidative stress. Biochemical and Biophysical Research Communications *418*, 301-306.

Kyriakis, J.M., Banerjee, P., Nikolakaki, E., Dai, T., Rubie, E.A., Ahmad, M.F., Avruch, J., and Woodgett, J.R. (1994). The stress-activated protein kinase subfamily of c-Jun kinases. Nature *369*, 156-160.

Musti, A.M., Treier, M., and Bohmann, D. (1997). Reduced ubiquitin-dependent degradation of c-Jun after phosphorylation by MAP kinases. Science *275*, 400-402.

Papavassiliou, A.G., Treier, M., and Bohmann, D. (1995). Intramolecular signal transduction in c-Jun. The EMBO Journal *14*, 2014-2019.

Pulverer, B.J., Kyriakis, J.M., Avruch, J., Nikolakaki, E., and Woodgett, J.R. (1991). Phosphorylation of c-jun mediated by MAP kinases. Nature *353*, 670-674.

Riesgo-Escovar, J., Jenni, M., Fritz, A., and Hafen, E. (1996). The Drosophila Jun-N-terminal kinase is required for cell morphogenesis but not for DJun-dependent cell fate specification in the eye. Genes & Development *10*, 2759-2768.

Rios-Barrera, L.D., and Riesgo-Escovar, J.R. (2013). Regulating cell morphogenesis: the Drosophila Jun N-terminal kinase pathway. Genesis *51*, 147-162.

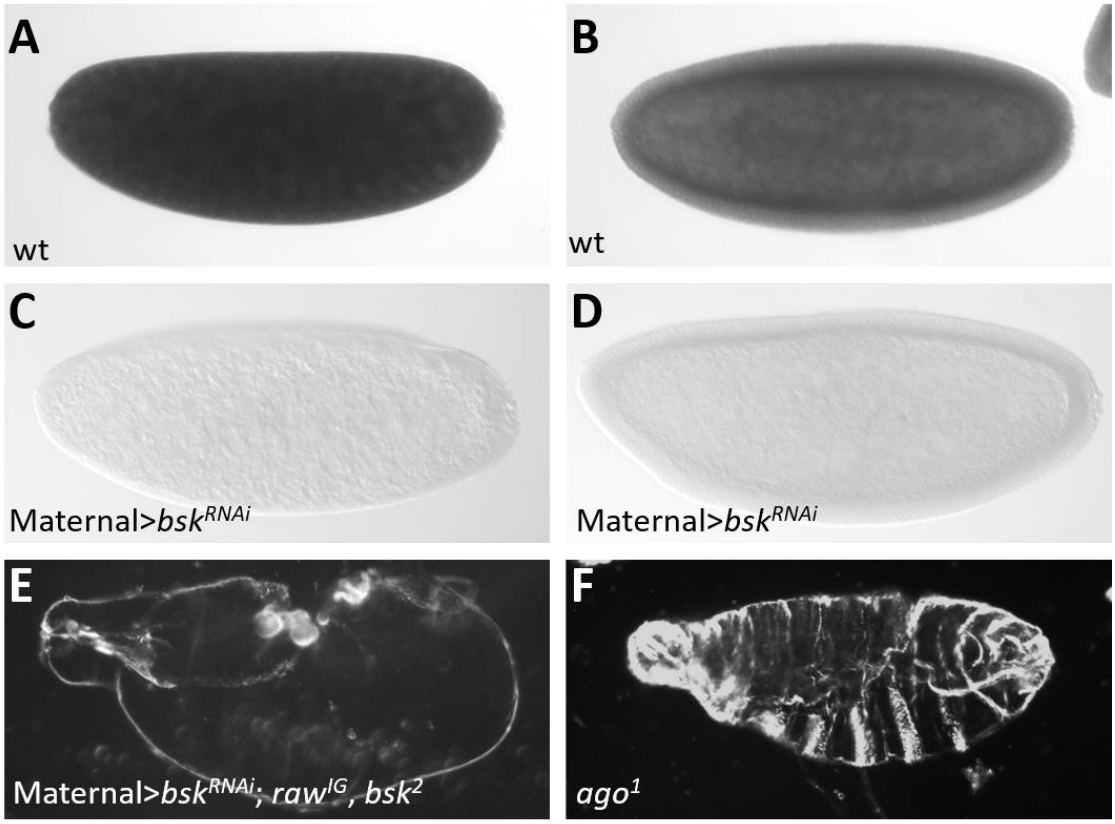

Fig. B.1. Maternal *bsk* does not contribute to the *raw* phenotype. *bsk* is maternally loaded and zygotically expressed in wild-type embryos (A-B) and expression is ablated using maternal bsk^{RNAi} in *raw bsk* mutant embryos (C-D). Loss of maternal *bsk* and zygotic *raw* and *bsk* (E) results in cuticle phenotypes indistinguishable from *raw* embryos. ago^{1} embryos exhibit raw-like phenotypes (F).

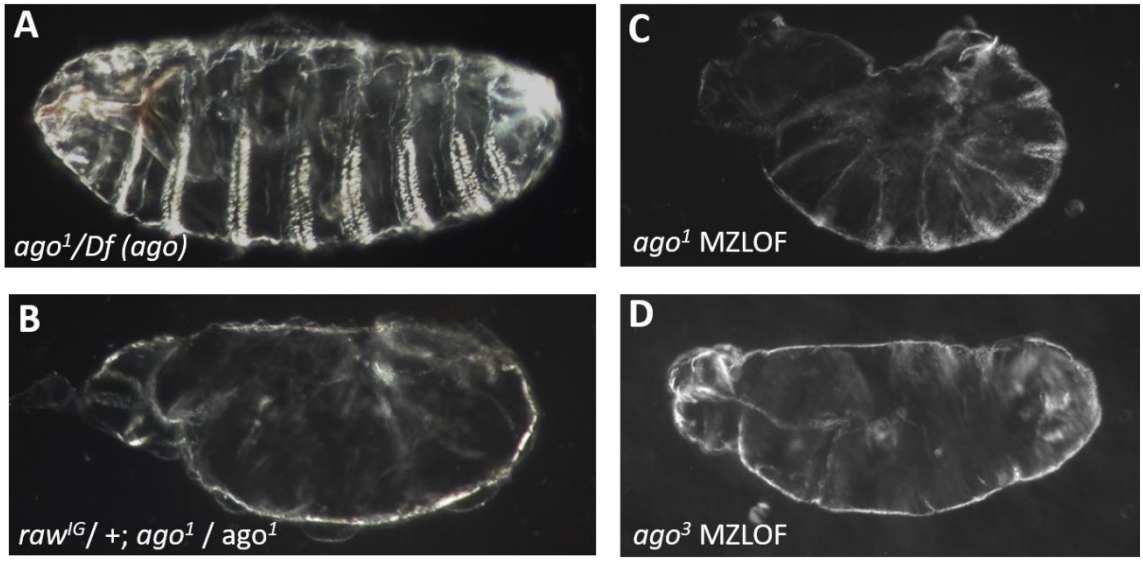

Fig. B.2. *ago* and *raw* genetically interact and maternally-derived *ago* contributes to embryogenesis. *ago*^{1} is defined as a null in this study as the *ago*^{1} allele in trans to a deficiency (A) does not worsen the *ago*^{1} phenotype previously reported (A). Loss of *ago* in a *raw*/+ background worsens the phenotype of *ago* alone (B). Loss of maternally- and zygotically-derived *ago* result in worsened phenotypes compared to *ago* alone (C-D).

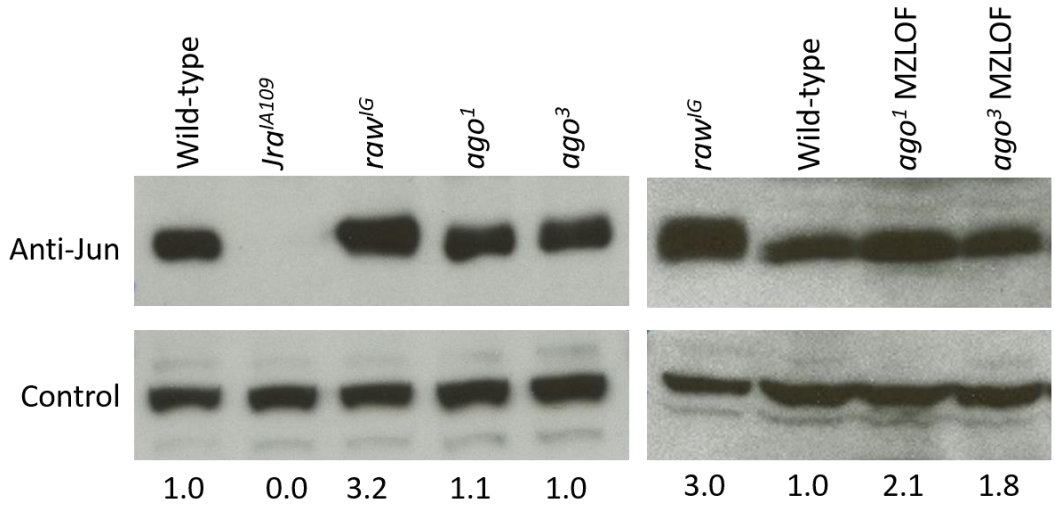

Fig. B.3. Ago is required for degradation of Jun. Jun levels are increased in *raw* as previously reported (A) but not significantly increased in *ago* zygotic mutants. However, depletion of *ago* maternally and zygotically results in increased Jun protein levels compared to wild-type (B).